

Advances in Alkyne Metathesis:

Catalysts with Multivalent Siloxy Ligands

&

Formal Total Synthesis of (+)-Aspicilin

&

Stabilization of α -Helical Peptide Structures

Dissertation

zur Erlangung des akademischen Grades eines
Doktors der Naturwissenschaften
(Dr. rer. nat.)
des Fachbereichs Chemie der Technischen Universität Dortmund

vorgelegt von
Sebastian Schaubach
geboren am 24.09.1987
in Ludwigsburg

Mülheim an der Ruhr, 2016

Hiermit versichere ich, dass ich die eingereichte Dissertation selbständig verfasst und keine anderen als die angegebenen Quellen und Hilfsmittel benutzt sowie Zitate kenntlich gemacht habe.

(Ort, Datum)

(Unterschrift)

Die vorliegende Arbeit entstand unter Anleitung von Herrn Prof. Dr. Alois Fürstner in der Zeit von April 2013 bis April 2016 am Max-Planck-Institut für Kohlenforschung in Mülheim an der Ruhr. Teile dieser Arbeit wurden in folgenden Beiträgen veröffentlicht:

- "Orthogonal Ring-Closing Alkyne and Olefin Metathesis for the Synthesis of Small GTPase-Targeting Bicyclic Peptides"
P. Cromm, S. Schaubach, J. Spiegel, A. Fürstner, T. Grossmann, H. Waldmann, *Nat. Commun.* **2016**, *Accepted Article*, doi.org/10.1038/ncomms11300
- "A Two-Component Alkyne Metathesis Catalyst System with an Improved Substrate Scope and Functional Group Tolerance: Development and Applications to Natural Product Synthesis"
S. Schaubach, K. Gebauer, F. Ungeheuer, L. Hoffmeister, M. K. Ilg, C. Wirtz, A. Fürstner, *Chem. Eur. J.* **2016**, *Accepted Article*, doi.org/10.1002/chem.201601163.

Die praktischen Arbeiten entstanden teilweise in Zusammenarbeit mit Marina Ilg (Kapitel 3), Kenichi Michigami (Kapitel 4) sowie Philipp Cromm (Kapitel 5). Die beschriebenen Ergebnisse bilden eine vollständige Darstellung dieser gemeinsamen Arbeiten. Die von diesen Mitarbeitern alleinverantwortlich erzielten Ergebnisse wurden als solche an entsprechender Stelle gekennzeichnet.

1. Berichterstatter: Herr Prof. Dr. Alois Fürstner

2. Berichterstatter: Herr Prof. Dr. Martin Hiersemann

Danksagung

Mein herzlicher Dank gilt Herrn Prof. Dr. Alois Fürstner für die Aufnahme in seine Arbeitsgruppe, die interessante Themenstellung sowie seine allzeit hervorragende Betreuung und Unterstützung. Die ausgezeichneten Arbeitsbedingungen, die wissenschaftliche Freiheit und die Vielfältigkeit der bearbeiteten Projekte haben meine Promotion zu einer höchst lehrreichen und abwechslungsreichen Zeit gemacht, wofür ich ihm sehr danken möchte.

Ich danke Herrn Prof. Dr. Martin Hiersemann von der Technischen Universität Dortmund für die freundliche Übernahme des Korreferats. Für die hervorragende Zusammenarbeit während der Syntheseprojekte danke ich Philipp Cromm, Chris Hartding, Marina Ilg und Kenichi Michigami. Den technischen Mitarbeitern der Abteilung Fürstner, namentlich Sebastian Auris, Helga Krause, Daniel Laurich, Roswitha Leichtweiß, Karin Radkowski, Günter Seidel, Saskia Schulthoff und Christian Wille, möchte ich für die hilfsbereite Unterstützung bei der Laborarbeit danken.

Den Mitarbeitern der analytischen Abteilungen danke ich für die schnelle und gewissenhafte Messung zahlreicher Proben sowie deren Auswertung. Mein Dank gilt insbesondere Alfred Deege und Heike Hinrichs für die Durchführung chromatographischer Analysen und Trennungen. Marion Blumenthal, Heinz-Werner Klein, Simone Marcus und Daniel Margold danke ich für die massenspektrometrischen Analysen. Angelika Dreier und Dr. Richard Goddard möchte ich für Röntgenstrukturanalysen danken.

Monika Lickfeld danke ich für ihre große Hilfe in allen organisatorischen Angelegenheiten. Ein weiterer Dank gilt Andreas Ahlers, Sylvester Größl, Dr. Brendan Monks, Daniel Schaubach, Heiko Sommer, Daniel Tindall und Dr. Christophe Werlé für das schnelle und sorgfältige Korrekturlesen dieser Arbeit. Allen derzeitigen und ehemaligen Mitarbeitern der Arbeitsgruppe Fürstner danke ich für die gute Zusammenarbeit, die zahlreichen inspirierenden Diskussionen und die schöne Zeit innerhalb und außerhalb des Labors.

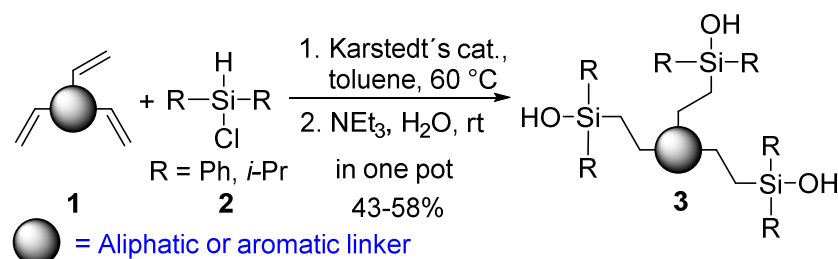
Mein ganz besonderer Dank gilt meiner Familie für die herzliche Unterstützung während meiner Promotionszeit.

Meiner Familie

Summary

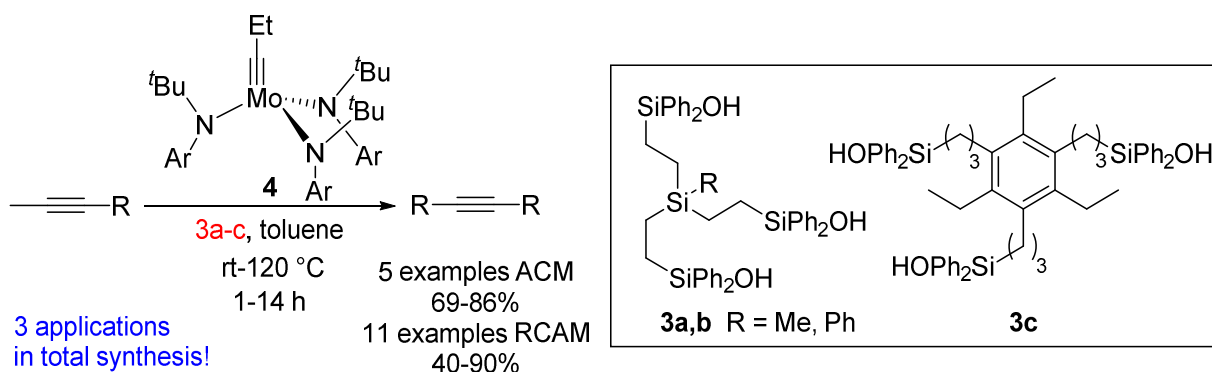
Development of New Two-Component Alkyne Metathesis Catalysts

The last couple of years have seen considerable progress in alkyne metathesis. This development led to catalysts with remarkable activity and functional-group tolerance as demonstrated in highly advanced applications.^[1] However, substrates with (multiple) protic sites still cause problems. Therefore we submitted the current catalyst generation based on Mo-alkylidynes with monodentate siloxy ligands to an extensive screening. The acquired information was then used for the design of a new catalyst generation based on multidentate siloxy ligands. We have established an efficient, scalable method to form tridentate silanols of type **3** via hydrosilylation of triolefin precursors **1** with chlorosilanes **2** and subsequent hydrolysis (**Scheme 1**).



Scheme 1: General synthesis for tridentate silanol ligands **3**.

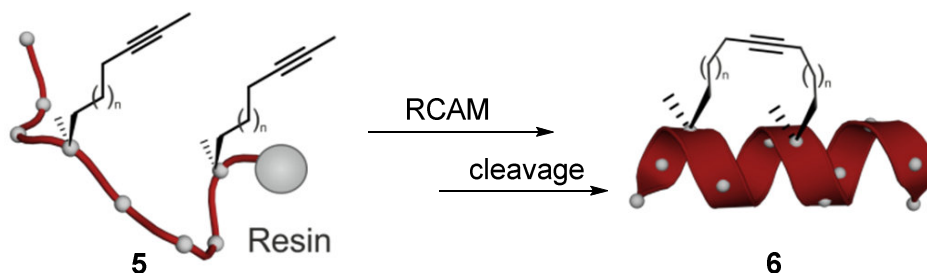
The catalysts are generated *in situ* from the known molybdenum alkylidyne^[2] **4** and silanols **3a-c** by ligand exchange (**Scheme 2**). Gratifyingly they show excellent stability and tolerate substrates containing free alcohols and highly coordinating groups. Their potential was further underlined by the ring closing alkyne metathesis (RCAM) reaction of diynes with two protected or unprotected hydroxy groups in propargylic positions. Moreover, they enabled three natural product syntheses where other commonly used catalysts failed.



Scheme 2: Metathesis reactions with new two-component catalyst systems.

Stabilization of α -Helical Peptides Using RCAM

Hydrocarbon-stapled peptides are a promising tool for targeting challenging protein-protein interactions, that are not accessible via classic small molecule approaches.^[3] One way to enforce an α -helical conformation is the introduction of an all-hydrocarbon macrocyclic bridge connecting two turns of a helix (**Scheme 3**).^[4] To accomplish this goal a hydrocarbon tether was introduced by RCAM using immobilized precursors **5**. Impressingly all (protected) functionalities present in the 20 proteinogenic amino acids were tolerated.

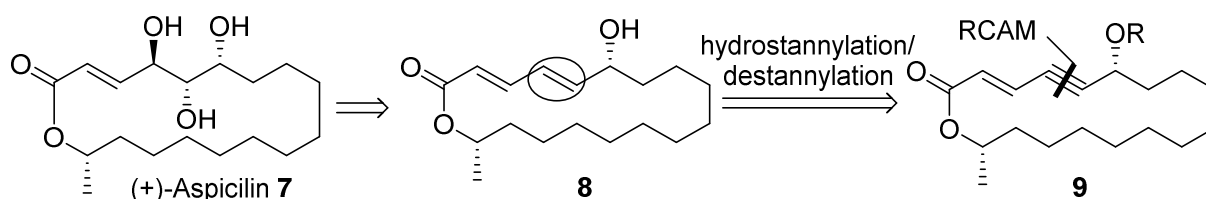


Scheme 3: RCAM approach to stabilize α -helical peptides.

Additionally, we successfully accomplished the synthesis of adjacent and intertwined bicyclic peptides via tandem ring closing olefin metathesis (RCM) and RCAM reactions. In order to further functionalize the macrocyclic scaffolds the immobilized alkyne was submitted to hydration, dibromination and azide-alkyne cycloadditions, which allowed us to introduce sidechains containing biomolecules such as sugars or biotin.

Formal Total Synthesis of (+)-Aspicilin

We have demonstrated the feasibility of constructing an *E,E*-diene in a macrocyclic molecule within a formal synthesis (+)-Aspicilin (**7**). In this synthesis we found that the 18-membered macrocyclic core structure **9** could be achieved via RCAM at high reaction temperature and under strict control of the reaction time (**Scheme 4**). Furthermore, we applied a newly developed hydrostannylation methodology for the first time on a macrocyclic 1,3-enyne.^[5] The formal synthesis of (+)-Aspicilin was completed in 14 steps with an overall yield of 10% for the longest linear sequence of ten steps.

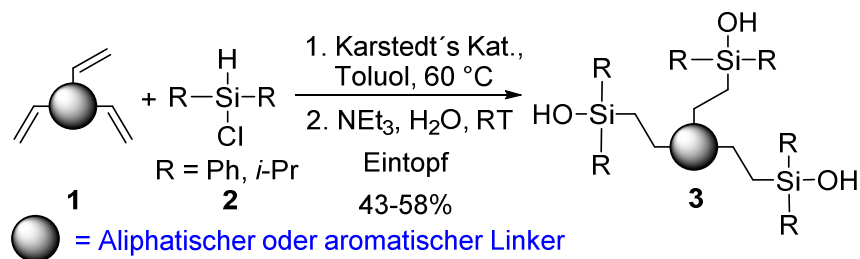


Scheme 4: Retrosynthetic analysis of (+)-Aspicilin **7**.

Zusammenfassung

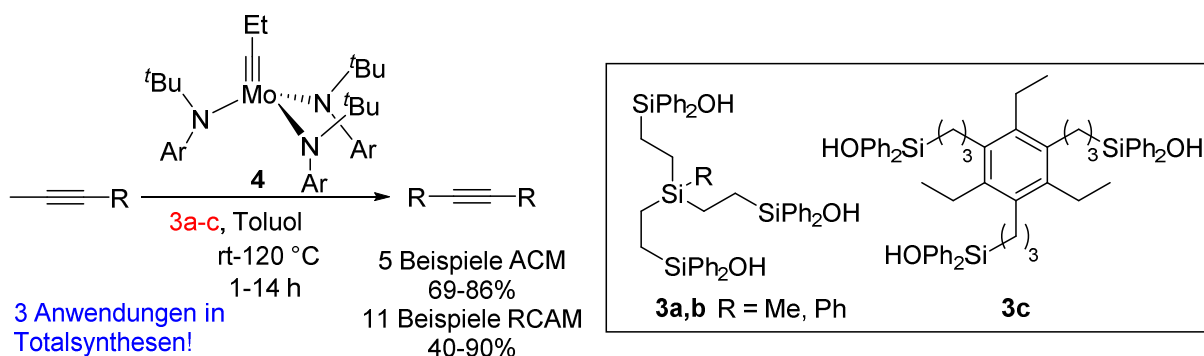
Entwicklung Neuer Zwei-Komponenten-Alkinmetathese-Katalysatoren

In den letzten Jahren wurden beträchtliche Fortschritte auf dem Gebiet der Alkinmetathese erzielt, was zu Katalysatoren mit bemerkenswerter Aktivität und Toleranz gegenüber funktionellen Gruppen führte. Dies wurde in zahlreichen herausfordernden Anwendungen demonstriert.^[1] Substrate mit einer oder mehreren protischen Funktionalitäten bleiben aber oft problematisch. Daher wurde die aktuelle Katalysatorgeneration einer erweiterten Substratkompatibilitätsprüfung unterzogen. Die so gewonnenen Informationen wurden in das Design neuer Katalysatoren einbezogen, welche auf multidentaten Siloxy Liganden **3** basieren. Für diese haben wir einen effizienten und skalierbaren Zugang ausgehend von Trioletinen **1** durch Silylierung und Hydrolyse geschaffen (**Schema 1**).



Schema 1: Generelle Synthese von tridentaten Silanolen **3**.

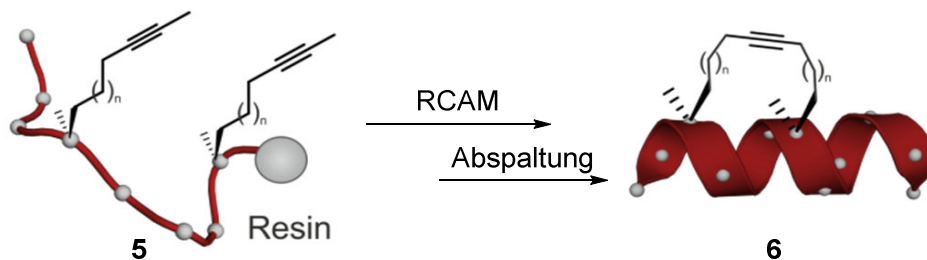
Die Katalysatoren wurden ausgehend vom Alkyldin **4** und dem jeweiligen Silanol **3a-c** *in situ* durch Ligandenaustausch hergestellt (**Schema 2**). Sie zeigten eine herausragende Stabilität selbst unter verschärften Reaktionsbedingungen. Des Weiteren wurde eine verbesserte Toleranz gegenüber Substraten mit freien Alkoholen sowie stark koordinierenden Gruppen beobachtet. Diese Befunde konnten z.B. durch die Ringschluss-Alkinmetathese (RCAM) Reaktionen von Substraten mit zwei geschützten oder ungeschützten Hydroxy-Gruppen in propargylier Position belegt werden. Ebenso konnten die neuen Katalysatoren in drei Totalsynthesen ihre Überlegenheit gegenüber den sonst üblichen Katalysatoren beweisen.



Schema 2: Metathesereaktionen mit den neuen Zwei-Komponenten-Katalysatoren.

Stabilisierung von α -Helikalen Peptiden durch RCAM

Peptide, die über Kohlenwasserstoffbrücken stabilisiert sind, gelten als vielversprechendes Werkzeug um Protein-Protein-Interaktionen zu adressieren; dies ist durch kleine Moleküle oft nicht möglich.^[3] Ein Weg zur Stabilisierung der α -helikalen Konformation ist die Einführung einer Kohlenwasserstoffbrücke^[4], die zwei Windungen der Helix miteinander verbindet. Dies ist uns ausgehend vom festphasengebundenen Vorläufer **5** durch RCAM zu **6** gelungen (**Schema 3**). Die Methodik tolerierte alle (geschützten) Funktionalitäten der 20 proteinogenen Aminosäuren.

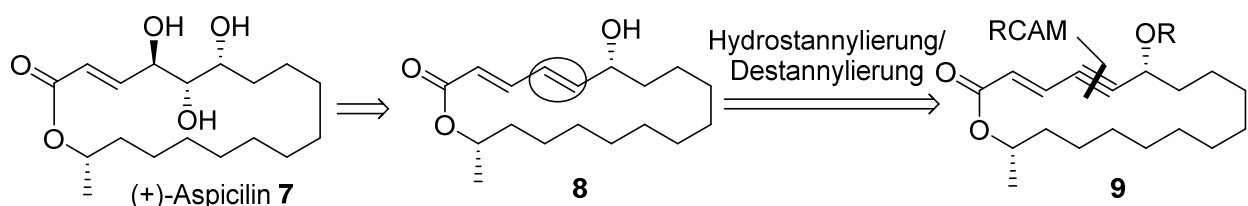


Schema 3: RCAM zur Stabilisierung α -helikaler Peptide.

Durch Kombination von Olefinmetathese und Alkinmetathese konnten bityklische Peptide mit benachbarten oder sich überschneidenden Brücken erzeugt werden. Wir konnten weiterhin zeigen, dass sich die Alkine mittels Hydratisierung, Dibromierung oder Azid-Alkin-Cycloaddition weiter funktionalisieren lassen. Letzteres ermöglichte die Einführung von Seitenketten mit Biomolekülen wie Biotin oder eines Zuckerderivates.

Formale Totalsynthese von (+)-Aspicilin mittels RCAM und Hydrostannylierung

Um die kürzlich erzielten Fortschritte in der Reaktionsführung von RCAM Reaktionen zu zeigen^[6], wurde eine formale Totalsynthese von (+)-Aspicilin (**7**) durchgeführt. Der 18-gliedrige Makrozyklus **9** wurde durch RCAM aufgebaut, was nur unter strikter Kontrolle von Reaktionszeit und Temperatur selektiv möglich war (**Schema 4**). Zudem wendeten wir erstmalig die neu entwickelte Hydrostannylierung auf ein makrozyklisches Enin an.^[5] Die formale Synthese von (+)-Aspicilin gelang in 14 Stufen mit einer Ausbeute von 10% in der längsten linearen Sequenz von zehn Stufen.



Schema 4: Schlüsselschritte in der formalen Totalsynthese von (+)-Aspicilin.

Content

1 Introduction.....	1
1.1 Fundamentals of Alkyne Metathesis.....	1
1.2 Applications of Alkyne Metathesis.....	3
2 Alkyne Metathesis Catalysts Based on Siloxy Ligands.....	6
2.1 Introduction.....	6
2.1.1 Molybdenum Nitrido Complexes with Siloxy Ligands.....	6
2.1.2 Molybdenum Alkylidyne Complexes with Siloxy Ligands.....	7
2.2 Aims and Scope.....	9
2.3 Extended Substrate Scope of [Mo(\equiv CC ₆ H ₄ OMe)(OSiPh ₃) ₃].....	9
2.3.1 Homo Metathesis Reactions.....	9
2.3.2 ACM Reactions.....	13
2.4 Conclusion.....	14
3 Alkyne Metathesis Catalysts Based on Multidentate Ligands.....	15
3.1 Introduction.....	15
3.1.1 Early Molybdenum-Based Alkyne Metathesis Catalysts.....	15
3.1.2 Alkyne Metathesis Catalysts with Multidentate Ligands.....	16
3.2 Aims and Scope.....	20
3.3 Catalyst and Ligand Synthesis.....	20
3.3.1 Initial Considerations.....	20
3.3.2 Multidentate Ligands with Silicon Linkers.....	21
3.3.3 Multidentate Ligands with Trisubstituted Aromatic Linkers.....	24
3.3.4 Multidentate Ligands with Hexasubstituted Aromatic Linkers.....	25
3.3.5 Calyx[4]arene- and Silsesquioxane-Based Systems.....	28
3.3.6 Conclusion.....	31
3.4 Substrate Scope of <i>In Situ</i> Generated Catalysts.....	32
3.4.1 Homometathesis Reactions.....	32
3.4.2 RCAM Reactions.....	34
3.4.3 Applications to Natural Product Synthesis.....	37
3.4.4 Conclusion.....	39
4 Formal Synthesis of (+)-Aspicilin.....	40
4.1 Introduction.....	40
4.1.1 Isolation, Structure Validation, and Biological Activity.....	40
4.1.2 Preceding Synthetic Studies.....	41
4.1.3 Oppolzer's Total Synthesis of (+)-Aspicilin by Asymmetric Alkenylation.....	42

4.1.4 Hoveyda's Formal Synthesis of (+)-Aspicilin by Z-selective RCM	43
4.2 Aims and Scope	44
4.3 Preliminary Studies and Formal Synthesis	45
4.3.1 Preliminary Studies on Monomer to Dimer Ratios in RCAM.....	45
4.3.2 Retrosynthetic Analysis of (+)-Aspicilin	47
4.3.3 Synthesis of Fragments 151 and 152	47
4.3.4 Ring Closing Alkyne Metathesis.....	49
4.3.5 Completion of the Formal Synthesis of (+)-Aspicilin	50
4.4 Conclusion	51
5 Synthesis of Stapled Peptides via Alkyne Metathesis	52
5.1 Introduction.....	52
5.1.1 Small Molecules, Biologics, and Peptides as Drugs	52
5.1.2 Small GTPases Addressed by Stapled Peptides	52
5.1.3 Overview of Methodologies to Generate Stapled Peptides.....	53
5.2 Aims and Scope	54
5.3 Stapled Peptides via Alkyne Metathesis.....	54
5.3.1 RCAM of Immobilized Alkynes	54
5.3.2 Bicyclic Peptides via Orthogonal RCM and RCAM.....	57
5.3.3 Biological Evaluation of Alkyne Stapled Peptides	58
5.4 Functionalization of Immobilized Alkynes.....	59
5.4.1 Gold-Catalyzed Hydration	60
5.4.2 Azide-Alkyne Cycloaddition	62
5.4.3 Further Functionalization Attempts	63
5.5 Conclusion	64
6 Summary and Conclusion	65
7 Experimental Procedures	71
7.1 General Experimental Details.....	71
7.2 Extended Substrate Scope of Catalyst 28	75
7.2.1 Synthesis of Metathesis Catalysts 28	75
7.2.2 Synthesis of Metathesis Substrates.....	75
7.2.3 Homo Metathesis Reactions	86
7.2.4 Cross Metathesis Reactions.....	93
7.3 Synthesis of Multidentate Ligands	95
7.3.1 Synthesis of Ligands with Silicon Linkers.....	95
7.3.2 Synthesis of Ligands with Trisubstituted Aromatic Linkers.....	98

7.3.3 Synthesis of Ligands with Hexasubstituted Aromatic Linkers	101
7.3.4 Synthesis of Calyx[4]arene Based Systems	106
7.4 Reactions with the Two-Component Catalyst System	110
7.4.1 Homocoupling Reactions	110
7.4.2 RCAM Reactions	113
7.5 Formal Synthesis of Aspicilin	117
7.5.1 Synthesis of Alcohol Fragment 151	117
7.5.2 Synthesis of Acid Fragment 152	120
7.5.3 Completion of the Formal Total Synthesis	121
7.6 Peptide Reactions	126
8 Appendix	128
8.1 List of Abbreviations	128
8.2 Crystallographic Data	133
8.2.1 Crystallographic Data of 97c	133
8.2.2 Crystallographic Data of 100c	135
8.2.3 Crystallographic Data of 105b	137
8.3 Bibliography	139

1 Introduction

1.1 Fundamentals of Alkyne Metathesis

Complex organic molecules play a crucial role in our modern daily life. A highly important methodology to generate those molecules is olefin metathesis. The success of olefin metathesis is based on a high level of functional group tolerance, chemoselectivity, reliability, user friendliness and the good commercial availability of the catalysts.^[7] A lot of energy was invested to develop efficient and user friendly systems, allowing this transformation to become one of the most commonly used organic reaction.^[7] The importance of olefin metathesis is also highlighted by the Nobel Prize in 2005, which was awarded to Schrock, Grubbs and Chauvin for their fundamental work in this field.^[8]

Alkyne metathesis is another effective way to form C-C bonds.^[1, 9] It was first described by Pennella et al. who showed that WO_3 on silica can convert a mixture of 2-pentyne and 2-butyne to 3-hexyne (Figure 1.1).^[10]

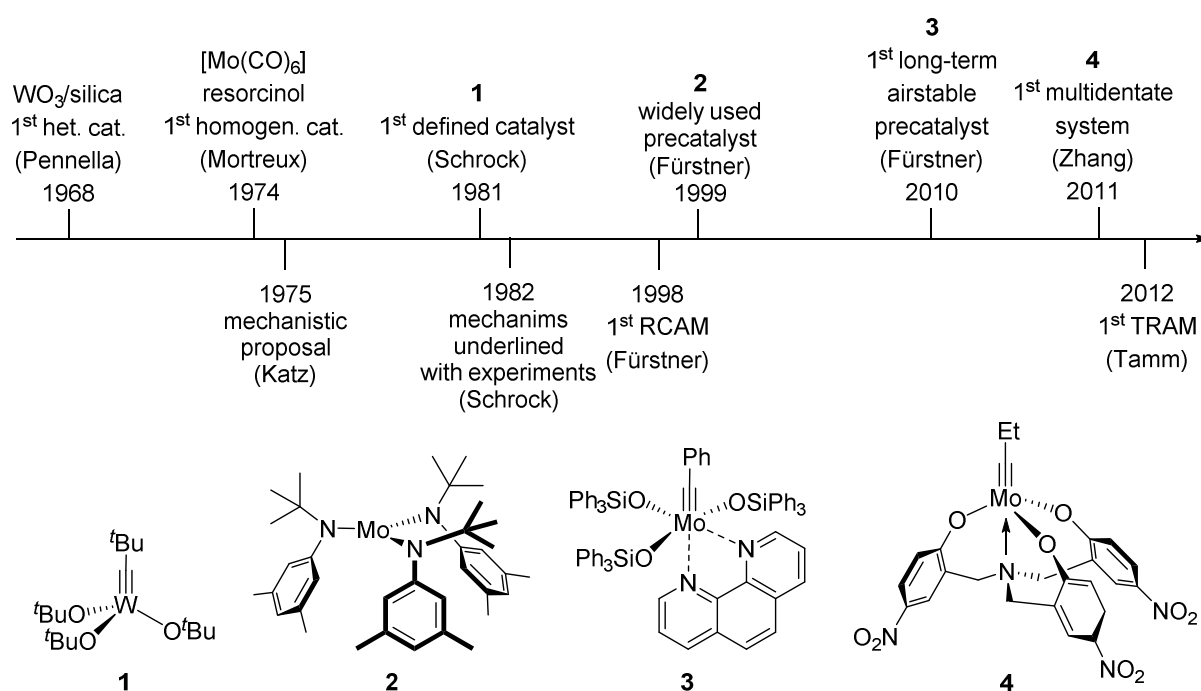
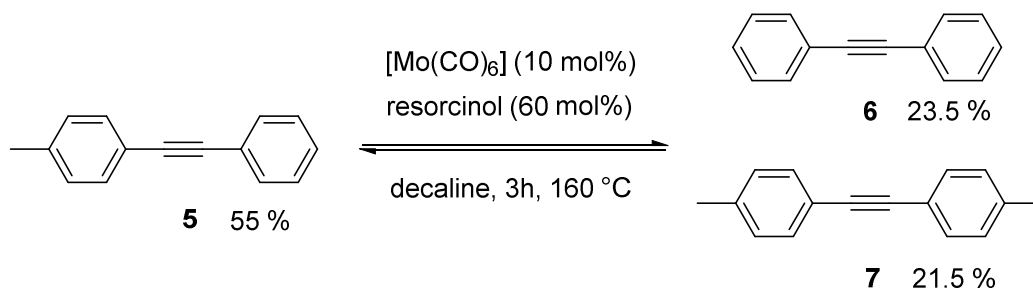


Figure 1.1: Milestones in alkyne metathesis research.^[10-11]

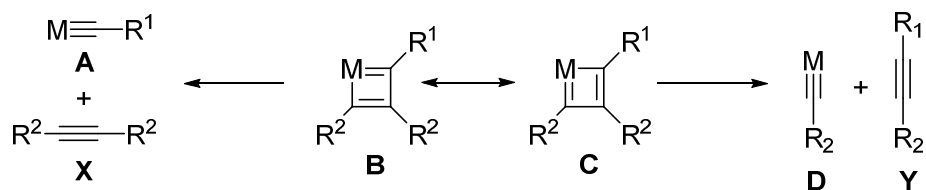
The first homogeneous catalyst for alkyne metathesis was developed by Mortreux and Blanchard.^[11a] Their work could show that heating a mixture of $[Mo(CO)_6]$ and resorcinol to 160 °C allowed the metathesis of methyltolane **5** to toluene **6** and dimethyltolane **7** to

proceed (Scheme 1.1). However, high reaction temperatures and limited functional group tolerance led to only a few applications.^[1]



Scheme 1.1: The first example for an alkyne metathesis with a homogeneous catalyst.

Later, considerable efforts have been placed in the synthesis of new alkyne metathesis catalysts as shown in Figure 1. The mechanism for alkyne metathesis was proposed by Katz and is related to the catalytic cycle proposed by Chauvin for olefin metathesis (Scheme 1.2).^[1, 11b] The alkylidyne **A** is reacting with the alkyne **X** in a formal [2+2]-cycloaddition to form a metallacyclobutadiene **B**, for which a second resonance structure **C** can be drawn. After cycloreversion, an alkyne **Y** and a new active alkylidyne **D** are formed, which eventually closes the catalytic cycle.



Scheme 1.2: Mechanism of alkyne metathesis reaction.

A couple of years later this mechanistic proposal could be substantiated by experimental results.^[11c] Schrock and coworkers managed to isolate metallacyclobutadiene species such as **8** and characterized them via NMR and X-ray analysis (Figure 1.2).^[11d, 12] They showed that metallacyclobutadienes **8** are catalytically active species, thereby proving that they play a role in the catalytic cycle of alkyne metathesis.

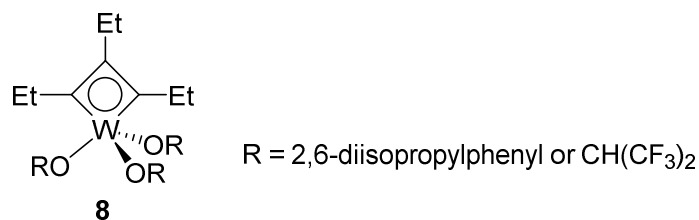
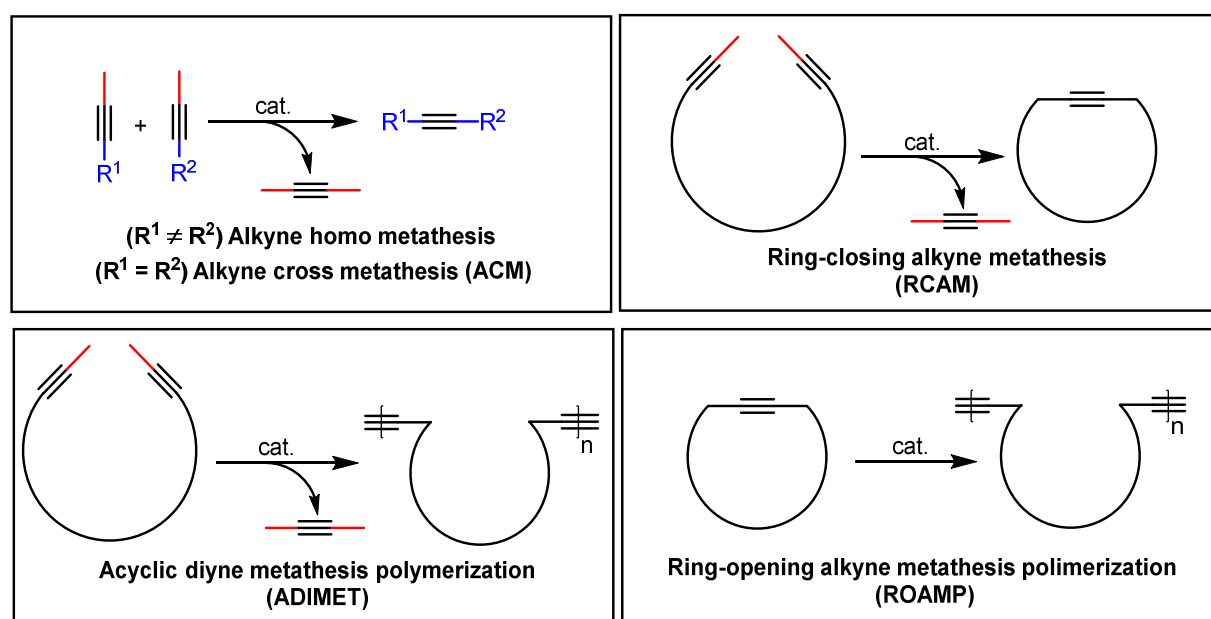


Figure 1.2: Metallacyclobutadiene complexes **8**, intermediates in alkyne metathesis reactions.

1.2 Applications of Alkyne Metathesis

In recent years considerable progress was made in catalyst development, leading to a variety of applications.^[1] Alkyne metathesis reactions can be assigned to four different classes (Scheme 1.3).^[9d] There are alkyne cross metathesis (ACM) reactions, in which two alkynes ($R^1 \neq R^2$) react with each other to furnish the cross metathesis product and a side product e.g. butyne. In a ring closing alkyne metathesis (RCAM) reaction a diyne is closed to furnish cyclic alkynes.



Scheme 1.3: Different reaction patterns of alkyne metathesis.^[13]

Furthermore there are two types of polymerization reactions, namely acyclic diyne metathesis polymerization (ADIMET) in which a diyne is polymerized under liberation of butyne, and ring-opening alkyne metathesis polymerization (ROAMP) where a cyclic alkyne is opened to generate polymeric structures.

Many interesting products arise from these reactions (Figure 1.3), for example carbazole-based macrocycle **9**, which can be generated through cyclic alkyne oligomerization with high selectivity.^[11g, 14] Its rigid, planar and conjugated backbone is an interesting structural motif to generate nanomaterials with internal channels that could find application in optoelectronic devices.^[9c]

Prostaglandin derivative **10** is an example for the application of an ACM reaction.^[15] ACM is especially successful when the coupling partners have different steric and/or electronic

properties to avoid a statistical product distribution.^[1] Furthermore, an effective ACM reaction of terminal alkynes with propynyl(trimethyl)silane was recently reported.^[16]

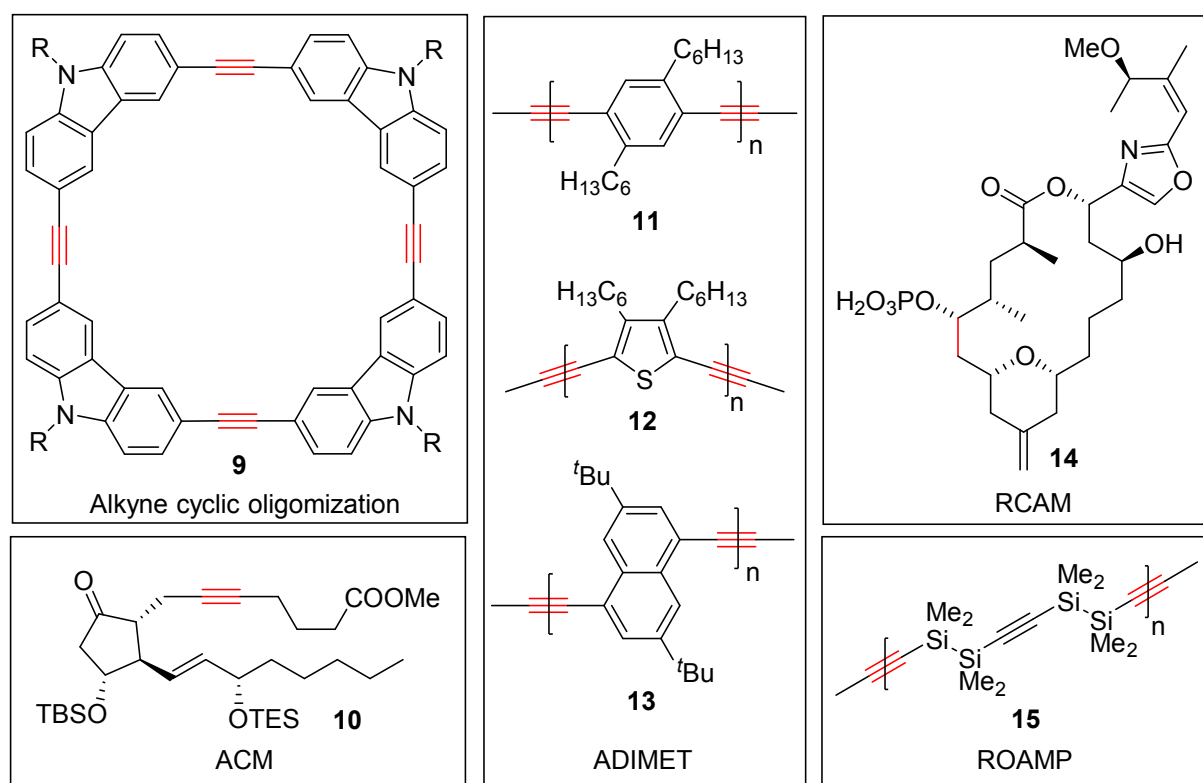


Figure 1.3: Examples for molecules generated with different alkyne metathesis approaches. The C-C bonds that were formed through the metathesis reaction are highlighted in red.

Poly(arylene-ethynylene)s (PAEs) **11-13** are attractive polymers, which can be generated via ADIMET in high molecular weights without diyne defects in the backbone that often pose a problem when accessing PAEs through Pd/Cu-catalyzed couplings.^[9c] PAEs are highly interesting for material science since they exhibit interesting electronic and optical properties.^[17]

RCAM has been applied in many natural product syntheses since the alkyne is a versatile structural motif for further functionalization as shown, for example, in the case of the total synthesis of Enigmazole A **14**.^[18] Furthermore, the first ring closing metathesis of terminal diynes (TRAM) was described recently.^[11i]

Disilane polymer **15**, which shows interesting optical properties and becomes conducting upon treatment with SbF_5 , is generated from a cyclodiyne through ROAMP.^[9c, 19] However,

there are only few application for ROAMP^[19-20] probably due to the lack of suitable substrates.^[9c]

The applications illustrated above show the variety of research fields that can benefit from alkyne methesis reactions, ranging from material science and supramolecular chemistry to the total synthesis of natural products aiming at the identification of drug candidates. A description of the catalysts utilized to synthesize most of the molecules displayed above is found in chapters 3 and 4.

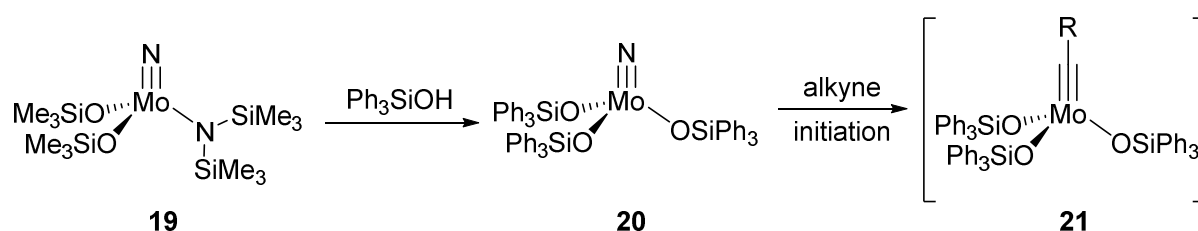
2 Alkyne Metathesis Catalysts Based on Siloxy Ligands

2.1 Introduction

2.1.1 Molybdenum Nitrido Complexes with Siloxy Ligands

In recent years remarkable progress was achieved leading to highly active, user friendly alkyne metathesis catalysts that bear a broad tolerance towards functional groups. This development has produced air-stable alkyne metathesis precatalysts that can be stored on the bench for several years and easily be activated *in situ*.^[11g, 21]

At the beginning of this development stood nitrido complex **19**, which was treated with different alcohols, phenols or silanols to generate precatalysts like **20** *in situ* (Scheme 2.1). Nitrido complex **20** is converted to the active alkylidyne **21** by reacting with alkynes.^[21] In this way, triphenylsilanol was found to be the ligand of choice since it is commercially available and offered highly active catalysts.^[21]



Scheme 2.1: Generation of the active alkylidyne **21** from nitrido precatalysts **19**.

The nitrido precatalysts **20** could be stabilized by pyridine^[21], which led to adduct **22** that can be handled in air (Figure 2.1). Pyridine adduct **22** is activated by heating to 80 °C in the reaction mixture. Basically unlimited stability was achieved by stabilizing the complex with 1,10-phenanthroline **23**.^[11g] In this case, the active species can be generated by treatment with MnCl₂.

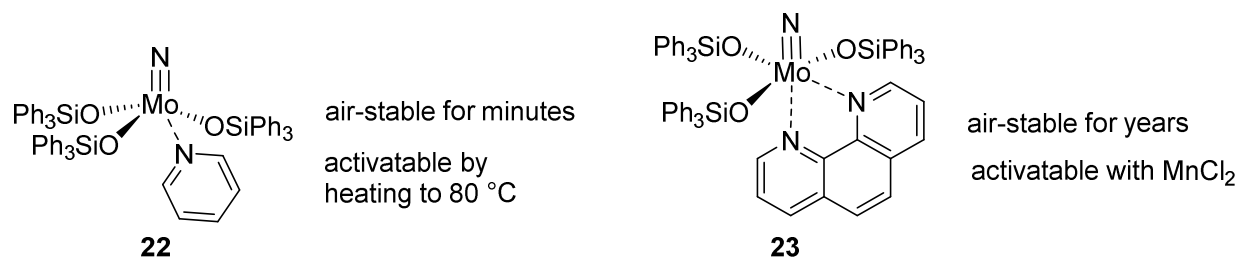
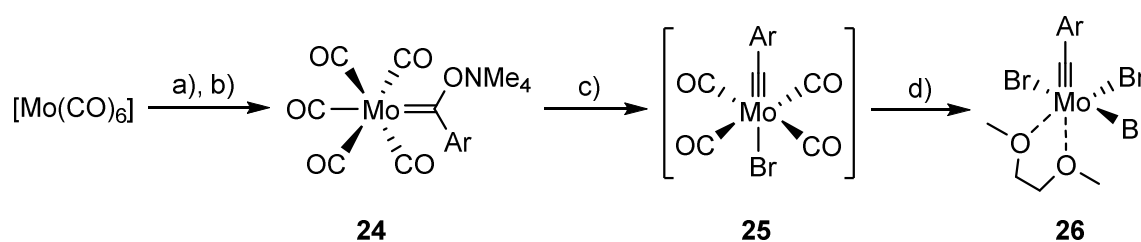


Figure 2.1: Stabilized forms of nitrido complex **20**.

The potential of these catalysts was proven in several natural product syntheses. The pyridine adduct **22** was successfully applied in the synthesis of (–)-Nakadomarin A^[22] and Cruentaren A^[23]. Mixtures of nitrido complex **19** and triphenylsilanol were used in the syntheses of Cruentaren A^[24] and (±)-Halicionacyclamine C^[25]. However, the development soon moved on to molybdenum alkylidyne complexes, since only a small portion of the nitrido complex **20** is reacting to the actual catalyst, alkylidyne **21**, indicating that already small amounts of the alkylidyne **21** are highly active.^[1]

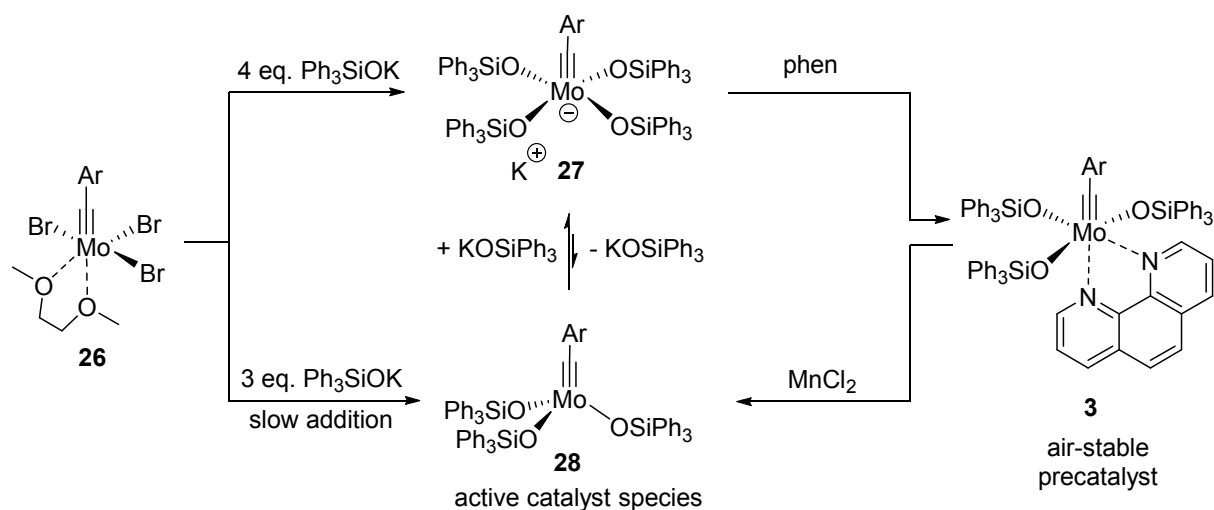
2.1.2 Molybdenum Alkylidyne Complexes with Siloxy Ligands

In order to get hold of the supposedly highly active alkylidyne, tribromo alkylidyne complex **26**, which is accessible through a scaleable and efficient synthesis from molybdenum hexacarbonyl via the Fischer-Carbene **24** and the Schrock-Alkylidyne **25**, was used as the starting compound (Scheme 2.2).^[26]



Scheme 2.2: Gram scale synthesis of catalyst precursor **26**. Conditions: a) ArLi, Et₂O, rt; b) Me₄NBr, H₂O, rt; c) oxalyl bromide, CH₂Cl₂, –78 °C to –20 °C; d) Br₂, DME, CH₂Cl₂, –78 °C to rt.

When using KOSiPh₃ as the ligand source, tribromo alkylidyne complex **26** was selectively transferred to the ate-complex **27** by using 4 equiv of the silanolate (Scheme 2.3).^[26a] With 3 equiv of KOSiPh₃ the neutral complex **28** could be selectively generated. In solution, the ate-complex **27** is in equilibrium with small amounts of the neutral complex **28**, which is actually the active species. Both compounds are highly active, but not stable in air. By adding 1,10-phenanthroline to the ate complex **27**, an air stable, easy to handle precatalyst **3** could be isolated on gram scale. Precatalyst **3** can be activated similarly to the nitro complex **23** by the addition of MnCl₂ or ZnCl₂.



Scheme 2.3: Synthesis of modern alkyne metathesis catalysts based on siloxy ligands.

Catalyst **28** and congeners tolerate a broad variety of functional groups such as esters, ethers, nitriles, pyridines, thiophenes and in some cases also protic groups.^[1, 6, 11g, 26a] To demonstrate the potential of those new catalysts, the ate-complex **27** was successfully applied in several total syntheses in our group, such as Tularin C^[27], (*R,Z*)-5-Muscenone^[28], 5,6-Dihydrocineromycin B^[29], Enigmazole A^[18], Hybridalactone^[30] and Ecklonialactones A, B, and C^[30]. The neutral complex **28** was successfully applied in the syntheses of Brefeldin A^[31], Mandelalide A^[32] and the formal total synthesis of Kendomycin^[33].

2.2 Aims and Scope

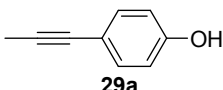
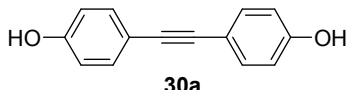
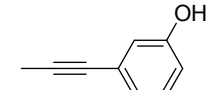
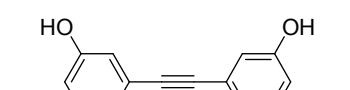
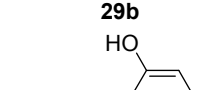
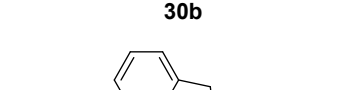
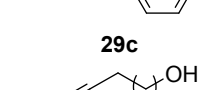
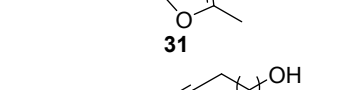

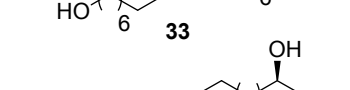
As discussed before, metathesis catalyst **28** tolerates a variety of functional groups. However, the functional group tolerance was not comprehensively tested, leaving out some synthetically interesting structural motifs such as secondary or tertiary amines, azides, primary alkyl halides, indoles, sulfoxides, sulfonamides among others. Therefore we sought to perform an extensive substrate scope screen for catalyst **28** to determine the limits of substrate tolerance. Furthermore, we set out to investigate the compatibility of free hydroxy groups, either aromatic or aliphatic, with alkyne metathesis.

2.3 Extended Substrate Scope of [Mo(≡CC₆H₄OMe)(OSiPh₃)₃]

2.3.1 Homo Metathesis Reactions

The syntheses of the investigated substrates are described in the experimental section (Chapter 7.2.2). The reactions were first carried out with a catalyst loading of 2 mol% at room temperature and the progress was monitored by TLC or GCMS. Catalyst loading, temperature and time were individually modified to achieve best results. Only the highest yielding conditions are displayed in the Table 2.1.

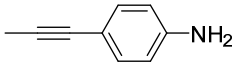
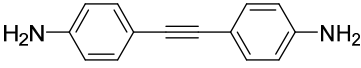
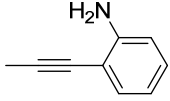
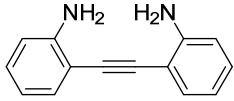
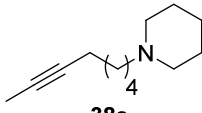
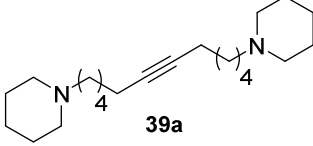
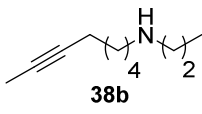
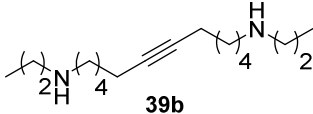
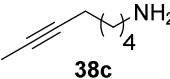

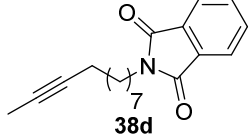

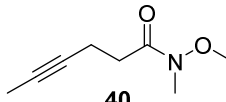
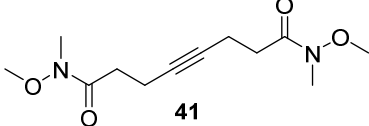
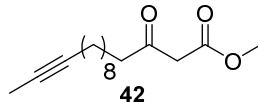
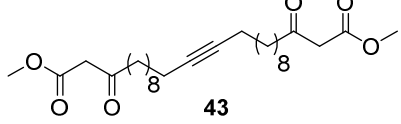
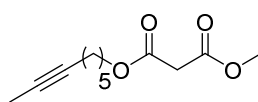
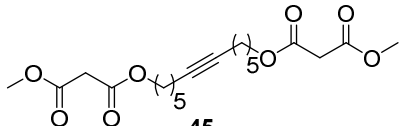
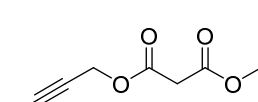
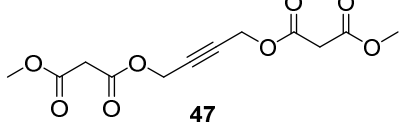
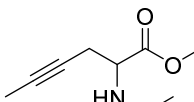
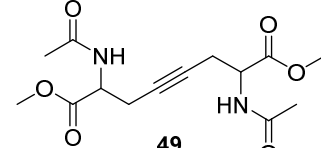
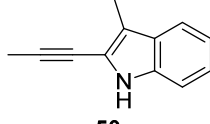
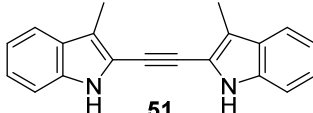
Table 2.1: Intermolecular metathesis reaction with [Mo(≡CC₆H₄OMe)(OSiPh₃)₃] (**28**) of alkynes of the general type RC≡CMe.

entry	substrate	product	temp. [°C]	28 [%]	time [h]	yield [%]
1			80	3	3	87
2			80	5	7	93
3			80	5	48	- ^a
4			120	5	14	- ^b
5			80	7	24	66

a) No dimerization product was observed, only starting material and cyclization product **31**

b) Only starting material recovered

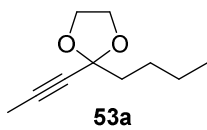
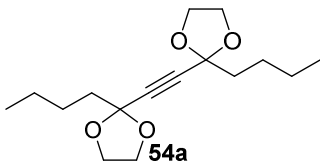
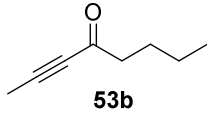
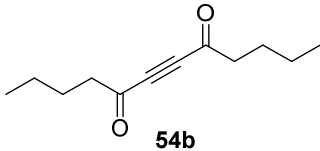
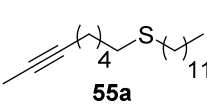
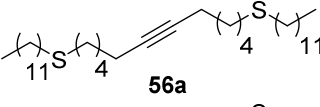
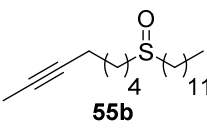
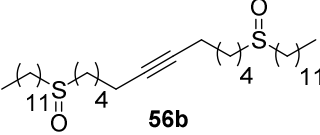
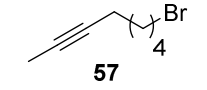
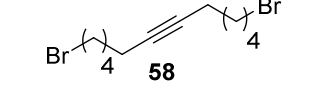
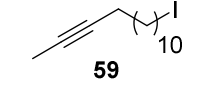
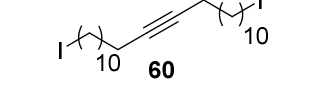
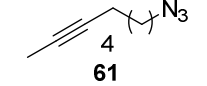

2 Alkyne Metathesis Catalysts Based on Siloxy Ligands

entry	substrate	product	temp. [°C]	28 [%]	time [h]	yield [%]
6	 36a	 37a	80	4	13	52
7	 36b	 37b	80	5	36	- ^a
8	 38a	 39a	rt	4	1	81
9	 38b	 39b	rt	3	16	77
10	 38c	 39c	120	5	5	- ^a
11	 38d	 39d	rt	4	1	92
12	 40	 41	80	6	40	66
13	 42	 43	80	14	20	72
14	 44	 45	80	2	4	94
15	 46	 47	80	2	48	- ^b
16	 48	 49	rt	6	1	89
17	 50	 51	rt	5	1	88

a) Starting material and decomposition

b) Only starting material recovered

2 Alkyne Metathesis Catalysts Based on Siloxy Ligands

entry	substrate	product	temp. [°C]	28 [%]	time [h]	yield [%]
18	 53a	 54a	rt	5	5	73
19	 53b	 54b	120	5	16	- ^a
20	 55a	 56a	rt	2	2	88
21	 55b	 56b	80	5	16	75
22	 57	 58	rt	1	1.5	91
23	 59	 60	rt	5	1.5	78
24	 61	 62	rt	1	15	85

a) Only starting material recovered

The investigations showed significant reactivity differences depending on the chemical surrounding of the hydroxy groups. In general, elevated temperatures were necessary to effectively convert substrates containing free hydroxy groups. Substrates **29a** and **29b** with phenolic –OH groups in the *para*- or *meta*-position respectively were tolerated (Table 2.1, Entry 1-2) while substrate **29c** with a hydroxy group in the *ortho*-position only led to benzofuran **31** (Table 2.1, Entry 3). Secondary alcohol **34** is still moderately well tolerated, while primary alcohol **32** deactivates the catalyst (Table 2.1, Entry 4-5). Furthermore, substrates with free hydroxy groups in propargylic or homopropargylic position did not undergo homo metathesis reaction at all.

For amines we observed similar trends. *Para*-substituted aniline **36a** did not lead to full conversion, therefore only moderate yields were observed, while *ortho* substituted aniline **36b** did not react at all (Table 2.1, Entry 6-7). The tertiary amine **38a** posed no problem,

while secondary amine **38b** needed prolonged reaction time, and the primary amine **38c** was not tolerated at all. When the primary amine **38c** was protected as a phthalimide **38d**, the metathesis reaction proceeded successfully (Table 2.1, Entry 8-11). This indicates that more sterically hindered amines are tolerated, while unhindered primary amines deactivate the catalyst.

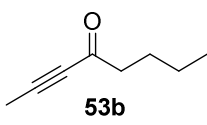
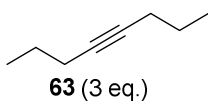
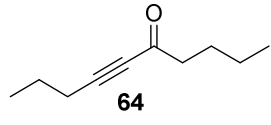
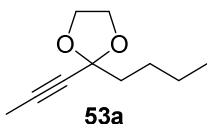
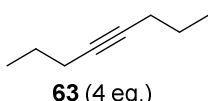
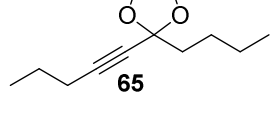
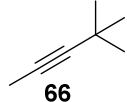
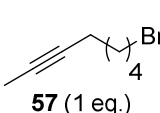
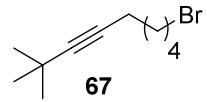
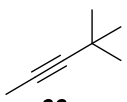
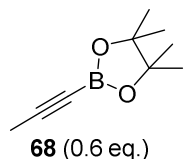
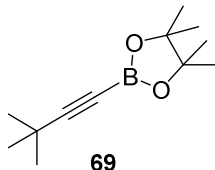
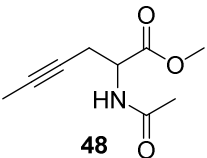
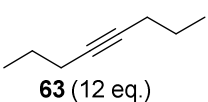
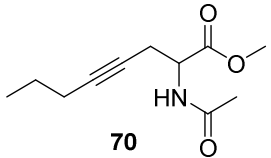
Highly coordinating Weinreb amide **40** needed a higher catalyst loading, an increased temperature and prolonged reaction time, and could only be metathesized in moderate yield due to incomplete conversion (Table 2.1, Entry 12). Furthermore, we compared a row of α -acidic compounds. While malonate **44** reacted smoothly, acetoacetate **42** needed a higher catalyst loading (Table 2.1, Entry 13-14). For substrate **46**, where the malonate is in propargylic position, no reaction was observed (Table 2.1, Entry 15). Amino acid derivative **48** and indole **50** could be effectively metathesized (Table 2.1, Entry 16-17).

A ketone next to the alkyne **53b** did not undergo a homo metathesis reaction, probably due to the electron poor character of the alkyne. Surprisingly the sterically demanding acetal derivative **53a** was metathesized efficiently (Table 2.1, Entry 18-19). Thioether **55a** was also accepted, while sulfoxide **55b** needed a higher temperature, as well as an increased catalyst loading and a longer reaction time, probably due to its coordinating character (Table 2.1, Entry 20-21). Bromide **57**, iodide **59** and azide **61** were tolerated without problems in homo metathesis reactions (Table 2.1, Entry 22-24).

2.3.2 ACM Reactions

Substrates **53b**, **66**, and **68** did not undergo homo metathesis in any of the attempted reaction conditions. However, this lack of reactivity does not allow for the evaluation of the substrates' capacity to undergo alkyne metathesis. Therefore we submitted these substrates to cross metathesis reactions with highly reactive alkynes such as 4-octyne (**63**) or bromo alkyne **57** in order to determine their ability to participate alkyne metathesis.

Table 2.2: Cross metathesis reactions with $[\text{Mo}(\equiv\text{CC}_6\text{H}_4\text{OMe})(\text{OSiPh}_3)_3]$ **28**.

entry	substrates	product	temp. [°C]	28 [%]	time [h]	yield [%]	
1	 53b	 63 (3 eq.)	 64	120	5	16	75 ^a
2	 53a	 63 (4 eq.)	 65	rt	5	0.5	74
3	 66	 57 (1 eq.)	 67	rt	5	1.5	53
4	 66	 68 (0.6 eq.)	 69	60	2	84	37
5	 48	 63 (12 eq.)	 70	rt	5	1	80

a) MnCl_2 (20 mol%) was added.

Since alkyne **53b** with a ketone in propargylic position did not undergo homo metathesis, we tried an ACM reaction with 4-octyne (**63**). Elevated temperatures and the addition of MnCl_2 , which probably coordinates to the ketone and therefore avoids its coordination to the molybdenum catalyst, were needed in order to allow the reaction to proceed (Table 2.2, Entry 1). Acetal derivative **53a** reacted smoothly with 4-octyne (**63**) (Table 2.2, Entry 2), in analogy to the homo metathesis results (Table 2.1, Entry 18). Neoheptyne **66**, which did not undergo homo metathesis due to sterical hindrance, could be coupled to bromo alkyne **57**. Coupling of neoheptyne **66** to the borane **68** was possible even though the yield was low due

to isolation problems (Table 2.2, Entry 3-4). We further examined amino acid derivative **48** which gave the desired cross metathesis product **70** when a high excess of 4-octyne (**63**) was used (Table 2.2, Entry 5). It is also noteworthy that a strict control of the reaction time was necessary in this case, since the homo coupling product of amino acid derivative **48** accumulated during the reaction.

2.4 Conclusion

In conclusion, catalyst **28** tolerates substrates with challenging structural motifs such as secondary or tertiary amines, an azide, primary alkyl halides, an indole, a thioether, a sulfoxide, or a sulfonamide. However, substrates with protic groups are not generally tolerable under reaction condition. While certain substrates with protic functionalities like phenols in *para*- or *meta*-position to the alkyne or a secondary alcohol could be successfully homo metathesized, a compound containing a primary alcohol failed to give the desired homo metathesis product. We hypothesize that protic substrates outcompete the Ph₃SiO-groups for the metal center thus forming an unreactive metal species incapable of catalysis. Furthermore, substrates with highly coordinating groups such as Weinreb amides or free primary amines may deactivate the catalyst by blocking the coordination site that is needed for the reaction. Sterically demanding substrates like neoheptyne **66** were found to be incompetent for homo metathesis reaction but capable of ACM reactions with sterically less demanding substrates.

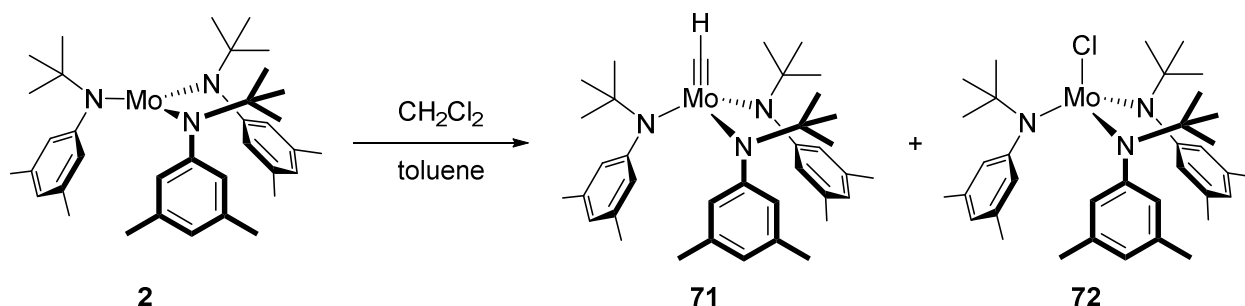
3 Alkyne Metathesis Catalysts Based on Multidentate Ligands

3.1 Introduction

Having demonstrated that substrates with protic groups can hinder alkyne metathesis (Chapter 2), we hypothesized that rendering the ligands more stable towards replacement by these substrates would improve the reactivity of the catalysts. In order to achieve these ends, multidentate ligands and their chelating effect will be discussed in this chapter.

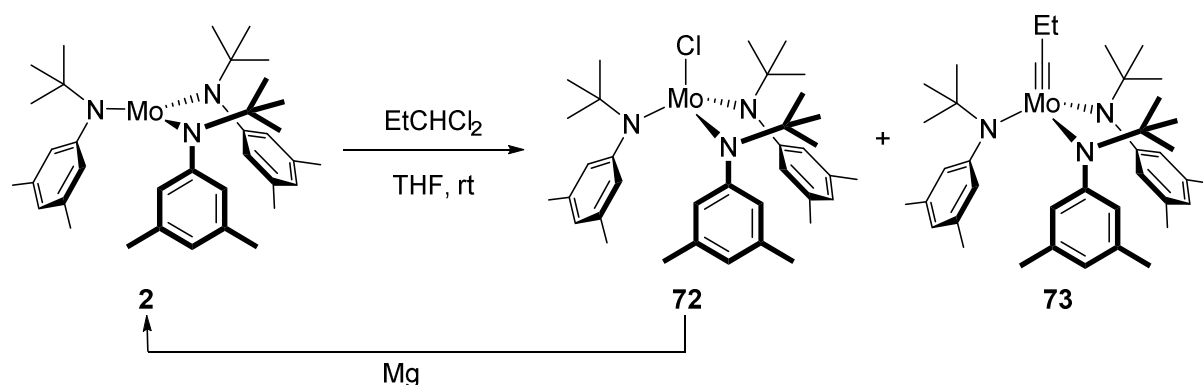
3.1.1 Early Molybdenum-Based Alkyne Metathesis Catalysts

The molybdenum-based alkyne metathesis precatalyst **72** can be generated from a molybdenum(III) species **2**, which was originally introduced for molecular nitrogen splitting by Cummins.^[34] Upon treatment with CH_2Cl_2 in toluene, **2** reacts to chlorocomplex **71** and methylidyne complex **72** (Scheme 3.1).^[1, 11f, 35] The catalytically active species has demonstrated good functional group tolerance as evident from its employment in the syntheses of natural products Latrunculin A, B, C, S^[36], Myxovirescin A₁^[37], Cruentaren A^[38], Amphidinolide V^[39], and Leiodermatolide^[40].



Scheme 3.1: Activation of Cummin's catalyst with CH_2Cl_2 .

Moore later showed that molybdenum(III) species **2** reacts with 1,1-dichloropropane to give the propylidyne complex **73** (Scheme 3.2).^[41] The undesired chlorocomplex **72** can be selectively reduced to the starting molybdenum(III) species with magnesium while propylidyne complex **73** stays unaffected. The synthesis can be done on a gram scale.^[42]

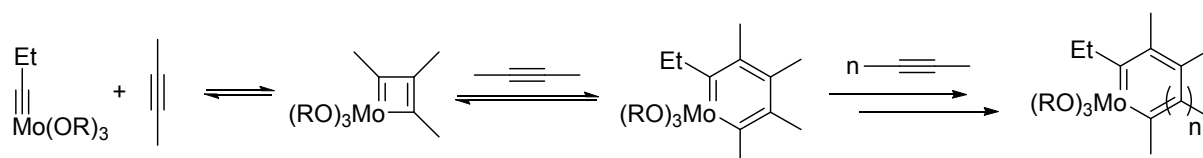


Scheme 3.2: Reductive recycle approach to molybdenum(VI) alkyldiyne complex **73**.

The main drawback of this catalyst is that molybdenum(III) species such as **2** are highly sensitive to hydrolysis or oxidation and even react with N_2 , which leads to preparative difficulties.^[1] Nevertheless, molybdenum alkyldiyne **73** has found several applications in synthesis as a precatalyst, which can generate highly active catalysts *in situ* by treatment with three equivalents of phenols (in particular *p*-nitrophenol).^[14a, 41, 43] Additionally, alkyldiyne **73** can be immobilized on silica to yield highly active heterogeneous metathesis catalysts.^[44]

3.1.2 Alkyne Metathesis Catalysts with Multidentate Ligands

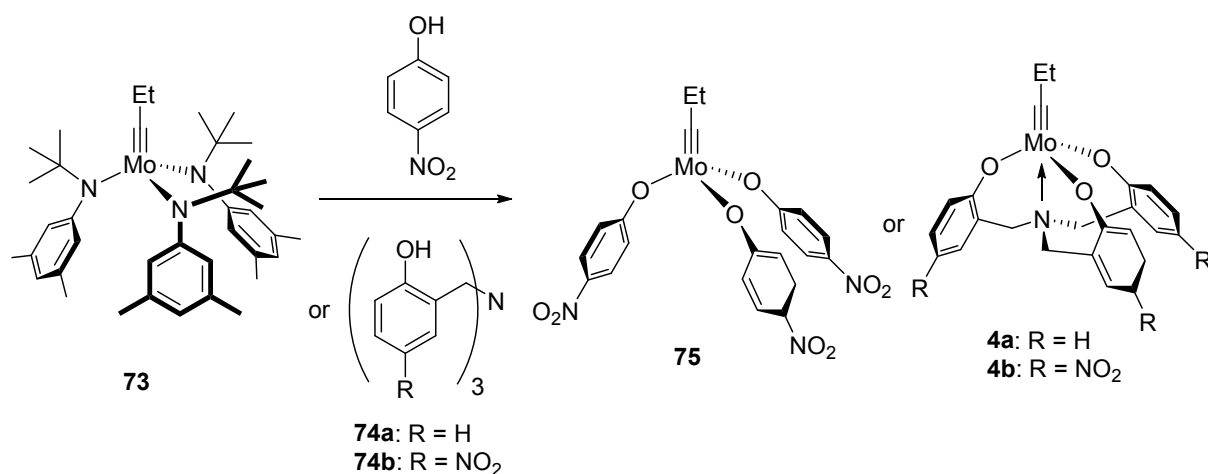
Studies by Moore and coworkers have shown that sterically undemanding ligands such as *p*-nitrophenol can lead to the polymerization of small substrates like 2-butyne.^[2] This happens by a ring expansion mechanism through a repeated insertion of the alkyne substrates into the Mo-C bond (Scheme 3.3).



Scheme 3.3: Ring expansion side reaction deactivating metathesis catalysts.

Furthermore, alkyne metathesis catalysts based on monodentate phenol ligands show stability issues which are limiting their spectrum of applications. To address these problems, Zhang investigated the use of multidentate phenol ligands.^[11h] Their chelating effect should increase the stability and lifetime of the catalyst and the linker could block the free coordinating site on the metal to prevent polymerization as well as non-productive substrate binding.^[45]

Zhang's catalysts **4a** and **4b** are generated *in situ* from molybdenum propylidyne **73** with the trisubstituted amine ligands **74a** and **74b** respectively (Scheme 3.4).



Scheme 3.4: Phenol-based, *in situ* generated metathesis catalysts.

4a was unable to promote the metathesis reaction of 4-propyneanisole even at elevated temperatures (70 °C). In sharp contrast, **4b** proved reactive and showed a significant improvement of catalytic activity, lifetime and substrate scope compared to the monodentate analogue **75**.^[45] The Lewis acidity of the molybdenum center is highly reduced by the donating effect of the nitrogen linker and the nitro groups in **4b** are needed to render the phenol more electron deficient.^[46] It had already been shown before, that lower electron density on the molybdenum center improves the catalytic activity.^[47]

To address this problem Zhang's group designed catalysts **76a-c** based on tri(arylmethyl)-ammonium ligands with a non-coordinating quaternary nitrogen linkers (Figure 3.1).^[45] The introduction of a quaternary nitrogen linker increased the electrophilicity of the molybdenum center in catalysts **76a-c** as compared to catalyst **4b**. This increase in electrophilicity resulted in the improved catalytic activity of catalysts **76a-c** when compared to **4b**. Furthermore, no alkyne polymerization side reactions were observed when catalysts **76a-c** were used. However, the ionic character of the ligand led to solubility issues in organic solvents.^[46] They also studied the electronic effects on metathesis activity by varying the substitution pattern of the phenol using 4-nitropropynylbenzene as test substrate. While catalyst **76a** showed a low conversion of 43%, catalysts **76b** and **76c** enabled conversions of 61% and 64% respectively, which demonstrates the importance of electrophilicity at the metal center.^[45]

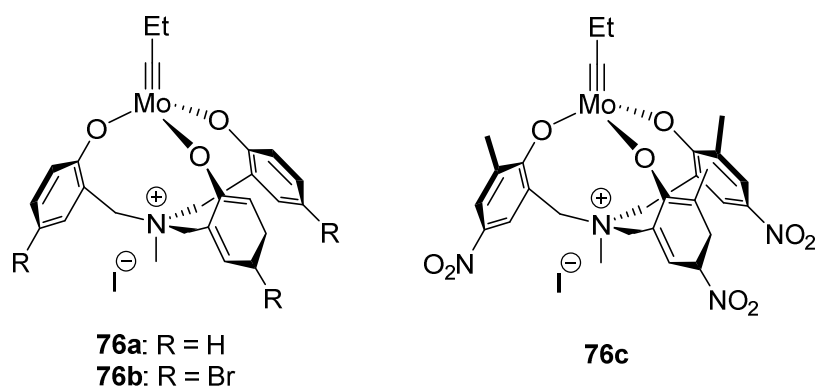
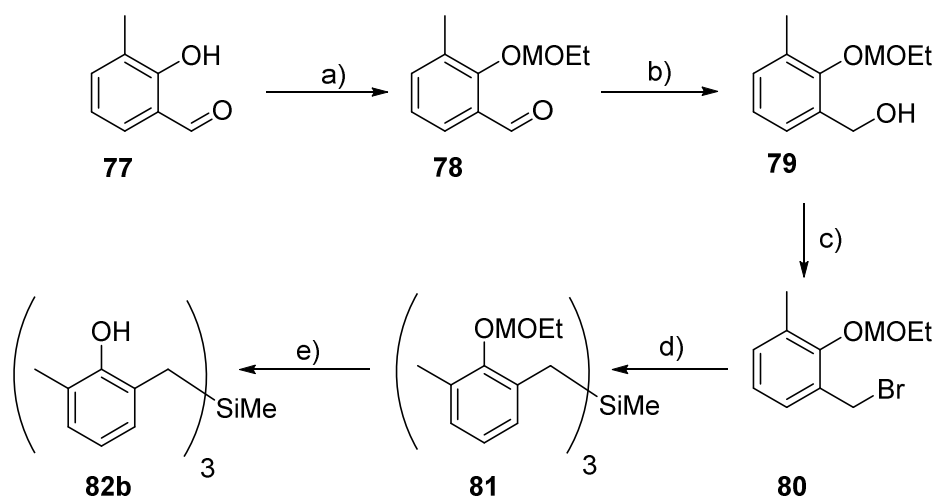


Figure 3.1: *In situ* generated metathesis catalysts **76a-c** based on quaternary-nitrogen-linked ligands.

Zhang further continued this project and designed ligands such as triphenol **82b** with a silicon linker in order to avoid the previously mentioned problems caused by tertiary or quaternary nitrogen linkers.^[46] The access to ligand **82b** is achieved through a five step synthesis from commercially available aldehyde **77** (Scheme 3.5). Aldehyde **77** is converted through ethoxymethyl protection and subsequent reduction to alcohol **79**. Alcohol **79** is brominated with NBS to bromide **80** that is metallated and reacted with MeSiCl₃ to give, after deprotection of acetal **81**, the desired triphenolsilane-based ligand **82b**.



Scheme 3.5: Representative synthesis of multidentate triphenol silane ligand **82b**. Conditions: a) EtOMCl, DIPEA, DMAP, CH₂Cl₂, rt, 97%; b) NaBH₄, MeOH, 0 °C, quant.; c) NBS, PPh₃, CH₂Cl₂, rt, 77%; d) Mg, THF, rt, then MeSiCl₃, rt, 82%; e) PPTS, *i*-PrOH, 70 °C, 66%.

With ligand **82b** in hand, catalyst **83b** was generated *in situ* upon addition of alkylidyne complex **73** (Figure 3.2).^[46] Catalyst **83b** proved to be a highly reactive species allowing for the homo metathesis of challenging substrates such 3-(prop-1-yn-1-yl)phenol (**29b**). The

catalyst generated with ligand **82b** remained active in solution for days at room temperature.

The catalytic activities of *in situ* generated catalysts **83** were evaluated by using 4-nitropropynylbenzene as a test substrate. Catalyst **83a** gave an isolated yield of 54%, catalyst **83b** gave 58%, and catalyst **83c** furnished 54%, indicating that the ligands' sterics barely affects the catalysts' activity.

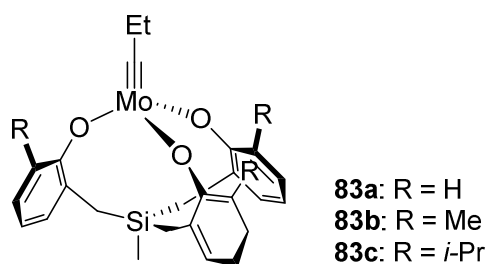


Figure 3.2: *In situ* generated triphenol silane catalysts **83a-c**.

Zhang could successfully apply his catalysts in a variety of applications like the synthesis of shape persistent porphyrin-based molecular cages^[48], interlocked organic cages^[49], ionic covalent organic frameworks with spiroborate linkage^[50] and highly porous poly(arylene-ethynylene) networks^[51]. A major drawback of these catalysts is that the reactions are carried out in the highly cancerogenic and expensive solvent tetrachloromethane which makes this system unattractive especially for RCAM where high dilutions are needed.^[46] Until now catalysts that are based on monodentate siloxy ligands are still superior concerning activity, synthesis and handling.^[11g, 26a] It seems promising to combine the concept of multidentate ligands with the superior electronic properties of siloxy ligands.

3.2 Aims and Scope

As described in chapter 2, the latest generation of alkyne metathesis catalysts based on siloxy ligands are powerful systems, being able to convert a broad variety of substrates. Nevertheless several applications showed that free hydroxy groups can deactivate the catalysts presumably through a ligand exchange which renders the catalyst inactive. In order to avoid this problem we decided to design more stable ligands which should improve the catalysts' performance. So far siloxy-based ligands proved to be superior to other ligand types due to their favorable electronic character. Therefore we decided to keep this structural motif but link the silanolates on a common backbone to generate multidentate ligands. The stability of the catalysts generated with these multidentate ligands should be higher due to their beneficial chelating effect.

3.3 Catalyst and Ligand Synthesis

3.3.1 Initial Considerations

We designed our first target ligands based on the ligand utilized in Zhang's catalyst **83a** (Figure 3.3). More precisely, we adopted the ligand-geometry in catalyst **83a** for the backbone of our ligand as represented in structure **E**. However, we chose to substitute the phenolates of catalyst **83a** with silanolates to arrive at alkyldiyne complexes such as **84**.

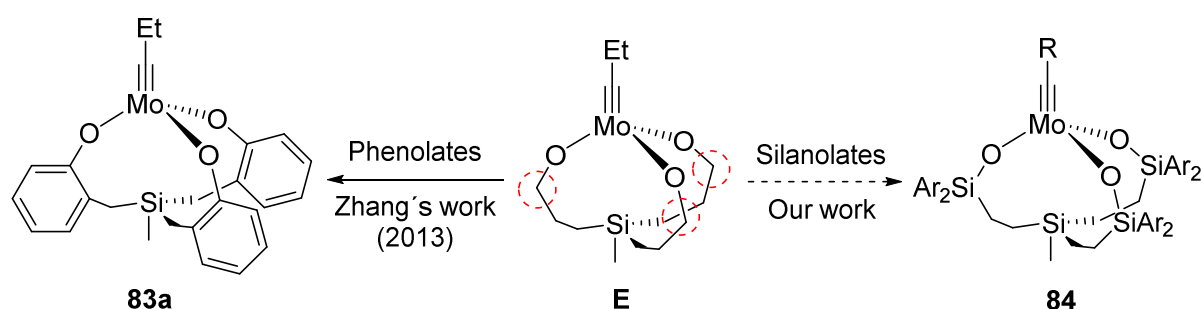
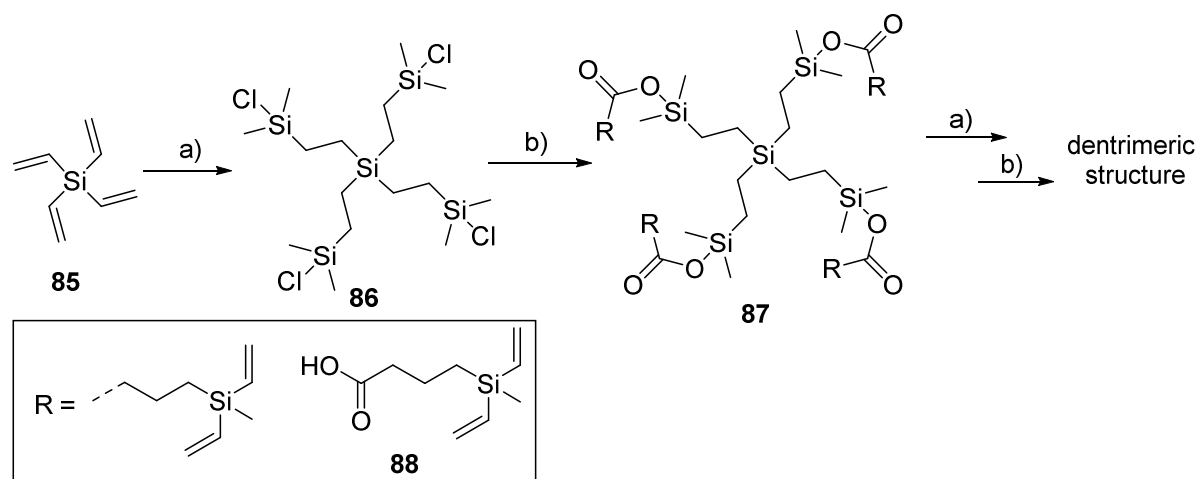


Figure 3.3: Design considerations for multidentate siloxy ligands.

An important point that needs to be kept in mind is the flexibility of the ligands. Ideally they should be flexible enough to provide an unhampered access to the molybdenum center even for bulky substrates, but on the other hand they must be rigid enough to allow the generation and isolation of a defined catalyst species.

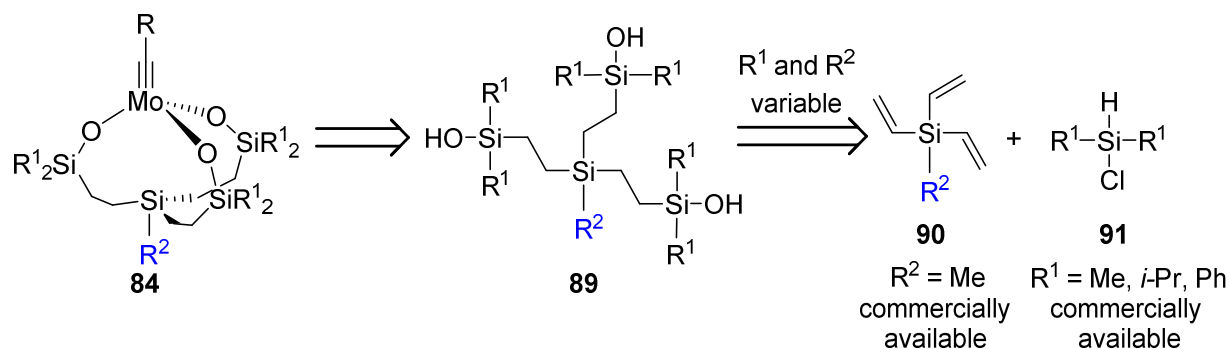
3.3.2 Multidentate Ligands with Silicon Linkers

Our first approach towards multidentate siloxy ligands was inspired by Kung, who synthesized dendrimeric structures through the hydrosilylation of tetravinylsilane (**85**) to chlorosilane **86**, which was converted to acyloxysilane **87** via esterification (Scheme 3.6).^[52] By repeating this procedure he successfully generated dendrimeric structures.



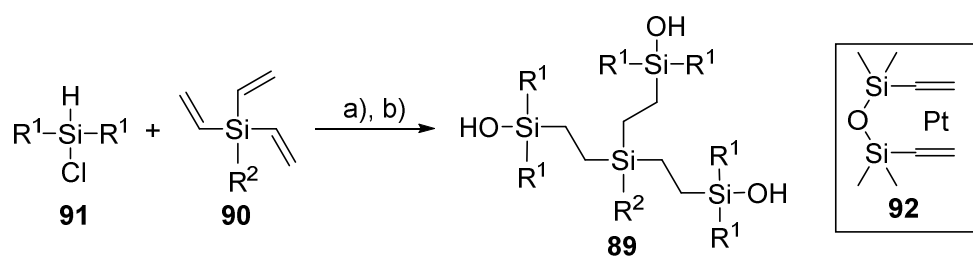
Scheme 3.6: Literature example for the generation of dendrimeric structures via hydrosilylation. Conditions: a) chlorodimethylsilane, Karstedt's cat., THF, reflux; b) pyridine, **88**, toluene, rt.

Inspired by these results, we planned the synthesis of our target ligands starting from trivinylsilanes **90**, which should be converted to silanols **89** through hydrosilylation with different commercially available chlorosilanes **91** and subsequent hydrolysis (Scheme 3.7). **89** could be reacted with a molybdenum alkylidyne precursor in order to generate metathesis catalysts **84**. The synthesis is designed in a way as to allow for an easy variation of R^1 and R^2 in order to investigate electronic and steric effects on catalyst formation, stability and reactivity.



Scheme 3.7: Synthetic approach to multidentate silanol ligands via hydrosilylation strategy.

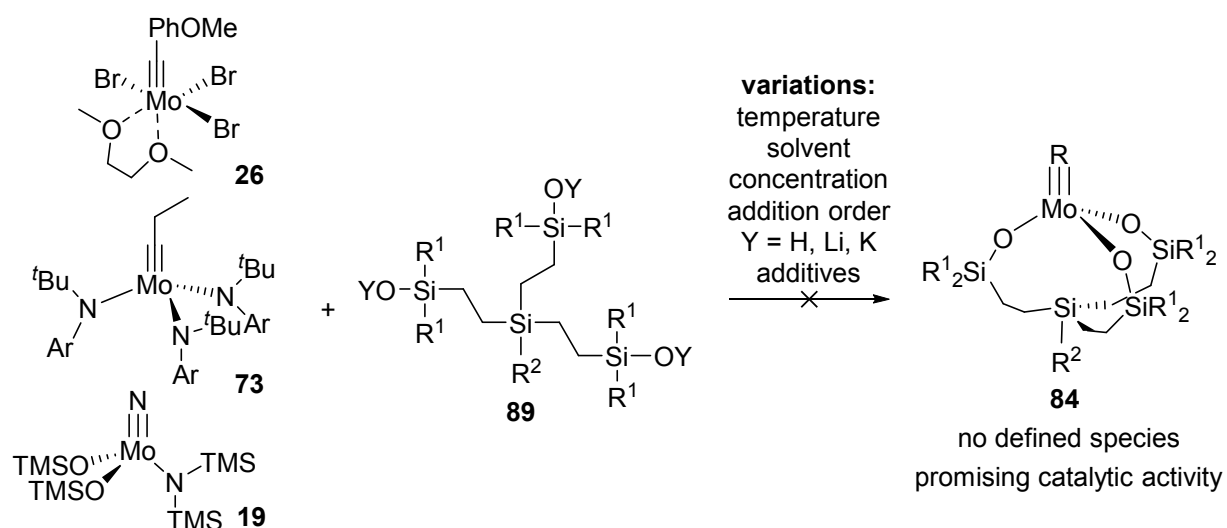
The synthesis of target silanols **89** from chlorosilanes **91** and trivinylsilanes **90** proceeded in moderate yield on gram scale using Karstedt's catalyst **92** for the hydrosilylation reactions (Scheme 3.8, Entry 1, 2, 4). We further tried to synthesize a methyl derivative **89c**, but our attempts only led to polymeric materials (Scheme 3.8, Entry 3). Mesityl derivative **89e**, which we planned to synthesize in order to examine the effect of a sterically demanding substituent R^2 was not accessible by this strategy due to incomplete hydrosilylation, probably caused by steric hindrance (Scheme 3.8, Entry 5).



entry	Product	R^1	R^2	yield [%]	scale [g]
1	89a	Ph	Me	56	2.4
2	89b	<i>i</i> Pr	Me	43	0.7
3	89c	Me	Me	-	-
4	89d	Ph	Ph	58	2.3
5	89e	Ph	Mes	-	-

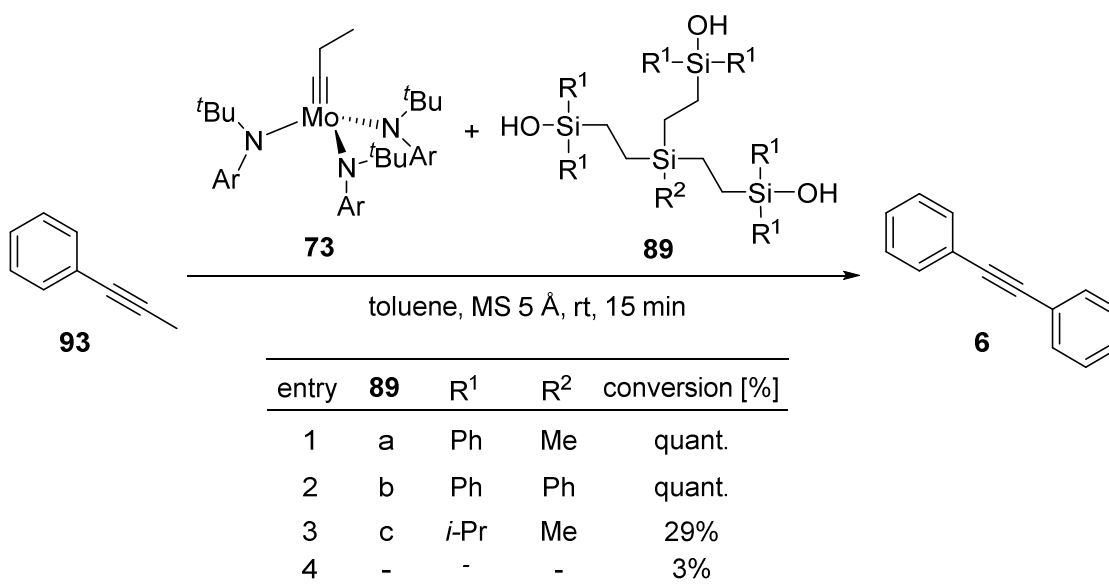
Scheme 3.8: Synthesis of multidentate ligands **89** with a silicon connecting unit. Conditions: a) Karstedt's cat. **92**, toluene, 50 °C to 70 °C; b) NEt_3 , H_2O , rt.

With these ligands in hand we tried to generate the proposed catalysts **84**. Despite considerable efforts we did not manage to isolate a defined catalyst species. All attempts to synthesize a monomeric species led to inseparable mixtures of compounds probably due to the sterically flexible character of our ligands (Scheme 3.9). We think that the ligands generate networks between molybdenum centers, leading to oligomeric or polymeric materials.



Scheme 3.9: Summary of different approaches to generate a defined catalyst species **84**.

In order to evaluate the new ligands we generated the catalysts *in situ* from molybdenum alkylidyne **73** and the corresponding ligands **89** in analogy to Zhang's methodology described in chapter 3.1.2. Phenylpropyne **93** was used as test substrate. The results showed that silanols with aromatic substituents R^1 lead to fast homodimerization reaction (Scheme 3.10, Entry 1, 2). In contrast, a silanol with aliphatic substituents R^1 resulted in low conversion (Scheme 3.10, Entry 3). The beneficial effect of ligands **89** was verified by a control experiment in which molybdenum precatalyst **73** was tested without the addition of silanol ligands, which led to a low conversion (Scheme 3.10, Entry 4).

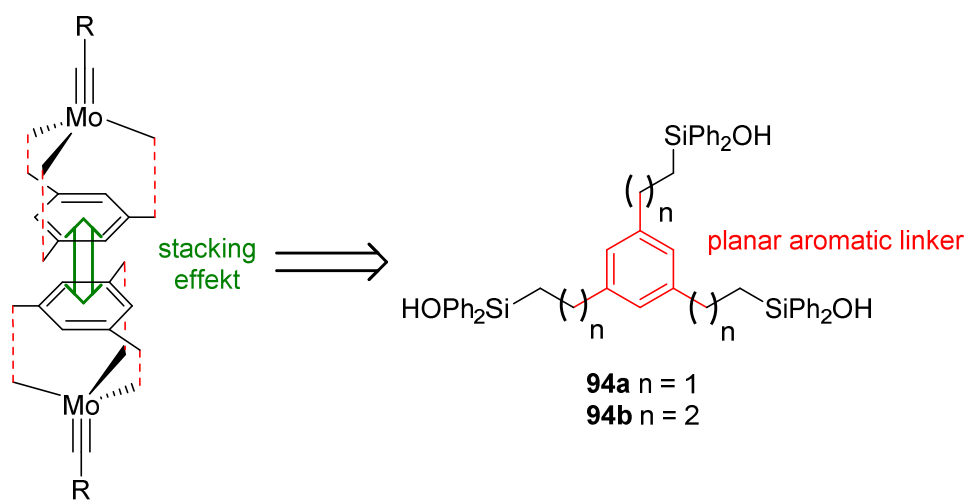


Scheme 3.10: Test reactions with *in situ* generated catalysts. Conditions: 5 mol% **73** and 5 mol% **89**.

The catalytic activity of the crude materials was highly promising and surpassed in some cases the results obtained with the previous catalyst generation **28** (Chapter 3.4, Tables 3.1, 3.2, 3.3). However, the ligands did not favor the formation of a defined catalyst species. Based on these findings we decided that the ligand design requires optimization. The new design should still contain the siloxy motif but a different ligand geometry needs to be found in order to get a defined catalyst species.

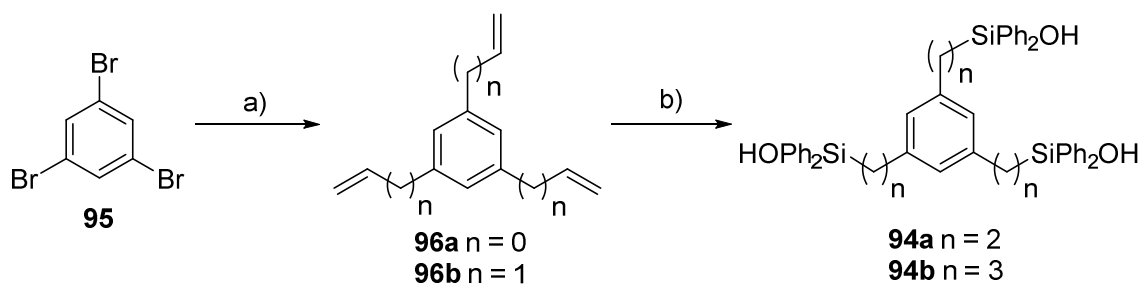
3.3.3 Multidentate Ligands with Trisubstituted Aromatic Linkers

To address the points mentioned above we planned to make use of π - π -interactions in order to generate a monomeric species. When using a trisubstituted aromatic linker unit, two of the ligands might undergo a stacking interaction and therefore lead to a preorientation of the sidechains, which should facilitate the generation of a defined species (Scheme 3.11). We decided to synthesize two ligands with different linker lengths: **94a** (two carbon atoms) and **94b** (three carbon atoms).



Scheme 3.11: Ligand design making use of stacking effects.

Their preparation started from commercial 1,3,5-tribromobenzene (**95**) which was converted to the corresponding trienes **96a** and **96b** by Stille coupling with vinyltributylstannane or allyltributylstannane, respectively (Scheme 3.12). Hydrosilylation of triolefins **96a** and **96b** followed by hydrolysis afforded triols **94a** and **94b**. The target ligands were synthesized over the two steps with an overall yield of 33% on a 150 mg scale for **94a** and with 36% on a 750 mg scale for **94b**.

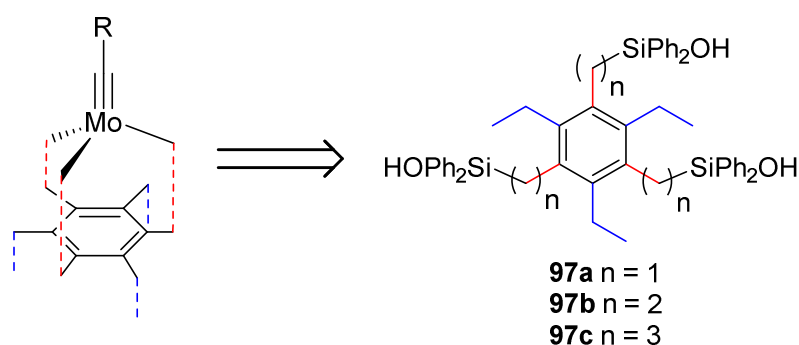


Scheme 3.12: Synthesis of multidentate ligand **94** with an aromatic connecting unit. Conditions: a) vinyltributylstannane, Pd(PPh₃)₄, DMF, 135 °C, 80% for **96a**; allyltributylstannane, Pd(PPh₃)₄, DMF, 120 °C, 76% for **96b**; b) Karstedt's cat., chlorodiphenylsilane, toluene, 70 °C; then NEt₃, H₂O, rt, 41% over 2 steps for **94a**; Karstedt's cat., chlorodiphenylsilane, toluene, 50 °C; then NEt₃, H₂O, rt, 47% over 2 steps for **94b**.

Disappointingly all attempts to generate a defined species with ligand **94a** and **94b** failed. The reactivity of the catalysts generated from molybdenum precatalyst **73** and the corresponding ligands **94a** and **94b** was highly promising. Both catalysts showed full conversions of phenylpropyne **93** to tolane **6** after 15 min reaction time at room temperature with a catalyst loading of 5 mol%.

3.3.4 Multidentate Ligands with Hexasubstituted Aromatic Linkers

Since trisubstituted aromatic linkers did not lead to a defined species, we decided to stick with the aromatic linker and make use of steric effects by introducing further substituents at the aromatic core. The envisaged target ligands should contain an aromatic linker with alternating ethyl groups and silanol containing sidechains (Scheme 3.13). It can be postulated that the substituents will arrange in an alternating orientation through steric effects like shown in the literature for comparable hexasubstituted arenes.^[53] This would lead to a preorientation that could favor the formation of a monomeric species. Therefore we decided to synthesize three ligands **97a-c** with different linker lengths.



Scheme 3.13: Ligand design with a hexasubstituted aromatic linker.

The tridentate silanol ligand **97c** also showed an alternating orientation of the substituents (Figure 3.5). In the solid state, however, the hydroxy groups all point to the outside. Based on this data it is not possible to conclude, how the ligand will behave in solution and whether a monomeric species is likely to be achieved.

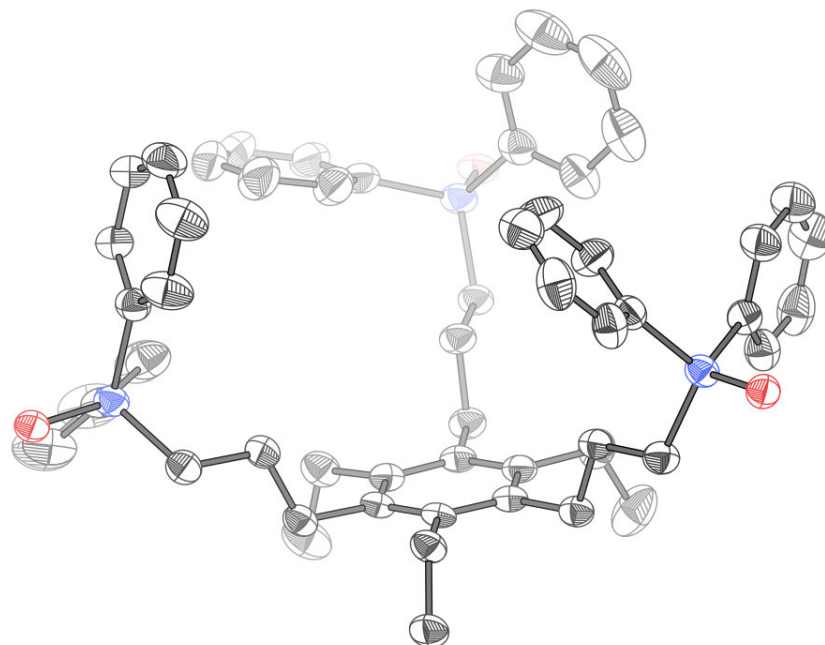
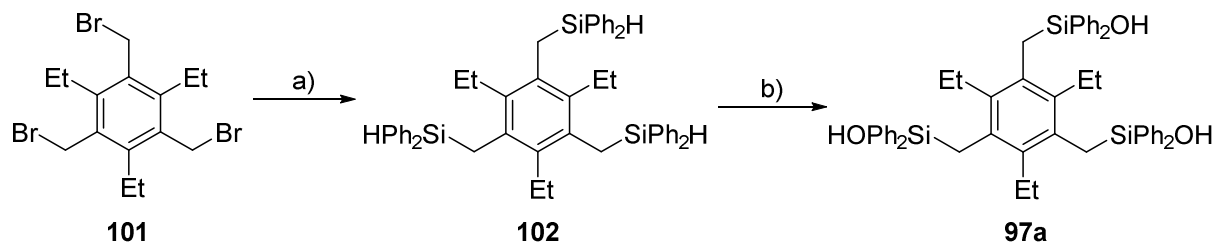


Figure 3.5: X-ray structure of multidentate ligand **97c** showing the alternating orientation of the side chains.

For the synthesis of the one carbon linker analog **97a** we utilized a procedure developed by Kabe and coworkers.^[53] The synthesis commenced with tribromide **101**, which was metallated and converted to trisilane **102** with chlorodiphenylsilane (Scheme 3.15). The target triol **97a** was generated through a bromination/hydrolysis sequence of trisilane **102**.



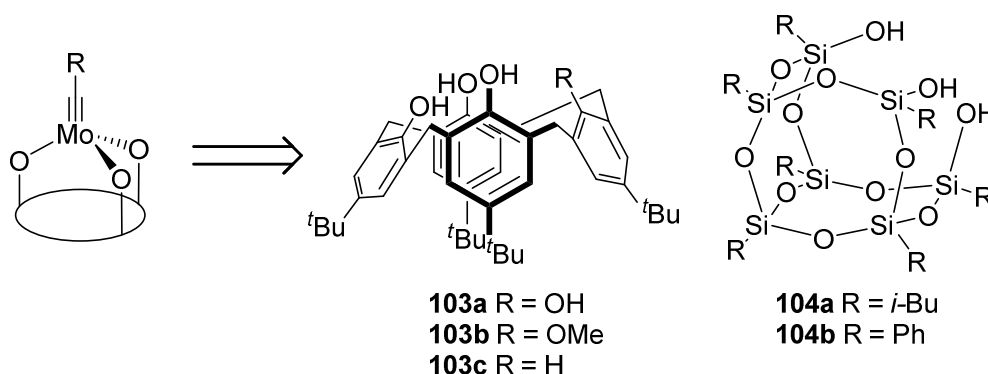
Scheme 3.15: Synthesis of multidentate ligand **97a** with a hexasubstituted aromatic linker. Conditions: a) Mg, chlorodiphenylsilane, THF, $-20\text{ }^{\circ}\text{C} \rightarrow \text{rt}$, 65%, b) NBS, CH_2Cl_2 , rt, then NEt_3 , H_2O , rt, 87% over 2 steps.

Neither ligand **97a** nor **97c** furnished a defined catalyst species. The catalysts generated from molybdenum precatalyst **73** and the corresponding ligands **97a** or **97c** were highly active,

showing full conversions of phenylpropyne **93** to tolane **6** for **97c** and a conversion of 95% for **97a** after 15 min reaction time at room temperature with 5 mol% catalyst loading. At this point we decided to evaluate the feasibility of more constrained ligands for the formation of a defined catalyst species.

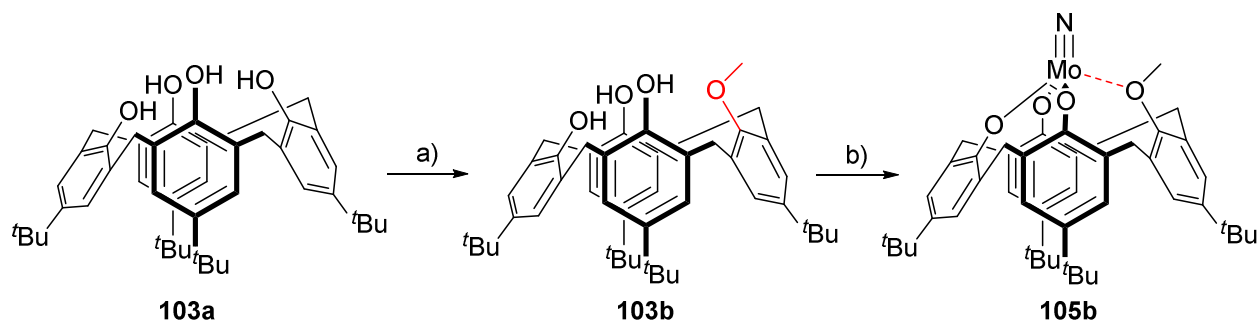
3.3.5 Calyx[4]arene- and Silsesquioxane-Based Systems

Since we were so far not able to isolate any crystalline species probably due to the high flexibility of the multidentate ligands shown in chapters 3.3.2 to 3.3.4, we decided to use sterically more constrained ligands like calyx[4]arenes **103** or silsesquioxanes **104** (Scheme 3.16).



Scheme 3.16: Structural considerations for constrained multidentate ligands.

In order to generate a neutral catalyst from calyx[4]arenes **103a** we used a protocol developed by Radius^[54] to selectively mono-methylate tetra hydroxy calyx[4]arene **103a**. The resulting calyx[4]arene derivative **103b** reacted with molybdenum nitrido complex **19** to generate nitrido complex **105** (Scheme 3.17). Nitrido complex **105** was previously described by Radius, but it was not evaluated in alkyne metathesis reactions.^[55] Even though complex **105** was air stable and a defined species, its metathesis activity was very low.



Scheme 3.17: Synthesis of calyx[4]arene based catalyst **105b** with a methyl-capped hydroxy group. Conditions: a) K_2CO_3 , MeI, MeCN, reflux, 58%; b) **19**, toluene, rt, 45%.

We assume that the low metathesis activity is a result of the coordination of the ether to the molybdenum center blocking the free site needed for substrate binding in the metathesis reaction (Figure 3.7). This assumption is supported by X-ray structure analysis, which shows an O1-Mo1 bond length of 2.228(3) Å (Figure 3.6).^[56]

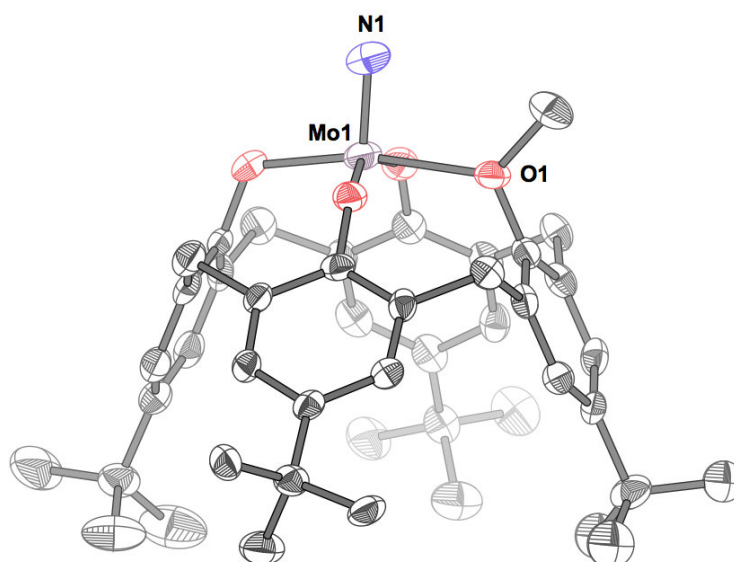


Figure 3.6: X-ray structure of methoxy calyx[4]arene nitrido complex **105b**.

In order to overcome this problem we decided to remove one of the oxygen atoms. A tridentate calyx[4]arenes **103c** could lead to complex **105c** which leaves a free coordination site at the molybdenum center. This should allow the unhindered coordination of the alkyne during the metathesis reaction.

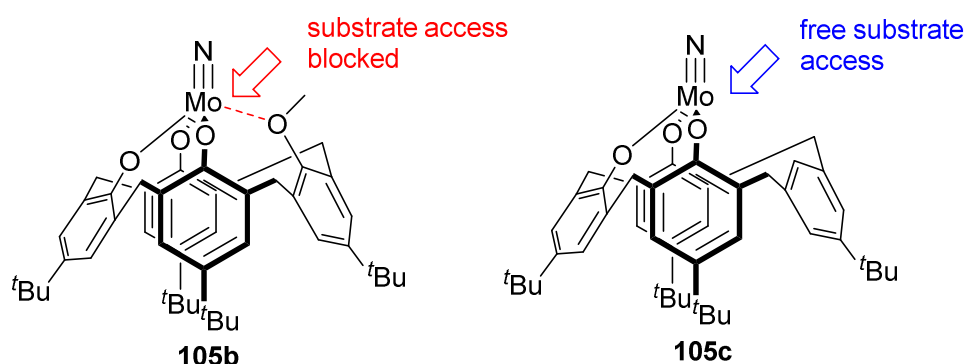
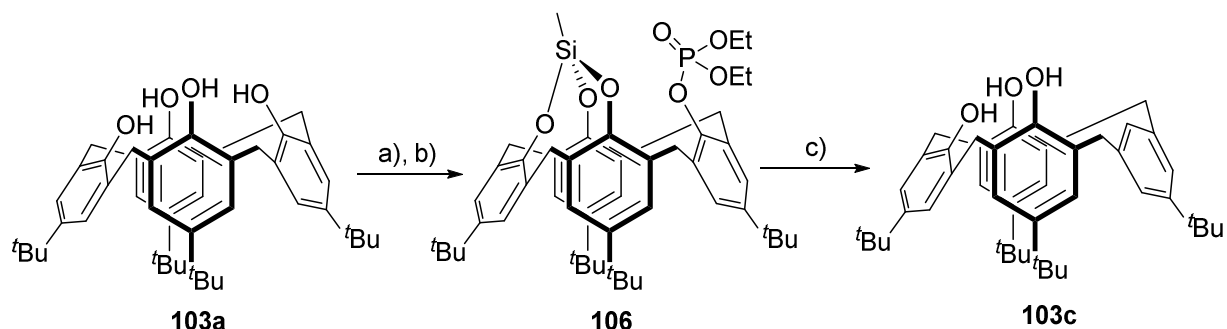


Figure 3.7: Catalyst design considerations for calyx[4]arene-based catalysts **105b** and **105c**.

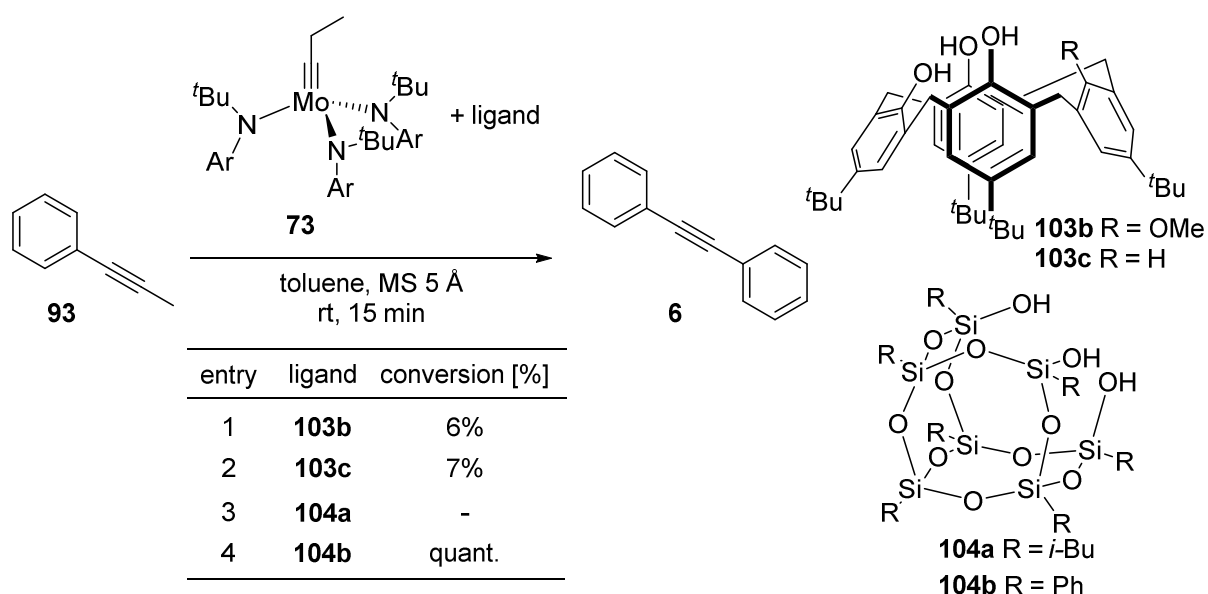
The synthesis of calyx[4]arene derivative **103c** was performed according to a procedure developed by Taoufik and coworkers (Scheme 3.18).^[57] Calyx[4]arene **103a** was converted to

the phosphorylated derivative **106** by a silylation/phosphorylation sequence. Birch reduction of intermediate **106** yielded the target triol **103c**.



Scheme 3.18: Synthesis of calyx[4]arene-based tridentate ligand **103c**. Conditions: a) MeSiCl_3 , TEA, toluene, rt; b) $n\text{-BuLi}$, CIP(O)(EtO)_2 , toluene, rt, 61% over 2 steps; c) K, NH_3 , toluene, -78°C , 48%.

Disappointingly ligand **103c** did not furnish an isolatable catalyst species on treatment with molybdenum nitrido complex **19** since the crude material could not be precipitated even from pentane at -78°C . Furthermore, the catalytic activity of the *in situ* generated systems from molybdenum precatalyst **73** and the corresponding ligands **103b** or **103c** was very low (Scheme 3.19, Entry 1, 2). This is probably due to the fact that phenols are electronically less favorable for alkyne metathesis applications than siloxy ligands.



Scheme 3.19: Test reactions with *in situ* generated catalysts. Conditions: 5 mol% **73** and 5 mol% of the corresponding ligands **103b-c** and **104a-b**.

We also utilized silsesquioxanes for which some preliminary studies had already been conducted by Moore.^[58] He successfully used catalysts generated from monodentate

silsesquioxanes with cyclopentyl residues in alkyne metathesis reactions. Moore also described an *in situ* generated system from a multidentate silsesquioxane with cyclopentyl residues and molybdenum alkylidyne **73** which was reported to lead to polymerization of the butyne side product. We examined two electronically different silsesquioxanes. While silsesquioxane **104a** with alkyl residues led to no activity (Scheme 3.19, Entry 3), its analog **104b** bearing aromatic residues afforded a catalytic species with high activity (Scheme 3.19, Entry 4). A mixture of **73** and **104b** was further evaluated in the homo metathesis reaction of primary alcohol **32**, leading to low conversion according to TLC. Both silsesquioxanes **104a** and **104b** did not lead to defined species.

3.3.6 Conclusion

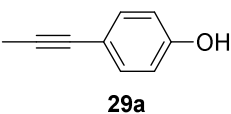
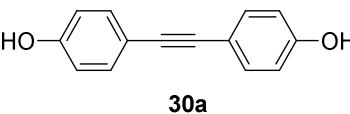
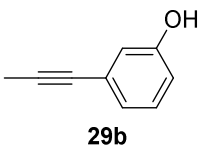
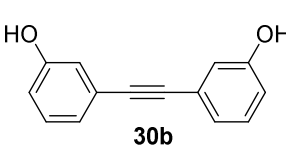
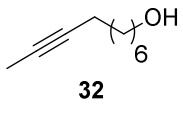
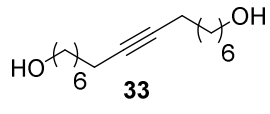
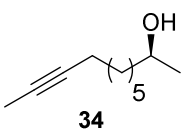
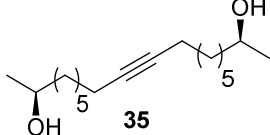
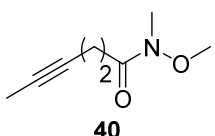
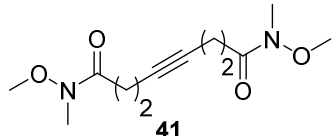
The studies described above show that multidentate siloxy ligands lead to highly active catalyst systems with molybdenum alkylidyne **73** as a precatalyst. The activity depends on the substituents on the silicon atom. While ligands with aromatic substituents such as **89a** and **89d** led to highly proficient systems, ligand **89b** with aliphatic substituents were less appropriate. Furthermore, the geometry of the ligand plays only a minor role, with ligand **89** (silicon linker) as well as ligands **94** and **97** (aromatic linkers) all forming highly active catalysts. In contrast constrained ligands like calyx[4]arenes and silsesquioxanes mainly furnished unreactive species probably due to electronic effects and a constrained geometry. The only exception was **104b**, which furnished a highly reactive system. Our attempts to isolate a defined, highly active complex failed due to the formation of product mixtures. Gratifyingly, the systems generated *in situ* from multidentate silanol ligands and molybdenum alkylidyne **73** show very good results with complex molecules and in many cases significantly surpass the performance of the previous catalyst generation **28** as described in the next chapter.

3.4 Substrate Scope of *In Situ* Generated Catalysts

3.4.1 Homometathesis Reactions

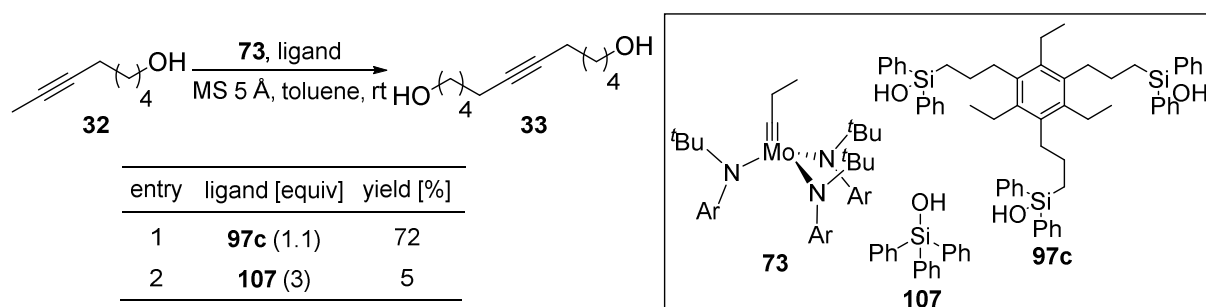
Some of the catalysts that were generated from molybdenum alkylidyne **73** and the siloxy ligands described in Chapter 3.3 showed a promising reactivity. Therefore we decided to evaluate the performance of these catalysts with substrates that were found to be troublesome for catalyst **28**.

Table 3.1: Homo metathesis reactions. Comparison of $[\text{Mo}(\equiv\text{CC}_6\text{H}_4\text{OMe})(\text{OSiPh}_3)_3]$ (**28**) with systems generated *in situ* from molybdenum alkylidyne **73** and multidentate silanols **89a** and **97c**.

entry	substrate	product	system	temp. [°C]	cat. [mol%]	time [h]	yield [%]
			28	80	3	3	87
1			28	rt	10	14	69
			73/89a	rt	3	16	78
			73/89a	rt	10	1	81
			73/97c	rt	10	4	84
2			28	rt	10	14	84
			73/89a	rt	10	14	80
			73/97c	rt	10	14	80
3			28	rt	10	14	0
			28	110	10	14	7
			73/89a	rt	10	14	69
			73/97c	rt	10	4	72
4			28	80	7	24	66
			28	rt	10	14	34
			73/89a	rt	10	0.5	81
			73/97c	rt	10	4	76
5			28	80	6	40	66
			28	rt	10	16	47
			73/89a	rt	10	0.5	86
			73/97c	rt	10	4	75

Homo dimerization experiments showed that catalyst **28** gives good yields at elevated temperatures when dealing with substrates containing phenolic hydroxy groups (Table 3.1, Entry 1-2). When working at room temperature, the performance of catalyst **28** is surpassed by the multidentate systems in the case of *p*-phenol substrate **29a**. Substrate **32** containing a primary hydroxy group underwent metathesis reaction when using multidentate systems, while **28** did not lead to any significant yields even at elevated temperatures (Table 3.1, Entry 3). For substrate **34** containing a secondary alcohol, the yield achieved with monodentate system **28** dropped considerably when running the reaction at room temperature, while the multidentate systems still produced good yields (Table 3.1, Entry 4). Improvements were also observed for the strongly coordinating Weinreb amide **40** when using the multidentate systems (Table 3.1, Entry 5). Surprisingly, we did not detect a significant difference in the performance of **89a** and **97c**, indicating that the type of linker is rather unimportant for the activity of the catalysts (Table 3.1, Entry 1-5).

The results can be rationalized by chelating effects which render catalysts with multidentate siloxy ligands more stable compared to their analogs with monodentate siloxy ligands. We assume that the monodentate ligand in catalyst **28** is more prone to be replaced by protic substrates which would render the catalysts less reactive/unreactive. In order to evaluate this postulate and to exclude effects that may be caused by the different alkylidynes in complex **28** (aryl) and complex **73** (alkyl), we compared catalysts that were generated from complex **73** with monodentate ligand **107** or multidentate ligand **97c**. 8-Decinol (**32**) was used as a test substrate and both reactions were run for 14 h at room temperature. The homodimerization product **33** was isolated in 5% yield when the catalyst generated with the monodentate ligand **107** was used (Scheme 3.20, Entry 1). The catalyst generated with the multidentate ligand **97c** furnished 72% yield, which supports the notion that the multidentate geometry improves the stability towards ligand replacement (Scheme 3.20, Entry 2).



Scheme 3.20: Comparison of *in situ* generated metathesis catalysts from multidentate ligand **97c** and monodentate ligand **107**.

In general the position of a free hydroxy group is very important for the outcome of alkyne metathesis reactions. This is illustrated by the fact that alkynes **108** and **109** with free hydroxy groups in either propargylic or homo-propargylic position did not undergo homo metathesis reactions (Figure 3.8). Also the *o*-phenol **29c** was not tolerated as well as acid **110**.

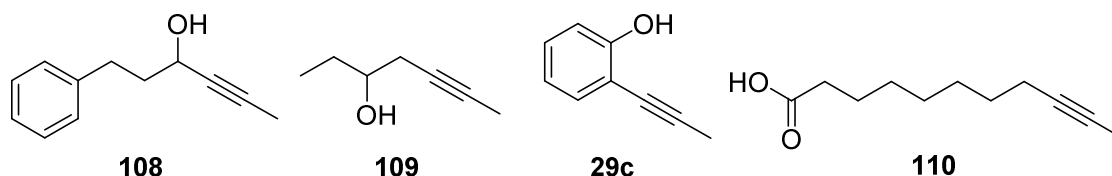


Figure 3.8: Substrates that did not undergo homo metathesis reactions with either multidentate or monodentate systems.

3.4.2 RCAM Reactions

We compared the efficiency of metathesis catalyst **28** and systems generated from complex **73** with multidentate ligands in the RCAM reactions of substrates containing protected or unprotected hydroxy groups in propargylic position.

For mono-MOM/TES protected substrates **111a** and **111b** the RCAM reaction proceeded in acceptable yield when the system based on complex **73** and multidentate ligand **97c** was used, while the use of catalyst **28** did not furnish any RCAM products (Table 3.2, Entry 1). Mono acetate/benzoate protected substrates **111c** and **111d** did not lead to cyclization products with any of the examined catalysts.

The crude NMR spectra of the RCAM reactions of diynes **111c** and **111d**, in which one of the hydroxy groups is acylated, showed that an ethyl group is transferred to the side with the free hydroxy group (Figure 3.9). Further reaction seems to be unfavorable since no RCAM products were observed.

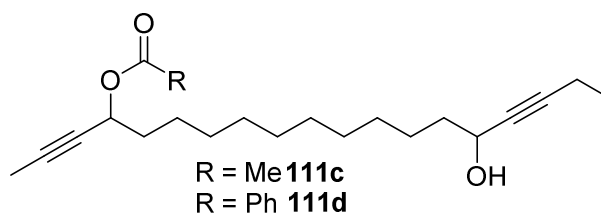
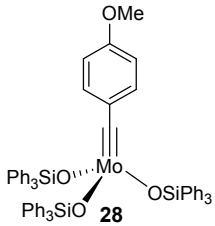
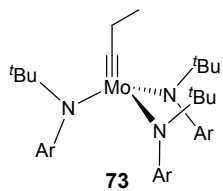
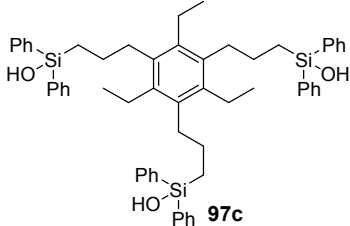
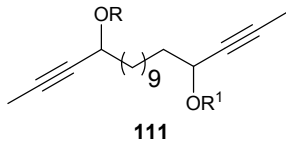
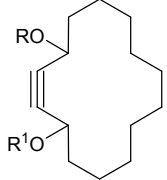
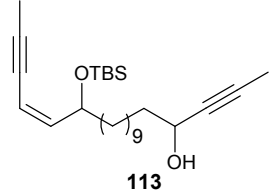
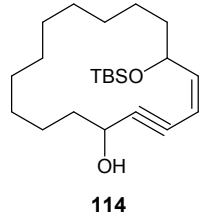
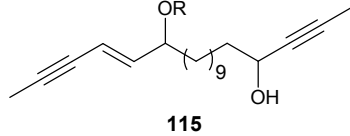
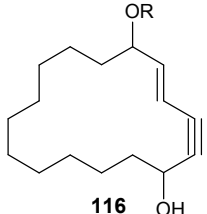


Figure 3.9: Ethyl transfer product generated in the RCAM reactions of mono acetate or mono benzoate protected diynes **111c-d**.

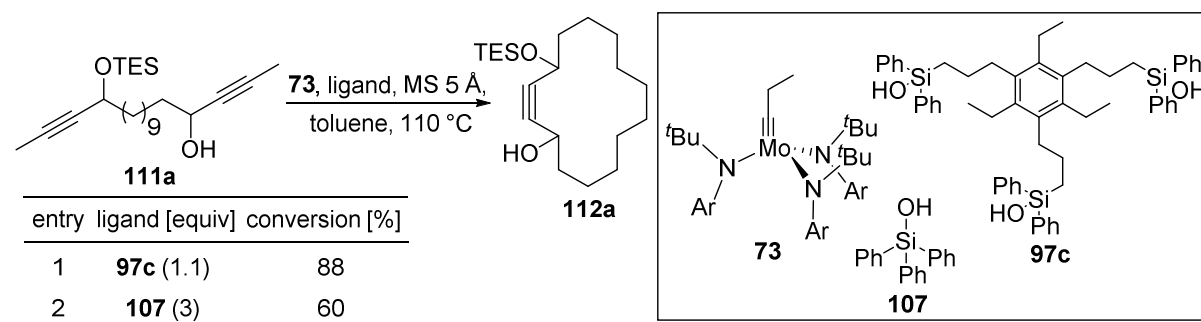
Table 3.2: RCAM reactions. Comparison of $[\text{Mo}(\equiv\text{CC}_6\text{H}_4\text{OMe})(\text{OSiPh}_3)_3]$ (**28**) with systems generated *in situ* from molybdenum alkylidyne **73** and multidentate silanol **97c**.

entry	substrate	product	R	R ¹	73/97c yield [%]	28 yield [%]
						
						
1			a: TES b: MOM c: Ac d: Bz e: TES f: MOM g: Ac h: Bz i: H	H H H H TES MOM Ac Bz H	64 ^a 67 ^a 0 ^a 0 ^a 71 ^a 70 ^a 0 ^a 0 ^a 53 ^a	0 ^b 0 ^b 0 ^b 0 ^b 0 ^b 54 ^b 0 ^b 0 ^b 0 ^b
2			-	-	90 ^{c,d}	0 ^{b,d}
3			a: TBS b: H	- -	76 ^{c,d} 40 ^a	0 ^{b,d} 0 ^b

a) (22 mol%) **97c**, (20 mol%) **73**, MS 5 Å, toluene, 110 °C; b) **28** (20 mol%), MS 5 Å, toluene, 110 °C; c) (20 mol%) **97c**, (20 mol%) **73**, MS 5 Å, toluene, 60 °C; c) (25 mol%) **97c**, (20 mol%) **73**, MS 5 Å, toluene, 110 °C; d) Experiments conducted by M. Ilg.

The RCAM reactions of bis-TES and bis-MOM protected substrates **111e-f** proceeded in good yields when the multidentate system was used (Table 3.2, Entry 1). Acetate and benzoate protected substrates **111g-h** did not lead to cyclization products. The bis-MOM protected substrate **111f** was the only case in which catalyst **28** furnished any RCAM product. Impressingly even the completely unprotected diol **111i** could be cyclized with moderate yield when using the multidentate system.

In order to find reasons for the superior performance of the multidentate system (Table 3.2, Entry 1), we conducted experiments in which we compared catalysts generated *in situ* from molybdenum alkylidyne **73** and either tridentate ligand **97c** or monodentate ligand **107** (Scheme 3.21). Surprisingly the system generated with the monodentate ligand also catalyzed the reaction, even though it stopped at 60% conversion (Scheme 3.21, Entry 2). This indicates that the nature of the alkylidyne is important for the initiation step. Furthermore it shows that the longtime stability of the multidentate system is better compared to that of the monodentate analog.



Scheme 3.21: Comparison of catalysts generated *in situ* with multidentate **97c** and monodentate **107** ligands.

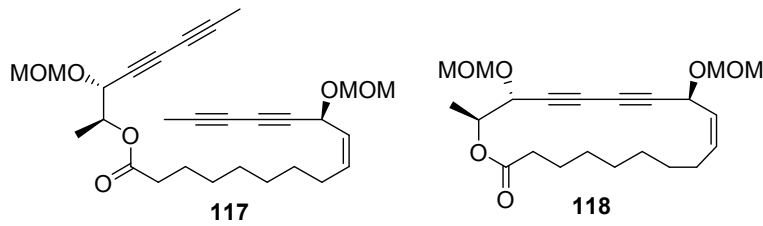
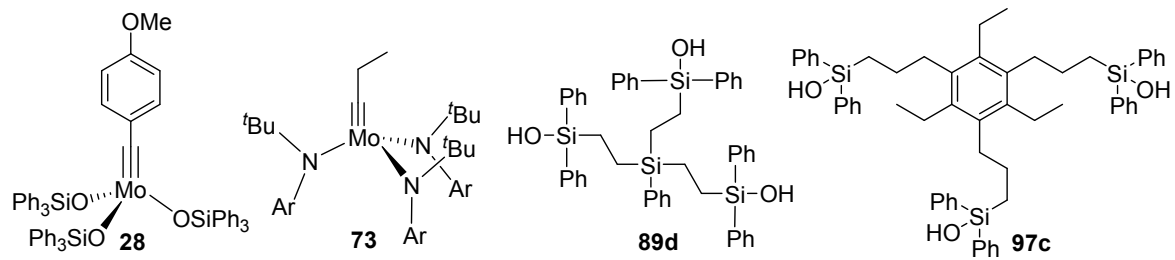
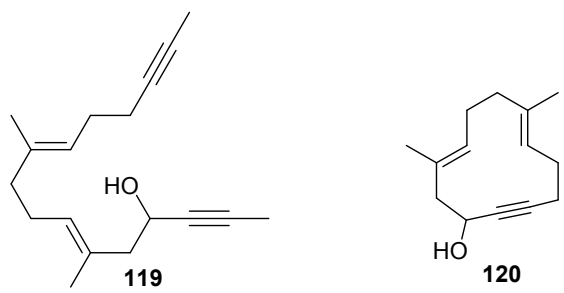
Alkylidyne **73** is a catalytically active species at elevated temperature, therefore we performed a control experiment in which we submitted diyne **111i** to molybdenum alkylidyne **73** at 110 °C without the addition of siloxy ligands. Only traces of the desired product **112i** were detected in the crude product and the mass balance led to the conclusion that this reaction suffered from a significant material loss probably due to ring expansion polymerization reaction.

Substrates with a propargylic hydroxy-group on one side and a protected alcohol next to an enyne motif **113** and **115a** were successfully metathesized using the multidentate system (Table 3.2, Entry 2-3).^[59] Interestingly *Z*-enyne **114** was formed in better yield compared to *E*-enyne **116a**. The RCAM reaction of completely unprotected *E*-enyne **115b** could only be accomplished in low yield (Table 3.2, Entry 3).

3.4.3 Applications to Natural Product Synthesis

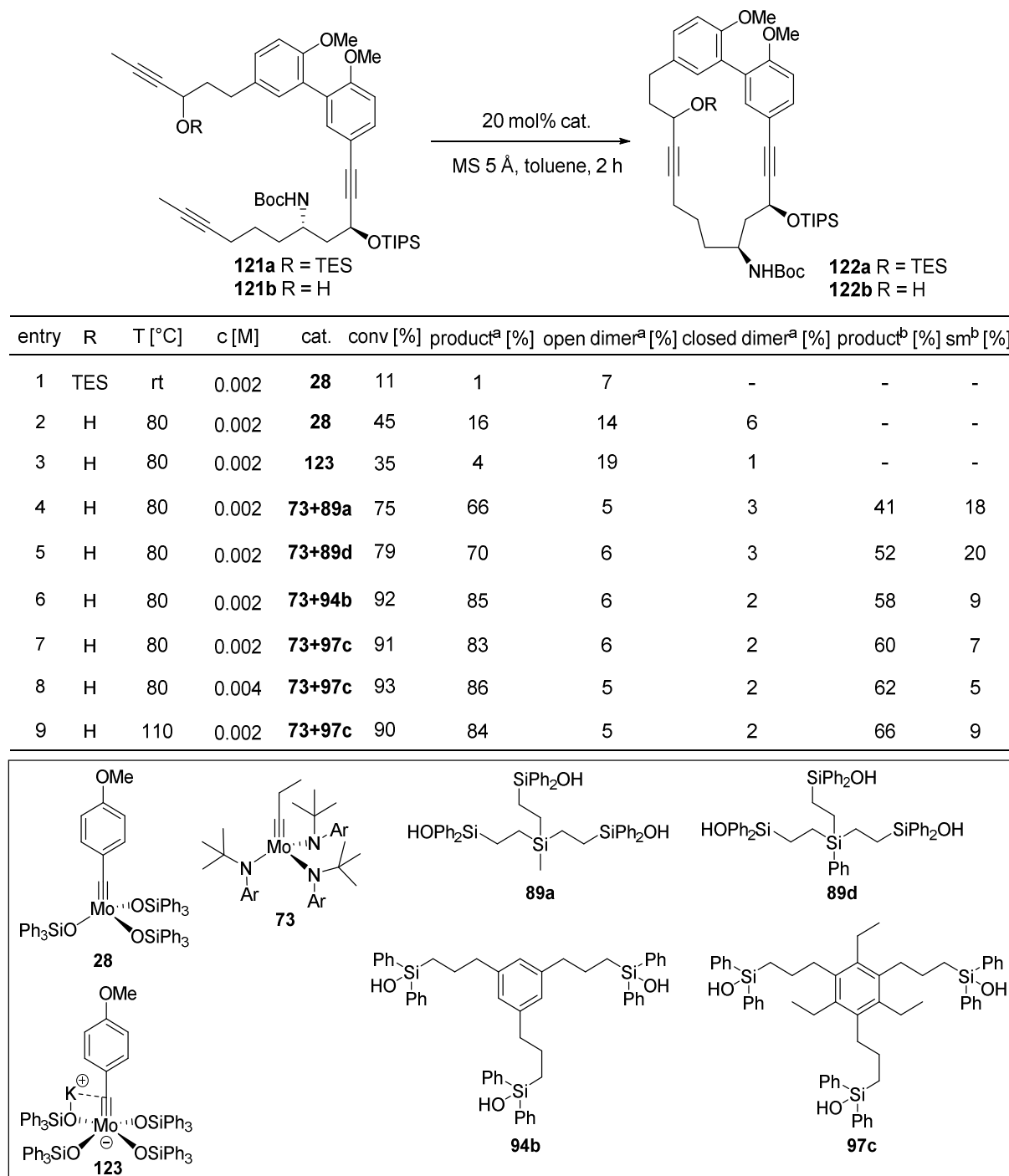
The newly developed alkyne metathesis catalysts were applied in the total syntheses of two natural products; Ivorenolide A and Manshurolide.^[59] Additionally these catalysts were successfully employed in studies towards the synthesis of Lythrancepines.^[59] In the total synthesis of Ivorenolide A, the diyne metathesis of substrate **117** to diyne **118** was accomplished in good yield when applying the multidentate system, whereas **28** only furnished low yields (Table 3.3, Entry 1). The multidentate system could further proof its value in the total synthesis of Manshurolide. The key RCAM reaction failed with the standard system **28**, but the system generated with molybdenum alkylidyne **73** and multidentate silanol **89d** furnished the highly strained *E,E*-diene macrocycle **120** in good yield (Table 3.3, Entry 2).

Table 3.3: RCAM reactions in natural product synthesis. Comparison of $[\text{Mo}(\equiv\text{CC}_6\text{H}_4\text{OMe})(\text{OSiPh}_3)_3]$ (**28**) with systems generated *in situ* from molybdenum alkylidyne **73** and multidentate silanols.

entry	substrate	product	yield [%]	yield [%]
1	 <p>117 → 118</p>	 <p>28, 73, 89d, 97c</p>	78 ^{a,c}	38 ^{b,c}
2	 <p>119 → 120</p>		83 ^{d,f}	0 ^{e,f}

a) (20 mol%) **97c**, (20 mol%) **73**, MS 5 Å, toluene, 60 °C; b) **28** (35 mol%), MS 5 Å, toluene, 60 °C; c) Experiments conducted by F. Ungeheuer; d) (10 mol%) **89d**, (10 mol%) **73**, MS 5 Å, toluene, 120 °C; e) **28** (20 mol%), MS 5 Å, toluene, 120 °C; f) Experiments conducted by Dr. L. Hoffmeister.

Furthermore we demonstrated the usefulness of the newly developed catalysts in a synthetic approach towards the Lythrancepines. The key step in this synthesis, RCAM of triyne **121b** to diyne **122b**, was used as a proficiency test for various catalysts in this highly challenging transformation (Scheme 3.22).^[60]



Scheme 3.22: Application of catalysts with multidentate ligands in the total synthesis of Lythrancepines. The experiments were performed by Dr. K. Gebauer. a) Yields were determined by LC-MS of the crude reaction mixture; b) Isolated yields.

The standard catalyst **28** was not able to effectively convert triyne **121a** into diyne **122a** with a TES-protected hydroxy group in one of the propargylic positions (Scheme 3.22, Entry 1). Removal of the sterically demanding TES group led to some conversion when using the neutral complex **28** or ate complex **123**, but the yield of the desired product **122b** was still very low (Scheme 3.22, Entry 2-3). A screening of different multidentate ligands led to significantly better results (Scheme 3.22, Entry 4-9). While the systems with silicon linkers **89a,d** did not produce satisfactory yields (Scheme 3.22, Entry 4-5), the systems with aromatic linkers **94b** and **97c** led to good conversions and acceptable yields (Scheme 3.22, Entry 6-8). The yield could be further improved by raising the reaction temperature to 110 °C to give the desired macrocycle in 66% yield when utilizing the hexasubstituted arene **97c** (Scheme 3.22, Entry 9).

It is especially noteworthy that the ratio of monomeric cycle to open and closed dimeric species significantly improved when using the multidentate systems.

3.4.4 Conclusion

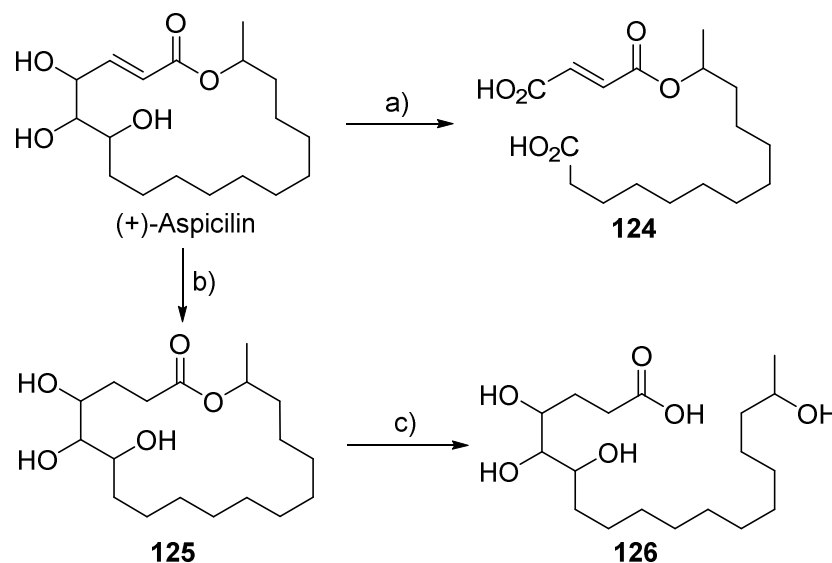
The newly developed *in situ* generated alkyne metathesis catalysts based on multidentate siloxy ligands showed their potential in various challenging ACM and RCAM reactions where the previous generation of metathesis catalysts **28** faced problems or completely failed to work. This opens the way to address new structural motifs in total synthesis via alkyne metathesis.

4 Formal Synthesis of (+)-Aspicilin

4.1 Introduction

4.1.1 Isolation, Structure Validation, and Biological Activity

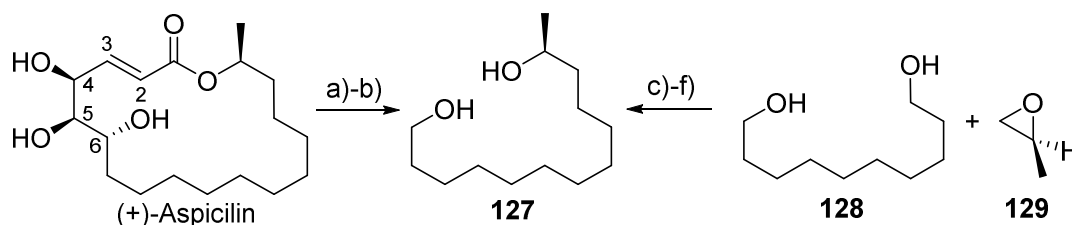
(+)-Aspicilin was first isolated in 1900 from lichen *Aspicilia calcarea* which belongs to the *Lecanoraceae* family.^[61] Its constitution was determined by Huneck nearly 75 years later via mass spectroscopy, IR spectroscopy and NMR spectroscopy in addition to chemical degradation experiments (Scheme 4.1).^[62] The triol motif was confirmed by NMR spectroscopy as well as through chemical degradation with Jones reagent to diacid **124**. The (*E*)-olefin motif was validated by NMR and reduction to macrocycle **125** which consumed 1 equiv of hydrogen. Furthermore, the unsaturation was identified to be in α,β -position to the carbonyl via UV-spectroscopy (211 nm). The lactone motif was confirmed by the IR carbonyl band, as well as through hydrolysis of macrocycle **125** to open chain acid **126**.



Scheme 4.1: Structure validation of (+)-Aspicilin. Conditions: a) $\text{CrO}_3/\text{H}_2\text{SO}_4$, acetone, rt; b) Pt/C, H_2 , EtOH, rt; c) KOH, MeOH, reflux.

The absolute configuration was determined by Quinkert through a combination of NMR and X-ray analysis, as well as chemical degradation/fragment synthesis (Scheme 4.2).^[63] The relative configuration was determined by single-crystal X-ray analysis and $^1\text{H-NMR}$ (COSY and NOE) analysis of the acetonide (C4-C5) of (+)-Aspicilin (to reduce the conformational

flexibility). To determine the absolute configuration, (+)-Aspicilin was disassembled by periodate cleavage and reduction to give diol **127**, for which the configuration could be determined through chemical synthesis from 1,10-decanediol (**128**) and (*S*)-propylene oxide (**129**).



Scheme 4.2: Proving the absolute configuration by chemical synthesis of degradation product **127**. Conditions: a) NaIO_4 , $\text{MeOH}/\text{H}_2\text{O}$ (9:1), rt; b) LiAlH_4 , Et_2O , rt; c) HBr , petroleum ether, 80°C ; d) dihydropyran, PPTS, CH_2Cl_2 , rt; e) Mg , THF; f) 1,5-cyclooctadiene, CuCl , rt.

(+)-Aspicilin was tested against various cancer cell lines in an MTT assay.^[64] It exhibits inhibitory activity on the proliferation of cancer cell lines A549 ($\text{IC}_{50} = 14.7 \mu\text{M}$ over 24 h), HeLa ($\text{IC}_{50} = 17.9 \mu\text{M}$ over 24 h) and MCF7 ($\text{IC}_{50} = 12.0 \mu\text{M}$ over 24 h), whereas Neuro2a, and MDA-MB-231 were not affected. No potential antibacterial and antifungal activities were observed.

4.1.2 Preceding Synthetic Studies

(+)-Aspicilin has received considerable attraction by organic chemists, leading to 16 total syntheses (Quinkert,^[65] Keinan,^[66] Oppolzer,^[67] Enders,^[68] Kobayashi,^[69] Hatakeyama,^[70] Tanaka,^[71] Ley,^[72] Banwell,^[73] Raghavan,^[74] Markó,^[75] Yadav,^[76] Reddy,^[64] Hou,^[77] Gandhi,^[78] Shaw^[79]), one formal synthesis (Hoveyda^[80]) and two syntheses of the enantiomer (–)-Aspicilin (Zwanenburg,^[81] Solladié^[82]) (Figure 4.1). The macrocycle was closed in most of those syntheses via Yamaguchi macrolactonization or ring closing olefin metathesis (RCM). In the following, there is a short description of Oppolzer’s approach since our formal synthesis intercepts his intermediate **132**. Moreover, Hoveyda’s synthesis is discussed since he disconnects the same C-C bond to form the macrocycle of (+)-Aspicilin as we plan for our synthesis.

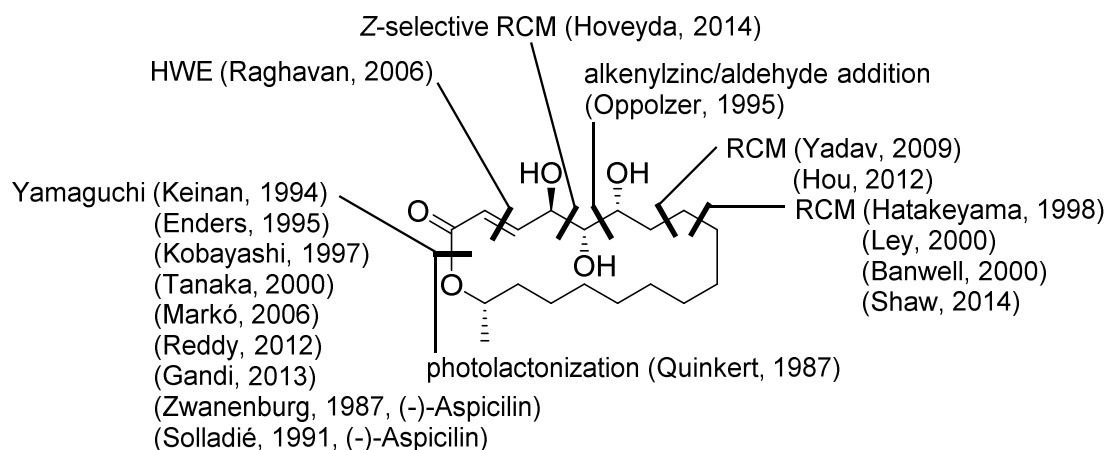
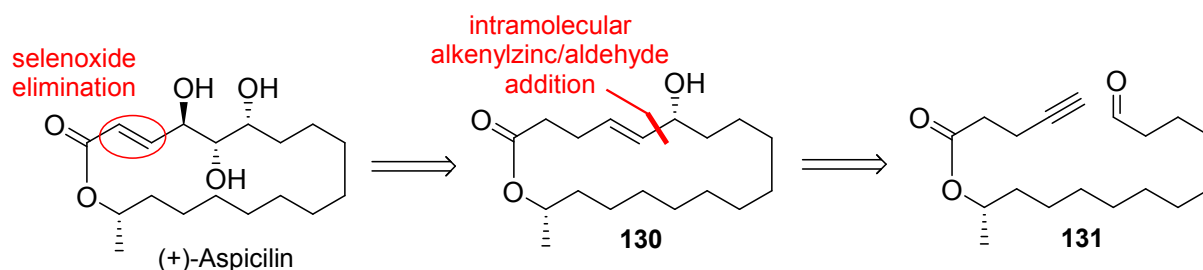


Figure 4.1: Overview of previous retrosynthetic disconnections.

4.1.3 Oppolzer's Total Synthesis of (+)-Aspicilin by Asymmetric Alkenylation

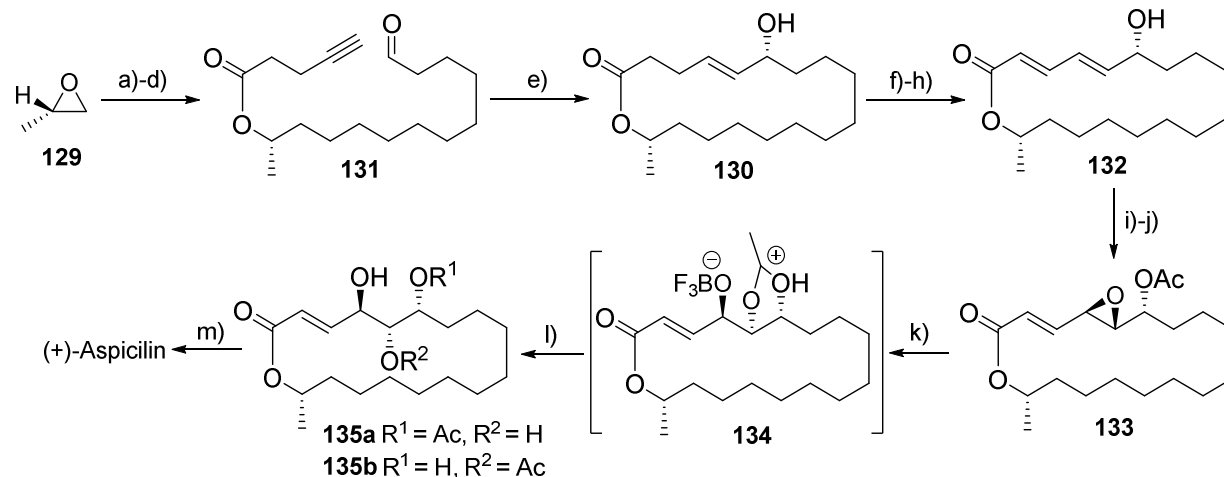
The Oppolzer group planned to introduce the unsaturation at a late stage by selenoxide elimination (Scheme 4.3).^[67] The triol motif was to be introduced via epoxidation/epoxide opening, with stereocontrol by the already existing allylic stereocenter of macrocycle **130**. For the closure of the macrocycle **130**, an intramolecular alkenylzinc/aldehyde addition from open chain precursor **131** was envisaged. This transformation was chosen due to its previous successful employment in the synthesis of (*R*)-(-)-muscone.^[83]



Scheme 4.3: Retrosynthetic analysis of (+)-Aspicilin by Oppolzer *et al.*^[67]

The synthesis (Scheme 4.4) commenced with (*S*)-propylene oxide (**129**), which was converted via copper-catalyzed epoxide opening, esterification, acetal cleavage and subsequent Swern oxidation to open chain aldehyde **131**. As the key step, they closed the macrocycle with an asymmetric cyclization that proceeded via hydroboration, boron/zinc-transmetalation and dimethylaminoisoborneol catalyzed intramolecular addition to afford macrocycle **130** with 60% yield and a diastereoselectivity of 91%. The α,β -unsaturation was installed after protection of alcohol **130** by a phenylselenation/selenide-oxidation/selenoxide-elimination process to yield (*E,E*)-dienol **132** after deprotection. They continued their synthesis with a hydroxyl-directed epoxidation and acetylation to give

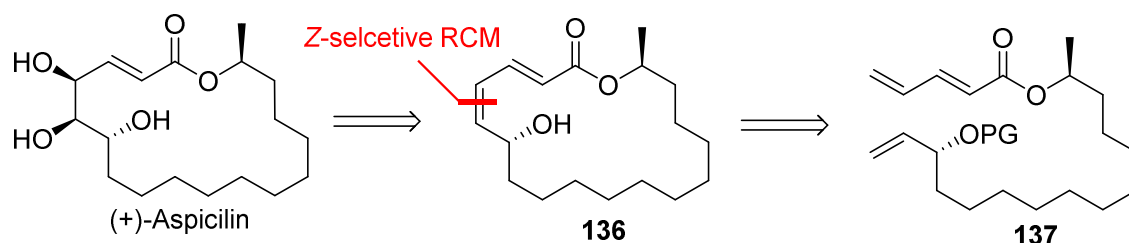
product **133**. Subsequent treatment with $\text{BF}_3 \cdot \text{Et}_2\text{O}$ gave cyclic oxonium ion **134** that was converted to a 1:1 mixture of monoacetates **135a** and **135b** upon treatment with water. Deprotection furnished (+)-Aspicilin in a total of twelve steps from literature known compounds (2 extra steps from commercially available 1,10-decanediol (**128**)) and 22% overall yield.



Scheme 4.4: Oppolzer's asymmetric macrocyclization approach. Conditions: a) $\text{BrMg}(\text{CH}_2)_{10}\text{OTHP}$, $\text{Cu}(\text{COD})\text{Cl}$; b) 4-pentynoic acid, DCC, DMAP; c) TsOH , MeOH; d) $(\text{COCl})_2$, DMSO, NEt_3 , 76% over 4 steps; e) $(\text{c-hex})_2\text{BH}$, Et_2Zn , (-)-DAIB, 60%, 91% ds.; f) TBSCl, DBU; g) LICA, THF, -78°C , then TBSCl, HMPA, then PhSeBr , magnesium monoperoxyphthalate; h) HF-py, 82% over 3 steps; i) $t\text{-BuOOH}$, $\text{VO}(\text{acac})_2$, 77%; j) Ac_2O , NEt_3 , DMAP, quant.; k) $\text{BF}_3 \cdot \text{Et}_2\text{O}$, rt; l) NaHCO_3aq , 81%; m) 1% HCl, MeOH, rt, 97%.

4.1.4 Hoveyda's Formal Synthesis of (+)-Aspicilin by Z-selective RCM

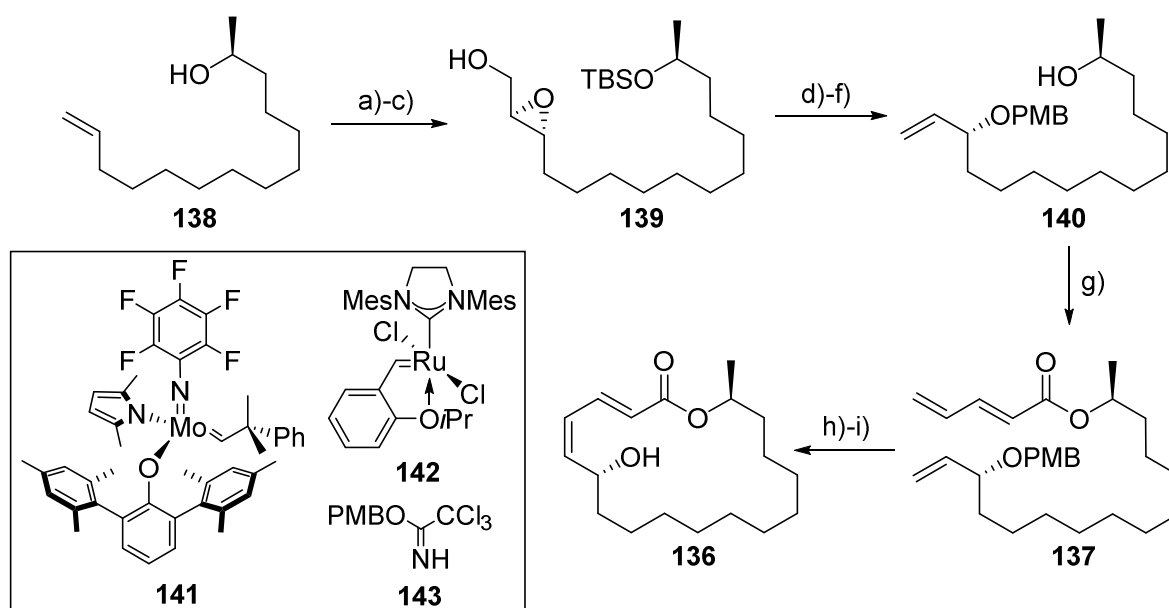
Another interesting approach was described by Hoveyda's group, who designed a formal synthesis of (+)-Aspicilin in which the macrocycle **136** was formed from triene **137** with a newly developed Z-selective olefin metathesis catalysts **141** (Scheme 4.5).^[80]



Scheme 4.5: Retrosynthetic analysis of (+)-Aspicilin by Hoveyda *et al.*^[80]

Their synthesis started from literature known olefin **138** that was converted to epoxide **139** via a sequence of TBS protection, olefin cross metathesis and Sharpless epoxidation (Scheme 4.6). Epoxide **139** was converted to alcohol **140** by a three step sequence; a radical epoxide-

opening/hydroxy-eliminating transformation, a PMB protection, and a TBS deprotection. Following the three step synthesis, alcohol **140** was converted to metathesis precursor **137** via esterification. RCM of ester **137** with catalyst **141** afforded stereoisomerically pure (*E,Z*)-dienoate **136** after deprotection. Accessing Quinkert's intermediate, dienoate **136**, thus completed the formal synthesis of (+)-Aspicilin.^[65a] Hoveyda's approach took 9 steps from literature known olefin **138** with an overall yield of 9%. This was the first example of a catalyst-controlled stereoselective macrocyclic RCM reaction to generate (*E,Z*)-dienoates.



Scheme 4.6: Hoveyda's stereoselective RCM approach. Conditions: synthesis of **138** literature known^[69] a) (*t*-Bu)Me₂SiCl, imidazole, DMF, rt; b) (*Z*)-but-2-ene-1,4-diol, 2mol% **142**, CH₂Cl₂, 71% over 2 steps; c) (–)-diethyl tartrate, Ti(*Oi*-Pr)₄, *t*-BuOOH, CH₂Cl₂, –20 °C, 56%; d) Cp₂TiCl₂, Zn, ZnCl₂, THF, rt, 69%; e) **142**, La(OTf)₃, toluene, rt; f) (*n*-Bu)₄NF, THF, rt, 65% over 2 steps; g) pentadienoic acid, pivaloyl chloride, DMAP, NEt₃, rt, 80%; h) 10 mol% **141**, benzene, rt, 133 mbar, 69%, >98:2 *Z/E*; i) DDQ, CH₂Cl₂/H₂O, 0 °C, 91%; see ref.^[65a] for the completion of the synthesis.

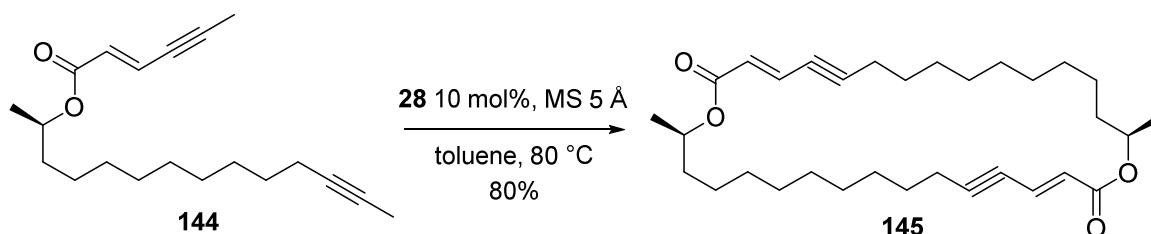
4.2 Aims and Scope

Our formal synthesis of (+)-Aspicilin targeted Oppolzer's *E,E*-diene intermediate **132**. The *E,E*-diene should be built by utilizing RCAM in concert with a post-metathetic modification based on a hydrostannylation/destannylation sequence. This synthesis was chosen as a challenge for the recently developed ruthenium-catalyzed *trans*-hydrostannylation.^[5] Furthermore, the molecule was chosen as a trial for RCAM since the formation of macrocyclic *E*-enynes has proven difficult due to the formation of cyclic dimers.^[6]

4.3 Preliminary Studies and Formal Synthesis

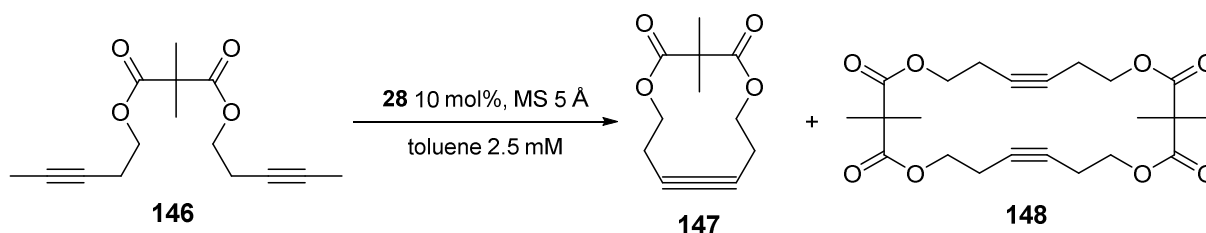
4.3.1 Preliminary Studies on Monomer to Dimer Ratios in RCAM

A previous study had demonstrated that a compound containing an enyne motif was incapable of forming the desired monomer in a RCAM.^[6] When diyne **144** was submitted to metathesis conditions, only dimeric macrocycle **145** was observed (even at high dilutions of 0.1 mM) instead of the desired 16-membered target product (Scheme 4.7). Normally 16-membered rings are well within the range of this methodology, with an eleven-membered ring being so far the smallest ring size that could be closed by RCAM.^[35]



Scheme 4.7: RCAM reaction of enyne **144** leading to undesired dimeric macrocycle **145**.

In order to get a better understanding of how to influence the ratio of monomeric and dimeric macrocycles, we decided to evaluate the effects of temperature and time. We chose **146** as a model substrate, since its reaction can be easily monitored by ¹H NMR spectroscopy of the crude reaction mixtures, due to the fact that the proton signals next to the ester motif are quite characteristic (4.31 ppm for the monomer **147** but 4.12 ppm for the dimer **148**) (Scheme 4.8).^[35]



Scheme 4.8: Test reaction to evaluate the influence of time and temperature on monomer **147** to dimer **148** ratio.

We first evaluated possible temperature effects (Chart 4.1) and observed that elevated temperatures favor the formation of the monomer **147** over the dimer **148**. This can be explained by the fact that the dimeric macrocycle **148** is the kinetically favored product, whereas the monomeric macrocycle **147** is the thermodynamically favored product.^[84]

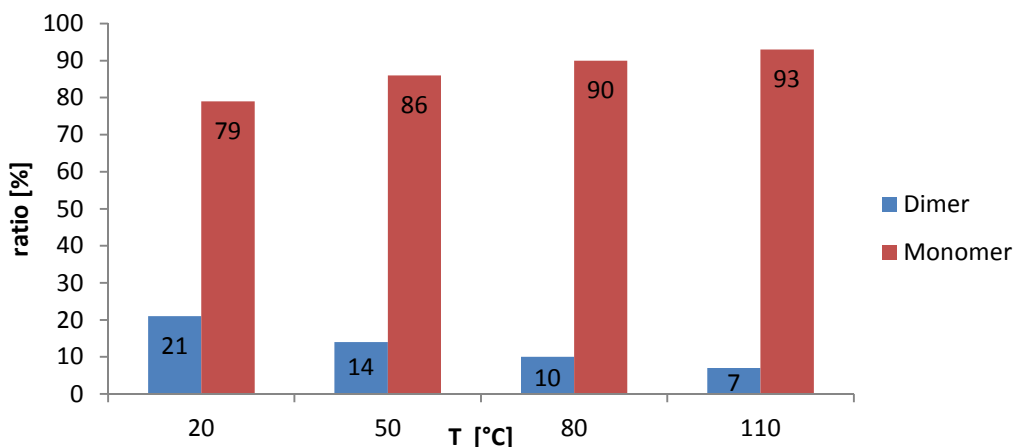


Chart 4.1: Temperature dependency of monomer **147** to dimer **148** ratio in RCAM reaction. Conditions: 10 mol% **28**, MS 5 Å, toluene 2.5 mM, 10 min reaction time. The ratios were determined by ^1H NMR of the crude reaction mixture.

The reaction time is also influencing the ratio of monomer **147** to dimer **148** in the sense that short reaction times are leading to higher monomer to dimer ratios (Chart 4.2). Increased reaction times lead to reopening of the highly strained monomeric macrocycle **147**.

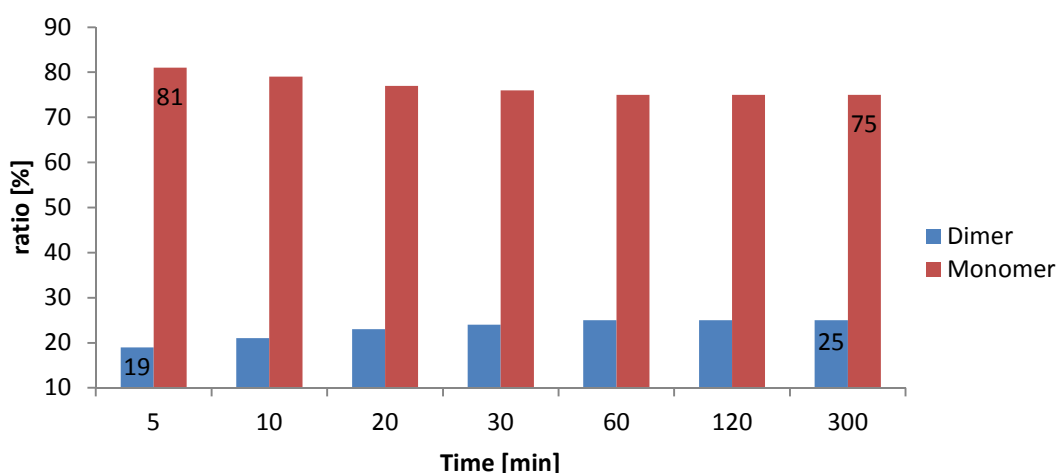


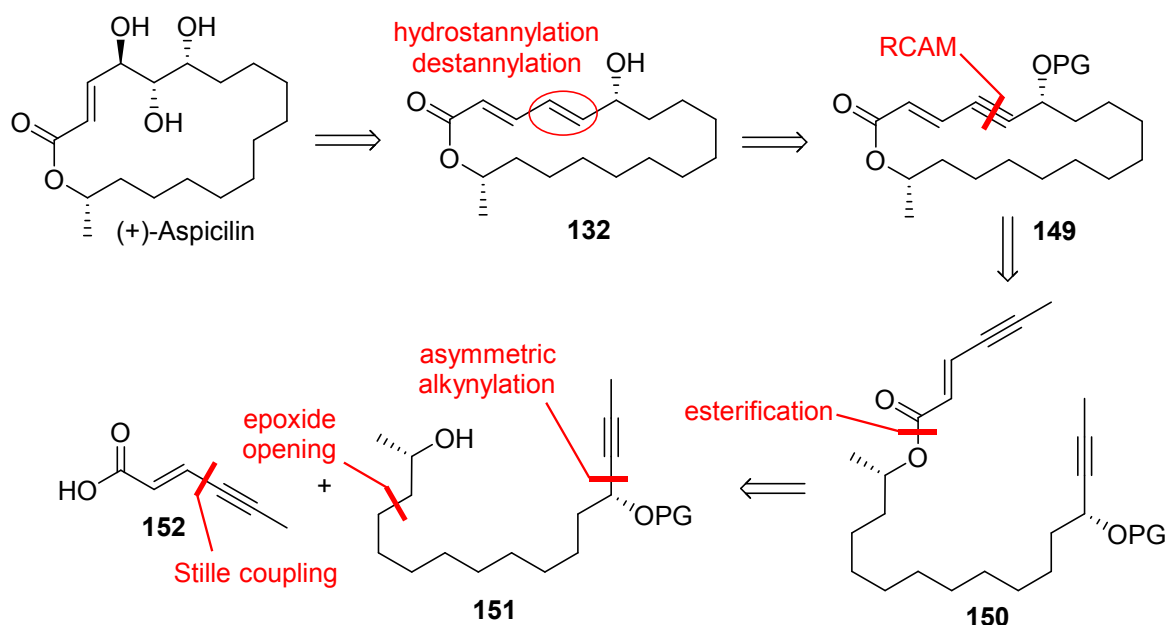
Chart 4.2: Time dependency of monomer **147** to dimer **148** ratio in RCAM reaction. Conditions: 10 mol% **28**, MS 5 Å, toluene 2.5 mM, 20 °C. The ratios were determined by ^1H NMR of the crude reaction mixture.

In conclusion, high temperatures and short reaction times favor the formation of the monomeric cycle **147**, providing crucial information towards our formal synthesis of (+)-Aspicilin.

4.3.2 Retrosynthetic Analysis of (+)-Aspicilin

We decided to target the known diene **132** of Oppolzer's synthesis of (+)-Aspicilin (Scheme 4.9).^[67] The diene motif was considered a result of a hydrostannylation/destannylation sequence from enyne **149**, utilizing the protocol recently developed in our group.^[5] The latter was proposed to derive from diyne **150**, which can be synthesized from alcohol fragment **151** and acid fragment **152** by esterification.

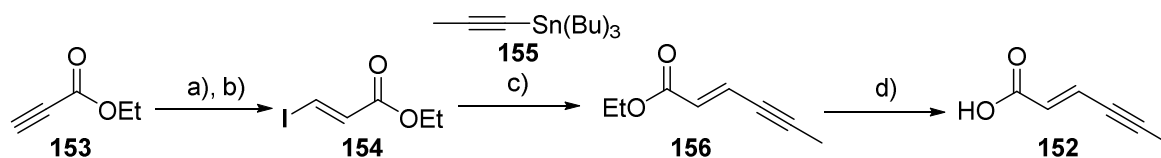
The intended acid fragment **152** can be constructed via Stille coupling based on a procedure described by Dr. Josep Llaveria Cros.^[85] For the alcohol fragment **151**, the secondary alcohol could be introduced by an epoxide opening. Furthermore, we envisaged that the propargyl alkyne could be introduced via asymmetric alkylation procedures.



Scheme 4.9: Retrosynthetic analysis of (+)-Aspicilin.

4.3.3 Synthesis of Fragments 151 and 152

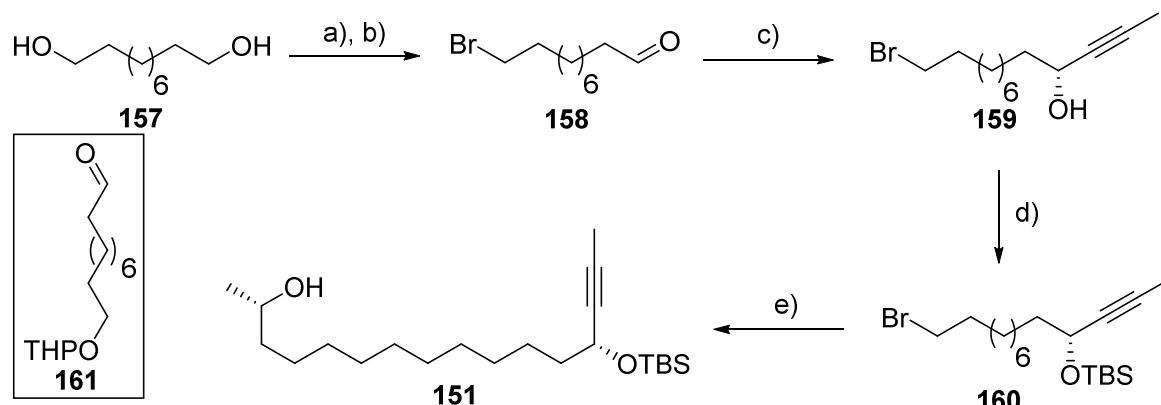
The synthesis of acid **152** starts from commercially available ethyl propiolate (**153**), which was converted to (*E*)-iodoacrylate **154** by an iodination/isomerization sequence (Scheme 4.10). The (*E*)-iodide **154** was submitted to a Stille cross-coupling with propynyl stannane **155**, which was synthesized according to literature^[86] to furnish (*E*)-enyne **156** which was hydrolyzed to obtain the target compound **152** in four steps with an overall yield of 64%.



Scheme 4.10: Synthesis of the acid fragment **152**. Conditions: a) NaI, MeCN, reflux; b) HI_{aq} , toluene, 80 °C, 77% over 2 steps; c) **155**, 4 mol% bis-(acetonitrile)-palladium(II)-chloride, DMF, rt, 91%; d) LiOH, $\text{H}_2\text{O}/\text{THF}/\text{EtOH}$ 5/5/1, rt, 91%.

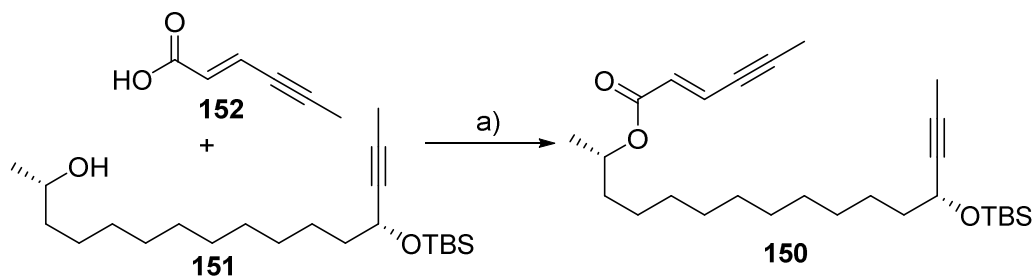
The synthesis of alcohol fragment **151** begins with diol **157**, which was converted to aldehyde **158** via mono bromination and subsequent oxidation, using a convenient procedure developed by Stahl and coworkers (Scheme 4.11).^[87] In an earlier version of our synthesis, we tried various conditions to introduce the alkyne on THP protected aldehyde **161**. Utilizing the methodology from Pu's group^[88], we could only achieve a moderate yield of 42%. Trost's Zn-propenol-catalyzed asymmetric alkyne addition^[89] furnished the target alkyne, with a low yield of 56% and an enantiomeric excess of only 81%. Carreira's alkynylation protocol^[90] led to acceptable yields of 65% and an excellent *ee* of 96%.

Therefore we utilized Carreira's alkynylation procedure^[90] without further screening. The alkyne was introduced with a high enantiomeric excess of 94% using (+)-*N*-methylephedrine as a chiral additive.^[90] The propargylic alcohol **159** was isolated with a moderate yield of 65%, due to partial *N*-alkylation of (+)-*N*-methylephedrine by bromides **158** and **159**. Alcohol **159** was TBS protected to furnish TBS-ether **160**. The hydrocarbon chain of TBS-ether **160** was elongated by a copper-catalyzed epoxide opening reaction to yield the desired alcohol **151** in five steps with an overall yield of 30%.



Scheme 4.11: Synthesis of the alcohol fragment **151**. Conditions: a) HBr_{aq} , toluene, reflux, 73%; b) 5 mol% $\text{Cu}(\text{MeCN})_4(\text{PF}_6)$, bpy, NMI, TEMPO, MeCN, air, rt, quant.; c) propyne, (+)-*N*-methylephedrine, $\text{Zn}(\text{OTf})_2$, NEt_3 , toluene, rt, 65%, 94% *ee*; d) TBSCl, imidazole, CH_2Cl_2 , 0 °C to rt, 90%; e) Mg, I_2 (cat.), THF, reflux; then 4 mol% Li_2CuCl_4 , (*S*)-propylene oxide, THF, 0 °C, 71%.

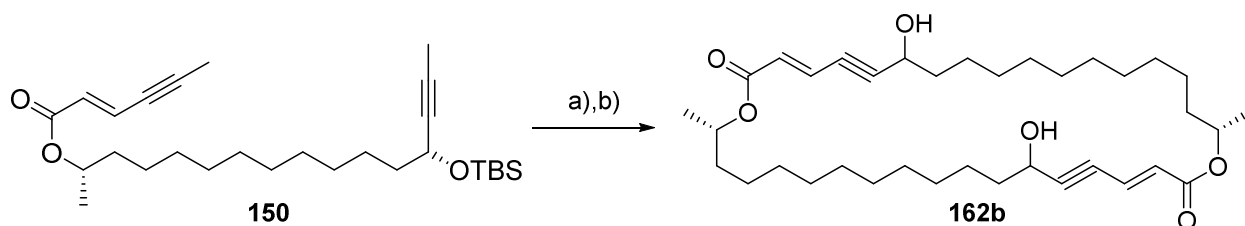
Esterification of alcohol **51** and acid **152** under standard conditions proceeded uneventfully to yield metathesis precursor **150** (Scheme 4.12).



Scheme 4.12: Coupling of alcohol fragment **151** and acid fragment **152** to metathesis precursor **150**. Conditions: a) DCC, DMAP, CH₂Cl₂, 0 °C, 93%.

4.3.4 Ring Closing Alkyne Metathesis

The RCAM key step needed some optimization. Our first attempt, in which we tried to close the macrocycle at room temperature, furnished the cyclic dimer **162b** after deprotection as the main product with 58% yield over both steps (Scheme 4.13).



Scheme 4.13: Initial RCAM of diyne **150** with non-optimized conditions. Conditions: a) 10 mol% [(Ph₃SiO)₃Mo≡CC₆H₄OMe] **28**, MS 5 Å, toluene, rt, 2h; b) TBAF, THF, rt, 58% over 2 steps.

We applied the knowledge from our model studies and screened different temperatures and reaction times for the RCAM reaction of diyne **150**. The ratio of monomer **149a** to dimer **149b** was improved to 3 to 1 when the reaction was run at 110 °C for one hour. By optimizing the reaction time, the monomer to dimer ratio could further be improved to 12 to 1 (Chart 4.3).

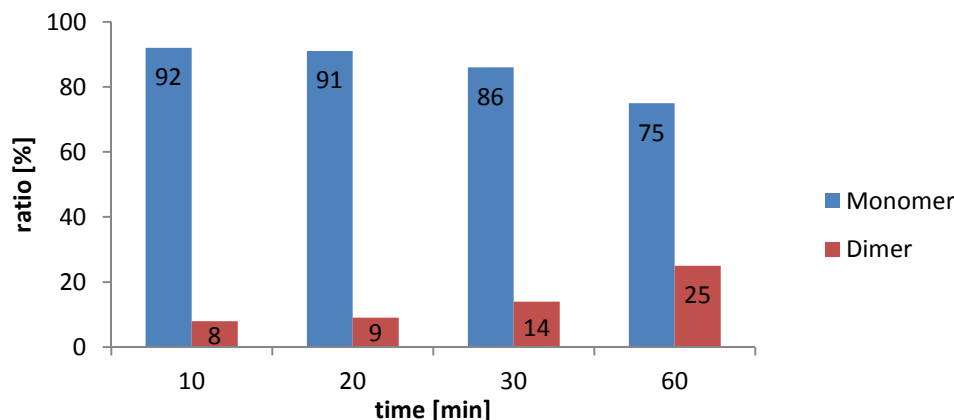
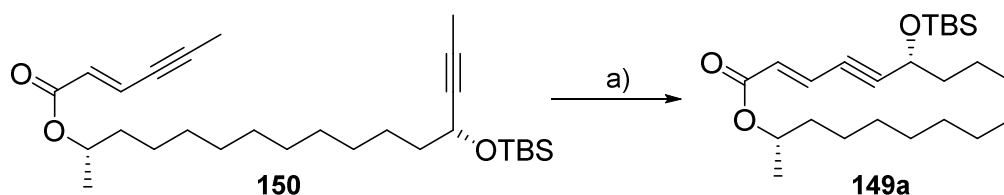


Chart 4.3: Time dependency of monomer **149a** to dimer **149b** ratio in RCAM reaction. The reactions were carried out with 20 mol% $[(\text{Ph}_3\text{SiO})_3\text{Mo}\equiv\text{CC}_6\text{H}_4\text{OMe}]$ **28** at 110 °C. Ratios were determined by HPLC.

With the optimized conditions in hand we could successfully close the macrocycle on a 500 mg scale to yield the desired enyne **149a** in 78% isolated yield (Scheme 4.14).

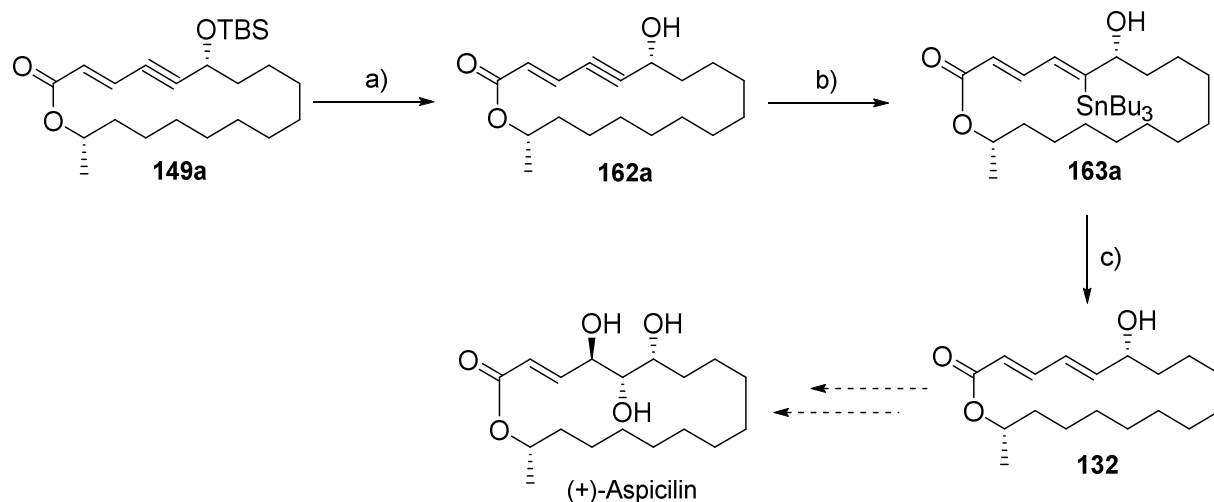


Scheme 4.14: Optimized conditions for the formation of cyclic enyne **149a** via RCAM. Conditions: a) 10 mol% $[(\text{Ph}_3\text{SiO})_3\text{Mo}\equiv\text{CC}_6\text{H}_4\text{OMe}]$ **28**, MS 5 Å, toluene, 110 °C, 78% (monomer to dimer = 12 : 1).

4.3.5 Completion of the Formal Synthesis of (+)-Aspicilin

To complete the synthesis, we deprotected the macrocycle **149a** to yield enyne **162a** with a free hydroxy group in the propargylic position which was needed as a directing group for the *trans*-hydrostannylation step (Scheme 4.15). Literature studies have indicated that alkynes as part of an 1,3-enyne motif are challenging substrates to address by Ru-catalyzed *trans*-additions.^[91] These difficulties are caused by the high affinity of the electron rich 1,3-enyne moiety engaging its 4π electrons in coordination to the ruthenium center. However, the problem can be addressed with a hydroxy group adjacent to the alkyne. This can be explained by hydrogen bonding between the –OH group and the chlorine anion of the catalyst $[\text{RuCp}^*\text{Cl}]_4$, which favors the binding of the proximal alkyne over the competing 1,3-enyne.^[91] The hydrostannylation proceeded with excellent regioselectivity and furnished

only the proximally stannylated products **163a** and **163b** (Figure 4.2) with a good *cis/trans* selectivity of 12.5 : 1. The formal synthesis was completed by destannylation of *trans*-stannane **163a** with CuTC to yield Oppolzer's (*E,E*)-diene intermediate **132**.



Scheme 4.15: *Trans*-hydrostannylation/destannylation sequence to reduce enyne **149a** to (*E,E*)-diene **132**. Conditions: a) TBAF, THF, 0 °C to rt, 85%; b) 2 mol% [RuCp*Cl]₄, HSnBu₃, CH₂Cl₂, rt, 66% (crude ratio of stereoisomers: 12.5 to 1); c) CuTC, DMF, rt, 83%.

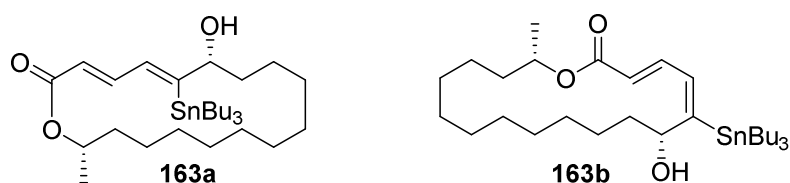


Figure 4.2: *Trans*-hydrostannylation products **163a** and **163b**.

4.4 Conclusion

We managed to complete our formal synthesis of (+)-Aspicilin in 14 steps and ten steps in the longest linear sequence from commercially available 1,10-decanediol (**157**) with an overall yield of 10%. The synthesis illustrates how important a strict control of temperature and reaction time is for the monomer-to-dimer ratio in RCAM reactions. Furthermore, it shows that *trans*-hydrostannylation can be performed on macrocyclic 1,3-enynes with excellent regioselectivity and good stereoselectivity.

5 Synthesis of Stapled Peptides via Alkyne Metathesis

5.1 Introduction

5.1.1 Small Molecules, Biologics, and Peptides as Drugs

Almost all therapeutic agents currently used as pharmaceuticals can be classified as either small molecules or “biologics”.^[3] Small molecules, compounds with a mass below ca. 500 Da, are typically able to penetrate through the cell membrane.^[92] Their targets are often proteins with hydrophobic binding pockets. If the target protein has a shallow surface small molecules cannot interact effectively. In such cases, protein-based molecules (biologics) with a molecular mass above 5 kDa can be designed that bind to the target protein’s surface. However, biologics can only be used for extracellular applications since they are not capable of penetrating the cell membrane. Due to these macromolecules’ inability to pass through the cell membrane as well as the incapability of small molecules to address certain proteins, there exist numerous intracellular targets that cannot be addressed. Peptide-based drugs have the potential to close this gap since they have excellent surface recognition properties and a lower toxicity compared to small molecule therapeutics.^[3, 93] However, it is necessary to chemically stabilize the bioactive peptide conformation since peptides otherwise adopt a flexible conformation in solution, which leads to low cell membrane permeability and proteolytic instability.

Peptide based pharmaceuticals are important, with currently more than 60 FDA-approved peptide products on the market, approximately 140 in clinical trial, and more than 500 in preclinical study.^[94] Amongst the most widely used peptide based drugs is Copaxone for the treatment of multiple sclerosis, Lupron and Zoladex for breast and prostate cancer therapy, and Sandostatin which is used for the treatment of acromegaly and cancer.^[92] The importance of these compounds is illustrated by the sales of each compound exceeding 1 billion dollars annually.

5.1.2 Small GTPases Addressed by Stapled Peptides

Small GTPases are a group of pharmaceutically relevant targets, which have proven difficult to address.^[95] Even though the pharmaceutical industry and academia put a lot of effort in

the development of efficient modulators to address small GTPases, no approved drugs are available so far.^[95g] Rab proteins, a subfamily of the small GTPases, are important regulators of intracellular vesicular transport and trafficking. They are regulated through protein-protein interactions and play an important role in neurodegenerative diseases and various forms of cancer.^[4, 96] Waldmann and coworkers could show that Rab-GTPases can be effectively targeted with hydrocarbon-stapled peptides generated via RCM.^[4]

5.1.3 Overview of Methodologies to Generate Stapled Peptides

Since α -helical moieties of proteins are involved in many protein-protein interactions, their stabilization in smaller bioactive peptide derivatives has been established with a variety of methods, for example side-chain cross-linking.^[3, 97] Some of these methodologies can be applied to peptides with only natural amino acids in their sequence, such as the formation of lactam-bridges between lysine and aspartic acid^[98] as schematically shown in amide **164**, disulfide bridges between two cysteine moieties^[99] like in disulfide **165**, cross-linkers between two cysteine sidechains^[100] as demonstrated by bipyridine **166**, and cross-linkers between two lysine moieties^[101] as in amide **167** (Figure 5.1).

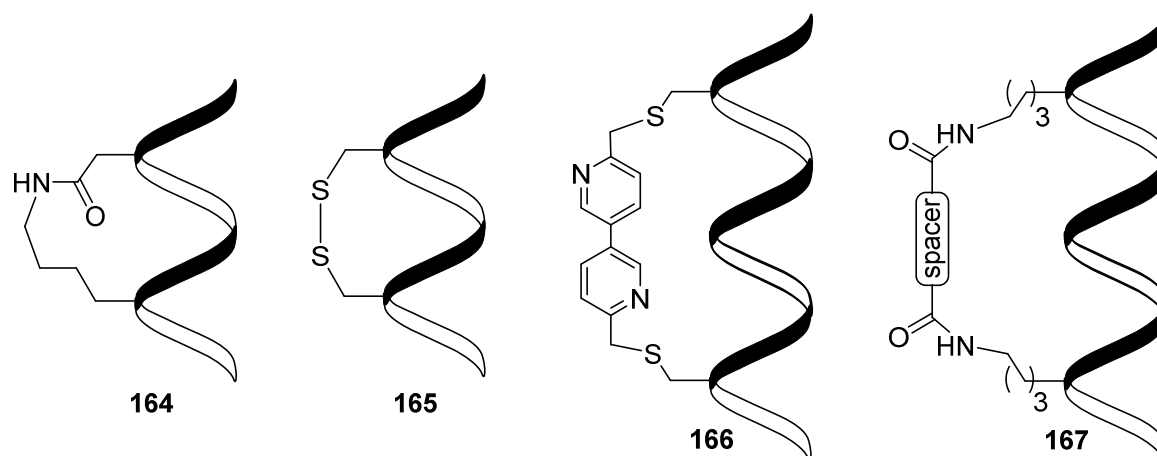


Figure 5.1: Different approaches to stapled peptides by utilizing only natural amino acids in the peptide chain.

Furthermore, there are several approaches using unnatural amino acids to generate stapled peptide structures, amongst which are azide-alkyne cycloaddition^[102] as shown in triazole **168**, C–H activation of tryptophan and coupling with iodo tyrosine or iodo phenyl-alanine^[103] as shown in indole **169**, olefin-bridges formed via RCM between two modified serine moieties^[104] like in olefin **170**, and all-hydrocarbon olefin-bridges formed via RCM spanning one or two turns of the α -helix as in peptides **171** or **172** respectively (Figure 5.2).^[105]

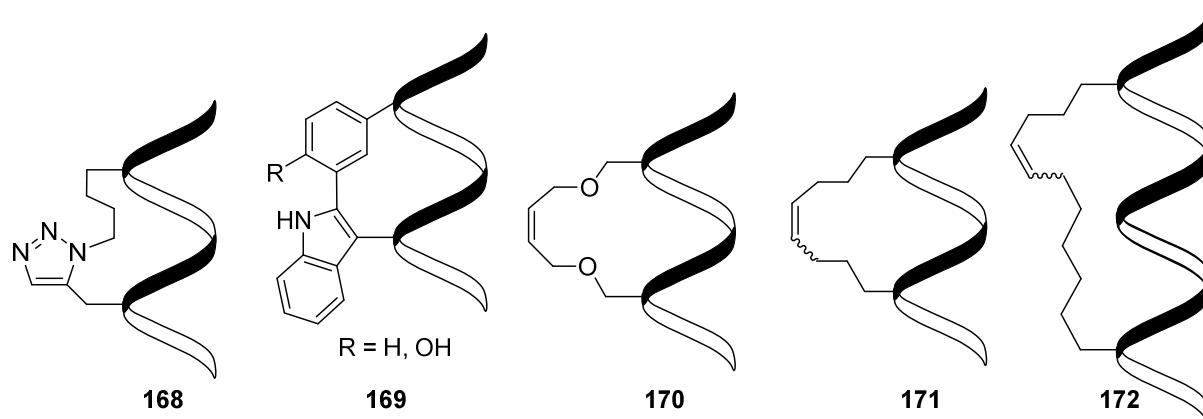


Figure 5.2: Different approaches to stapled peptides by utilizing unusual amino acids in the peptide chain.

5.2 Aims and Scope

Even though there already exists a variety of methods to generate stapled peptides, seen in the light of possible applications in pharmaceuticals, it seems worthwhile to establish further methodologies. Stapled peptides can be generated through RCM (Chapter 5.1). However, unlike RCM, RCAM still has to be demonstrated as a suitable reaction for this cause. Additionally, once RCAM is capable of peptides stapling, the alkyne moiety would serve as a useful handle for further functionalization of the macrocycles. Finally, with both forms of metathesis successful in the formation of macrocyclic peptides, one can imagine the selective formation of bicyclic structures where one ring is closed via RCM and the other ring via RCAM. Based on these ambitions, we sought to synthesize hydrocarbon-stapled peptides and study their effects on Rab-GTPase.

5.3 Stapled Peptides via Alkyne Metathesis

5.3.1 RCAM of Immobilized Alkynes

The peptides used in this work were synthesized on solid-support using the Fmoc-strategy.^[106] They were bound to the solid support with Rink amide linkers.^[106] We first evaluated different solid support materials concerning their compatibility with the RCAM reaction (Figure 5.3). All resins needed to be dried by suspending them in toluene over MS 5 Å for four days, while exchanging the solvent daily. The best results concerning RCAM conversions were observed when using a polystyrene based solid support with a polyethylene glycol linker as in amine **175** to which the Rink amide was attached. Solid supports in which the Rink amide was directly attached to either a polyethylene glycol core

like in amine **173** or a polystyrene core as shown in compound **174** resulted in low conversions. One explanation could be that through the ethylene glycol linking chain the peptide is further away from the polymeric support, thereby increasing the accessibility for the metathesis catalyst.

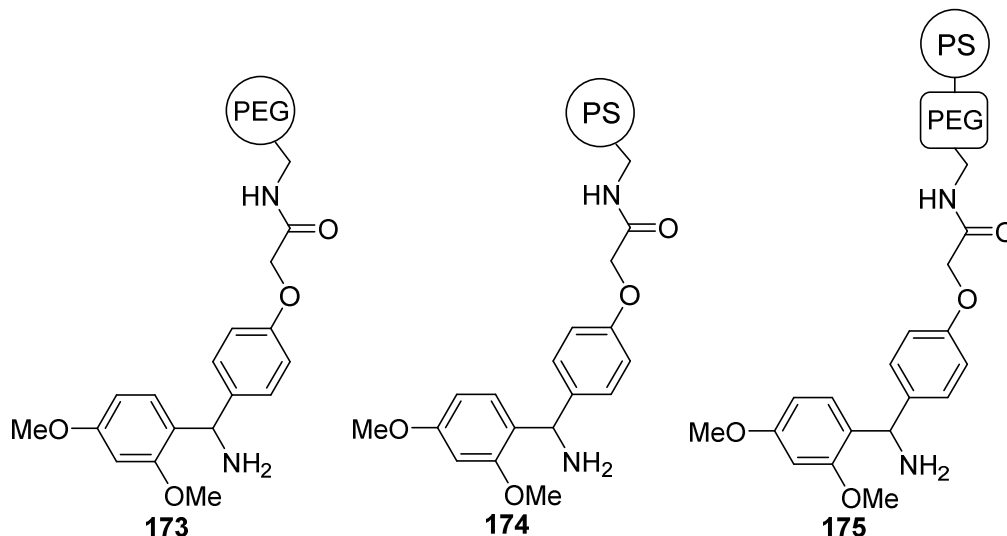


Figure 5.3: Different solid supports with Rink amide linkers.

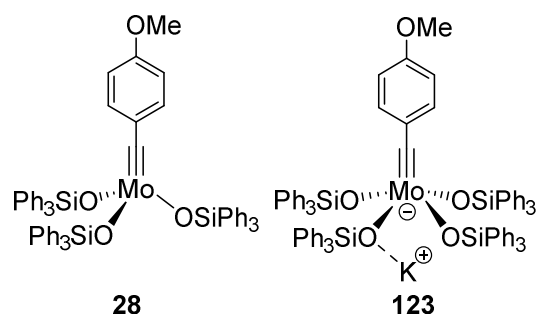
In order to prove the robustness of our methodology, we performed the RCAM on peptide **176a** (Figure 5.4) that contained all functionalities present in the 20 proteinogenic amino acids (Table 5.1). Impressingly the metathesis reaction proceeded smoothly, but it was necessary to use 1.5 equivalents of catalyst **28** to reach full conversion. This is probably due to residual moisture in the solid support and technical problems when handling very small amounts of the catalyst. The neutral complex **28** led to better results than the ate-complex **123**, which might be explained by unfavorable interactions of the charged species **123** with the highly functionalized peptide **176a**.

Table 5.1: Comparison of different solid supports and alkyne metathesis catalysts for the RCAM of peptide **176a**. The reactions were performed in 0.15 mL of dry toluene in the presence of MS 5 Å in a flame-dried Schlenk tube under argon for 3 h at 40 ° C. Conversions were determined by LC-MS.

resin	conversion ^[a] [%]	conversion ^[b] [%]
PS PEG	complete	12
PEG	36	0
PS	16	0

[a] 1.5 eq. of complex **28** according to resin loading

[b] 1.5 eq. of complex **123** according to resin loading



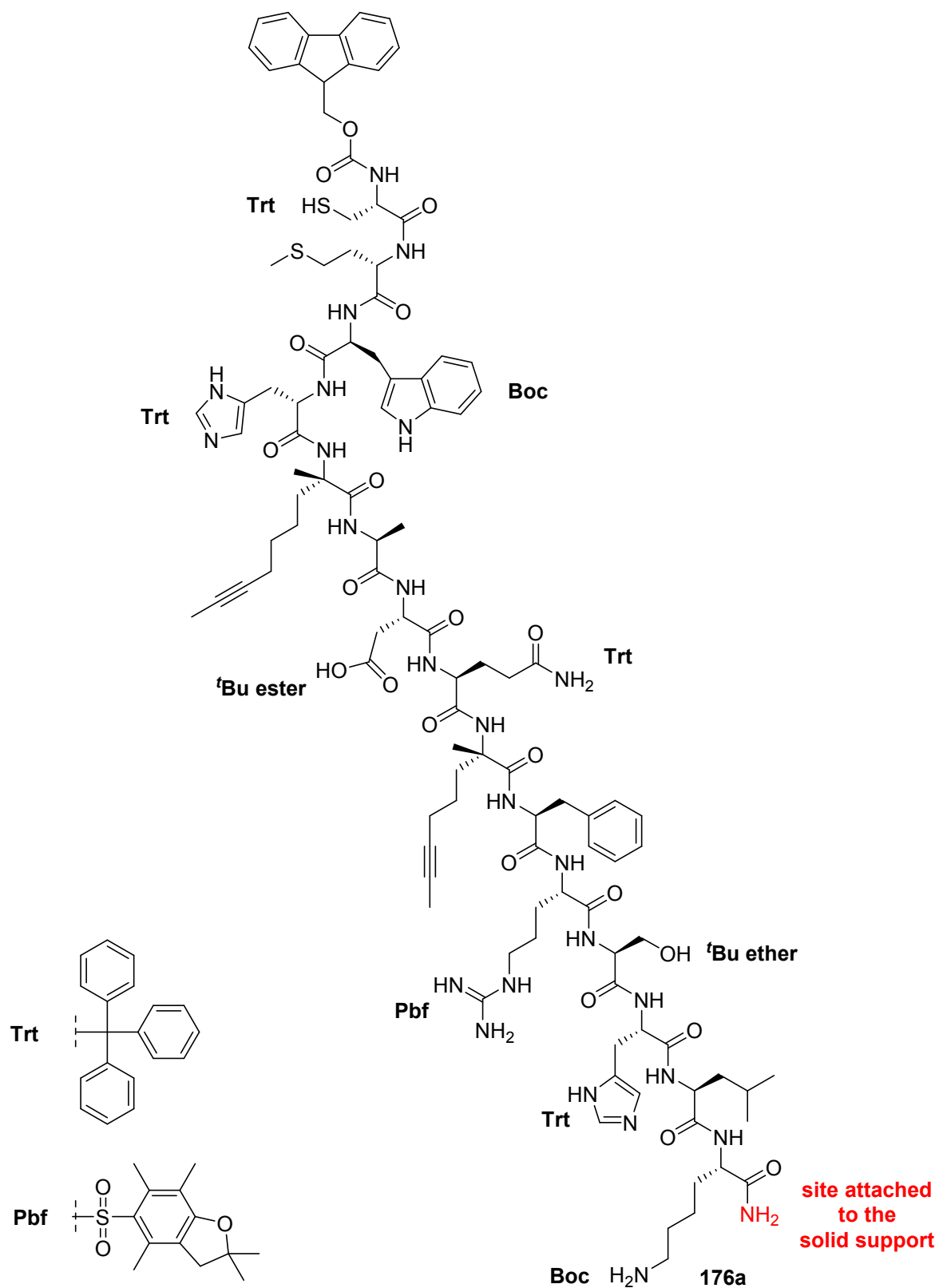
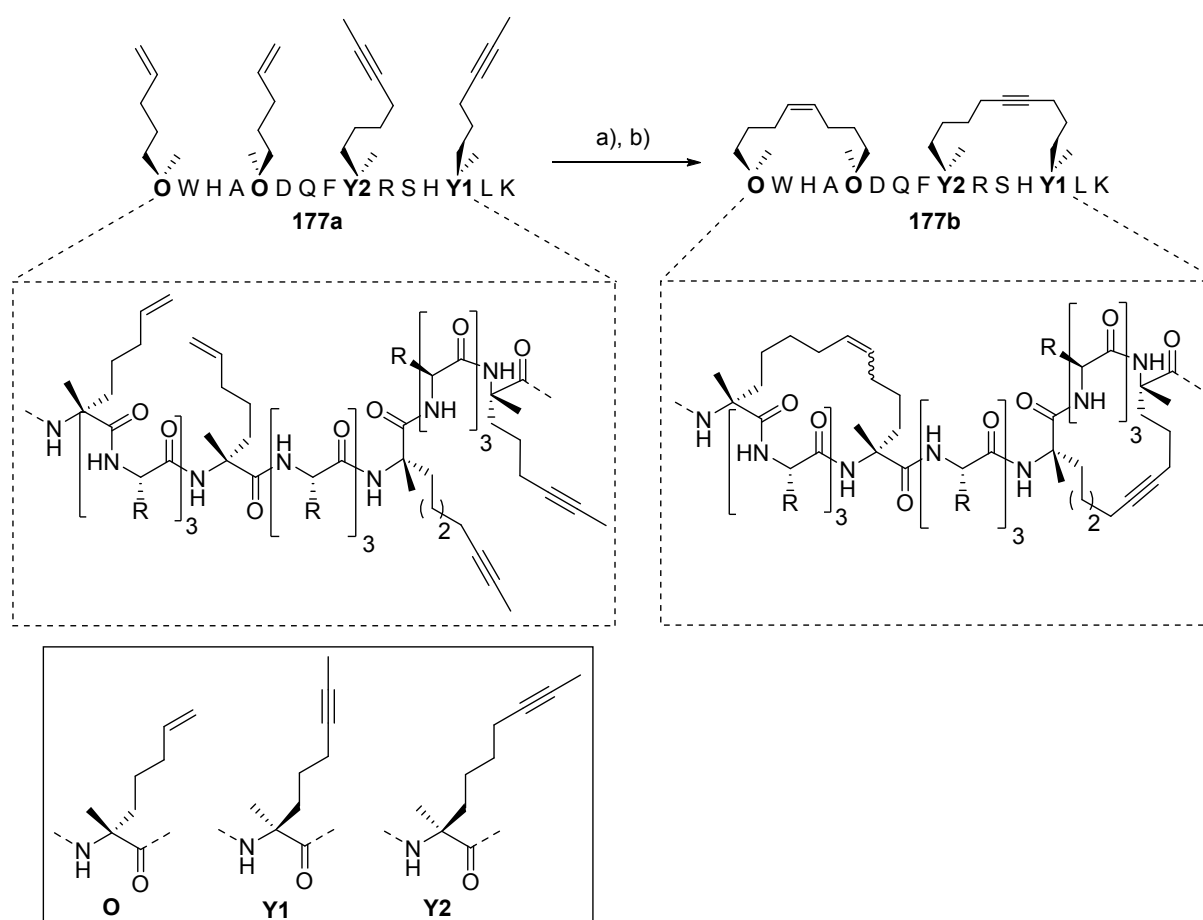


Figure 5.4: Test peptide **176a** for the RCAM reaction on solid support. The protecting groups that were present during metathesis reaction are indicated. The shown structure corresponds to the peptide that is isolated after cleavage from the solid support prior to running the RCAM reaction.

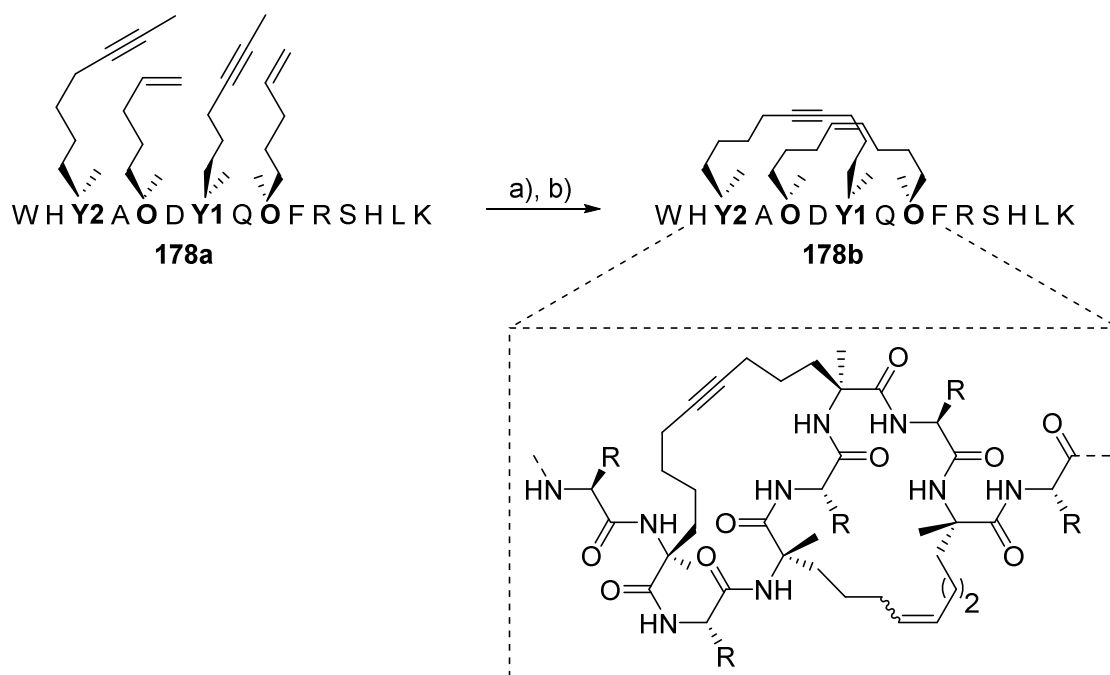
5.3.2 Bicyclic Peptides via Orthogonal RCM and RCAM

With suitable RCAM conditions in hand, we established a methodology to chemo- and regioselectively generate bicyclic peptides via a combination of RCM and RCAM (Scheme 5.1).^[107] Starting from solid support bound peptide **177a** containing two alkyne-functionalized building blocks **Y1/Y2** and two olefin-functionalized amino acids **O**, the bicyclic peptide **177b** was selectively generated through a one-pot RCM/RCAM procedure. Test peptide **177a** was designed to contain all functionalities of proteinogenic amino acids, excluding sulfur containing amino acids.



Scheme 5.1: Synthesis of an adjacent bicyclic peptide **177b** via tandem RCM and RCAM in a one-pot reaction. R = side chain of a proteinogenic amino acid except Cys or Met. Conditions: a) Alkyne metathesis catalyst **28**, Grubbs 1st generation catalyst, toluene, 40 °C, 2 × 1.5 h. b) cleavage from solid support and deprotection. The experiments were conducted by P. Cromm.

It was even possible to selectively generate the intertwined bicyclic peptide **178b** starting from immobilized peptide **178a** with alternating alkyne- and olefin-containing amino acids in the chain (Scheme 5.2).^[107] This led to an edge-on bicyclic structure with a more constrained geometry.



Scheme 5.2: Synthesis of intertwined bicyclic peptide **178b** via tandem RCM and RCAM in a one-pot reaction. R = side chain of a proteinogenic amino acid except Cys or Met. Conditions: a) Alkyne metathesis catalyst **28**, Grubbs 1st generation catalyst, dry toluene, 40 °C, 2 × 1.5 h. b) cleavage from solid support and deprotection. The experiments were conducted by P. Cromm.

5.3.3 Biological Evaluation of Alkyne Stapled Peptides

In order to evaluate the biological affinity of alkyne stapled peptides, the Waldmann group synthesized a row of monocyclic and bicyclic peptides with different architectures and compared their binding affinity towards the small GTPase Rab8a (GppNHp) (see Chapter 5.1.2).^[107] The sequence and architecture of those peptides is based on the interaction motif of Rab6 interacting protein wt-R6IP. **wtRIP**, an unmodified sequence of Rab6-interacting protein wt-R6IP, was shown to bind the small GTPase Rab8a with moderate affinity (Table 5.2, Entry 1). However, **StRIP3**, a hydrocarbon-stapled monocyclic peptide, whose sequence resembles that of **wtRIP**, shows a 5-fold improvement in binding affinity compared to **wtRIP** (Table 5.2, Entry 2).^[4] Building upon this knowledge, analogue **179b**, an alkyne stapled monocyclic peptide, showed a 10-fold improvement in binding affinity compared to **wtRIP** (Table 5.2, Entry 3). More Impressingly, bicyclic peptide derivatives **180b** and **181b** showed even further improvement relative to their monocyclic analogs **179b** and **StRIP3** (Table 5.2, Entry 4, 5). Bicyclic peptide **180b** is so far the most potent binder of an activated Rab GTPase.

Table 5.2: a) Affinity of wild-type sequence of Rab6 interacting protein **wtRIP** (aa 900 – 916) and mono-alkene **StRIP3**, mono-alkyne **179b** and bicyclic peptide derivatives **180b**, **181b** towards Rab8a₆₋₁₇₆(GppNHp). The affinities towards Rab8a₆₋₁₇₆(GppNHp) were determined by fluorescence polarization assays (rel. $K_d = K_d/K_d$ [StRIP3]); b) Sequence of peptide **180b**, the most potent binder to an activated Rab GTPase known. The experiments were conducted by P. Cromm.

a)

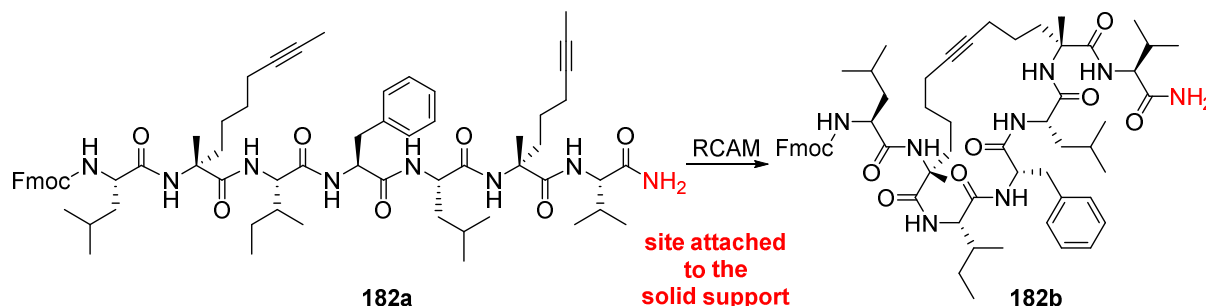
entry	peptide	aa 903	aa 907	aa 911	aa 915	rel. K_d	K_d [μ M]
1	wtRIP	K	L	L	A	n.d.	102 \pm 6.7
2	StRIP3	O	O	L	A	1.00	20.7 \pm 0.7
3	179b	Y2	Y2	L	A	0.40	10.7 \pm 0.5
4	180b	O	O	Y1	Y2	0.27	6.6 \pm 0.4
5	181b	Y1	Y2	O	O	0.42	9.6 \pm 0.4

b)

DDEOEQFOYHLY1SFNY2V **180b**

5.4 Functionalization of Immobilized Alkynes

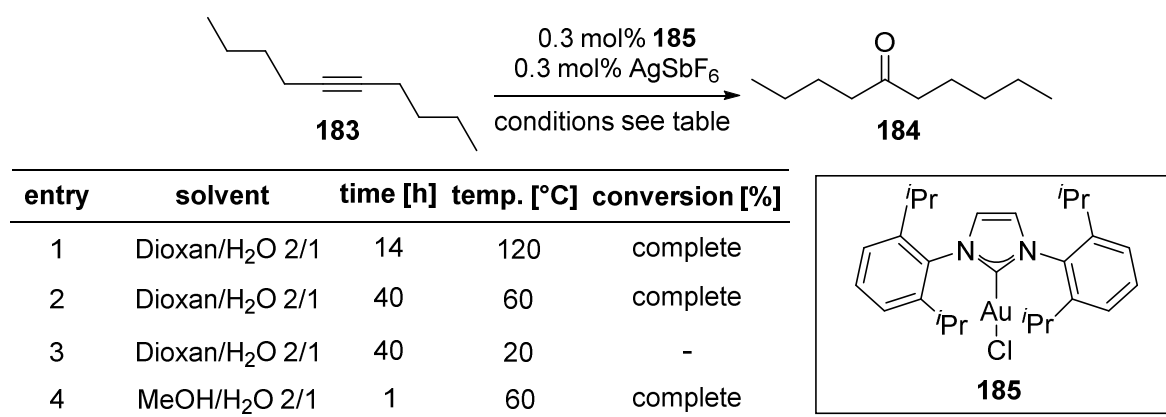
Our next goal was to establish conditions to functionalize the triple bond generated via RCAM. Towards this end, hydration, azide-alkyne cycloaddition, Pauson-Khand reaction, hydrostannylation, hydroborylation, and dibromination reactions were envisioned on alkyne containing peptides. With these reactions interesting approaches to further modify the stapled peptides could be accomplished. In order to find suitable reaction conditions and limit incompatibilities with the amino acid side chains, we used the simplified test peptide **182b** (Scheme 5.3).



Scheme 5.3: Test peptide **182b** for alkyne functionalization reactions on solid support. The shown structures correspond to the peptides which are isolated after cleavage from the solid support. RCAM conditions: catalyst **28**, toluene, 40 °C, 3 h.

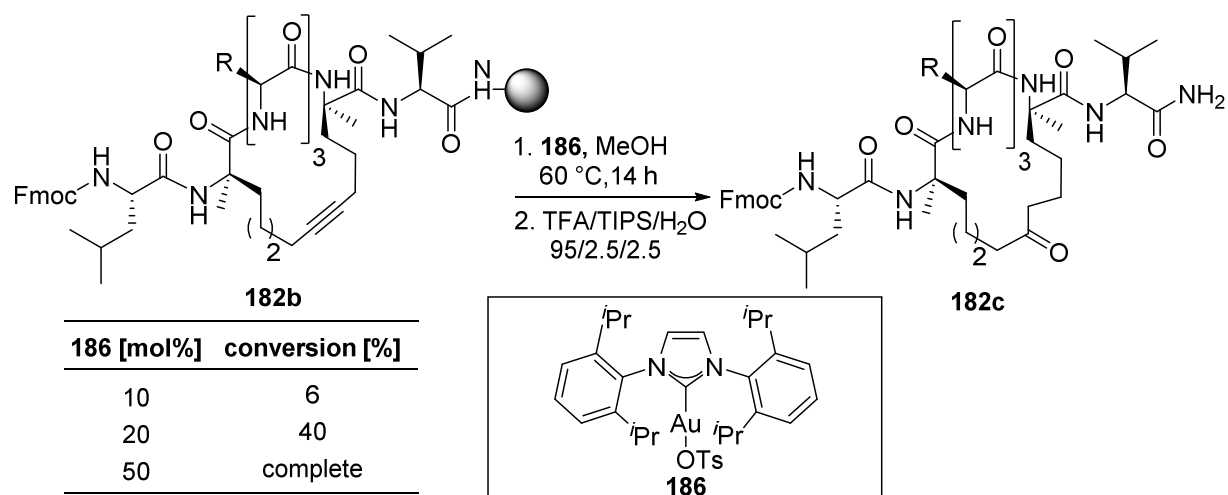
5.4.1 Gold-Catalyzed Hydration

In order to hydrate the alkyne, we used a gold-catalyzed methodology developed by Nolan and coworkers.^[108] The reaction is normally performed at 120 °C which would be troublesome for the peptide's stability. Therefore we first screened different reaction conditions with 5-decyne as a test substrate (Scheme 5.4). The experiments revealed that the reaction is also possible at 60 °C when the reaction times are increased (Scheme 5.4, Entry 1-3). The solid support showed better swelling properties in MeOH compared to 1,4-dioxane, therefore the reaction was run in MeOH/H₂O (2/1), which lowered the reaction time significantly (Scheme 5.4, Entry 4).



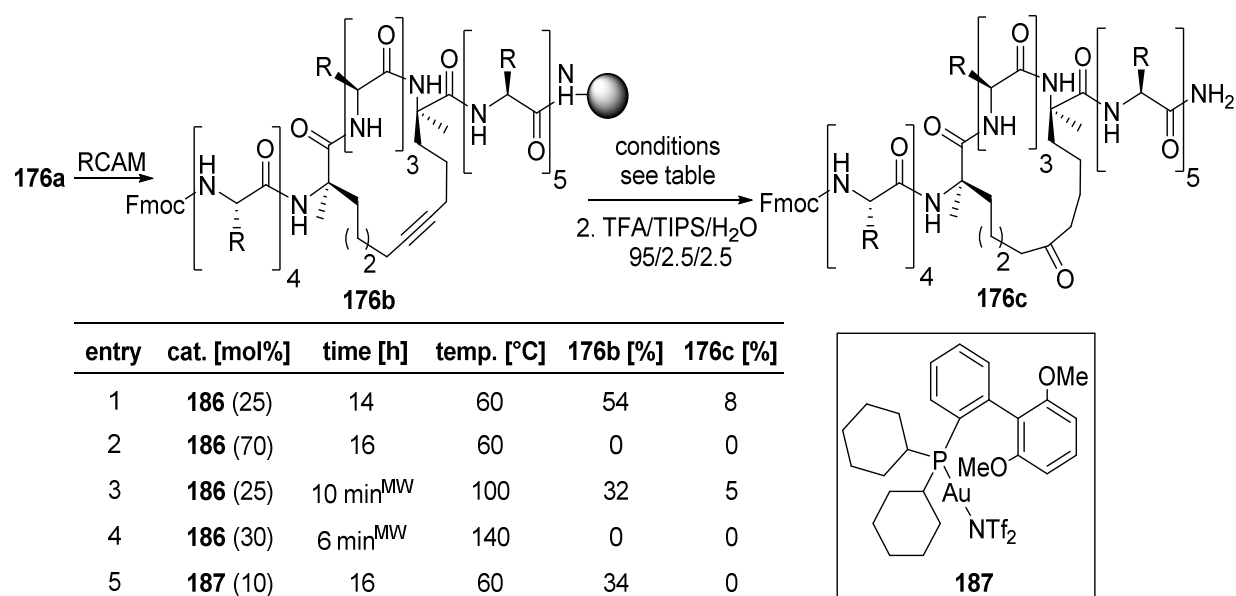
Scheme 5.4: Condition screening for the gold-catalyzed hydration of alkynes. Conversions were monitored by GC-MS.

Gold-catalyst **186**, which was generated from complex **185** by treatment with silver *p*-toluenesulfonate according to the literature^[109], was used for the hydration of test peptide **182b** (Scheme 5.5). The reaction was performed in pure MeOH since water prevented the solid support from swelling properly. In order to achieve full conversion, the catalyst loading had to be increased to 50%. The reaction proceeded smoothly to achieve the target peptide **182c** after cleavage from the solid support. LC-MS did not reveal any regioselectivity.



Scheme 5.5: Gold-catalyzed hydration of test peptide **182b**. The side chains R are defined in Scheme 5.3. Conversions were determined by LC-MS.

The same conditions were applied to the more complex peptide **176b** but the desired product **176c** was only generated in trace quantities (Scheme 5.6). The reactions mainly lead to extensive decomposition (Scheme 5.6, Entry 1, 2). This can perhaps be attributed to the high density of functional groups present in peptide **176b** which can interact with the gold catalyst. The long reaction time could be one reason for decomposition; therefore the reaction was tried in a microwave reactor with superheated solvent and shorter reaction time (Scheme 5.6, Entry 3, 4). However, these changes did not improve the reaction outcome either. Additionally, a more electrophilic gold complex **187** was used, hypothesizing that this would increase the affinity towards the alkyne but only starting material and extensive decomposition was observed (Scheme 5.6, Entry 5).

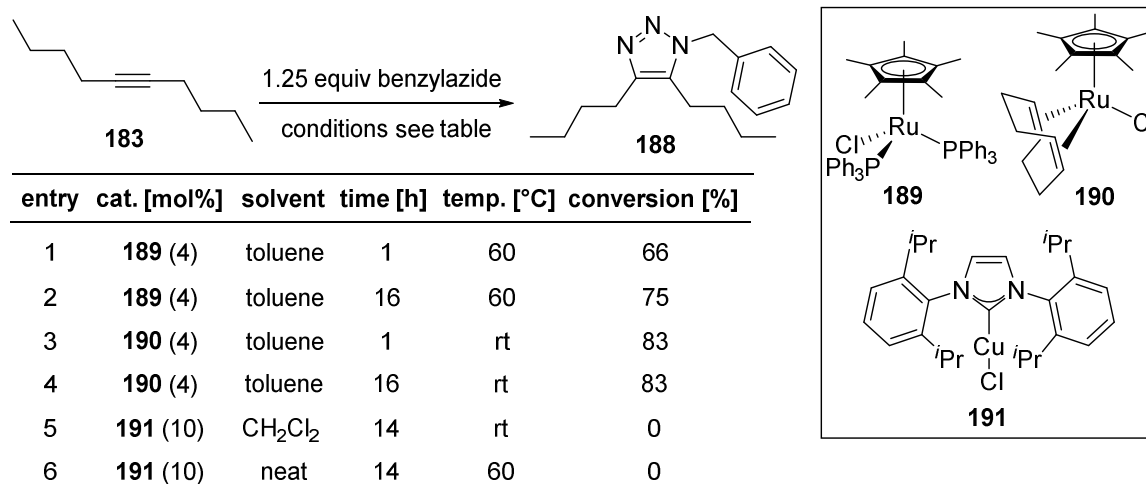


Scheme 5.6: Gold-catalyzed hydration of test peptide **176b**. The side chains R are defined in Figure 5.4. For RCAM conditions see Table 5.1. The reactions yielded complex mixtures that were analyzed by LC-MS.

Even though the hydration methodology can be used on immobilized peptides, certain amino acids seem to deactivate the catalyst and lead to decomposition. It is likely that the S-containing methionine binds to the gold catalyst.

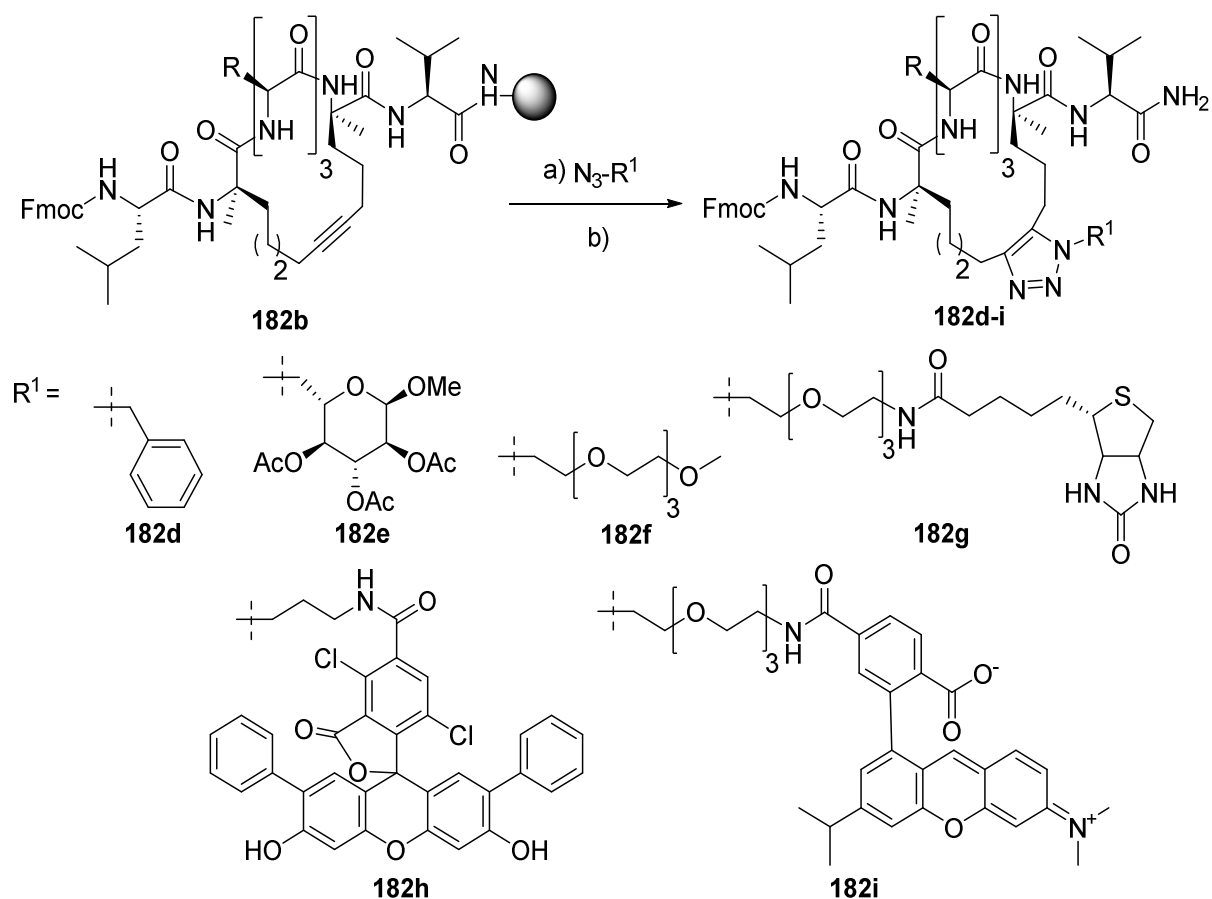
5.4.2 Azide-Alkyne Cycloaddition

Another versatile way to functionalize alkynes is through azide-alkyne cycloaddition (AAC).^[110] Terminal alkynes are the substrates of choice, whereas there are far less reports in the literature for unstrained internal alkynes. 5-Decyne (**183**) was employed as a test substrate to evaluate suitable methods, such as a ruthenium-AAC methodology developed by Fokin and coworkers.^[110b] When phosphine-based ruthenium-catalyst **189** was used at 60 °C, moderate conversions and significant (20%) amounts of a (*E*)-*N*-benzyl-1-phenylmethanimine were observed (Scheme 5.7, Entry 1, 2). Ruthenium-COD catalyst **190** allowed the reaction to proceed at room temperature and led to good conversions already after 1 h reaction time (Scheme 5.7, Entry 3, 4). Attempts to utilize a copper-catalyzed AAC methodology developed by Nolan and coworkers^[111] failed with CuIPr catalyst **191** (Scheme 5.7, Entry 5, 6).



Scheme 5.7: Condition screening for the ruthenium-catalyzed azide alkyne cyclization. Conversions were monitored by GC-MS.

With suitable conditions in hand, several structural motifs were successfully coupled to peptide **182b** leading to benzyl derivative **182d**, sugar derivative **182e**, PEG derivative **182f** and biotin derivative **182g** (Scheme 5.8). Coupling of dye-containing azides did not give the desired products **182h** and **182i**, probably due to unfavorable interactions of the Ru-catalyst with the aromatic moiety of the dye molecules.



Scheme 5.8: Ruthenium-AAC to couple various azide-containing structural motifs to test peptide **182b**. The side chains R are defined in Scheme 5.3. Conditions: a) **190**, toluene, 60 °C; b) TFA/TIPS/H₂O (95/2.5/2.5), rt. The reactions were monitored via LC-MS.

All attempts to apply the azide-alkyne cyclization protocol to the highly functionalized test peptide **176b** failed. In this case many decomposition products and residual starting material were observed.

5.4.3 Further Functionalization Attempts

We further managed to successfully dibrominate^[112] the alkyne in a monocyclic peptide with CuBr₂. Our attempts to functionalize the alkyne via Pauson-Khand^[113] reaction failed under all tested conditions and only led to decomposition. Hydrostannylation^[5, 91] led to extensive material loss, probably due to residual water in the solid support which caused the decomposition of the ruthenium-catalyst while generating HCl, which cleaved the peptide off the solid support during the reaction.

5.5 Conclusion

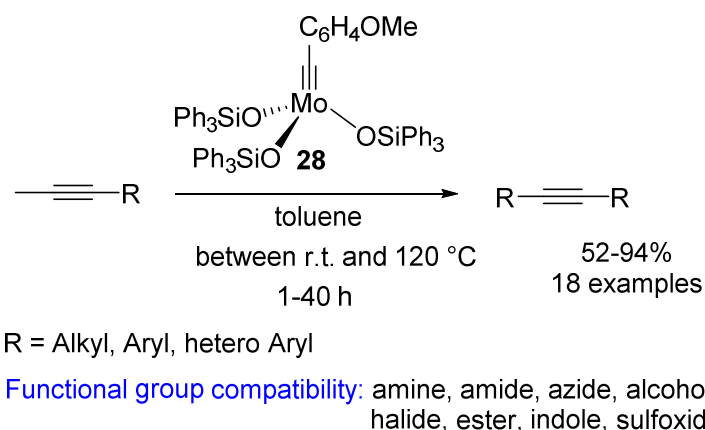
In conclusion we have demonstrated that RCAM can be applied to immobilized peptides to generate macrocycles. Impressingly all (protected) functionalities present in the 20 proteinogenic amino acids were tolerated. Additionally, we successfully accomplished the synthesis of adjacent and intertwined bicyclic peptides via tandem RCM and RCAM reactions. The immobilized alkynes were further functionalized via hydration, azide-alkyne cycloaddition or dibromination. However, it seems that certain amino acids are not tolerated. In order to get a clearer picture, further experiments with different amino acid combinations in the sequence are needed.

6 Summary and Conclusion

The last couple of years have seen considerable progress in alkyne metathesis. This development led to catalysts with remarkable activity and functional group tolerance as demonstrated in highly elaborate applications.^[1] However, despite these advances there are still unmet needs in the field. The objective of this thesis was therefore to develop new alkyne metathesis catalysts and extend the scope of application for this transformation.

1) Extended substrate scope of catalyst **28**

The latest generation of siloxy-based alkyne metathesis catalysts developed in the Fürstner group has proven its quality in a wide range of applications in total synthesis.^[1] However, the functional group tolerance was so far not comprehensively screened, leaving out some synthetically interesting structural motifs. Therefore, an extensive substrate scope screening for catalyst **28** was performed to determine the limits of substrate tolerance.

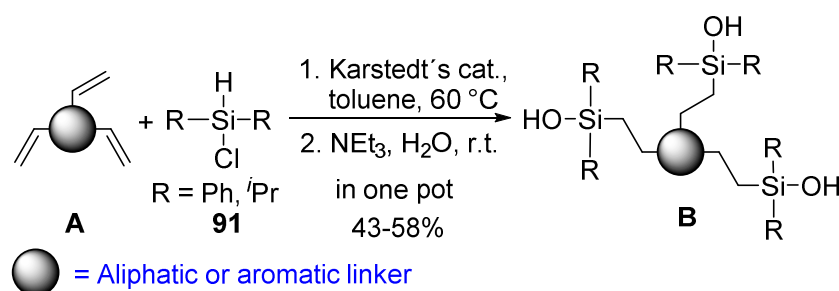


Scheme 6.1: Metathesis reactions of methyl capped alkynes to homo dimers with catalyst **28**.

Catalyst **28** was found to tolerate a broad variety of substrates with challenging structural motifs such as secondary or tertiary amines, an azide, primary alkyl halides, an indole, a thioether, a sulfoxide or a sulfonamide (Scheme 6.1). However, substrates with protic groups were not generally tolerated. We assumed that these incompatibilities are caused by ligand/substrate competition and therefore decided to design catalysts with multidentate siloxy ligands exploiting their stabilizing chelate effect.

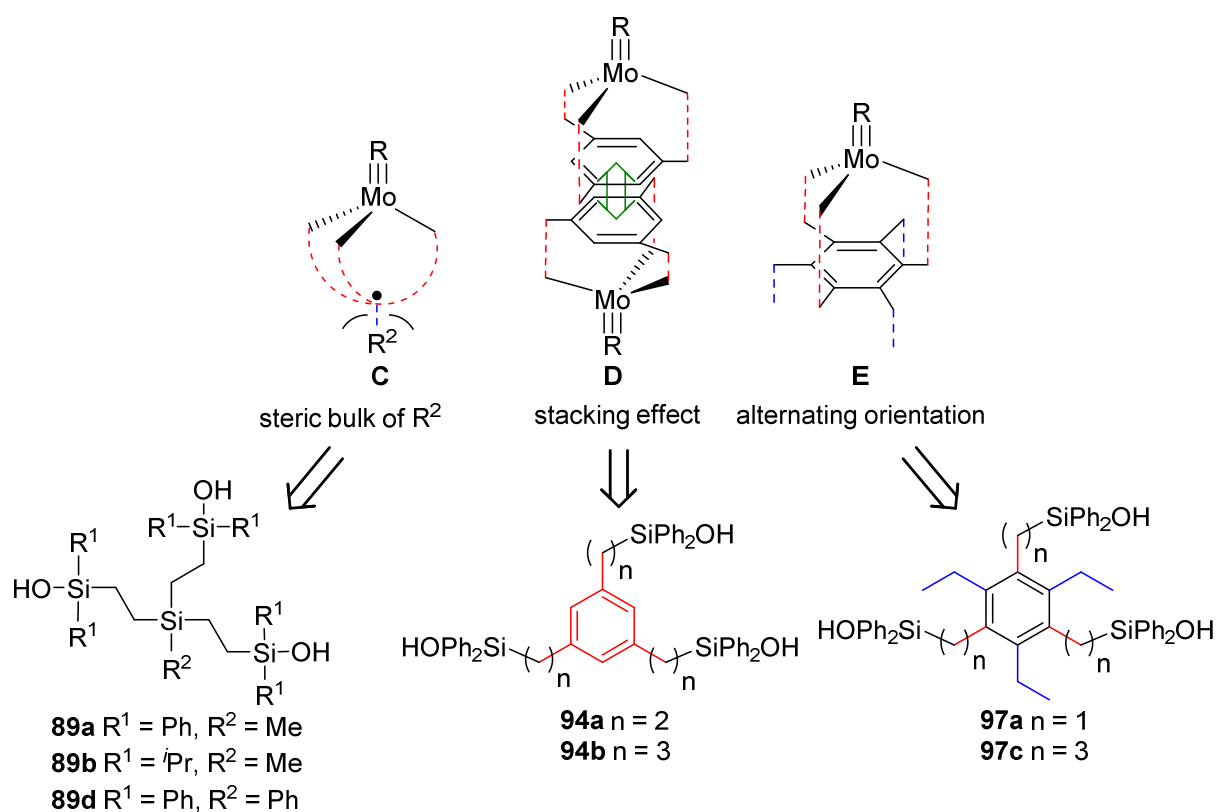
2) Alkyne metathesis catalysts based on multidentate siloxy ligands

Zhang *et al.* have demonstrated that alkyne metathesis catalysts based on multidentate phenol ligands are more stable than their monodentate analogs.^[46] Furthermore, our group has demonstrated that siloxy-based alkyne metathesis catalysts are amongst the most active and selective alkyne metathesis catalysts.^[1] Both principles were combined in the design of tridentate silanols of type **B** (Scheme 6.2). An efficient and scalable method was established to synthesize these tridentate ligands **B** via hydrosilylation of triolefin precursors **A** with chlorosilanes **91** and subsequent hydrolysis.



Scheme 6.2: General synthesis of tridentate silanols **B**.

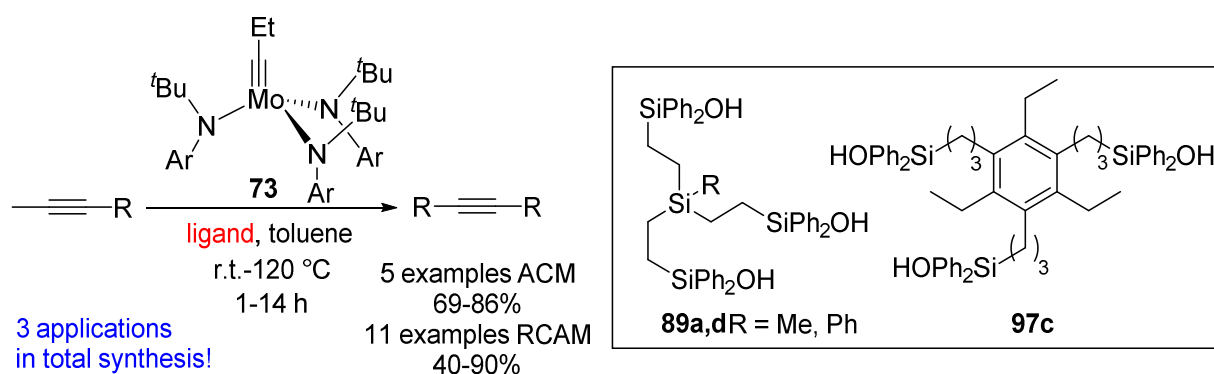
Different ligand geometries were investigated, aiming for the formation of a defined catalyst species as illustrated in structures **C**, **D**, **E** (Scheme 6.3).



Scheme 6.3: Strategies to generate a defined species ($\text{R} = \text{CEt}$, $\text{CC}_6\text{H}_4\text{OMe}$ or N).

However, all attempts to isolate a defined catalyst species failed due to the formation of product mixtures. Therefore, the catalysts were generated *in situ* from the multidentate siloxy ligands and molybdenum alkylidyne **73**. While ligands with aromatic substituents such as **89a** and **89d** led to highly active systems, the use of ligand **89b** with aliphatic substituents was inadequate. The geometry of the ligand plays only a minor role, which is demonstrated by the fact that ligands **89a, b** (silicon linker) as well as ligands **94** and **97** (aromatic linkers) performed similarly well. In contrast, constrained ligands like calyx[4]arenes **103b, c** and silsesquioxanes **104a, b** mainly furnished unreactive systems probably due to electronic effects and a constrained geometry.

The catalysts that were generated *in situ* from molybdenum alkylidyne **73** and silanols **89a, d** or **97c** were tested in a number of challenging alkyne metathesis reactions (Scheme 6.4).^[59] Gratifyingly they showed excellent stability and tolerated substrates containing free alcohols and highly coordinating groups. Their potential was further underlined by the RCAM reaction of diynes with two protected or unprotected hydroxy groups in propargylic positions.



Scheme 6.4: Metathesis reactions with new two-component catalyst systems.

In parallel work in this laboratory, these catalysts enabled the RCAM in three natural product synthesis projects (Ivorenolide A, Manshurolide, Lythrancepines) where other commonly used catalysts failed (Figure 6.1).^[59]

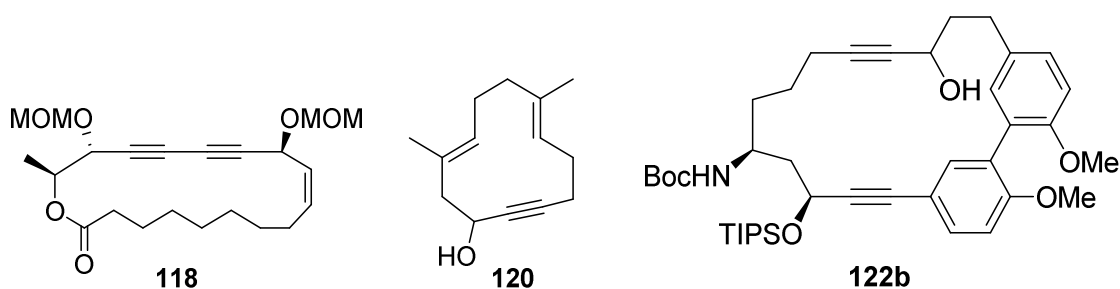
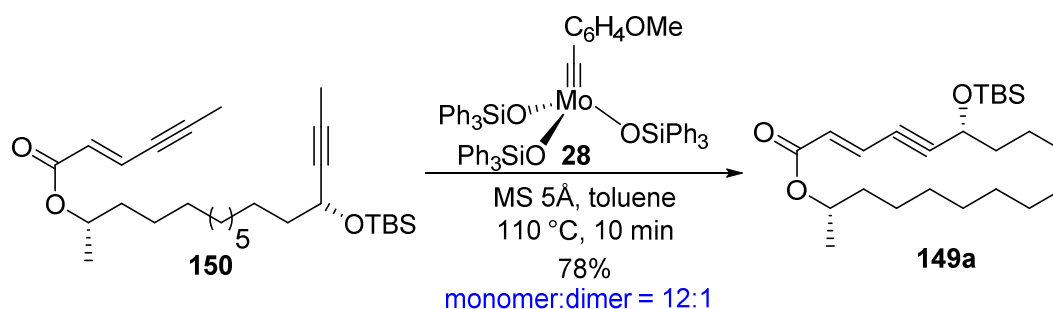


Figure 6.1: Key intermediates in natural product syntheses formed by the new two-component catalyst systems.

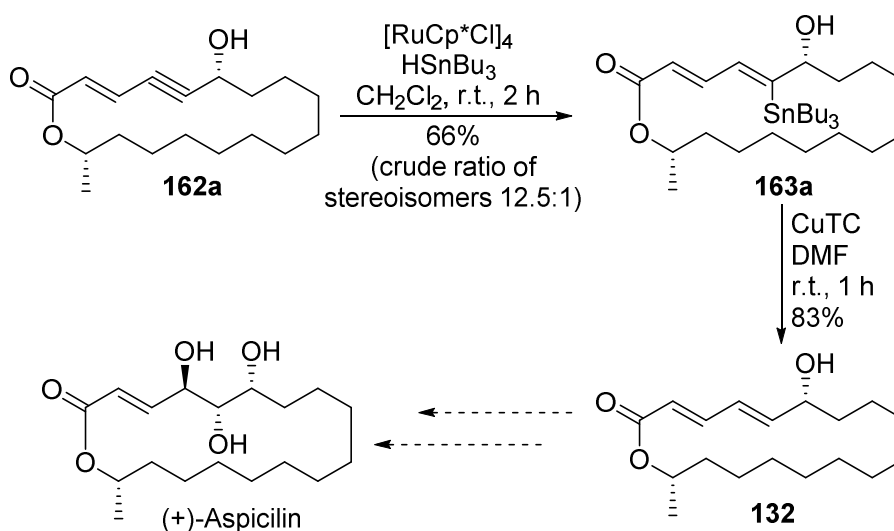
3) Formal total synthesis of (+)-Aspicilin

The feasibility of constructing an *E,E*-diene in a macrocyclic molecule by a sequence of RCAM and *trans*-hydrostannylation/destannylation was demonstrated within the formal synthesis of (+)-Aspicilin. The 18-membered macrocyclic core structure **149a** could be generated via RCAM at high temperature and under strict control of the reaction time (Scheme 6.5).



Scheme 6.5: RCAM of diyne **150** to generate enyne **149a**.

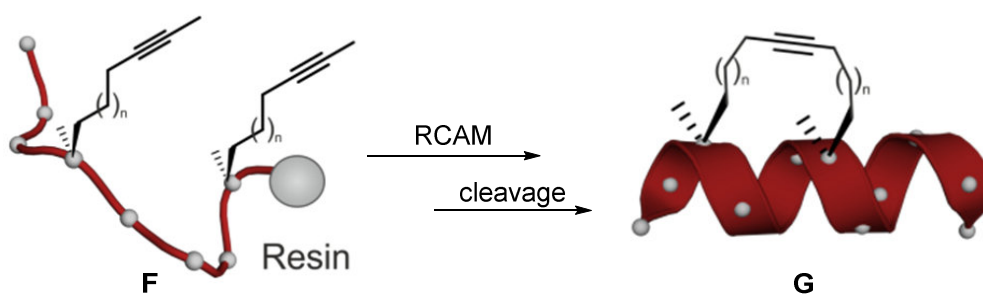
Furthermore, a newly developed hydrostannylation methodology was applied for the first time on a macrocyclic 1,3-enyne.^[5] Enyne **162a** was converted to stannane **163a** with excellent regioselectivity and a favorable *cis/trans* selectivity of 12.5 : 1 (Scheme 6.6). Subsequent destannylation of *trans*-stannane **163a** with CuTC furnished the target of our synthesis *E,E*-diene **132**. The formal synthesis of (+)-Aspicilin was completed with an overall yield of 10% for the longest linear sequence of ten steps.



Scheme 6.6: Hydrostannylation of enyne **162a** to stannane **163a** and subsequent destannylation to diene **132**.

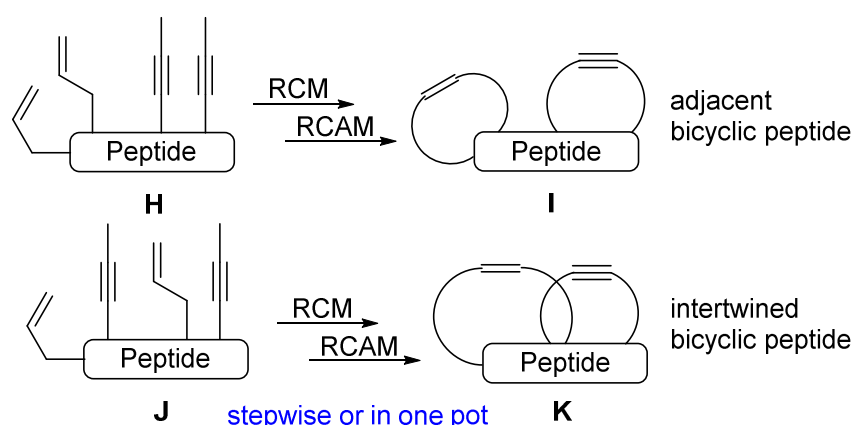
4) Stabilization of α -helical peptides using ring closing alkyne metathesis

Hydrocarbon-stapled peptides are a promising tool for targeting challenging protein-protein interactions, which are not accessible via classic small molecule approaches.^[3] One way to enforce an α -helical conformation is the introduction of an all-carbon macrocyclic bridge connecting two turns of a helix (Scheme 6.7).^[4] In order to accomplish this goal a hydrocarbon tether was introduced by RCAM using immobilized precursors **F**. Impressingly all (protected) functionalities present in the 20 proteinogenic amino acids were tolerated.^[107]



Scheme 6.7: RCAM to stabilize α -helical peptides.

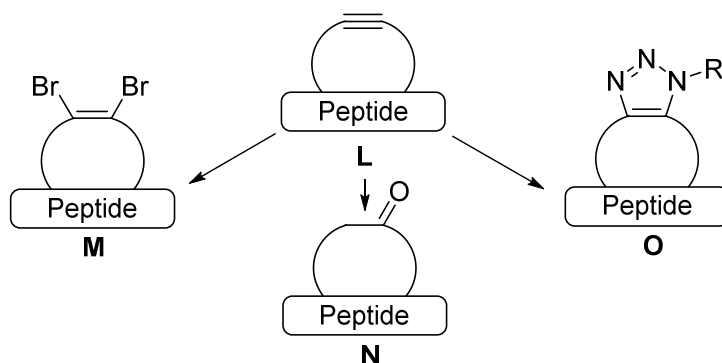
Additionally, the synthesis of adjacent bicyclic peptides **I** and intertwined bicyclic peptides **K** was successfully accomplished via tandem RCM and RCAM reactions (Scheme 6.8).^[107] The biological affinity of these alkyne stapled peptides was evaluated in binding affinity studies towards the small GTPase Rab8a. Bicyclic peptide **180b** was identified to be the most potent binder of an activated Rab GTPase.



Scheme 6.8: Formation of bicyclic peptides **I** and **K**.

In order to further functionalize the macrocyclic scaffold **L**, the immobilized alkyne was submitted to dibromination reaction to furnish dibromo olefins such as **M**, hydration to

ketones like **N**, and azide-alkyne cycloadditions to form triazoles such as **O** (Scheme 6.9). The latter allowed the introduction of sidechains containing biomolecules like sugars or biotin.



Scheme 6.9: Functionalization of immobilized peptides.

In conclusion, a new two-component system for alkyne metathesis was introduced which surpasses the known systems in reactions of alkynes bearing primary, secondary or phenolic –OH groups, as well as in reactions of (bis)propargylic alcohol derivatives. The potential of this system was proven by the total syntheses of Manshurolide and Ivorenolide A as well as by a study towards Lythrancepine I. Moreover, a formal synthesis (+)-Aspicilin was reached where the macrocyclic *E,E*-diene motive was constructed by a sequence of RCAM and *trans*-hydrostannylation/destannylation. Finally, the functionalization of immobilized peptides through RCAM and follow-up reactions of the thus formed alkynes were established. The work presented herein led to considerable progress in the field of alkyne metathesis allowing access to highly challenging macrocycles as well as cyclic peptides. This opened a variety of new possibilities in the synthesis of important bioactive compounds.

7 Experimental Procedures

7.1 General Experimental Details

All reactions with air- or moisture sensitive compounds were conducted in flame-dried glassware under argon using Schlenk technique, unless otherwise stated. The solvents were purified by distillation over the drying agents indicated and were transferred under Ar: THF, Et₂O (Mg/anthracene), CH₂Cl₂, toluene (Na/K), MeOH (Mg, stored over MS 3 Å); DMF, acetonitrile and NEt₃ were dried by an adsorption solvent purification system based on molecular sieves. Commercially available chemicals were used without further purification, unless otherwise stated. The molecular sieves were activated at 200 °C and 10⁻³ mbar for 24 h and stored under argon.

Chromatography

Thin layer chromatography was performed with precoated plates (POLYGRAM®SIL/UV254) from Machery-Nagel. Detection was done under UV-light at 254 nm and by dipping the plate in either cerium ammonium nitrate (CAN), basic KMnO₄ or acidic vanilin solution and development by heating. Flash chromatography was performed using Merck silica gel 60 (40–63 µm) under a slight over pressure. The utilized solvent mixtures are indicated in the corresponding experiments. Analytical gas chromatography measurements were performed on a Hewlett Packard HP 6890 device with a HP 5973 (GC/MS) detector.

Analytical high pressure liquid chromatography (HPLC) was performed with a Shimadzu LCMS2020 instrument (pumps LC-20AD, autosampler SIL-20AC, column oven CTO-20AC, diode array detector SPD-M20A, controller CBM-20A, ESI detector with Labsolutions as software) using a ZORBAX Eclipse Plus C18 column (1.8 µm, 3.0 or 4.6 mm ID × 50 mm) (Agilent). The oven temperature was set to 35 °C and 254 nm were used as detection wavelength. Preparative liquid chromatography was performed on a Shimadzu LC-20A prominence system (pumps LC-20AP, column oven CTO-20AC, diode array detector SPD-M20A, fraction collector FRC-10A, controller CBM-20A with LC-solution as software). The analyses were partially performed in cooperation with Roswitha Leichtweiß.

NMR-Spectroscopy

NMR spectra were recorded on Bruker DPX 300, AV 400, AV 500 spectrometers in the indicated solvents. The chemical shifts (δ) are given in ppm relative to TMS, coupling constants (J) are given in Hz. The solvent signals were used as a reference and the chemical shifts were converted to the TMS scale ([D₃]-acetonitrile: $\delta_C = 118.3$ ppm, $\delta_H = 1.94$ ppm; CDCl₃: $\delta_C = 77.0$ ppm, $\delta_H = 7.26$ ppm; CD₂Cl₂: $\delta_C = 53.8$ ppm, $\delta_H = 5.32$ ppm; [D₈]-toluene: $\delta_C = 20.7$ ppm, $\delta_H = 2.09$ ppm) The following abbreviations are used for multiplets: s: singlet, d: doublet, t: triplet, q: quartet, m: multiplet. Broad signals are indicated by b in front of the multiplicity. The values for ¹H are rounded to two digits, those for ¹³C to one digit after the decimal point. ¹³C-NMR spectra are recorded in ¹H decoupled mode. CD₂Cl₂ and [D₈]-toluene were stored over MS 3 Å.

IR-Spectroscopy

IR spectra were measured at room temperature via ATR (attenuated total reflection) on a Spectrum One (Perkin-Elmer) spectrometer. The characteristic absorptions are given in wavenumbers ($\tilde{\nu}$) [cm⁻¹].

Mass-Spectrometry

Measurements of mass spectra were undertaken by the mass spectrometry department of the Max-Planck-Institut für Kohlenforschung. EI-spectra were measured on a Finnigan MAT 8200 (70 eV) or on a Finnigan MAT 8400 (70 eV) spectrometer. ESI-spectra were measured on a Bruker ESQ 3000 spectrometer. All values are given in mass units per elementary charge (m/z). Intensities are given in percent relative to the basis peak. High resolution mass spectra (HRMS) were recorded on a Finnigan MAT 95 spectrometer (EI) or a Bruker APEX III FT-ICR-MS (7 Tesla magnet, ESI).

X-ray Analysis

X-ray diffraction measurements were performed by the department "Chemische Kristallographie" of the Max-Planck-Institut für Kohlenforschung. The measurements were done on a Bruker-AXS X8 Proteum diffractometer.

Melting Points

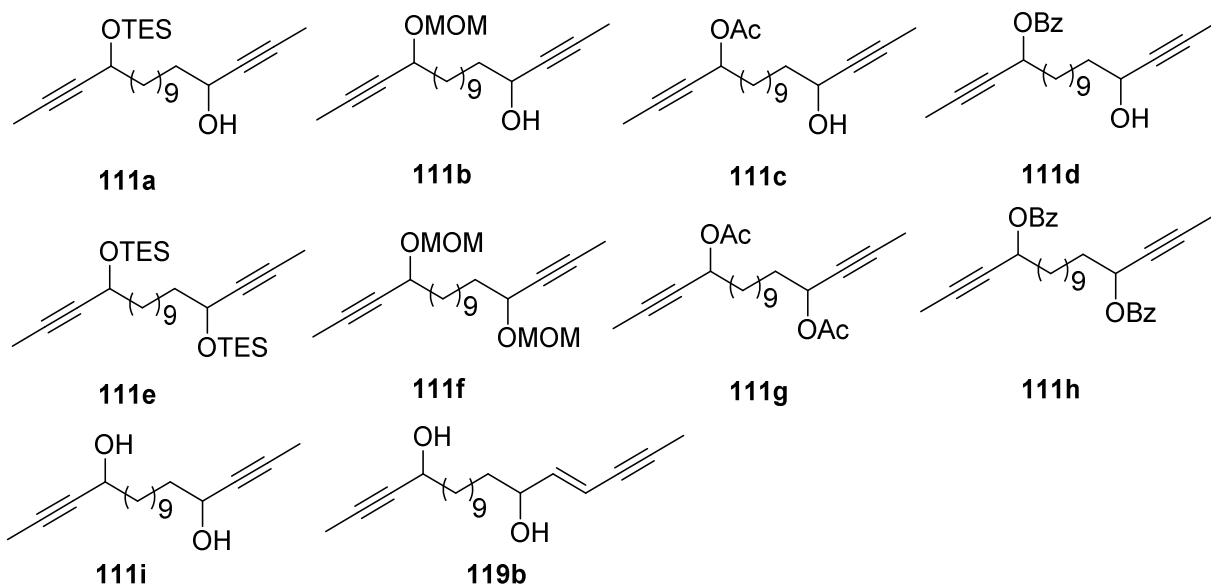
Melting points were measured in open capillary on a Büchi (*B-540*) melting point device.

Optical Rotations

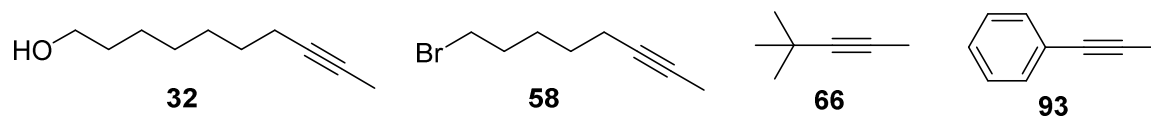
Optical rotations ($[\alpha]_D^{20}$) were measured with a Perkin-Elmer Model 343 polarimeter. The values are reported as specific optical rotations with the corresponding temperature, concentration (c (10 mg/mL)) and solvent at a wavelength of 589 nm.

The following compounds were synthesized in our group by the people indicated.

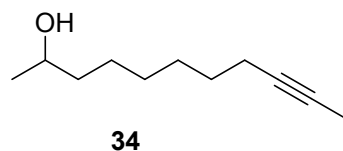
M. Ilg:



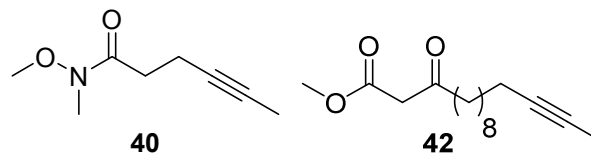
G. Seidel:



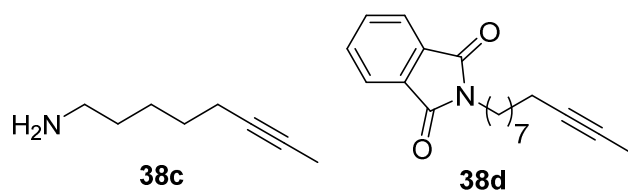
K. Radkowski:



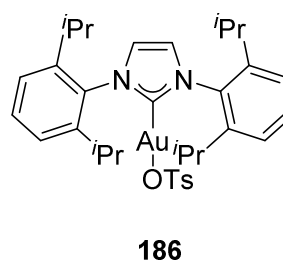
R. Stade:



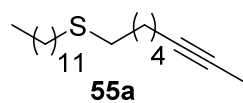
O. Guth:



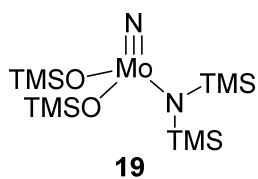
A. Ahlers:



Y. Suzuki:



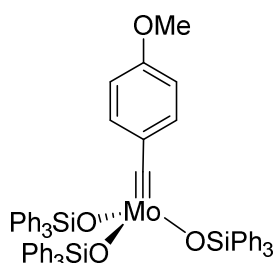
J. Heppekausen:



7.2 Extended Substrate Scope of Catalyst 28

7.2.1 Synthesis of Metathesis Catalysts 28

((Methylsilanetriyl)tris(ethane-2,1-diyl))tris(diphenylsilanol) (**28**)



According to a modified literature procedure^[26a], tribromo alkylidyne **26** (2.40 g, 4.40 mmol) was suspended in toluene (80 mL) and stirred for 10 min at 0 °C. The reaction mixture was cooled to -20 °C before a solution of Ph₃SiOK (4.14 g, 13.2 mmol) in toluene (40 mL) was added over 90 min at -20 °C. Stirring was continued for 10 min at -20 °C, for 30 min at 0 °C, and for 30 min at room temperature before the mixture was concentrated to 40 mL under reduced pressure. The suspension was filtered through a plug of Celite® that was washed with toluene (20 mL). The solvent was removed in vacuum to give a brown slurry which was dried for 15 min in high vacuum. The residue was dissolved in Et₂O (10 mL). After stirring at 0 °C for 30 min a yellow solid precipitated. The solid was filtered off and washed with cold Et₂O (8 mL) to give the title compound **28** (1.00 g, 22%) as a yellow powder which contained ca. 5% of the ate complex **27**.

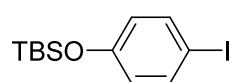
¹H NMR (400 MHz, CD₂Cl₂) δ = 7.54 (d, *J* = 6.9 Hz, 18H), 7.37 (t, *J* = 7.7 Hz, 9H), 7.19 (t, *J* = 7.5 Hz, 18H), 6.06 (d, *J* = 8.8 Hz, 2H), 5.19 (d, *J* = 8.8 Hz, 2H), 3.63 ppm (s, 3H); ¹³C NMR (100 MHz, CD₂Cl₂) δ = 300.7, 158.8, 140.2, 136.4, 135.8, 131.1, 130.4, 128.4, 112.2, 55.6 ppm.

The analytical and spectroscopic data are in agreement with those reported in the literature.^[26a]

7.2.2 Synthesis of Metathesis Substrates

General procedure 1: Suzuki cross-coupling of aryl iodides with sodium 1-propynyl

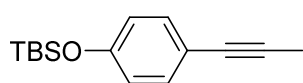
Trimethylborate (1.2 equiv) was added to a suspension of sodium 1-propynyl (1.2 equiv) in THF. The mixture was stirred for 30 min at ambient temperature, until a clear solution was observed. Pd(PPh₃)₄ (1 mol%) and the individual aryl iodide (1.0 equiv) were added and stirring continued for 14 h at reflux temperature. The mixture was then allowed to reach ambient temperature before H₂O was added. The phases were separated and the aqueous layer was extracted with ethyl acetate. The combined extracts were dried over MgSO₄, the solvent was evaporated, and the crude product was purified by flash chromatography.

***tert*-Butyl(4-iodophenoxy)dimethylsilane (EP1)**

4-Iodophenol (7.36 g, 33.4 mmol) was added to a solution of TBSCl (6.30 g, 41.8 mmol) in CH_2Cl_2 (60 mL) at room temperature. NEt_3 (5.81 mL, 41.8 mmol) was added at 0 °C and the reaction mixture was stirred for 3 h at room temperature. The reaction was quenched by addition of water (100 mL) and the aqueous phase was extracted with ethyl acetate (3 × 100 mL). The combined organic layers were dried over MgSO_4 , the solvent was evaporated, and the crude product was purified by flash chromatography (SiO_2 , hexanes) to give the title compound as a colorless oil (9.80 g, 88%).

^1H NMR (400 MHz, CDCl_3): δ = 7.51 (d, J = 8.8 Hz, 2H), 6.61 (d, J = 8.8 Hz, 2H), 0.98 (s, 9H), 0.19 ppm (s, 6H); ^{13}C NMR (100 MHz, CDCl_3): δ = 155.9, 138.5, 122.8, 83.9, 25.9, 18.3, -4.3 ppm.

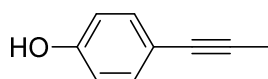
The analytical and spectroscopic data are in agreement with those reported in the literature.^[114]

***tert*-Butyldimethyl(4-(prop-1-yn-1-yl)phenoxy)silane (EP2)**

tert-Butyl(4-iodophenoxy)dimethylsilane (EP1) (8.30 g, 24.8 mmol) in THF (60 mL) was reacted with sodium 1-propynyl (1.97 g, 31.7 mmol), trimethylborate (3.29 mL, 31.7 mmol) and $\text{Pd}(\text{PPh}_3)_4$ (283 mg, 0.25 mmol, 1 mol%) according to general procedure 1. Flash chromatography (SiO_2 , hexanes/ethyl acetate, 50/1) afforded the title compound as a yellow oil (4.50 g, 79%).

^1H NMR (400 MHz, CDCl_3): δ = 7.26 (d, J = 8.4 Hz, 2H), 6.74 (d, J = 8.4 Hz, 2H), 2.03 (s, 3H), 0.97 (s, 9H), 0.19 ppm (s, 6H); ^{13}C NMR (100 MHz, CDCl_3): δ = 155.5, 133.1, 120.3, 116.9, 84.5, 79.8, 25.8, 18.4, 4.5, -4.2 ppm; IR (film): $\tilde{\nu}$ = 3040, 2956, 2930, 2886, 2857, 1602, 1505, 1471, 1391, 1362, 1273, 1251, 1165, 1098, 1007, 973, 906, 835, 805, 779, 739, 722, 674, 595, 532, 453, 421 cm^{-1} ; MS (EI): m/z (%) = 246 (31), 191 (14), 190 (29), 189 (100), 115 (35), 75 (11); HRMS (EI (DE)): m/z : calcd. for $[\text{C}_{15}\text{H}_{22}\text{OSi}_1]^+$: 246.1438, found: 246.1440.

The compound is literature known, but the SI containing the spectroscopic data is not available.^[115]

4-(Prop-1-yn-1-yl)phenol (29a)

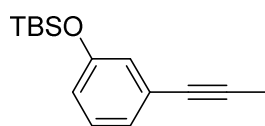
TBAF (1 M in THF, 20.0 mL, 20.0 mmol) was added to a solution of *tert*-butyldimethyl(4-(prop-1-yn-1-yl)phenoxy)silane (EP2) (4.50 g,

19.6 mol) in THF (40 mL) at room temperature. The mixture was stirred for 1.5 h at room temperature before the reaction was quenched with aq. sat. NH_4Cl (20 mL). The aqueous layer was extracted with ethyl acetate (3 × 50 mL). The combined extracts were washed with aq. sat. NaCl (30 mL) and dried over MgSO_4 . The solvent was evaporated and the residue was purified by flash chromatography (SiO_2 , hexanes/ethyl acetate, 15/1 to 4/1) to give the title compound as a colorless solid (2.51 g, 97%).

^1H NMR (400 MHz, CD_3CN): δ = 7.21 (d, J = 8.6 Hz, 2H), 7.10 (s, 1H), 6.74 (d, J = 8.6 Hz, 2H), 1.99 ppm (s, 3H); ^{13}C NMR (100 MHz, CD_3CN): δ = 157.6, 133.8, 116.3, 116.2, 84.6, 80.1, 4.1 ppm.

The analytical and spectroscopic data are in agreement with those reported in the literature.^[116]

***tert*-Butyldimethyl(3-(prop-1-yn-1-yl)phenoxy)silane (EP3)**

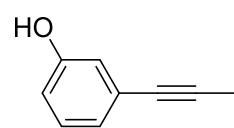


tert-Butyl(3-iodophenoxy)dimethylsilane (1.67 g, 5.00 mmol) in THF (10 mL) was reacted with sodium 1-propynyl (341 mg, 5.50 mmol), trimethylborate (626 μL , 5.50 mmol) and $\text{Pd}(\text{PPh}_3)_4$ (272 mg, 79 μmol , 2 mol%) according to general procedure 1. Flash chromatography (SiO_2 , hexanes/ethyl acetate, 50/1) afforded the title compound as a colorless oil (1.13 g, 92%).

^1H NMR (400 MHz, CDCl_3): δ = 7.13 (t, J = 7.8 Hz, 1H), 6.98 (d, J = 7.8 Hz, 1H), 6.87 (s, 1H), 6.76 (d, J = 7.8 Hz, 1H), 2.04 (s, 3H), 0.98 (s, 9H), 0.19 ppm (s, 6H); ^{13}C NMR (100 MHz, CDCl_3): δ = 155.5, 129.4, 125.2, 124.8, 123.2, 120.0, 85.7, 79.7, 25.8, 18.3, 4.5, -4.3 ppm; MS (EI): m/z (%) = 246 (17), 189 (100), 173 (2), 161 (8), 128 (3), 115 (20), 75 (3); HRMS (ESI(pos)): m/z : calcd. for $[\text{C}_{15}\text{H}_{22}\text{OSi}+\text{Na}]^+$: 269.1327, found: 269.1332.

The analytical and spectroscopic data are in agreement with those reported in the literature.^[117]

3-(Prop-1-yn-1-yl)phenol (29b)



TBAF (1 M in THF, 2.00 mL, 2.00 mmol) was added to a solution of *tert*-butyldimethyl(3-(prop-1-yn-1-yl)phenoxy)silane (**EP3**) (460 mg, 2.00 mmol) in THF (5 mL) at room temperature. The mixture was stirred

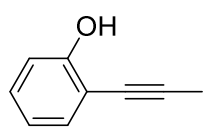
for 1 h at room temperature before the reaction was quenched with aq. sat. NH_4Cl (5 mL). The aqueous layer was extracted with ethyl acetate (3 × 30 mL). The combined extracts were

washed with aq. sat. NaCl (10 mL) and dried over MgSO₄. The solvent was evaporated and the residue was purified by flash chromatography (SiO₂, hexanes/ethyl acetate, 15/1 to 10/1) to give the title compound as a colorless solid (254 mg, 96%).

¹H NMR (400 MHz, CDCl₃): δ = 7.15 (t, *J* = 7.9 Hz, 1H), 6.97 (dt, *J* = 7.6, 1.4 Hz, 1H), 6.86 (dd, *J* = 2.7, 1.4 Hz, 1H), 6.75 (ddd, *J* = 8.2, 2.7, 1.0 Hz, 1H), 4.75 (s, 1H), 2.04 ppm (s, 3H).

The compound is literature known. However, spectroscopic data are not available.^[118]

2-(Prop-1-yn-1-yl)phenol (29c)



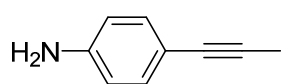
2-Iodophenol (1.37 g, 6.23 mmol) in THF (30 mL) was reacted with sodium 1-propynyl (1.97 g, 13.1 mmol), trimethylborate (1.37 mL, 13.2 mmol) and Pd(PPh₃)₄ (250 mg, 0.22 mmol, 3 mol%) according to general procedure 1.

Flash chromatography (SiO₂, hexanes/ethyl acetate, 6/1 to 4/1) afforded the title compound as a slightly yellow solid (648 mg, 79%).

¹H NMR (400 MHz, (CD₃)₂CO): δ = 8.04 (s, 1H), 7.26 (d, *J* = 7.6 Hz, 1H), 7.16 (t, *J* = 7.6 Hz, 1H), 6.87 (d, *J* = 8.3 Hz, 1H), 7.00 (t, *J* = 7.5 Hz, 1H), 2.04 ppm (s, 3H); ¹³C NMR (100 MHz, (CD₃)₂CO): δ = 158.8, 133.1, 129.8, 119.9, 116.2, 112.0, 91.7, 75.7, 3.9 ppm.

The analytical and spectroscopic data are in agreement with those reported in the literature.^[119]

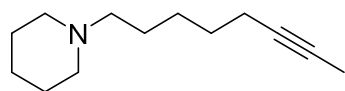
4-(Prop-1-yn-1-yl)aniline (36a)



4-Iodoaniline (3.03 g, 13.8 mmol) in THF (80 mL) was reacted with sodium 1-propynyl (2.33 g, 37.6 mmol), trimethylborate (4.32 mL, 38.0 mmol) and Pd(PPh₃)₄ (238 mg, 0.21 mmol, 2 mol%) according to general procedure 1. Flash chromatography (SiO₂, hexanes/ethyl acetate, 4/1 + 2% NEt₃) afforded the title compound as a brown oil (1.53 g, 85%).

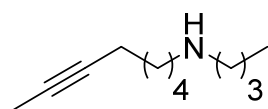
¹H NMR (400 MHz, CD₃CN): δ = 7.06 (d, *J* = 8.6 Hz, 2H), 6.53 (d, *J* = 8.6 Hz, 2H), 4.35 – 4.15 (bs, 2H), 1.94 ppm (s, 3H); ¹³C NMR (100 MHz, CD₃CN): δ = 149.1, 133.8, 115.5, 113.3, 83.9, 81.3, 4.5 ppm.

The analytical and spectroscopic data are in agreement with those reported in the literature.^[116]

1-(Oct-6-yn-1-yl)piperidine (38a)

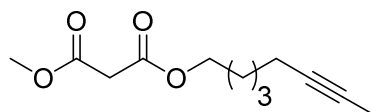
K_2CO_3 (1.93 g, 14.0 mmol), 1,4,7,10,13,16-hexa-oxacyclo-octadecane (150 mg, 567 μmol) and 1-bromo-6-octyne (2.00 g, 10.6 mmol) were successively added to a solution of piperidine (880 μl , 9.00 mmol) in acetonitrile (12 mL) at ambient temperature. The reaction mixture was stirred at reflux temperature for 22 h. The mixture was filtered through a plug of silica, which was rinsed with ethyl acetate (80 mL). The solvent was evaporated and the crude material was purified by distillation (65 $^\circ\text{C}$, 10^{-3} mbar) to give the title compound as a colorless oil (1.34 g, 77%).

^1H NMR (400 MHz, CDCl_3): δ = 2.35 (bs, 4H), 2.29 – 2.24 (m, 2H), 2.14 – 2.08 (m, 2H), 1.77 (t, J = 2.6 Hz, 3H), 1.61 – 1.54 (m, 4H), 1.53 – 1.31 ppm (m, 8H); ^{13}C NMR (100 MHz, CDCl_3): δ = 79.4, 75.6, 59.6, 54.8, 29.2, 27.2, 26.7, 26.1, 24.7, 18.8, 3.6 ppm; IR (film): $\tilde{\nu}$ = 2931, 2855, 2799, 2762, 1442, 1376, 1351, 1328, 1307, 1269, 1154, 1122, 1094, 1040, 990, 862, 779, 732 cm^{-1} ; MS (EI): m/z (%) = 193 (1), 151 (2), 125 (3), 124 (3), 99 (7), 98 (100), 96 (2), 84 (4), 70 (5), 69 (2), 67 (2), 56 (2), 55 (5), 53 (2), 44 (2), 42 (4), 41 (5); HRMS (EI): m/z : calcd. for $[\text{C}_{13}\text{H}_{23}\text{N}]^+$: 193.1831, found: 193.1830.

N-Butyloct-6-yn-1-amine (38b)

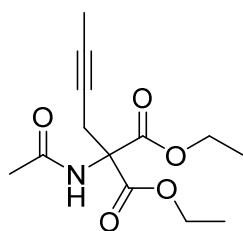
A solution of 8-bromo-2-octyne (300 mg, 1.59 mmol) in *n*-butylamine (370 mg, 500 μL , 5.06 mmol) was stirred at 50 $^\circ\text{C}$ for 16 h. The solvent was evaporated and the crude product was dried at 50 $^\circ\text{C}$ for 3 h under high vacuum to afford the title compound as a colorless solid (279 mg, 97%).

M.p. = 180 – 190 $^\circ\text{C}$; ^1H NMR (400 MHz, CDCl_3): δ = 6.65 (bs, 1H), 2.99 – 2.93 (m, 4H), 2.17 – 2.10 (m, 2H), 1.98 – 1.86 (m, 4H), 1.76 (t, J = 2.5 Hz, 3H), 1.54 – 1.37 (m, 6H), 0.95 ppm (t, J = 7.3 Hz, 3H); ^{13}C NMR (100 MHz, CDCl_3): δ = 78.6, 76.1, 47.8, 47.7, 28.4, 27.9, 26.1, 25.5, 20.3, 18.7, 13.6, 3.57 ppm; IR (film): $\tilde{\nu}$ = 2937, 1867, 1807, 1752, 1536, 2438, 1476, 1440, 1405, 1378, 1346, 1290, 1266, 1134, 1044, 989, 977, 879, 823, 799, 727, 495 cm^{-1} ; MS (EI): m/z (%) = 181 (0.4), 166 (8), 138 (47), 125 (25), 112 (14), 110 (8), 96 (8), 95 (14), 93 (17), 86 (100), 84 (15), 81 (11), 79 (16), 72 (8), 70 (12), 67 (22), 57 (12), 56 (13), 55 (16), 53 (9), 44 (24); HRMS (EI): m/z : calcd. for $[\text{C}_{12}\text{H}_{23}\text{N}]^+$: 181.1829, found: 181.1830.

Methyl oct-6-yn-1-yl malonate (42)

NEt₃ (3 mL) was added to a solution of oct-6-yne-1-ol (630 mg, 5.00 mmol) in CH₂Cl₂ (10 mL) at room temperature. A solution of methyl malonyl chloride (751 mg, 5.50 mmol) in CH₂Cl₂ (5 mL) was added to the stirred solution at 0 °C. The mixture was stirred at room temperature for 2 h before the reaction was quenched with HCl (2 M, 5 mL). The water layer was extracted with CH₂Cl₂ (3 × 25 mL) and the combined organic layers were washed with aq. NaHCO₃ (10 mL) and water (20 mL). The combined extracts were dried over MgSO₄, the solvent was evaporated, and the crude material was purified by flash chromatography (SiO₂, hexanes/ethyl acetate, 10/1 to 6/1) to give the title compound as a colorless oil (830 mg, 74%).

¹H NMR (400 MHz, CDCl₃): δ = 4.15 (t, *J* = 6.9 Hz, 2H), 3.75 (s, 3H), 3.38 (s, 2H), 2.16 – 2.10 (m, 2H), 1.77 (t, *J* = 2.5 Hz, 3H), 1.70 – 1.61 (m, 2H), 1.54 – 1.39 ppm (m, 4H); ¹³C NMR (100 MHz, CDCl₃): δ = 167.2, 166.7, 79.0, 75.9, 65.7, 52.6, 41.6, 28.7, 28.2, 25.2, 18.8, 3.6 ppm; IR (film): $\tilde{\nu}$ = 2951, 2862, 2219, 1731, 1673, 1437, 1411, 1333, 1272, 1199, 1148, 1019, 849, 685, 582 cm⁻¹; MS (EI): *m/z* (%) = 153 (9), 119 (21), 108 (21), 101 (42), 93 (100), 91 (27), 81 (17), 80 (17), 79 (51), 77 (20), 69 (14), 68 (27), 67 (40), 66 (38), 59 (25), 57 (11), 55 (28), 54 (13), 53 (15), 43 (10), 41 (22), 39 (12); HRMS (ESI(pos)): *m/z*: calcd. for [C₁₂H₁₈O₄+Na]⁺: 249.1099, found: 249.1097.

Diethyl 2-acetamido-2-(but-2-yn-1-yl)malonate (EP4)

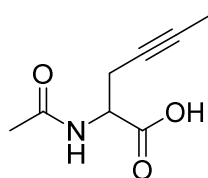
In analogy to the literature^[120], a solution of diethyl acetamidomalonate (1.04 g, 5.00 mmol) in DMF (5 mL) was added to a suspension of NaH (142 mg, 5.92 mmol) in DMF (5 mL) at 0 °C. The mixture was allowed to reach room temperature before 1-bromo-butyne (825 mg, 6.20 mmol) was added. After stirring for 3 h at 90 °C the solvent was evaporated. The residue was dissolved in water (20 mL) and the mixture was extracted with ethyl acetate (4 × 25 mL). The combined organic layers were dried over MgSO₄, the solvent was evaporated, and the residue was purified by flash chromatography (SiO₂, hexanes/ethyl acetate, 4/1 to 2/1) to give the title compound as a colorless oil (752 mg, 59%).

¹H NMR (400 MHz, CDCl₃): δ = 6.89 (bs, 1H), 4.31 – 4.19 (m, 4H), 3.21 – 3.17 (m, 2H), 2.05 (s, 3H), 1.73 (t, *J* = 2.6 Hz, 3H), 1.26 ppm (t, *J* = 7.1 Hz, 6H); ¹³C NMR (100 MHz, CDCl₃): δ = 169.2,

167.1, 78.9, 72.9, 65.8, 62.9, 24.3, 23.2, 14.1, 3.6 ppm; IR (film): $\tilde{\nu}$ = 3227, 3033, 2927, 2937, 1738, 1638, 1529, 1430, 1369, 1313, 1285, 1229, 1190, 1095, 1055, 1012, 952, 869, 810, 665, 619, 530, 455 cm^{-1} ; MS (EI): m/z (%) = 210 (16), 197 (12), 196 (97), 174 (45), 165 (10), 155 (11), 154 (100), 153 (27), 150 (43), 146 (13), 136 (812), 126 (56), 125 (14), 110 (16), 108 (37), 82 (17), 81 (12), 80 (45), 79 (14), 53 (23), 45 (12), 43 (55); HRMS (ESI(pos)): m/z : calcd. for $[\text{C}_{13}\text{H}_{19}\text{NO}_5+\text{Na}]^+$: 292.1155, found: 292.1157.

The analytical and spectroscopic data are in agreement with those reported in the literature.^[120]

2-Acetamidohex-4-ynoic acid (EP5)



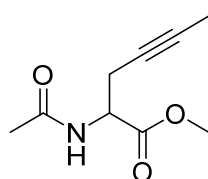
In analogy to the literature^[120], NaOH (120 mg, 3.00 mmol) was added to as solution of diethyl 2-acetamido-2-(but-2-yn-1-yl)malonate (EP4) (650 mg, 2.40 mmol) in a mixture of EtOH (15 mL) and water (10 mL) at room temperature. The mixture was stirred at reflux temperature for 26 h

before the solvent was reduced to 5 mL under vacuum. Aq. HCl (2 M, 4 mL) was added and the water layer was extracted with ethyl acetate (3 × 25 mL). Aq. NaHCO_3 (25 mL) was added to the aqueous layer before extraction with ethyl acetate (3 × 25 mL). The combined organic layers were dried over MgSO_4 and the solvent was evaporated to give the title compound as a colorless solid (317 mg, 78%).

^1H NMR (400 MHz, CDCl_3): δ = 6.38 (bd, J = 7.8 Hz, 1H), 6.20 – 5.50 (bs, 1H), 4.70 (dt, J = 7.8, 4.8 Hz, 1H), 2.83 – 2.67 (m, 2H), 2.10 (s, 3H), 1.78 ppm (t, J = 2.5 Hz, 3H); ^{13}C NMR (100 MHz, CDCl_3): δ = 173.6, 171.1, 79.8, 72.9, 51.2, 23.2, 22.5, 3.7 ppm; MS (EI): m/z (%) = 169 (12), 124 (35), 116 (7), 110 (24), 88 (6), 82 (58), 80 (11), 74 (860), 67 (12), 60 (51), 53 (14), 43 (100), 39 (12), 28 (19); HRMS (EI): m/z : calcd. for $[\text{C}_8\text{H}_{11}\text{NO}_3]$: 169.0739, found: 169.0739.

The analytical and spectroscopic data are in agreement with those reported in the literature.^[120]

Methyl 2-acetamidohex-4-ynoate (48)



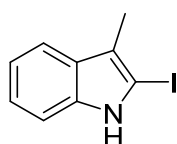
In analogy to the literature^[120], thionyl chloride (238 mg, 145 μL , 2.00 mmol) was added to a solution of 2-acetamidohex-4-ynoic acid (EP5) (307 mg, 1.82 mmol) in MeOH (10 mL) at 0 °C. The reaction mixture was allowed to warm to room temperature and stirred for 5 h before the

solvent was evaporated. The crude material was purified by flash chromatography (SiO₂, hexanes/ethyl acetate, 1/2 to 0/1) to give the title compound as a colorless solid (298 mg, 90%).

¹H NMR (400 MHz, CDCl₃): δ = 6.34 – 6.26 (bs, 1H), 4.74 – 4.66 (m, 1H), 3.76 (s, 3H), 2.74 – 2.62 (m, 2H), 2.05 (s, 3H), 1.76 ppm (s, 3H); ¹³C NMR (100 MHz, CDCl₃): δ = 171.6, 170.5, 79.4, 73.0, 52.8, 51.1, 23.4, 22.9, 3.6 ppm; IR (film): $\tilde{\nu}$ = 3305, 2951, 1751, 1645, 1552, 1429, 1372, 1350, 1283, 1229, 1201, 1131, 1054, 1022, 936, 907, 804, 710, 677 cm⁻¹; MS (EI): *m/z* (%) = 193 (4), 130 (11), 124 (100), 109 (6), 93 (6), 88 (81), 82 (63), 67 (10), 60 (21), 55 (6), 43 (42); HRMS (EI): *m/z*: calcd. for [C₉H₁₃NO₃]: 183.0896, found: 183.0895.

The analytical and spectroscopic data are in agreement with those reported in the literature.^[120]

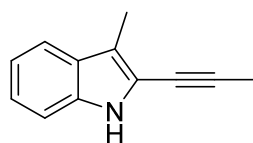
2-Iodo-3-methyl-1H-indole (EP6)



In analogy to the literature^[121], *n*-BuLi (27.8 mL, 44.5 mmol, 1.6 M in hexane) was added over 90 min to a solution of 3-methylindole (5.60 g, 42.7 mmol) in THF (100 mL) at –78 °C. The mixture was stirred for 30 min at –78 °C before CO₂ was introduced to the solution for 20 min at this temperature. The solvent was evaporated at 0 °C. THF (80 mL) and *t*-BuLi (1.7 M pentane, 26.5 mL, 45.1 mmol) were successively added at –78 °C. The mixture was stirred for 1 h at –78 °C. 1,2-Diiodoethane (14.4 g, 51.1 mmol, dissolved in 15 mL THF) was added at –78 °C and the mixture was stirred for 14 h at –78 °C. Water (5 mL) was added before the mixture was slowly warmed to room temperature. Aq. sat. NH₄Cl (50 mL) was added and the aqueous layer was extracted with ethyl acetate (2 × 100 mL). The combined extracts were washed with aq. sat. Na₂S₂O₃ (80 mL) and brine (50 mL) before they were dried over MgSO₄. The solvent was evaporated and the crude material was purified by flash chromatography (SiO₂, hexanes/ethyl acetate, 15/1 to 10/1) to give the title compound as a yellow brown solid (4.61 g, 42%).

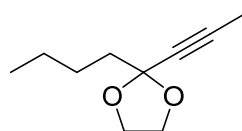
¹H NMR (400 MHz, CDCl₃): δ = 7.84 (bs, 1H), 7.49 (d, *J* = 7.7 Hz, 1H), 7.25 (d, *J* = 7.7 Hz, 1H), 7.13 – 7.05 (m, 2H), 2.27 ppm (s, 3H); ¹³C NMR (100 MHz, CDCl₃): δ = 138.9, 128.2, 122.4, 119.8, 118.3, 78.1, 12.0 ppm.

The analytical and spectroscopic data are in agreement with those reported in the literature.^[122]

3-Methyl-2-(prop-1-yn-1-yl)-1H-indole (50)

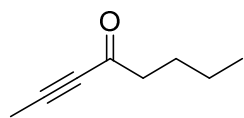
2-Iodo-3-methyl-1H-indole (**EP6**) (850 mg, 3.31 mmol) in THF (50 mL) was reacted with sodium 1-propynyl (1.05 g, 17.0 mmol), trimethylborate (1.95 mL, 17.3 mmol) and Pd(PPh₃)₄ (203 mg, 176 μmol, 5 mol%) according to general procedure 1. Flash chromatography (SiO₂, hexanes/ethyl acetate, 30/1 to 15/1) afforded the title compound as an orange solid (243 mg, 44%).

M.p. = 71.0 – 71.5 °C; ¹H NMR (400 MHz, CDCl₃): δ = 7.83 (bs, 1H), 7.50 (d, *J* = 7.7 Hz, 1H), 7.23 (d, *J* = 7.7 Hz, 1H), 7.18 (t, *J* = 7.7 Hz, 1H), 7.09 (t, *J* = 7.7 Hz, 1H), 2.36 (s, 3H), 2.14 ppm (s, 3H); ¹³C NMR (100 MHz, CDCl₃): δ = 135.6, 128.2, 123.2, 119.8, 119.2, 117.4, 116.8, 110.7, 91.8, 71.9, 9.7, 4.9 ppm; IR (film): $\tilde{\nu}$ = 3416, 3387, 3053, 2912, 1612, 1524, 1457, 1434, 1337, 1306, 1240, 1157, 1005, 957, 928, 738, 665, 576, 530, 463, 432 cm⁻¹; MS (EI): *m/z* (%) = 169 (100), 154 (5), 139 (9), 128 (5), 115 (6), 101 (3), 84 (20), 77 (8), 70 (6), 63 (5); HRMS (EI): *m/z*: calcd. for [C₁₂H₁₁N]⁺: 169.0890, found: 169.0891.

2-Butyl-2-(prop-1-yn-1-yl)-1,3-dioxolane (53a)

In analogy to the literature^[123], 1,2-bis(trimethylsiloxy)ethane (350 mg, 1.60 mmol) and oct-2-yne-4-one (53b) (100 mg, 0.81 mmol) were added to a solution of TMSOTf (5 mg, 22 μmol) in CH₂Cl₂ (3 mL) at –78 °C. The reaction mixture was stirred for 14 h at –30 °C and for 5 h at –20 °C. Aq. sat. NaHCO₃ (5 mL) was added and the water layer was extracted with CH₂Cl₂ (3 × 20 mL). The combined organic layers were washed with brine (10 mL) and dried over MgSO₄. The solvent was evaporated and the crude material was purified by flash chromatography (SiO₂, pentane/Et₂O, 30/1) to give the title compound as a colorless oil (101 mg, 75%).

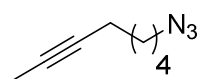
¹H NMR (400 MHz, CDCl₃): δ = 4.08 – 4.04 (m, 2H), 3.96 – 3.92 (m, 2H), 1.86 – 1.82 (m, 2H), 1.84 (s, 3H), 1.54 – 1.47 (m, 2H), 1.40 – 1.30 (m, 2H), 0.91 ppm (t, *J* = 7.4 Hz, 3H); ¹³C NMR (100 MHz, CDCl₃): δ = 103.7, 80.6, 77.6, 64.7, 39.6, 26.4, 22.9, 14.3, 3.5 ppm; IR (film): $\tilde{\nu}$ = 2956, 2932, 2874, 2236, 1736, 1468, 1380, 1343, 1296, 1240, 1196, 1164, 1116, 1084, 1032, 963, 946, 881, 750, 672 cm⁻¹; MS (EI): *m/z* (%) = 168 (0.1), 153 (10), 126 (7), 111 (100), 95 (3), 83 (4), 77 (4), 67 (35), 55 (5), 39 (5); HRMS (Cl(DE) *i*-Butane): *m/z*: calcd. for [C₁₀H₁₇O₂]⁺: 169.1227, found: 169.1229.

Oct-2-yn-4-one (53b)

In analogy to the literature^[123], 1-propynylmagnesium bromide (0.5 M in THF, 15.0 mL, 7.50 mmol) was added to a mixture of ZnCl₂ (1 M in Et₂O, 7.50 mL, 7.50 mmol) and THF (10 mL) at 0 °C. After stirring for 15 min, valeroyl chloride (600 mg, 4.98 mmol) was added and stirring continued for 1 h at 0 °C. Aq. sat. NH₄Cl (5 mL) was added at -10 °C. The aqueous layer was extracted with ethyl acetate (3 × 30 mL). The combined organic layers were dried over MgSO₄, the solvent was evaporated, and the crude material was purified by flash chromatography (SiO₂, hexanes/ethyl acetate, 50/1 to 30/1) to give the title compound as a colorless oil (235 mg, 38%).

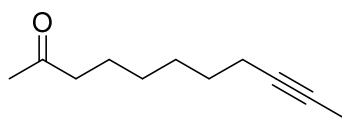
¹H NMR (400 MHz, CDCl₃): δ = 2.52 (t, *J* = 7.5 Hz, 2H), 2.01 (s, 3H), 1.68 – 1.60 (m, 2H), 1.39 – 1.29 (m, 2H), 0.91 ppm (t, *J* = 7.4 Hz, 3H); ¹³C NMR (100 MHz, CDCl₃): δ = 188.6, 89.9, 80.4, 45.3, 26.3, 22.3, 13.9, 4.2 ppm; IR (film): $\tilde{\nu}$ = 2959, 2933, 2873, 2219, 1735, 1670, 1465, 1407, 1379, 1315, 1248, 1171, 1104, 1001, 964, 951, 882, 766, 732, 652, 566 cm⁻¹; MS (EI): *m/z* (%) = 124 (0.4), 109 (9), 95 (5), 82 (53), 67 (100), 41 (6), 39 (9); HRMS (EI): *m/z*: calcd. for [C₈H₁₂O]⁺: 124.0887, found: 124.0888.

The analytical and spectroscopic data are in agreement with those reported in the literature.^[124]

8-Azidooct-2-yne (61)

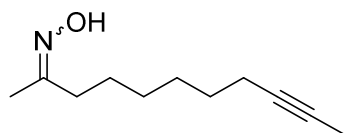
A mixture of NaN₃ (222 mg, 3.40 mmol), 8-bromo-2-octyne (189 mg, 1.00 mmol) and water (2 mL) was stirred in a microwave reactor for 2 h at 120 °C. The aqueous layer was extracted with methyl *t*-butyl ether (3 × 10 mL). The combined extracts were dried over MgSO₄, the solvent was evaporated, and the crude material was purified by flash chromatography (SiO₂, hexanes/ethyl acetate, 50/1) to give the title compound as a colorless oil (121 mg, 80%).

¹H NMR (400 MHz, CDCl₃): δ = 3.27 (t, *J* = 6.9 Hz, 2H), 2.18 – 2.11 (m, 2H), 1.78 (t, *J* = 2.6 Hz, 3H), 1.66 – 1.57 (m, 2H), 1.53 – 1.43 ppm (m, 4H); ¹³C NMR (100 MHz, CDCl₃): δ = 78.9, 76.0, 51.6, 28.7, 28.6, 26.1, 18.7, 3.6 ppm; IR (film): $\tilde{\nu}$ = 2930, 2859, 2093, 1727, 1679, 1578, 1456, 1349, 1245, 1123, 1072, 970, 897, 825, 744 cm⁻¹; MS (EI): *m/z* (%) = 151 (0.02), 122 (17), 108 (19), 105 (6), 94 (76), 91 (23), 80 (40), 77 (20), 70 (27), 67 (72), 56 (58), 53 (84), 41 (100), 39 (56), 30 (44), 29 (95); HRMS (CI(FE) *i*-Butane): *m/z*: calcd. for [C₈H₁₄N₃]⁺: 152.1189, found: 152.1188.

Undec-9-yn-2-one (EP7)

Oxalyl chloride (707 mg, 5.57 mmol) was added to a solution of DMSO (660 μ l, 9.30 mmol) in CH_2Cl_2 (10 mL) at -78°C . The mixture was stirred for 5 min before undec-9-yn-2-ol (**34**) (780 mg, 4.64 mmol) in CH_2Cl_2 (5 mL) was added over 5 min. After 90 min at -78°C , NEt_3 (2.58 mL, 18.6 mmol) was added and the reaction mixture was allowed to warm to room temperature before water (20 mL) was added. The aqueous layer was extracted with CH_2Cl_2 (30 mL). The combined organic layers were washed with aq. sat. NH_4Cl (5 mL), aq. sat. Na_2CO_3 (5 mL), and water (5 mL). The combined extracts were dried over MgSO_4 , the solvent was evaporated, and the crude material was purified by flash chromatography (SiO_2 , hexanes/ethyl acetate, 10/1) to give the title compound as a colorless oil (450 mg, 58%).

^1H NMR (400 MHz, CDCl_3): δ = 2.41 (t, J = 7.2 Hz, 2H), 2.12 (s, 3H), 2.12 – 2.06 (m, 2H), 1.76 (t, J = 2.6 Hz, 3H), 1.61 – 1.52 (m, 2H), 1.50 – 1.23 ppm (m, 6H); ^{13}C NMR (100 MHz, CDCl_3): δ = 209.3, 79.3, 75.6, 43.8, 30.0, 29.0, 28.8, 28.7, 23.9, 18.8, 3.6 ppm; IR (film): $\tilde{\nu}$ = 2932, 2857, 2219, 1712, 1434, 1357, 1164, 944, 720, 597, 521 cm^{-1} ; MS (EI): m/z (%) = 123 (7), 108 (16), 93 (21), 81 (18), 79 (22), 71 (14), 68 (34), 67 (24), 58 (27), 55 (18), 53 (12), 43 (100), 41 (18), 39 (11); HRMS (ESI(pos)): m/z : calcd. for $[\text{C}_{11}\text{H}_{18}\text{O}+\text{Na}]^+$: 189.1249, found: 189.1250.

Undec-9-yn-2-one oxime (EP8)

Undec-9-yn-2-one (**EP7**) (410 mg 2.47 mmol) was added to a solution of sodium acetate (243 mg, 2.96 mmol) and hydroxylammonium chloride (206 mg, 2.96 mmol) in a mixture of MeOH (5 mL) and water (100 μ L) at ambient temperature. The mixture was stirred for 2 h at reflux temperature. The mixture was allowed to reach room temperature before water (20 mL) was added. The aqueous layer was extracted with ethyl acetate (3 \times 30 mL). The combined extracts were dried over MgSO_4 , the solvent was evaporated, and the residue was purified by flash chromatography (SiO_2 , hexanes/ethyl acetate, 6/1 to 2/1) to give the title compound as a colorless oil (392 mg, 88%, mixture of diastereomers).

^1H NMR (400 MHz, CDCl_3): δ = 8.40 – 7.30 (bs, 1H), 2.18 (t, J = 7.6 Hz, 2H), 2.14 – 2.08 (m, 2H), 1.87 (s, 3H), 1.77 (t, J = 2.5 Hz, 3H), 1.56 – 1.26 ppm (m, 8H); ^{13}C NMR (100 MHz, CDCl_3): δ = 159.0, 79.4, 75.6, 36.0, 29.1, 28.9, 28.7, 26.3, 18.8, 13.4, 3.6 ppm; IR (film): $\tilde{\nu}$ = 3226, 2928, 2857, 1663, 1424, 1367, 1258, 1012, 925, 648 cm^{-1} . MS (EI): m/z (%) = 150 (7), 122 (6), 109

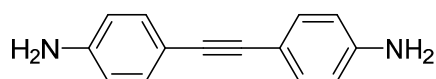
(5), 108 (8), 96 (7), 93 (6), 91 (6), 86 (11), 84 (5), 82 (6), 81 (9), 79 (12), 73 (48), 71 (5), 70 (45), 68 (6), 67 (13), 65 (5), 58 (7), 57 (100), 55 (19), 54 (7), 53 (13), 44 (5), 43 (7), 42 (43), 41 (29), 39 (14), 29 (15), 27 (10); HRMS (ESI(pos)): m/z : calcd. for $[C_{11}H_{19}NO+Na]^+$: 182.1540, found: 182.1539.

7.2.3 Homo Metathesis Reactions

General procedure 2: Alkyne homo metathesis reactions with catalyst **28**

The alkyne and MS 5 Å (1 g per mmol alkyne) were stirred in toluene (0.2 M based on the alkyne) for 30 min before metathesis catalyst **28** was added in one portion. The reaction mixture was stirred under the individual conditions. The suspension was filtered through a plug of Celite®, which was carefully rinsed with ethyl acetate. The solvent was evaporated and the residue was purified by flash chromatography.

4,4'-(Ethyne-1,2-diyl)dianiline (**37a**)

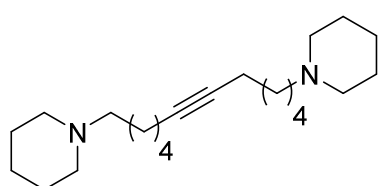


4-(Prop-1-yne-1-yl)aniline (**36a**) (65 mg, 0.50 mmol) was stirred with MS 5 Å (600 mg) and catalyst **28** (20.0 mg, 19.2 μmol, 4 mol%) in toluene (5 mL) for 13 h at 80 °C according to general procedure 2. Flash chromatography (SiO₂, hexanes/ethyl acetate, 2/1 to 0/1 + 1% NEt₃) afforded the title compound as a colorless solid (27 mg, 52%).

¹H NMR (400 MHz, CD₃OD): δ = 7.17 (d, J = 8.3 Hz, 4H), 6.65 (d, J = 8.3 Hz, 4H), 4.83 ppm (s, 6H); ¹³C NMR (100 MHz, CD₃OD): δ = 149.1, 133.3, 115.9, 114.0, 88.4 ppm; IR (film): $\tilde{\nu}$ = 3418, 3371, 2594, 2525, 2490, 2446, 1604, 1516, 1325, 1274, 1172, 1148, 1107, 822, 521 cm⁻¹; MS DE(EI): m/z (%) = 209 (17), 208 (100), 180 (7), 152 (5), 104 (9), 90 (5); HRMS (ESI(pos)): m/z : calcd. for $[C_{14}H_{12}N_2+H]^+$: 209.1072, found: 209.1073.

The compound is literature known. ¹H- and ¹³C-spectra were recorded in different solvents.^[115, 125]

1,12-Di(piperidin-1-yl)dodec-6-yne (**39a**)

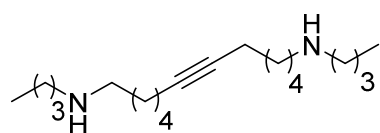


1-(Oct-6-yn-1-yl)piperidine (**38a**) (88 mg, 0.46 mmol) was stirred with MS 5 Å (840 mg) and catalyst **28** (18.2 mg, 17.5 μmol, 4 mol%) in toluene (5 mL) for 1 h at room temperature according to general procedure 2. Flash

chromatography (SiO₂, hexanes/ethyl acetate, 4/1 to 1/1 + 5% NEt₃) afforded the title compound as a colorless oil (63 mg, 81%).

¹H NMR (400 MHz, CDCl₃): δ = 2.42 – 2.30 (b, 8H), 2.30 – 2.24 (m, 4H), 2.13 (t, *J* = 7.0 Hz, 4H), 1.61 – 1.54 (m, 8H), 1.53 – 1.31 ppm (m, 16H); ¹³C NMR (100 MHz, CDCl₃): δ = 80.3, 59.7, 54.8, 29.3, 27.2, 26.7, 26.2, 24.7, 18.9 ppm; IR (film): $\tilde{\nu}$ = 3392, 2931, 2856, 2799, 2762, 2517, 1655, 1442, 1376, 1350, 1307, 1269, 1153, 1121, 1039, 962, 907, 860, 779, 731, 640, 514 cm⁻¹; MS (EI): *m/z* (%) = 332 (0.17), 248 (2), 234 (2), 206 (2), 204 (2), 178 (2), 151 (2), 124 (8), 111 (2), 98 (100), 96 (4), 84 (8), 70 (5), 67 (2), 55 (6); HRMS (ESI(pos)): *m/z*: calcd. for [C₂₂H₄₀N₂+H]⁺: 333.3264, found: 333.3264.

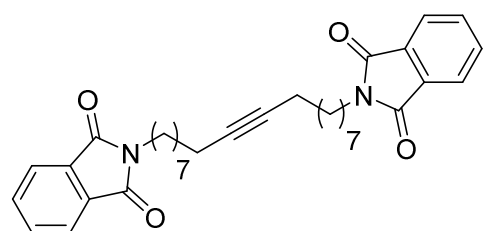
*N*¹,*N*¹²-Dibutyldodec-6-yne-1,12-diamine (**39b**)



N-Butyloct-6-yn-1-amine (**28b**) (90.0 mg, 0.496 mmol) was stirred with MS 5 Å (500 mg) and catalyst **28** (14.3 mg, 13.7 μmol, 3 mol%) in toluene (2.5 mL) for 16 h at room temperature according to general procedure 2. Flash chromatography (SiO₂, ethyl acetate/MeOH 10/1 to ethyl acetate/MeOH 5/1 + 5% NEt₃) afforded the title compound as a colorless solid (59.1 mg, 77%).

M.p. = 230 °C (decomp.); ¹H NMR (400 MHz, CDCl₃): δ = 3.68 (s, 2H), 2.71 – 2.61 (m, 8H), 2.20 – 2.10 (m, 4H), 1.64 – 1.30 (m, 20H), 0.91 ppm (t, *J* = 7.3 Hz, 6H); ¹³C NMR (100 MHz, CDCl₃): δ = 80.3, 49.7, 49.5, 31.5, 28.9, 26.6, 20.6, 18.8, 14.1 ppm; IR (film): $\tilde{\nu}$ = 2953, 2867, 2798, 2450, 1442, 1344, 1042, 888, 790, 758 cm⁻¹; MS (EI): *m/z* (%) = 308 (6), 266 (13), 265 (59), 252 (8), 251 (40), 236 (15), 194 (24), 192 (19), 167 (11), 166 (27), 154 (26), 112 (50), 111 (14), 93 (11), 86 (100), 84 (14), 81 (22), 67 (16), 44 (58); HRMS (ESI(pos)): *m/z*: calcd. for [C₂₀H₄₀N₂+H]⁺: 309.3264, found: 309.3264.

2,2'-(Octadec-9-yne-1,18-diyl)bis(isoindoline-1,3-dione) (**39d**)

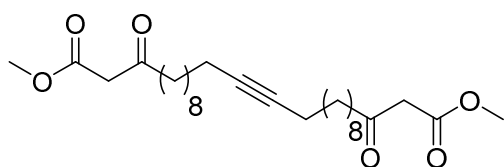


2-(Undec-9-yn-1-yl)isoindoline-1,3-dione (**38d**) (145 mg, 0.488 mmol) was stirred with MS 5 Å (540 mg) and catalyst **28** (21.3 mg, 20.5 μmol, 4 mol%) in toluene (4 mL) for 1 h at room temperature according to general procedure 2. Flash

chromatography (SiO₂, hexanes/ethyl acetate, 6/1 to 4/1) afforded the title compound as a colorless solid (121 mg, 92%).

M.p. = 75 – 76 °C, ¹H NMR (400 MHz, CDCl₃): δ = 7.85 – 7.80 (m, 4H), 7.72 – 7.67 (m, 4H), 3.66 (t, *J* = 7.3 Hz, 4H), 2.11 (t, *J* = 7.0 Hz, 4H), 1.71 – 1.60 (m, 4H), 1.49 – 1.40 (m, 4H), 1.39 – 1.24 ppm (m, 16H); ¹³C NMR (100 MHz, CDCl₃): δ = 168.6, 133.9, 132.3, 123.3, 80.3, 38.2, 29.2, 29.1, 28.9, 28.7, 27.0, 18.9 ppm; IR (film): $\tilde{\nu}$ = 2927, 2851, 1772, 1723, 1464, 1343, 1393, 1359, 1331, 1187, 1119, 1054, 997, 924, 873, 801, 711, 624, 554, 531, 512, 475 cm⁻¹; MS (EI): *m/z* (%) = 540 (7), 393 (18), 230 (8), 202 (7), 164 (40), 161 (20), 160 (100), 150 (53), 148 (20), 135 (9), 133 (7), 130 (13), 121 (9), 95 (11), 81 (13), 67 (12), 55 (7); HRMS (ESI(pos)): *m/z*: calcd. for [C₃₄H₄₀N₂O₄+Na]⁺: 563.2880, found: 563.2880.

Dimethyl 3,24-dioxohexacos-13-yne-1,12-dioate (43)

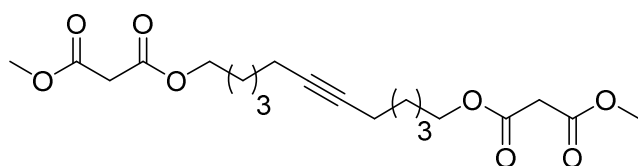


Methyl 3-oxopentadec-13-ynoate (**42**) (23.1 mg, 87 μmol) was stirred with MS 5 Å (270 mg) and catalyst **28** (12.5 mg, 12.0 μmol, 14 mol%) in toluene (2 mL) for 20 h at 80 °C according to general

procedure 2. Flash chromatography (SiO₂, hexanes/ethyl acetate, 10/1 to 4/1) afforded the title compound as a colorless solid (14.9 mg, 72%).

M.p. = 78.5 – 79 °C. ¹H NMR (400 MHz, CDCl₃): δ = 3.74 (s, 6H), 3.44 (s, 4H), 2.52 (t, *J* = 7.3 Hz, 4H), 2.13 (t, *J* = 7.0 Hz, 4H), 1.62 – 1.53 (m, 4H), 1.50 – 1.42 (m, 4H), 1.39 – 1.24 ppm (m, 20H); ¹³C NMR (100 MHz, CDCl₃): δ = 202.9, 168.0, 80.4, 52.4, 49.2, 43.2, 29.5, 29.4, 29.3, 29.2, 29.1, 29.0, 23.6, 18.9 ppm; IR (film): $\tilde{\nu}$ = 2923, 2867, 2807, 2438, 1441, 1266, 1044, 879, 823, 799, 728, 495 cm⁻¹; MS (ESI(pos)) *m/z* (%) = 501.3 (100 [M+Na]⁺); HRMS (ESI(pos)): *m/z*: calcd. for [C₂₈H₄₆O₆+Na]⁺: 501.3191, found: 501.3187.

O,O'-(Dodec-6-yne-1,12-diyl) dimethyl dimalonate (45)

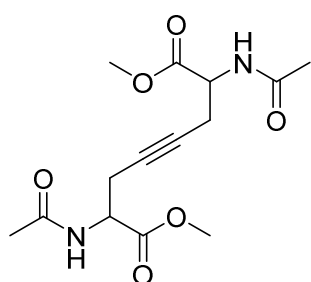


Methyl oct-6-yn-1-yl malonate (**44**) (205 mg, 0.91 mmol) was stirred with MS 5 Å (1.1 g) and catalyst **28** (15.0 mg,

14.4 μmol, 2 mol%) in toluene (5 mL) for 4 h at 80 °C according to general procedure 2. Flash chromatography (SiO₂, hexanes/ethyl acetate, 6/1 to 2/1) afforded the title compound as a colorless oil (169 mg, 94%).

^1H NMR (400 MHz, CDCl_3): δ = 4.14 (t, J = 6.6 Hz, 4H), 3.74 (s, 6H), 3.37 (s, 4H), 2.15 (t, J = 6.8 Hz, 4H), 1.70 – 1.62 (m, 4H), 1.54 – 1.39 ppm (m, 8H); ^{13}C NMR (100 MHz, CDCl_3): δ = 167.2, 166.7, 80.1, 65.7, 52.6, 41.5, 28.8, 28.2, 25.1, 18.8 ppm; IR (film): $\tilde{\nu}$ = 2953, 2864, 2212, 1728, 1673, 1437, 1411, 1334, 1272, 1198, 1147, 1018, 908, 850, 787, 685, 579 cm^{-1} ; MS (ESI(pos)) m/z (%) = 421 (100 [$\text{M}+\text{Na}^+$]); HRMS (ESI(pos)): m/z : calcd. for $[\text{C}_{20}\text{H}_{30}\text{O}_8+\text{Na}]^+$: 421.1837, found: 421.1833.

Dimethyl 2,7-diacetamidooct-4-ynedioate (**49**)

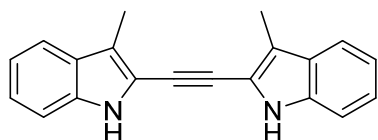


Methyl 2-acetamidohex-4-ynoate (**48**) (50 mg, 273 μmol) was stirred with MS 5 Å (720 mg) and catalyst **28** (16.0 mg, 15.4 μmol , 6 mol%) in toluene (5 mL) for 1 h at room temperature according to general procedure 2. Flash chromatography (SiO_2 , ethyl acetate/MeOH, 1/0 to 10/1) afforded the title compound as a colorless solid (38 mg, 89%, mixture of diastereomers).

^1H NMR (400 MHz, CDCl_3): δ = 7.19 (bd, J = 9.1 Hz, 2H), 6.54 (bd, J = 8.5 Hz, 2H), 4.90 (dt, J = 9.3, 3.8 Hz, 2H), 4.81 (dt, J = 8.4, 4.1 Hz, 2H), 3.80 (s, 6H), 3.80 (s, 6H), 2.74 – 2.54 (m, 8H), 2.14 (s, 6H), 2.13 ppm (s, 6H); ^{13}C NMR (100 MHz, CDCl_3): δ = 172.7, 171.54, 170.50, 170.4, 78.6, 78.0, 52.9, 50.7, 50.4, 23.6, 23.3, 23.2, 22.9 ppm; IR (film): $\tilde{\nu}$ = 3302, 2955, 2453, 1722, 1638, 1552, 1474, 1417, 1345, 1282, 1264, 1239, 1202, 1034, 1007, 788, 684, 595, 512, 458 cm^{-1} ; MS (EI): m/z (%) = 312 (27), 253 (26), 238 (15), 211 (90), 182 (100), 169 (88), 151 (11), 140 (14), 131 (11), 124 (30), 109 (32), 99 (11), 88 (86), 82 (42), 80 (36), 60 (13), 43 (89); HRMS (ESI(pos)): m/z : calcd. for $[\text{C}_{14}\text{H}_{20}\text{N}_2\text{O}_6+\text{Na}]^+$: 335.1211, found: 335.121.

The analytical and spectroscopic data are in agreement with those reported in the literature.^[120]

1,2-Bis(3-methyl-1H-indol-2-yl)ethyne (**51**)

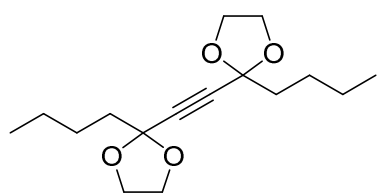


3-Methyl-2-(prop-1-yn-1-yl)-1H-indole (**50**) (33.0 mg, 195 μmol) was stirred with MS 5 Å (240 mg) and catalyst **28** (9.3 mg, 8.9 μmol , 5 mol%) in toluene (5 mL) for 1 h at room

temperature according to general procedure 2. The crude material was washed with CH_2Cl_2 (1 mL) to afford the title compound as a colorless solid (24.3 mg, 88%).

M.p. = decomp. 260 °C; ^1H NMR (400 MHz, $\text{CO}(\text{CH}_3)_2$): δ = 10.42 (bs, 2H), 7.55 (d, J = 8.1 Hz, 2H), 7.37 (d, J = 8.1 Hz, 2H), 7.20 (t, J = 7.6 Hz, 2H), 7.08 (t, J = 7.6 Hz, 2H), 2.45 ppm (s, 6H); ^{13}C NMR (100 MHz, $\text{CO}(\text{CH}_3)_2$): δ = 137.7, 128.8, 124.3, 120.4, 119.9, 118.2, 117.6, 112.0, 87.8, 10.0 ppm; IR (film): $\tilde{\nu}$ = 3393, 3049, 2914, 2528, 1466, 1440, 1373, 1338, 1318, 1242, 1161, 1116, 1063, 1028, 1003, 959, 925, 871, 834, 742, 680, 663, 573, 537, 503, 474, 444, 422 cm^{-1} ; MS (EI): m/z (%) = 284 (100), 283 (29), 282 (7), 281 (8), 269 (17), 268 (7), 241 (2), 167 (2), 154 (5), 142 (10), 141 (15), 128 (3), 127 (3), 77 (2); HRMS (EI): m/z : calcd. for $[\text{C}_{20}\text{H}_{16}\text{N}_2]^+$: 284.1313, found: 284.1313.

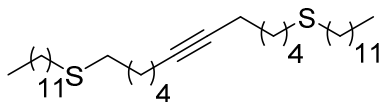
1,2-Bis(2-butyl-1,3-dioxolan-2-yl)ethyne (54a)



2-Butyl-2-(prop-1-yn-1-yl)-1,3-dioxolane (**53a**) (21.1 mg, 0.125 mmol) was stirred with MS 5 Å (260 mg) and catalyst **28** (7.0 mg, 6.7 μmol , 5 mol%) in toluene (2 mL) for 5 h at room temperature according to general procedure 2. Flash chromatography (SiO_2 , hexanes/ethyl acetate, 30/1 to 10/1) afforded the title compound as a colorless oil (14.8 mg, 73%).

^1H NMR (400 MHz, CDCl_3): δ = 4.08 – 4.01 (m, 4H), 4.00 – 3.94 (m, 4H), 1.89 – 1.85 (m, 4H), 1.54 – 1.48 (m, 4H), 1.40 – 1.33 (m, 4H), 0.91 ppm (t, J = 7.3 Hz, 6H); ^{13}C NMR (100 MHz, CDCl_3): δ = 103.4, 81.6, 64.7, 38.9, 26.2, 22.7, 14.1 ppm; IR (film): $\tilde{\nu}$ = 2956, 2931, 2892, 2874, 1468, 1380, 1342, 1296, 1259, 1236, 1198, 1160, 1118, 1048, 1029, 968, 945, 886, 587 cm^{-1} ; MS (EI): m/z (%) = 282 (0.21), 225 (100), 183 (29), 169 (3), 153 (15), 129 (24), 123 (26), 97 (48), 79 (6), 57 (10); HRMS (ESI(pos)): m/z : calcd. for $[\text{C}_{16}\text{H}_{26}\text{O}_4+\text{Na}]^+$: 305.1724, found: 305.1723.

1,12-Bis(tridecylthio)dodec-6-yne (56a)

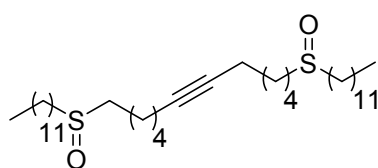


Oct-6-yn-1-yl(tridecyl)sulfane (**55a**) (144 mg, 0.46 mmol) was stirred with MS 5 Å (840 mg) and catalyst **28** (11.5 mg, 11.0 μmol , 2 mol%) in toluene (5 mL) for 2 h at room temperature according to general procedure 2. Flash chromatography (SiO_2 , pentane/ CH_2Cl_2 , 6/1 to 2/1) afforded the title compound as a colorless solid (112 mg, 85%).

M.p. = 55 – 56 °C, ^1H NMR (400 MHz, CDCl_3): δ = 2.53 – 2.47 (m, 8H), 2.17 – 2.12 (m, 4H), 1.64 – 1.53 (m, 8H), 1.51 – 1.45 (m, 8H), 1.42 – 1.21 (m, 36H), 0.88 ppm (t, J = 6.9 Hz, 6H); ^{13}C

NMR (100 MHz, CDCl₃): δ = 80.3, 32.4, 32.3, 32.1, 29.9, 29.81, 29.78, 29.76, 29.7, 29.5, 29.44, 29.41, 29.1, 28.9, 28.3, 22.8, 18.8, 14.3 ppm; IR (film): $\tilde{\nu}$ = 2953, 2917, 2847, 1459, 1426, 1370, 1297, 1250, 1199, 1186, 1026, 813, 762, 725, 512 cm⁻¹; MS (EI): m/z (%) = 566 (4), 397 (88), 365 (100), 311 (5), 229 (13), 197 (36), 195 (27), 141 (11), 107 (5), 101 (10), 95 (10), 87 (14), 81 (13), 69 (11), 67 (10), 57 (19), 55 (17), 43 (22); HRMS (EI): m/z : calcd. for [C₃₆H₇₀S₂]⁺: 566.4917, found: 566.4919.

1,12-Bis(tridecylsulfinyl)dodec-6-yne (56b)

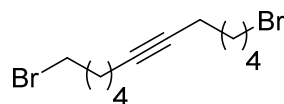


1-(Oct-6-yn-1-ylsulfinyl)tridecane (**55b**) (86.0 mg, 263 μ mol) was stirred with MS 5 Å (850 mg) and catalyst **28** (15.2 mg, 14.6 μ mol, 5 mol%) in toluene (5 mL) for 16 h at 80 °C according to general procedure 2. Flash chromatography

(SiO₂, CH₂Cl₂/ethyl acetate 1/1 to CH₂Cl₂/MeOH 10/1) afforded the title compound as a colorless solid (59 mg, 75%).

M.p. = 108 – 110 °C, ¹H NMR (400 MHz, CDCl₃): δ = 2.73 – 2.56 (m, 8H), 2.20 – 2.13 (m, 4H), 1.83 – 1.68 (m, 8H), 1.61 – 1.38 (m, 12H), 1.36 – 1.20 (m, 32H), 0.87 ppm (t, J = 6.9 Hz, 6H); ¹³C NMR (100 MHz, CDCl₃): δ = 80.2, 52.7, 52.5, 32.0, 29.74, 29.73, 29.67, 29.51, 29.46, 29.4, 29.0, 28.8, 28.2, 22.81, 22.76, 22.4, 18.7, 14.2 ppm; IR (film): $\tilde{\nu}$ = 2912, 2848, 1466, 1081, 1015, 723, 463 cm⁻¹. MS (EI): m/z (%) = 598 (22), 581 (20), 430 (39), 429 (54), 381 (26), 365 (43), 363 (67), 201 (87), 97 (28), 95 (38), 93 (27), 91 (22), 87 (23), 85 (22), 83 (41), 81 (61), 71 (34), 70 (20), 69 (59), 67 (47), 57 (78), 56 (25), 55 (88), 43 (100), 41 (73), 29 (28); HRMS (ESI(pos)): m/z : calcd. for [C₃₆H₇₀O₂S₂+Na]⁺: 621.4711, found: 621.4709.

1,12-Dibromododec-6-yne (58)



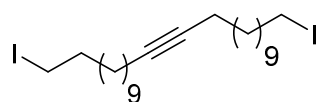
8-Bromo-oct-2-yne (**57**) (250 mg, 1.32 mmol) was stirred with MS 5 Å (1.25 g) and catalyst **28** (15.0 mg, 16 μ mol, 1 mol%) in toluene (6 mL) for 2 h at room temperature according to general procedure

2. Flash chromatography (SiO₂, pentane) afforded the title compound as a colorless oil (212 mg, 91%).

¹H NMR (400 MHz, CDCl₃): δ = 3.41 (t, J = 6.9 Hz, 4H), 2.16 (t, J = 6.5 Hz, 4H), 1.87 (dt, J = 6.9, 6.9 Hz, 4H), 1.58 – 1.45 ppm (m, 8H); ¹³C NMR (100 MHz, CDCl₃): δ = 80.3, 33.9, 32.6, 28.4, 27.6, 18.8 ppm; IR (film): $\tilde{\nu}$ = 3302, 2936, 2860, 2213, 1904, 1732, 1671, 1431, 1349, 1230,

1199, 1023, 732, 642 cm^{-1} ; MS (EI): m/z (%) = 324 (1), 245 (9), 243 (9), 203 (9), 201 (9), 189 (10), 187 (10), 163 (11), 135 (20), 121 (14), 109 (39), 95 (90), 81 (100), 67 (94), 55 (68), 41 (47), 29 (20); HRMS (EI): m/z : calcd. for $[\text{C}_{12}\text{H}_{20}\text{Br}_2]^+$: 321.9928, found: 321.9932.

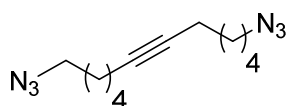
1,24-Diiodotetracos-11-yne (60)



14-Iodotetradec-2-yne (**59**) (71 mg, 0.22 mmol) was stirred with MS 5 Å (345 mg) and catalyst **28** (11.0 mg, 10.6 μmol , 5 mol%) in toluene (4 mL) for 90 min at room temperature according to general procedure 2. Flash chromatography (SiO_2 , hexanes/ethyl acetate, 1/0 to 50/1) afforded the title compound as a colorless solid (52 mg, 78%).

M.p. = 54 – 54.5 $^\circ\text{C}$, ^1H NMR (400 MHz, CDCl_3): δ = 3.18 (t, J = 7.1 Hz, 4H), 2.12 (t, J = 7.1 Hz, 4H), 1.85 – 1.77 (m, 4H), 1.49 – 1.42 (m, 4H), 1.40 – 1.24 ppm (m, 28H); ^{13}C NMR (100 MHz, CDCl_3): δ = 80.5, 33.7, 30.6, 29.6, 29.5, 29.31, 29.27, 29.0, 28.7, 18.9, 7.4 ppm; IR (film): $\tilde{\nu}$ = 2953, 2917, 2846, 1457, 1422, 1336, 1314, 1289, 1259, 1229, 1197, 1163, 1097, 1050, 1035, 982, 802, 724, 602, 527, 456 cm^{-1} ; MS (EI): m/z (%) = 586 (15), 459 (8), 361 (7), 305 (9), 210 (5), 155 (13), 151 (10), 137 (20), 123 (33), 111 (18), 109 (59), 95 (100), 81 (91), 67 (68), 57 (16), 55 (69), 43 (28), 41 (43); HRMS (EI): m/z : calcd. for $[\text{C}_{24}\text{H}_{44}\text{I}_2]^+$: 586.1528, found: 586.1532.

1,12-Diazidododec-6-yne (62)



8-Azido-oct-2-yne (**61**) (151 mg, 1.00 mmol) was stirred with MS 5 Å (1 g) and catalyst **28** (13.8 mg, 13.3 μmol , 2 mol%) in toluene (5 mL) for 16 h at room temperature according to general procedure 2. Flash chromatography (SiO_2 , hexanes/ethyl acetate, 100/1 to 50/1) afforded the title compound as a colorless oil (119 mg, 85%).

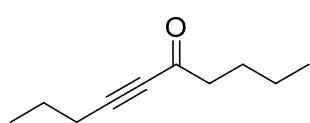
^1H NMR (400 MHz, CDCl_3): δ = 3.27 (t, J = 6.9 Hz, 4H), 2.19 – 2.14 (m, 4H), 1.66 – 1.57 (m, 4H), 1.55 – 1.42 ppm (m, 8H); ^{13}C NMR (100 MHz, CDCl_3): δ = 80.2, 51.5, 28.7, 28.6, 26.1, 18.7 ppm; IR (film): $\tilde{\nu}$ = 2936, 2861, 2087, 1456, 1349, 1333, 1257, 1097, 1026, 896, 839, 733, 668, 637, 557 cm^{-1} ; MS (EI): m/z (%) = 206 (2), 178 (17), 164 (23), 163 (24), 150 (15), 136 (30), 122 (66), 108 (42), 94 (45), 91 (48), 84 (10), 79 (62), 77 (59), 67 (63), 55 (75), 41 (100), 28 (62); HRMS (CI(DE), *i*-Butane): m/z : calcd. for $[\text{C}_{12}\text{H}_{21}\text{N}_6]^+$: 249.1826, found: 249.1828.

7.2.4 Cross Metathesis Reactions

General procedure 3: Alkyne cross metathesis with catalyst [Mo(\equiv CC₆H₄OMe)(OSiPh₃)₃] **28**

The alkynes were stirred with MS 5 Å (1 g per mmol alkyne) in toluene (0.2 M based on the alkyne) for 30 min before metathesis catalyst **28** was added in one portion. The reaction mixture was stirred under the individual conditions. The crude material was filtered through a plug of Celite[®], which was carefully rinsed with ethyl acetate. The solvent was evaporated and the residue was purified by flash chromatography.

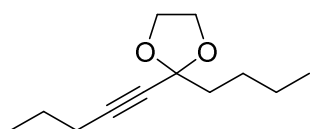
Dec-6-yn-5-one (**64**)



Oct-2-yn-4-one (**53b**) (21.8 mg, 0.176 mmol) and 4-octyne (**63**) (82.5 mg, 0.749 mmol) were stirred with MS 5 Å (370 mg), MnCl₂ (5.1 mg, 0.041 mmol), and catalyst **28** (9.8 mg, 9.4 μmol, 6 mol%) in toluene (2.5 mL) for 16 h at 120 °C according to general procedure 3. Flash chromatography (SiO₂, hexanes/ethyl acetate, 50/1) afforded the title compound as a colorless oil (20.2 mg, 75%).

¹H NMR (400 MHz, CDCl₃): δ = 2.52 (t, *J* = 7.5 Hz, 2H), 2.34 (t, *J* = 7.1 Hz, 2H), 1.69 – 1.56 (m, 4H), 1.40 – 1.29 (m, 2H), 1.02 (t, *J* = 7.3 Hz, 3H), 0.92 ppm (t, *J* = 7.3 Hz, 3H); ¹³C NMR (100 MHz, CDCl₃): δ = 188.7, 94.2, 81.2, 45.4, 26.4, 22.3, 21.4, 21.0, 13.9, 13.6 ppm; IR (film): $\tilde{\nu}$ = 3070, 2966, 2935, 2874, 2230, 2708, 1462, 1429, 1366, 1339, 1246, 1157, 1115, 1069, 1028, 997, 834, 752, 711, 700, 516 cm⁻¹; MS (EI): *m/z* (%) = 137 (7), 110 (35), 96 (7), 95 (100), 82 (12), 67 (16), 53 (15), 41 (11), 39 (7); HRMS (CI, (FE) *i*-Butane): *m/z*: calcd. for [C₁₀H₁₇O]⁺: 153.1281, found: 153.1279.

2-Butyl-2-(pent-1-yn-1-yl)-1,3-dioxolane (**65**)

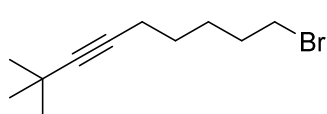


2-Butyl-2-(prop-1-yn-1-yl)-1,3-dioxolane (**53a**) (59.0 mg, 0.351 mmol) and 4-octyne (**63**) (150 mg, 1.36 mmol) were stirred with MS 5 Å (1 g) and catalyst **28** (23.1 mg, 22.2 μmol, 6 mol%) in toluene (5 mL) for 30 min at room temperature according to general procedure 3. Flash chromatography (SiO₂, hexanes/ethyl acetate, 50/1) afforded the title compound as a colorless oil (51.2 mg, 74%).

¹H NMR (400 MHz, CDCl₃): δ = 4.10 – 4.02 (m, 2H), 4.01 – 3.91 (m, 2H), 2.19 (t, *J* = 7.2 Hz, 2H), 1.89 – 1.82 (m, 2H), 1.58 – 1.48 (m, 4H), 1.42 – 1.31 (m, 2H), 0.98 (t, *J* = 7.4 Hz, 3H),

0.91 ppm (t, $J = 7.2$ Hz, 3H); ^{13}C NMR (100 MHz, CDCl_3): $\delta = 103.7, 84.9, 78.5, 64.6, 39.5, 26.4, 22.8, 22.1, 20.7, 14.1, 13.6$ ppm; IR (film): $\tilde{\nu} = 2958, 2932, 2873, 2233, 1463, 1379, 1339, 1294, 1238, 1196, 1161, 1116, 1089, 1070, 1038, 965, 884, 787, 740, 671$ cm^{-1} ; MS (EI): m/z (%) = 196 (0.1), 154 (5), 153 (20), 139 (100), 125 (5), 95 (32), 83 (5), 79 (9), 77 (5), 67 (9), 66 (5), 65 (6), 55 (7), 53 (7), 41 (9), 39 (5); HRMS (ESI(pos)): m/z : calcd. for $[\text{C}_{12}\text{H}_{20}\text{O}_3+\text{Na}]^+$: 219.1356, found: 219.1356.

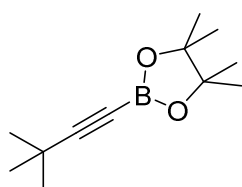
9-Bromo-2,2-dimethylnon-3-yne (67)



8-Bromooct-2-yne (**57**) (95 mg, 0.5 mmol) and 4,4-dimethylpent-2-yne (**66**) (48 mg, 0.5 mmol) were stirred with MS 5 Å (1 g) and catalyst **28** (50 mg, 48.0 μmol , 10 mol%) in toluene (5 mL) for 2.5 h at room temperature according to general procedure 3. Flash chromatography (SiO_2 , hexanes/ethyl acetate, 1/0 to 100/1) afforded the title compound as a colorless oil (61 mg, 53%).

^1H NMR (400 MHz, CDCl_3): $\delta = 3.42$ (t, $J = 6.8$ Hz, 2H), 2.16 (t, $J = 6.5$ Hz, 2H), 1.92 – 1.84 (m, 2H), 1.58 – 1.46 (m, 4H), 1.20 ppm (s, 9H); ^{13}C NMR (100 MHz, CDCl_3): $\delta = 89.6, 78.1, 33.9, 32.5, 31.6, 28.4, 27.4, 19.7$ ppm; IR (film): $\tilde{\nu} = 2966, 2937, 2862, 1475, 1456, 1437, 1390, 1361, 1332, 1265, 1241, 1205, 1068, 1031, 928, 895, 819, 731, 643, 563, 538, 513, 412$ cm^{-1} ; MS (EI): m/z (%) = 230 (0.3), 217 (11), 215 (11), 175 (5), 173 (5), 161 (7), 159 (6), 137 (5), 135 (14), 123 (9), 121 (6), 109 (45), 107 (38), 95 (96), 91 (25), 83 (31), 81 (100), 69 (49), 67 (65), 65 (16), 57 (27), 55 (46), 53 (18), 43 (14), 41 (20); HRMS (EI): m/z : calcd. for $[\text{C}_{11}\text{H}_{19}\text{Br}]^+$: 230.0673, found: 230.0670.

2-(3,3-Dimethylbut-1-yn-1-yl)-4,4,5,5-tetramethyl-1,3,2-dioxaborolane (69)

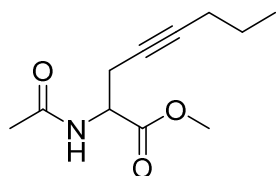


4,4,5,5-Tetramethyl-2-(prop-1-yn-1-yl)-1,3,2-dioxaborolane (**68**) (249 mg, 1.50 mmol) and 4,4-dimethylpent-2-yne (**66**) (240 mg, 2.50 mmol) were stirred with MS 5 Å (2.5 g) and catalyst **28** (30.3 mg, 29.1 μmol , 2 mol%) in toluene (12.5 mL) for 84 h at 60 °C according to general procedure 3. Sublimation (10^{-3} mbar, 60 °C) afforded the title compound as a colorless solid (116mg, 37%).

^1H NMR (400 MHz, CDCl_3): $\delta = 1.27$ (s, 12H), 1.24 (s, 9H); ^{13}C NMR (100 MHz, CDCl_3): $\delta = 84.2, 30.7, 28.6, 24.9, 24.8$ ppm.

The analytical and spectroscopic data are in agreement with those reported in the literature.^[126]

Methyl 2-acetamidooct-4-ynoate (70)



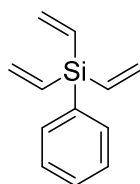
Methyl 2-acetamidohex-4-ynoate (**48**) (24.3 mg, 0.133 mmol) and 4-octyne (**63**) (225 mg, 2.04 mmol) were stirred with MS 5 Å (300 mg) and catalyst **28** (30.3 mg, 29.1 μmol, 22 mol%) in toluene (2 mL) for 1 h at room temperature according to general procedure 3. Flash chromatography (SiO₂, hexanes/ethyl acetate, 2/1) afforded the title compound as a colorless oil (22.4 mg, 80%).

¹H NMR (400 MHz, CDCl₃): δ = 6.25 (d, *J* = 6.9 Hz, 1H), 4.70 (dt, *J* = 8.1, 4.2 Hz, 1H), 3.76 (s, 3H), 2.77 – 2.63 (m, 2H), 2.10 (tt, *J* = 7.0, 2.4 Hz, 2H), 2.04 (s, 3H), 1.52 – 1.42 (m, 2H), 0.94 ppm (t, *J* = 7.3 Hz, 3H); ¹³C NMR (100 MHz, CDCl₃): δ = 171.4, 169.8, 84.0, 74.1, 52.7, 51.2, 23.3, 23.0, 22.4, 20.7, 13.5 ppm; IR (film): $\tilde{\nu}$ = 3298, 3086, 2926, 2929, 2863, 1738, 1650, 1553, 1430, 1373, 1352, 1302, 1284, 1227, 1201, 1181, 1131, 1055, 1022, 935, 910, 808, 791, 718, 677, 600, 518, 456 cm⁻¹; MS (EI): *m/z* (%) = 211 (2), 183 (7), 153 (5), 152 (44), 137 (19), 124 (41), 110 (38), 109 (8), 93 (5), 88 (100), 80 (11), 79 (6), 68 (18), 60 (12), 53 (6), 43 (33); HRMS (ESI(pos)): *m/z*: calcd. for [C₁₁H₁₇N₁O₃+Na]⁺: 234.1101, found: 234.1101.

7.3 Synthesis of Multidentate Ligands

7.3.1 Synthesis of Ligands with Silicon Linkers

Phenyltrivinylsilane (90d)

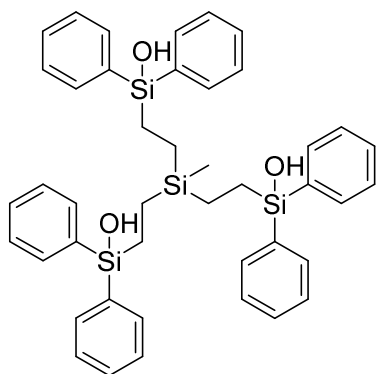


Trichloromethylsilane (2.12 g, 10.0 mmol) was added dropwise at room temperature over 60 min to a solution of vinylmagnesium bromide (1 M in THF, 31.0 mL, 31.0 mmol) in THF (20 mL). After stirring for 16 h the reaction mixture was cooled to 0 °C and aq. sat. NH₄Cl (30 mL) was added. Stirring was continued for 10 min at room temperature before the aqueous layer was extracted with ethyl acetate (2 × 50 mL) and the combined extracts were dried over MgSO₄. Evaporation of the solvent and purification of the residue by flash chromatography (SiO₂, hexanes) afforded the title compound as a colorless oil (1.23 g, 66%).

^1H NMR (400 MHz, CDCl_3): δ = 7.54 – 7.59 (m, 2H), 7.35 – 7.42 (m, 3H), 6.35 (dd, J = 19.9, 14.6 Hz, 3H), 6.21 (dd, J = 14.6, 4.0 Hz, 3H), 5.84 ppm (dd, J = 19.9, 4.0 Hz, 3H); ^{13}C NMR (100 MHz, CDCl_3): δ = 136.1, 135.2, 134.6, 133.9, 129.6, 128.0 ppm; IR (film): $\tilde{\nu}$ = 3051, 3007, 2969, 2944, 1590, 1428, 1400, 1266, 1110, 1006, 956, 809, 699, 619, 549, 471 cm^{-1} ; MS (EI): m/z (%) = 186 (12), 159 (38), 158 (100), 157 (13), 133 (50), 132 (23), 131 (47), 130 (22), 128 (13), 108 (11), 107 (47), 106 (10), 105 (34), 82 (23), 81 (10), 53 (12); HRMS (EI (FE)): m/z : calcd. for $[\text{C}_{12}\text{H}_{14}\text{Si}]^+$: 186.0864, found: 186.0865.

The analytical and spectroscopic data are in agreement with those reported in the literature.^[127]

((Methylsilanetriyl)tris(ethane-2,1-diyl))tris(diphenylsilanol) (89a)



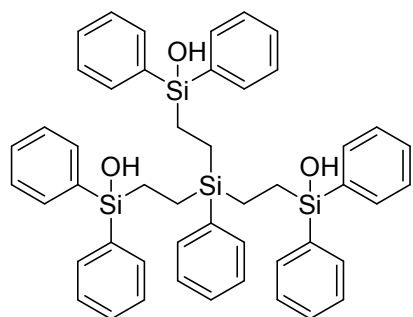
Trivinylmethylsilane (746 mg, 6.00 mmol) was dissolved in toluene (50 mL) in a flame-dried Schlenk flask. After addition of Karstedt's catalyst (0.1 M in poly(dimethylsiloxane), 0.3 mL, 0.03 mmol) the mixture was heated to 60 °C and diphenylchlorosilane (4.05 g, 18.5 mmol) was added dropwise and stirring was continued for 20 h at 60 °C. The mixture was then allowed to reach ambient temperature

before H_2O (10 mL) and NEt_3 (0.5 mL) were added. After stirring for 20 min aq. sat. NH_4Cl (5 mL) was added and stirring continued for another 10 min. The aqueous layer was extracted with ethyl acetate (3×100 mL) and the combined organic layers were dried over MgSO_4 . The solvent was evaporated and the crude product was purified by column chromatography (SiO_2 , hexanes/ethyl acetate, 4/1 to 3/1). The material was dissolved in CH_2Cl_2 (20 mL) and MS 3 Å (2 g) was added. After gentle stirring of the suspension for 2 h at room temperature, the MS was filtered off and the filtrate was evaporated. The product was dried for 4 h under high vacuum to afford the title compound as a colorless hygroscopic solid (2.43 g, 56%).

M.p.: 55 – 65 °C; ^1H NMR (400 MHz, CD_3OD): δ = 7.54 – 7.48 (m, 12H), 7.35 – 7.26 (m, 18H), 0.90 – 0.79 (m, 6H), 0.56 – 0.47 (m, 6H), –0.11 ppm (s, 3H); ^{13}C NMR (100 MHz, CD_3OD): δ = 138.2, 135.3, 130.6, 128.8, 8.2, 4.7, –6.4 ppm; IR (film): $\tilde{\nu}$ = 3258, 3068, 3047, 3012, 2908, 2879, 1589, 1427, 1249, 1111, 1053, 1027, 997, 818, 695, 664, 636, 499, 479, 445 cm^{-1} ; MS

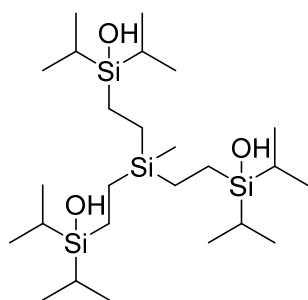
(ESI(pos)): m/z (%) = 747.3 $[M+Na]^+$ (100); HRMS (ESI(pos)): m/z : calcd. for $[C_{43}H_{48}O_3Si_4+Na]^+$: 747.2569, found: 747.2573.

((Phenylsilanetriyl)tris(ethane-2,1-diyl))tris(diphenylsilanol) (89d)



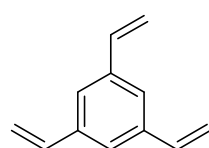
Phenyltrivinylmethylsilane **90d** (950 mg, 5.10 mmol) was dissolved in toluene (20 mL) in a flame-dried Schlenk flask. After addition of Karstedt's catalyst (0.1 M in poly(dimethylsiloxane), 0.4 mL, 0.04 mmol) the mixture was heated to 50 °C and diphenylchlorosilane (3.91 g, 17.9 mmol) was added dropwise and stirring was continued for 16 h at this temperature before a second portion of Karstedt's catalyst (0.1 M in poly(dimethylsiloxane), 0.1 mL, 0.01 mmol) was added and stirring was continued for another 2 h at 65 °C. The mixture was then allowed to reach ambient temperature before H₂O (20 mL) and NEt₃ (0.5 mL) were added. After stirring for 20 min, aq. sat. NH₄Cl (5 mL) was introduced and stirring was continued for 10 min. The aqueous layer was extracted with ethyl acetate (3 × 100 mL) and the combined organic layers were dried over MgSO₄. The solvent was evaporated and the crude product was purified by flash chromatography (SiO₂, hexanes/ethyl acetate, 4/1 to 2/1). The material was dissolved in CH₂Cl₂ (20 mL) and MS 3 Å (2 g) was added. After gentle stirring of the suspension for 2 h at room temperature, the MS was filtered off and the filtrate was evaporated. The product was dried for 4 h under high vacuum to afford the title compound as a colorless hygroscopic solid (2.31 g, 58%).

M.p.: 56 – 60 °C; ¹H NMR (400 MHz, CDCl₃): δ = 7.51 – 7.55 (m, 12H), 7.30 – 7.42 (m, 23H), 2.38 – 2.41 (m, 3H), 0.84 – 1.00 ppm (m, 12H); ¹³C NMR (100 MHz, CDCl₃): δ = 136.3, 136.0, 134.5, 134.3, 130.0, 129.2, 128.0, 127.9, 7.0, 2.3 ppm; IR (film): $\tilde{\nu}$ = 3298, 3067, 3046, 2910, 1705, 1589, 1486, 1427, 1304, 1262, 1110, 1049, 997, 828, 694, 665, 643, 501, 471, 445 cm⁻¹; MS (ESI(pos)): m/z (%) = 809.4 $[M+Na]^+$ (100); HRMS (ESI(pos)): m/z : calcd. for $[C_{48}H_{50}O_3Si_4+Na]^+$: 809.2729, found: 809.2729.

((Methylsilanetriyl)tris(ethane-2,1-diyl))tris(diisopropylsilanol) (89b)

Trivinylmethylsilane (373 mg, 3.00 mmol) was dissolved in toluene (10 mL) in a flame-dried Schlenk flask. After addition of Karstedt's catalyst (0.1 M in poly(dimethyl-siloxane), 0.30 mL, 0.03 mmol) the mixture was heated to 70 °C and diphenylchlorosilane (1.87 mL, 1.63 g, 10.8 mmol) was added dropwise and stirring continued for 16 h at this temperature. The mixture was then allowed to reach ambient temperature before water (10 mL) and NEt_3 (1 mL) were added. After stirring for 20 min aq. sat. NH_4Cl (5 mL) was added and stirring was continued for another 10 min. The aqueous layer was extracted with ethyl acetate (3×50 mL) and the combined organic layers were dried over MgSO_4 . The solvent was evaporated and the crude product was purified by flash chromatography (SiO_2 , hexanes/ethyl acetate, 4/1 to 2/1). The material was dissolved in CH_2Cl_2 (20 mL) and MS 3 Å (2 g) was added. After gentle stirring of the suspension for 2 h at room temperature, the MS was filtered off and the filtrate was evaporated. The product was dried for 4 h under high vacuum to afford the title compound as a colorless hygroscopic solid (675 mg, 43%).

M.p.: 73 – 75 °C; ^1H NMR (400 MHz, CDCl_3): δ = 1.53 (bs, 3H), 0.98 – 1.04 (m, 42H), 0.51 (s, 12H), –0.04 ppm (s, 3H); ^{13}C NMR (100 MHz, CDCl_3): δ = 17.6, 12.8, 4.1, 3.4, –6.6 ppm; IR (film): $\tilde{\nu}$ = 3297, 2941, 2891, 2864, 1461, 1406, 1383, 1365, 1248, 1133, 1065, 992, 919, 882, 807, 722, 702, 650, 466 cm^{-1} ; MS (EI): m/z (%) = 361 (33), 343 (100), 301 (4), 273 (3), 247 (2), 201 (4), 159 (5), 131 (5), 103 (4), 75 (5); HRMS (ESI(pos)): m/z : calcd. for $[\text{C}_{25}\text{H}_{60}\text{O}_3\text{Si}_4+\text{Na}]^+$: 543.3512, found: 543.3508.

7.3.2 Synthesis of Ligands with Trisubstituted Aromatic Linkers**1,3,5-Trivinylbenzene (96a)**

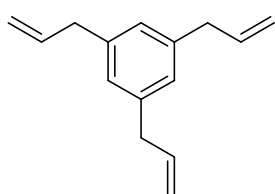
A solution of 1,3,5-tribromobenzene (378 mg, 1.20 mmol), vinyltributylstannane (1.46 g, 4.60 mmol), CsF (577 mg, 3.80 mmol) and $(\text{Ph}_3\text{P})_4\text{Pd}$ (231 mg, 0.20 mmol, 17 mol%) in DMF (10 mL) was stirred for 3.5 h at 135 °C in a closed JYoung tube. After cooling to room temperature, the reaction was quenched with aq. sat. KF (100 mL). The mixture was diluted with methyl *t*-butyl ether (200 mL) and stirred for 10 min before water (100 mL) and aq. sat. Na/K-tartrate (100 mL)

were added. The aqueous layer was extracted with methyl *t*-butyl ether (3 × 150 mL), the combined extracts were dried over MgSO₄ and the solvent was evaporated. The crude product was purified by flash chromatography (SiO₂, hexanes) to give the title compound as a colorless solid (150 mg, 80%).

¹H NMR (400 MHz, CDCl₃): δ = 7.36 (s, 3H), 6.73 (dd, *J* = 17.6, 10.9 Hz, 3H), 5.80 (dd, *J* = 17.6, 0.9 Hz, 3H), 5.29 ppm (dd, *J* = 10.9, 0.9 Hz, 3H); ¹³C NMR (100 MHz, CDCl₃): δ = 138.1, 136.7, 123.7, 114.5 ppm; IR (film): $\tilde{\nu}$ = 3087, 3042, 3007, 2981, 2958, 2926, 2854, 1822, 1770, 1702, 1633, 1585, 1444, 1413, 1396, 1299, 1274, 1257, 1166, 1080, 1052, 1029, 986, 903, 877, 715, 595, 544, 483 cm⁻¹; MS (EI): *m/z* (%) = 157 (12), 156 (100), 155 (23), 153 (16), 141 (26), 129 (16), 128 (25), 127 (12), 115 (33), 77 (10); HRMS (EI(DE)): *m/z*: calcd. for [C₁₂H₁₂]: 156.0940, found: 156.0939.

The analytical and spectroscopic data are in agreement with those reported in the literature.^[128]

1,3,5-Triallylbenzene (96b)

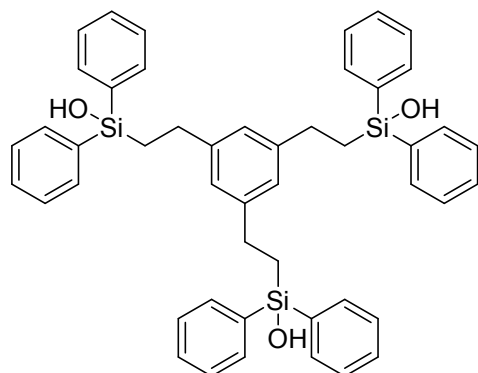


A solution of 1,3,5-tribromobenzene (1.67 g, 5.32 mmol), allyltributylstannane (5.50 mL, 5.87 g, 17.7 mmol) and (Ph₃P)₄Pd (1.54 g, 1.33 mmol, 25 mol%) in toluene (8 mL) was stirred for 18 h at 120 °C in a closed JYoung tube. After cooling to room temperature, the reaction was quenched with aq. sat. KF (20 mL). The mixture was diluted with methyl *t*-butyl ether (20 mL) and stirred for 15 min before water (30 mL) and aq. sat. Na/K-tartrate (10 mL) were added. The aqueous layer was extracted with ethyl acetate (3 × 50 mL), the combined organic layers were dried over MgSO₄ and the solvent was evaporated. The crude product was purified by distillation (10⁻³ mbar, 65 °C) to give the title compound as a colorless oil (801 mg, 76%).

¹H NMR (400 MHz, CDCl₃): δ = 6.87 (s, 3H), 5.96 (ddt, *J* = 17.0, 10.1, 6.8 Hz, 3H), 5.04 – 5.12 (m, 6H), 3.35 ppm (d, *J* = 6.8 Hz, 6H); ¹³C NMR (100 MHz, CDCl₃): δ = 140.5, 137.7, 126.8, 115.8, 40.3 ppm; IR (film): $\tilde{\nu}$ = 3078, 3005, 2978, 2957, 2904, 2872, 2850, 1833, 1639, 1601, 1456, 1431, 1412, 1377, 1340, 1281, 1189, 1157, 1098, 1072, 992, 962, 909, 845, 740, 715, 685, 654, 594, 557, 512, 451 cm⁻¹; MS (EI): *m/z* (%) = 198 (28), 157 (75), 155 (14), 153 (11), 142 (26), 141 (28), 130 (12), 129 (100), 128 (43), 127 (13), 116 (26), 115 (72), 91 (17), 77 (12), 41 (16); HRMS (EI(FE)): *m/z*: calcd. for [C₁₅H₁₈]: 198.1410, found: 198.1409.

The analytical and spectroscopic data are in agreement with those reported in the literature.^[129]

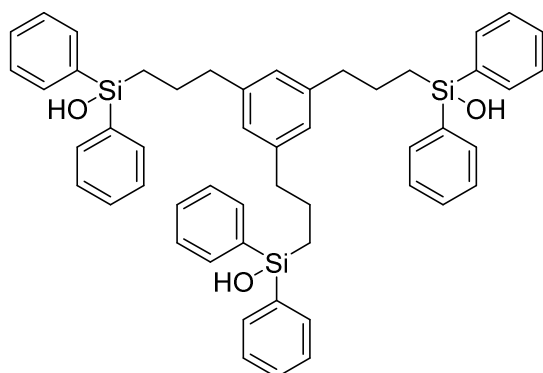
(Benzene-1,3,5-triyltris(ethane-2,1-diyl))tris(diphenylsilanol) (94a)



1,3,5-Triallylbenzene (**96a**) (75 mg, 0.48 mmol) was dissolved in toluene (5 mL) in a flame-dried Schlenk flask. After addition of Karstedt's catalyst (0.1 M in poly(dimethylsiloxane), 0.20 mL, 0.02 mmol) the mixture was heated to 70 °C and diphenylchlorosilane (0.39 mL, 437 mg, 2.00 mmol) was added dropwise and stirring continued for 16 h at 70 °C. The mixture

was allowed to reach ambient temperature before H₂O (10 mL) and NEt₃ (1 mL) were added and the mixture stirred for 20 min. Aq. sat. NH₄Cl (5 mL) was added and stirring was continued for another 10 min. The aqueous layer was extracted with ethyl acetate (3 × 50 mL) and the combined organic layers were dried over MgSO₄. Evaporation of the solvent and flash chromatography (SiO₂, hexanes/ethyl acetate, 6/1 to 2/1) of the residue gave the crude product which was dried with MS 3 Å (2 g) by stirring in CH₂Cl₂ (10 mL) for 2 h at room temperature. The MS was filtered off and the solvent was evaporated. The material was dried for 4 h under high vacuum to give the title compound as a colorless hygroscopic solid (150 mg, 41%).

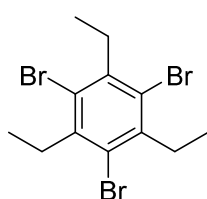
M.p.: 55 – 57 °C; ¹H NMR (400 MHz, CDCl₃): δ = 7.59 (d, *J* = 6.6 Hz, 12H), 7.43 – 7.32 (m, 18H), 6.72 (s, 3H), 2.66 – 2.75 (m, 9H), 1.48 ppm (t, *J* = 8.0 Hz, 6H); ¹³C NMR (100 MHz, CDCl₃): δ = 144.4, 136.3, 134.2, 130.0, 128.1, 125.5, 29.3, 17.0 ppm; IR (film): $\tilde{\nu}$ = 3321, 3069, 3049, 3012, 2975, 2920, 1708, 1591, 1454, 1427, 1376, 1319, 1262, 1175, 1113, 998, 908, 830, 757, 732, 696, 647, 603, 567, 481, 448 cm⁻¹; MS (EI): *m/z* (%) = 444 (7), 366 (6), 363 (5), 199 (19), 79 (7), 78 (100), 77 (23), 76 (5), 52 (14), 51 (816), 50 (10), 39 (7); HRMS (ESI(pos)): *m/z*: calcd. for [C₄₈H₄₈O₃Si₃+Na]⁺: 779.2802, found: 779.2804.

(Benzene-1,3,5-triyltris(propane-3,1-diyl))tris(diphenylsilanol) (94b)

Trialkene **96b** (397 mg, 2.00 mmol) was dissolved in toluene (10 mL) in a flame-dried Schlenk flask. After addition of Karstedt's catalyst (2% Pt. in xylene, 0.20 mL) the mixture was heated to 50 °C and diphenylchlorosilane (1.37 mL, 1.52 g, 7.0 mmol) was added dropwise. The mixture was stirred for 16 h at

this temperature before a second portion of Karstedt's catalyst (2% Pt. in xylene, 0.30 mL) and diphenylchlorosilane (0.30 mL, 0.33 g, 1.1 mmol) were added and stirring continued for another 2 h at 60 °C. The mixture was allowed to reach ambient temperature before H₂O (20 mL) and NEt₃ (1 mL) were added. After stirring for 20 min, aq. sat. NH₄Cl (5 mL) was added and stirring was continued for 10 min. The aqueous layer was extracted with ethyl acetate (3 × 50 mL) and the combined organic layers were dried over MgSO₄. The solvent was evaporated and the crude product was purified by flash chromatography (SiO₂, hexanes/ethyl acetate, 4/1 to 2/1). The material was dissolved in CH₂Cl₂ (20 mL) and MS 3 Å (2 g) was added. After gentle stirring for 2 h at room temperature, the MS was filtered off and the solvent was evaporated. The product was dried for 4 h under high vacuum to afford the title compound as a colorless hygroscopic solid (756 mg, 47%).

M.p.: 57 – 65 °C; ¹H NMR (400 MHz, CDCl₃): δ = 7.52 – 7.56 (m, 12H), 7.30 – 7.41 (m, 18H), 6.71 (s, 3H), 2.56 (t, *J* = 7.4 Hz, 6H), 2.32 – 2.38 (m, 3H), 1.70 – 1.80 (m, 6H), 1.12 – 1.17 ppm (m, 6H); ¹³C NMR (100 MHz, CDCl₃): δ = 142.1, 136.3, 134.3, 130.0, 128.0, 126.5, 39.3, 24.9, 14.8 ppm; IR (film): $\tilde{\nu}$ = 3241, 3067, 3046, 2999, 2923, 2857, 1590, 1427, 1112, 1067, 1045, 1027, 997, 823, 734, 695, 504, 480, 448 cm⁻¹; MS (ESI(pos)): *m/z* (%) = 821 [M+Na]⁺ (100); HRMS (ESI(pos)): *m/z*: calcd. for [C₅₁H₅₄O₃Si₃+Na]⁺: 821.3274, found: 821.3273.

7.3.3 Synthesis of Ligands with Hexasubstituted Aromatic Linkers**1,3,5-Tribromo-2,4,6-triethylbenzene (99)**

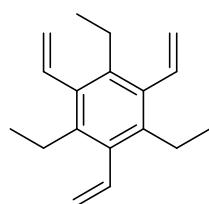
1,3,5-Triethylbenzene (4.48 mL, 3.86 g, 23.8 mmol) was added over 15 min to a mixture of bromine (20 mL) and iron powder (400 mg, 7.16 mmol) at 0 °C. The mixture was warmed to room temperature and stirred for 16 h before it was poured into aq. sat. Na₂S₂O₃ containing KOH

(30 g). After extraction of the aqueous layer with CH_2Cl_2 (3×200 mL), the combined extracts were dried over MgSO_4 . The solvent was removed and the residue recrystallized from ethanol to give the title compound as a colorless crystalline solid (7.20 g, 76%).

M.p.: 103 – 105 °C; ^1H NMR (400 MHz, CDCl_3): δ = 3.14 (q, J = 7.7 Hz, 6H), 1.17 ppm (t, J = 7.7 Hz, 9H); ^{13}C NMR (100 MHz, CDCl_3): δ = 142.6, 124.4, 32.8, 12.4 ppm; IR (film): $\tilde{\nu}$ = 2971, 2935, 2870, 1534, 1461, 1360, 1313, 1240, 1075, 1054, 1003, 893, 784, 663, 620 cm^{-1} ; MS (EI): m/z (%) = 402 (21), 400 (61), 398 (62), 396 (22), 387 (26), 385 (81), 381 (29), 319 (12), 223 (13), 144 (16), 143 (60), 142 (21), 141 (42), 130 (15), 129 (60), 128 (100), 127 (23), 116 (12), 115 (62), 103 (10), 102 (12), 91 (15), 77 (26), 75 (12), 71 (12), 70 (13), 64 (16), 63 (29), 51 (22), 39 (15); HRMS (EI(DE)): m/z : calcd. for $[\text{C}_{12}\text{H}_{15}\text{Br}_3]^+$: 395.8723, found: 395.8724.

The analytical and spectroscopic data are in agreement with those reported in the literature.^[130]

1,3,5-Trivinyl-2,4,6-triethylbenzene (100b)



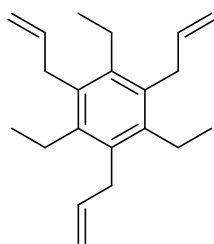
Vinyltributylstannane (2.17g, 6.84 mmol) was added to a solution of 1,3,5-tribromo-2,4,6-triethylbenzene (**99**) (678 mg, 1.70 mmol), $(\text{Ph}_3\text{P})_4\text{Pd}$ (395 mg, 342 μmol , 20 mol%) and CsF (858 mg, 5.65 mmol) in DMF (10 mL). The mixture was stirred for 3.5 h at 135 °C in a closed JYoung tube. After cooling to room temperature, methyl *t*-butyl ether (200 mL) and aq. sat. KF (100 mL) were added and stirring was continued for 10 min. Water (100 mL) and aq. sat. Na/K-tartrate (100 mL) were added and the aqueous layer was extracted with methyl *t*-butyl ether (3×150 mL). The combined extracts were dried over MgSO_4 , the solvent was evaporated and the crude product was purified by flash chromatography (SiO_2 , hexanes) to give the title compound as a colorless solid (150 mg, 37%).

^1H NMR (400 MHz, CDCl_3): δ = 6.80 (dd, J = 17.9, 11.4 Hz, 3H), 5.49 (dd, J = 11.4, 2.2 Hz, 3H), 5.24 (dd, J = 17.9, 2.2 Hz, 3H), 2.68 (q, J = 7.4 Hz, 6H), 1.02 ppm (t, J = 7.4 Hz, 9H); ^{13}C NMR (100 MHz, CDCl_3): δ = 138.9, 135.9, 135.8, 119.2, 24.1, 14.6 ppm; IR (film): $\tilde{\nu}$ = 3078, 2964, 2930, 2871, 1847, 1627, 1451, 1426, 1368, 1288, 1316, 1053, 1074, 991, 918, 836, 758, 626, 443 cm^{-1} ; MS (EI): m/z (%) = 241 (11), 240 (61), 226 (18), 225 (100), 212 (12), 211 (73), 197 (51), 196 (52), 195 (12), 183 (42), 182 (34), 181 (39), 179 (12), 178 (13), 169 (34), 168 (23), 167 (44), 166 (23), 165 (44), 155 (29), 154 (15), 153 (27), 152 (22), 141 (20), 128 (13), 115

(13), 91 (11), 89 (13), 77 (11); HRMS (EI(DE)): m/z : calcd. for $[C_{18}H_{24}]$: 240.1878, found: 240.1880.

The analytical and spectroscopic data are in agreement with those reported in the literature.^[131]

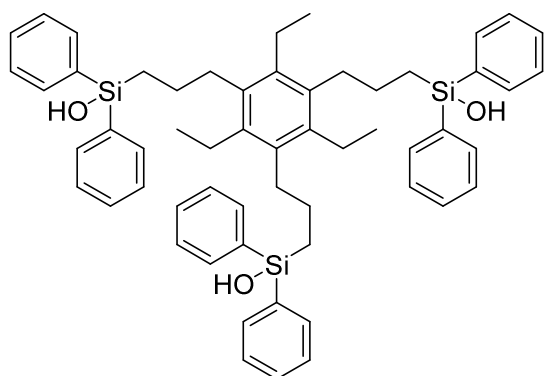
1,3,5-Triallyl-2,4,6-triethylbenzene (100c)



Allyltributylstannane (8.54 g, 25.8 mmol) was added to a solution of 1,3,5-tribromo-2,4,6-triethylbenzene (**99**) (2.57 g, 6.45 mmol), $(Ph_3P)_4Pd$ (1.16 g, 1.00 mmol, 16 mol%) and CsF (3.04 g, 20.0 mmol) in DMF (15 mL). The mixture was stirred for 3.5 h at 135 °C in a closed JYoung tube. After cooling to room temperature, methyl *t*-butyl ether (200 mL)

and aq. sat. KF (100 mL) were added and stirring was continued for 10 min. Water (100 mL) and aq. sat. Na/K-tartrate (100 mL) were added and the aqueous layer was extracted with methyl *t*-butyl ether (3 × 150 mL). The combined extracts were dried over $MgSO_4$ and the solvent was evaporated. Purification of the residue by flash chromatography (SiO_2 , hexanes) afforded the title compound as a colorless solid (1.10 g, 60%).

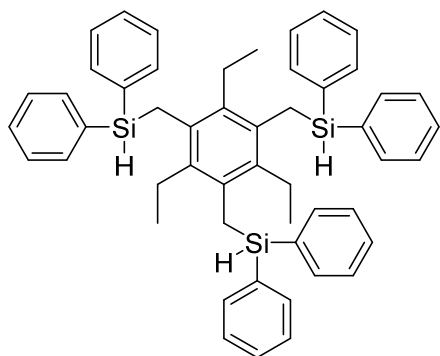
M.p.: 57 – 58 °C; 1H NMR (400 MHz, $CDCl_3$): δ = 6.03 (ddt, J = 17.1, 10.1, 5.0 Hz, 3H), 4.86 – 4.83 (m, 3H), 4.72 (dq, J = 17.1, 1.9 Hz, 3H), 3.42 (dt, J = 5.0, 1.9 Hz, 6H), 2.54 (q, J = 7.5 Hz, 6H), 1.17 ppm (t, J = 7.5 Hz, 9H); ^{13}C NMR (100 MHz, $CDCl_3$): δ = 140.3, 137.9, 133.0, 114.8, 33.0, 22.9, 15.5 ppm; IR (film): $\tilde{\nu}$ = 3080, 3001, 2962, 2927, 2897, 2869, 1817, 1636, 1485, 1448, 1422, 1403, 1376, 1291, 1227, 1198, 1117, 1059, 995, 927, 905, 823, 769, 629, 555 cm^{-1} ; MS (EI): m/z (%) = 283 (23), 232 (100), 267 (31), 253 (32), 241 (27), 226 (19), 225 (17), 213 (12), 212 (16), 211 (23), 200 (11), 199 (17), 197 (28), 185 (20), 183 (19), 181 (11), 171 (14), 169 (15), 167 (14), 155 (14); HRMS (EI(DE)): m/z : calcd. for $[C_{21}H_{30}]$: 282.2345, found: 282.2348.

((2,4,6-Triethylbenzene-1,3,5-triyl)tris(propane-3,1-diyl))tris(diphenylsilanol) (97c)

Trialkene **100c** (334 mg, 1.18 mmol) was dissolved in toluene (10 mL) in a flame-dried Schlenk flask. After addition of Karstedt's catalyst (0.1 M in poly(dimethylsiloxane), 0.50 mL, 0.05 mmol) the mixture was heated to 70 °C and diphenylchlorosilane (0.88 mL, 984 mg, 4.5 mmol) was added dropwise. The reaction

was stirred for 16 h at this temperature before a second portion of Karstedt's catalyst (0.1 M in poly(dimethylsiloxane), 0.1 mL, 0.01 mmol) and diphenylchlorosilane (0.15 mL, 168 mg, 0.78 mmol) were added and stirring continued for another 2 h at 70 °C. The mixture was allowed to reach ambient temperature before water (10 mL) and NEt₃ (1 mL) were added. After stirring for 20 min aq. sat. NH₄Cl (5 mL) was added and stirring was continued for 10 min. The aqueous layer was extracted with ethyl acetate (3 × 50 mL) and the combined organic layers were dried over MgSO₄. The solvent was evaporated and the crude product was purified by flash chromatography (SiO₂, hexanes/ethyl acetate, 6/1 to 2/1). The material was dissolved in CH₂Cl₂ (20 mL) and MS 3 Å (2 g) was added. After gentle stirring for 2 h at room temperature the MS was filtered off and the solvent was evaporated. The product was dried for 4 h under high vacuum to afford the title compound as a colorless hygroscopic solid (560 mg, 54%).

M.p.: 66 – 75 °C; ¹H NMR (400 MHz, CDCl₃): δ = 7.59 (d, *J* = 7.0 Hz, 12H), 7.32 – 7.44 (m, 18H), 2.50 – 2.59 (m, 6H), 2.38 (q, *J* = 7.2 Hz, 6H), 2.06 – 2.13 (m, 3H), 1.55 – 1.66 (m, 6H), 1.29 (t, *J* = 7.9 Hz, 6H), 1.06 ppm (t, *J* = 7.2 Hz, 9H); ¹³C NMR (100 MHz, CDCl₃): δ = 138.4, 136.4, 136.3, 134.3, 130.0, 128.1, 33.6, 25.0, 22.6, 16.5, 15.8 ppm; IR (film): $\tilde{\nu}$ = 3299, 3068, 3047, 2958, 2927, 2869, 1589, 1486, 1462, 1427, 1373, 1305, 1262, 1169, 1112, 1066, 1026, 997, 965, 944, 824, 762, 736, 696, 640, 504, 479, 449 cm⁻¹; MS (ESI(pos)): *m/z* (%) = 905 [M+Na]⁺ (100); HRMS (ESI(pos)): *m/z*: calcd. for [C₅₇H₆₆O₃Si₃+Na]⁺: 905.4212, found: 905.4212.

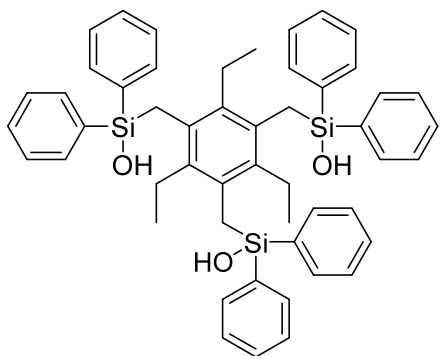
((2,4,6-Triethylbenzene-1,3,5-triyl)tris(methylene))tris(diphenylsilane) (102)

In analogy to the literature^[53], a suspension of diphenylchlorosilane (1.52 mL, 1.71 g, 7.81 mmol) and magnesium (190 mg, 7.81 mmol) in THF (5 mL) was added to a solution of 1,3,5-tris(bromomethyl)-2,4,6-triethylbenzene (1.00 g, 2.27 mmol) in THF (5 mL) at 0 °C. The mixture was stirred for 3 h at ambient temperature before aq. sat. NH₄Cl (5 mL) was added.

The aqueous layer was extracted with ethyl acetate (3 × 20 mL) and the combined organic layers were dried over MgSO₄. The solvent was evaporated and the crude product was purified by flash chromatography (SiO₂, hexanes) to give the title compound as a colorless solid (1.10 g, 65%).

¹H NMR (400 MHz, CDCl₃): δ = 7.48 (d, *J* = 6.6 Hz, 12H), 7.42 – 7.31 (m, 18H), 4.74 (t, *J* = 3.5 Hz, 3H), 2.58 (d, *J* = 3.6 Hz, 6H), 2.21 (q, *J* = 7.4 Hz, 6H), 1.02 ppm (t, *J* = 7.4 Hz, 9H); ¹³C NMR (100 MHz, CDCl₃): δ = 136.2, 135.2, 134.5, 132.6, 129.8, 128.0, 24.2, 16.2, 13.5 ppm.

The analytical and spectroscopic data are in agreement with those reported in the literature.^[53]

((2,4,6-Triethylbenzene-1,3,5-triyl)tris(methylene))tris(diphenylsilanol) (97a)

In analogy to the literature^[53], a solution of compound **102** (751 mg, 1.00 mmol) and *N*-bromosuccinimide (587 mg, 3.30 mmol) in CH₂Cl₂ (8 mL) was stirred for 2 h at room temperature. Water (2 mL) and NEt₃ (0.5 mL) were added and stirring was continued for 2 h before the solvent was removed under reduced pressure. The residue was extracted with ethyl acetate (3 × 20 mL).

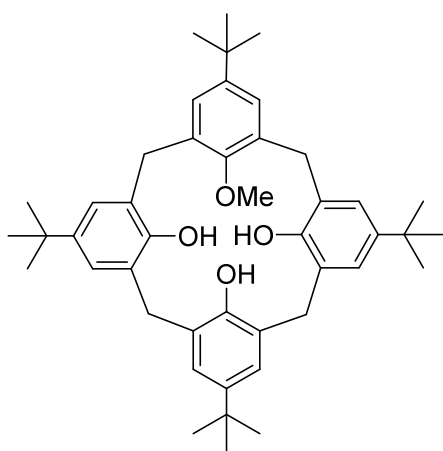
The combined extracts were washed with water (10 mL) and dried over MgSO₄. The solvent was evaporated and the crude product was purified by flash chromatography (SiO₂, hexanes/ethyl acetate, 6/1 to 2/1). The material was dissolved in CH₂Cl₂ (10 mL) and MS 3 Å (2 g) was added. After gentle stirring for 2 h at room temperature, the MS was filtered off and the solvent was evaporated. The product was dried for 4 h under high vacuum to afford the title compound as a colorless hygroscopic solid (700 mg, 87%).

^1H NMR (400 MHz, CDCl_3): δ = 7.52 (d, J = 6.5 Hz, 12H), 7.45 – 7.26 (m, 18H), 2.68 (s, 6H), 2.30 – 2.44 (bs, 3H), 2.24 (q, J = 7.4 Hz, 6H), 0.97 ppm (t, J = 7.4 Hz, 9H); ^{13}C NMR (100 MHz, CDCl_3): δ = 136.9, 136.6, 134.2, 132.1, 130.0, 128.0, 24.4, 19.1, 13.5 ppm.

The analytical and spectroscopic data are in agreement with those reported in the literature.^[53]

7.3.4 Synthesis of Calyx[4]arene Based Systems

Methoxy calyx[4]arene **103b**

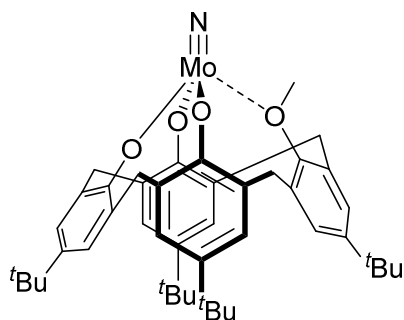


A suspension of 4-*tert*-butylcalix[4]arene **103a** (649 mg, 1.00 mmol) and K_2CO_3 (78.8 mg, 0.570 mmol) in acetonitrile (30 mL) was stirred at reflux temperature for 30 min before methyl iodide (1.42 g, 0.623 mL, 10.0 mmol) was added. The mixture was stirred for 4 d at this temperature. The solvent was evaporated and the residue was dissolved in CH_2Cl_2 (100 mL) and washed with aq. HCl (1 M, 2 \times 100 mL) and water (100 mL). The organic

layer was dried over MgSO_4 , the solvent was evaporated, and the crude product was purified by flash chromatography (SiO_2 , CH_2Cl_2 /pentane, 2/1 to 1/1) to give the title compound as a colorless solid (381 mg, 58%).

^1H NMR (400 MHz, CDCl_3): δ = 10.1 (s, 1H), 9.60 (s, 2H), 7.13 – 7.00 (m, 8H), 4.38 (d, J = 13.0 Hz, 2H), 4.29 (d, J = 13.5 Hz, 2H), 4.15 (s, 3H), 3.48 – 3.42 (m, 4H), 1.24 (s, 9H), 1.23 (s, 18H), 1.22 ppm (s, 9H); ^{13}C NMR (100 MHz, CDCl_3): δ = 150.6, 148.5, 148.4, 147.9, 143.8, 143.3, 133.5, 128.34, 128.31, 128.0, 126.6, 126.1, 125.9, 125.8, 125.7, 63.4, 34.4, 34.1, 34.0, 33.1, 32.3, 31.6, 31.5, 31.4 ppm. IR (film): $\tilde{\nu}$ = 3249, 3150, 3047, 3023, 2955, 2905, 2867, 1599, 1481, 1455, 1393, 1361, 1297, 1241, 1202, 1123, 1103, 1092, 1004, 945, 915, 871, 816, 782, 745, 720, 700, 674, 627, 603, 589, 573, 555, 526, 498, 483, 461, 444, 429 cm^{-1} ; MS (EI): m/z (%) = 664 (27), 663 (87), 662 (100), 649 (9), 648 (23), 647 (15), 607 (6), 606 (16), 592 (10), 591 (12), 550 (6), 549 (6), 535 (6), 493 (5), 175 (6), 57 (19); HRMS (ESI(pos)): m/z : calcd. for $[\text{C}_{45}\text{H}_{58}\text{O}_4+\text{Na}]^+$: 685.4222, found: 685.4227.

The analytical and spectroscopic data are in agreement with those reported in the literature.^[54]

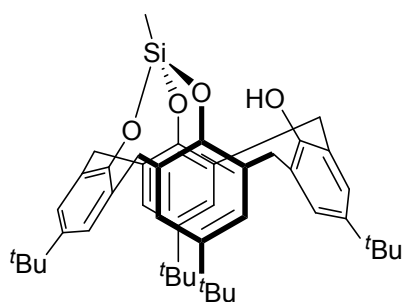
Nitrido calyx[4]arene **105b**

A solution of triol **103b** (144 mg, 0.217 mmol) in toluene (5 mL) was added over 5 min to a solution of complex **19** (97.5 mg, 0.217 mmol) in toluene (5 mL) at room temperature. The resulting mixture was stirred for 1 h at room temperature. The solvent was evaporated and the residue was recrystallized from Et₂O (3 mL) by cooling the

mixture to -78 °C over the course of 1 h. The solid was collected under argon and dried under high vacuum to give the title compound as an orange crystalline solid (75.0 mg, 49%).

¹H NMR (400 MHz, C₆D₆): δ = 7.20 – 7.17 (m, 4H), 6.91 – 6.89 (m, 2H), 6.84 – 6.81 (m, 2H), 4.73 (d, *J* = 12.7 Hz, 2H), 4.35 (d, *J* = 12.3 Hz, 2H), 4.27 – 4.23 (m, 3H), 3.15 (d, *J* = 12.8 Hz, 2H), 3.09 (d, *J* = 12.8 Hz, 2H), 1.36 (s, 18H), 0.85 – 0.80 (m, 9H), 0.77 – 0.71 ppm (m, 9H); ¹³C NMR (100 MHz, C₆D₆): δ = 156.1, 150.5, 146.0, 144.5, 134.5, 130.9, 129.32, 129.26, 126.7, 125.71, 125.68, 124.2, 76.0, 34.0, 33.7, 33.5, 33.2, 32.5, 31.7, 30.7, 30.4 ppm; IR (film): $\tilde{\nu}$ = 3634, 2951, 2902, 2864, 1579, 1460, 1433, 1393, 1361, 1302, 1263, 1247, 1196, 1124, 1108, 1088, 1041, 984, 946, 916, 888, 871, 834, 798, 759, 733, 712, 678, 646, 598, 556, 511, 480, 466, 430 cm⁻¹; MS (EI(DE)): *m/z* (%) = 771 (88), 756 (100), 743 (51), 616 (38); HRMS (ESI(pos)): *m/z*: calcd. for [C₄₅H₅₅MoNO₄+Na]⁺: 794.3076, found: 794.3078.

The analytical and spectroscopic data are in agreement with those reported in the literature.^[55]

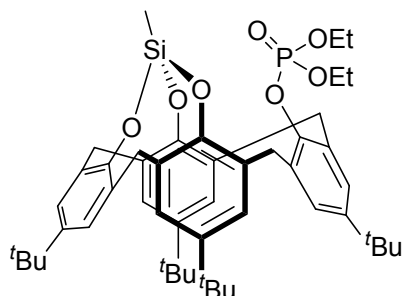
Calyx[4]arene silane EP9

In analogy to the literature^[57], NEt₃ (7.51 mL, 53.9 mmol) was added to a suspension of calyx[4]arene **103a** (10.0 g, 15.4 mmol) in toluene (800 mL) at room temperature. The reaction mixture was stirred for 20 min before methyltrichlorosilane (3.53 mL, 4.48 g, 30.0 mmol) was added dropwise and the reaction mixture was stirred at

room temperature for 16 h. The solid precipitate was filtered off and washed with hexanes (2 × 50 mL). The residue was dissolved in CH₂Cl₂ (50 mL) before methyl *t*-butyl ether (150 mL) was added, which caused a fine colorless solid to precipitate. The solid material was filtered over Celite® and the filtrate was evaporated to give the title compound as a

colorless solid (11.2 g, quant.). The material was used in the next step without further purification.

Calyx[4]arene phosphonate **106**



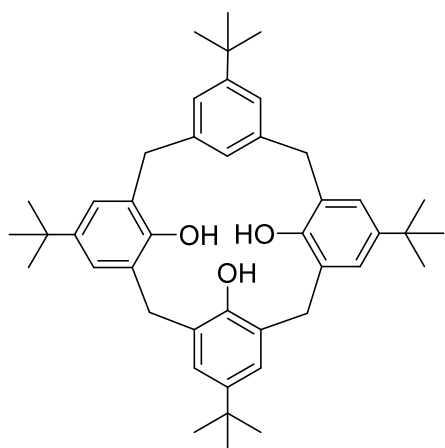
In analogy to the literature^[57], *n*-BuLi (1.6 M in hexane, 11.2 mL, 17.9 mmol) was added to a solution of calyx[4]arene silane **EP9** (11.2 g, 16.3 mmol) in toluene (500 mL) at room temperature. The mixture was stirred for 20 min at room temperature before diethyl chlorophosphate (3.53 mL, 4.22 g, 24.5 mmol) was added.

The mixture was stirred for 4 h at room temperature before it was filtered through Celite®. The solvent was evaporated, the residue was suspended in CH₂Cl₂ (100 mL) and the mixture was filtered over Celite®. The solvent was evaporated and the residue was suspended in hexanes (70 mL) at 0 °C. The solid was filtered off and dried under vacuum to give the title compound as a colorless solid (9.10 g, 68%).

¹H NMR (400 MHz, CDCl₃): δ = 7.15 – 7.08 (m, 8H), 4.44 (d, *J* = 14.7 Hz, 4H), 3.69 (d, *J* = 16.2 Hz, 2H), 3.55 – 3.40 (m, 6H), 1.35 (s, 18H), 1.30 (s, 9H), 1.23 (s, 9H), 0.73 (t, *J* = 7.1 Hz, 6H), –0.39 ppm (s, 3H); ¹³C NMR (100 MHz, CDCl₃): δ = 148.7, 147.7, 147.0, 146.0, 145.3, 144.5, 132.4, 130.8, 130.6, 130.1, 127.5, 126.6, 125.5, 124.8, 64.2, 37.3, 35.3, 34.41, 34.36, 34.1, 31.72, 31.67, 31.61, 15.8, –8.3 ppm.

The analytical and spectroscopic data are in agreement with those reported in the literature.^[57]

15,35,55,75-Tetra-*tert*-butyl-1,3,5,7(1,3)-tetrabenzenacyclooctaphane-12,32,52-triol (**103c**)



In analogy to the literature^[57], a suspension of phosphate **106** (5.00 g, 6.06 mmol) in Et₂O (60 mL) was added over 5 min to a mixture of potassium (12.0 g, 307 mmol) and ammonia (100 mL) at –78 °C. The reaction mixture was stirred for 1 h at –78 °C. NH₄Cl was added until the blue color disappeared. The mixture was allowed to warm to room temperature. The solid residue was extracted with CH₂Cl₂ (3 × 200 mL), the solvent was

evaporated, and the crude material was purified by flash chromatography (SiO₂, hexanes/ethyl acetate, 10/1 to 2/1) to give the title compound as a colorless solid (2.48 g, 65%).

¹H NMR (400 MHz, CDCl₃): δ = 7.17 – 7.01 (m, 8H), 3.91 (s, 4H), 3.86 (s, 4H), 1.29 (s, 9H), 1.25 (s, 9H), 1.23 ppm (s, 18H); ¹³C NMR (100 MHz, CDCl₃): δ = 151.7, 148.7, 147.4, 144.5, 143.9, 141.2, 127.6, 127.4, 126.2, 125.7, 124.8, 124.2, 38.2, 34.7, 34.2, 34.1, 32.8, 31.59, 31.57, 31.5 ppm; IR (film): $\tilde{\nu}$ = 3223, 2961, 2903, 2869, 1596, 1483, 1455, 1430, 1393, 1362, 1300, 1247, 1198, 1154, 1135, 1112, 1066, 962, 949, 915, 887, 871, 817, 799, 782, 752, 735, 715, 699, 566, 548, 518 cm⁻¹; MS (EI): m/z (%) = 634 (12), 633 (48), 632 (100), 618 (10), 617 (22), 577 (16), 576 (40), 575 (13), 562 (10), 561 (23), 520 (25), 519 (11), 505 (19), 57 (27); HRMS (ESI(neg)): m/z : calcd. for [C₄₄H₅₆O₃]⁻: 631.4163, found: 631.4157.

The analytical and spectroscopic data are in agreement with those reported in the literature.^[57]

7.4 Reactions with the Two-Component Catalyst System

7.4.1 Homocoupling Reactions

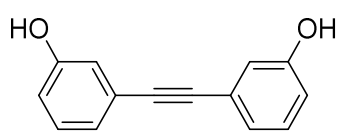
General procedure 4: Alkyne homo metathesis using *in situ* generated systems containing the multidentate ligand **89a** and precatalyst **73**^[42]

The alkyne was stirred with MS 5 Å (1 g per mmol alkyne) in toluene (0.2 M based on the alkyne) for 30 min before a freshly prepared solution of trisilanol **89a** and complex **73** in toluene, which had been stirred for 5 min, was added. The reaction mixture was stirred under the individual conditions. The crude material was filtered through a plug of Celite® which was carefully rinsed with ethyl acetate. The solvent was evaporated and the residue was purified by column chromatography.

General procedure 5: Alkyne homo metathesis using *in situ* generated systems containing the multidentate ligand **97c** and precatalyst **73**^[42]

The alkyne was stirred with MS 5 Å (1 g per mmol alkyne) in toluene (0.2 M based on the alkyne) for 30 min before a freshly prepared solution of trisilanol **97c** and complex **73** in toluene, which had been stirred for 5 min, was added. The reaction mixture was stirred under the individual conditions. The crude material was filtered through a plug of Celite® which was carefully rinsed with ethyl acetate. The solvent was evaporated and the residue was purified by column chromatography.

3,3'-(Ethin-1,2-diyl)diphenole (**30b**)



3-(Prop-1-yn-1-yl)phenol (**29b**) (33.0 mg, 0.25 mmol) was stirred with MS 5 Å (200 mg), trisilanol **97c** (22.1 mg, 25.0 μmol, 10 mol%), and complex **73** (16.6 mg, 25.0 μmol, 10 mol%) in

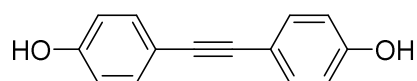
toluene (2 mL) for 14 h at room temperature according to general procedure 5. Flash chromatography (SiO₂, hexanes/ethyl acetate, 4/1 to 2/1) afforded the title compound as a colorless solid (21.0 mg, 80%).

¹H NMR (400 MHz, CDCl₃): δ = 7.17 (t, *J* = 8.0 Hz, 2H), 6.96 (ddd, *J* = 7.6, 1.5, 1.0 Hz, 2H), 6.90 (dd, *J* = 2.6, 1.5 Hz, 2H), 6.78 ppm (ddd, *J* = 8.0, 2.5, 1.0 Hz, 2H); ¹³C NMR (100 MHz, CDCl₃): δ = 158.5, 130.6, 125.5, 123.9, 119.0, 116.9, 89.6 ppm; IR (film): $\tilde{\nu}$ = 3236, 3059, 2992, 2613, 1574, 1497, 1451, 1322, 1309, 1252, 1182, 1159, 1085, 970, 873, 752, 682 cm⁻¹; MS (EI): *m/z*

(%) = 210 (100), 181 (18), 165 (5), 152 (28), 127 (5), 105 (8), 98 (2), 76 (9), 63 (7), 51 (4); HRMS (EI): m/z : calcd. for $[C_{14}H_{10}O_2]^+$: 210.0679, found: 210.0681.

The analytical and spectroscopic data are in agreement with those reported in the literature.^[132]

4,4'-(Ethin-1,2-diyl)diphenole (**30a**)

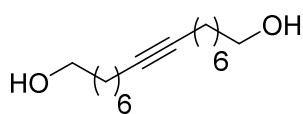


4-(Prop-1-yn-1-yl)phenol **29a** (33.0 mg, 0.25 mmol) was stirred with MS 5 Å (200 mg), trisilanol **97c** (22.1 mg, 25.0 μmol, 10 mol%), and complex **73** (16.6 mg, 25.0 μmol, 10 mol%) in toluene (2 mL) for 4 h at room temperature according to general procedure 5. Flash chromatography (SiO₂, hexanes/ethyl acetate, 4/1 to 1/1) afforded the title compound as a colorless solid (22.0 mg, 84%).

¹H NMR (400 MHz, CD₃CN): δ = 7.35 (d, J = 8.6 Hz, 4H), 7.22 (s, 2H), 6.81 ppm (d, J = 8.6 Hz, 4H); ¹³C NMR (100 MHz, CD₃CN): δ = 158.0, 133.8, 116.5, 115.6, 88.4 ppm; IR (film): $\tilde{\nu}$ = 3304, 1607, 1591, 1510, 1438, 1371, 1350, 1231, 1171, 1100, 766 cm⁻¹; MS (EI): m/z (%) = 210 (100), 181 (7), 152 (13), 105 (11), 76 (5); HRMS (EI): m/z : calcd. for $[C_{14}H_{10}O_2]^+$: 210.0680, found: 210.0681.

The analytical and spectroscopic data are in agreement with those reported in the literature.^[116]

Hexadec-8-yne-1,16-diol (**33**)

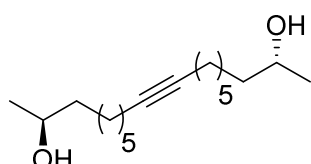


Dec-8-yn-1-ol **32** (38.6 mg, 0.25 mmol) was stirred with MS 5 Å (200 mg), trisilanol **97c** (22.1 mg, 25.0 μmol, 10 mol%), and complex **73** (16.6 mg, 25.0 μmol, 10 mol%) in toluene (2 mL) for 4 h at room temperature according to general procedure 5. Flash chromatography (SiO₂, hexanes/ethyl acetate, 4/1 to 0/1) afforded the title compound as a colorless solid (23.0 mg, 72%).

M.p.: 39 – 40 °C; ¹H NMR (400 MHz, CDCl₃): δ = 3.63 (t, J = 6.6 Hz, 4H), 2.19 – 2.09 (m, 4H), 1.62 – 1.29 ppm (m, 22H); ¹³C NMR (100 MHz, CDCl₃): δ = 80.4, 63.1, 32.9, 29.1, 29.1, 28.9, 25.8, 18.8 ppm; IR (film): $\tilde{\nu}$ = 3348, 3265, 2931, 2851, 1457, 1423, 1381, 1361, 1297, 1249, 1211, 1133, 1109, 1094, 1055, 1040, 1014, 1005, 970, 896, 815, 756, 725, 650, 548, 478, 452, 432, 416 cm⁻¹; MS (EI): m/z (%) = 150 (10), 136 (23), 135 (18), 125 (10), 122 (16), 121 (75),

112 (13), 111 (23), 110 (16), 109 (20), 108 (28), 107 (54), 98 (47), 97 (32), 96 (23), 95 (58), 94 (56), 93 (71), 91 (26), 85 (14), 84 (21), 83 (18), 82 (58), 81 (93), 80 (68), 79 (97), 77 (18), 72 (11), 71 (16), 69 (26), 68 (64), 67 (100), 66 (10), 55 (59), 54 (31), 53 (11), 43 (14), 41 (36), 39 (16); HRMS (ESI(pos)): m/z : calcd. for $[C_{16}H_{30}O_2+Na]^+$: 277.2140, found: 277.2138.

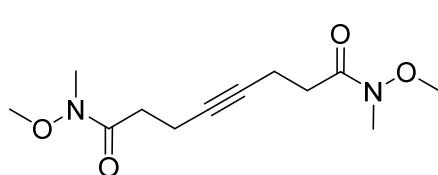
(2*R*,17*R*)-Octadec-9-yn-2,17-diole (35)



(*R*)-Undec-9-yn-2-ole **34** (42.1 mg, 0.25 mmol) was stirred with MS 5 Å (200 mg), trisilanol **97c** (22.1 mg, 25.0 μmol, 10 mol%), and complex **73** (16.6 mg, 25.0 μmol, 10 mol%) in toluene (2 mL) for 4 h at room temperature according to general procedure 5. Flash chromatography (SiO₂, hexanes/ethyl acetate, 4/1 to 1/1) afforded the title compound as a colorless solid (27.0 mg, 76%).

M.p.: 56 – 57 °C; ¹H NMR (400 MHz, CDCl₃): δ = 3.74 – 3.82 (m, 2H), 2.14 (t, *J* = 6.9 Hz, 4H), 1.27 – 1.51 (m, 22H), 1.18 ppm (d, *J* = 6.3 Hz, 6H); ¹³C NMR (100 MHz, CDCl₃): δ = 80.4, 68.3, 39.4, 29.3, 29.2, 28.9, 25.9, 23.7, 18.8 ppm; IR (film): $\tilde{\nu}$ = 3325, 3243, 2960, 2940, 2849, 1496, 1466, 1373, 1354, 1294, 1127, 1107, 1046, 1010, 926, 836, 720, 673 cm⁻¹; MS (EI): m/z (%) = 282 (1), 249 (4), 189 (5), 175 (7), 164 (8), 161 (10), 149 (22), 135 (58), 121 (56), 107 (48), 95 (77), 81 (100), 67 (97), 55 (75), 45 (99), 41 (50); HRMS (ESI(pos)): m/z : calcd. for $[C_{18}H_{34}O_2+Na]^+$: 305.2448, found: 305.2451.

***N*1,*N*8-dimethoxy-*N*1,*N*8-dimethyloct-4-ynediamide (41)**



N-methoxy-*N*-methylhex-4-ynamide **40** (38.8 mg, 0.25 mmol) was stirred with MS 5 Å (200 mg), trisilanol **97c** (22.1 mg, 25.0 μmol, 10 mol%), and complex **73** (16.6 mg, 25.0 μmol, 10 mol%) in toluene (2 mL) for 4 h at room temperature according to general procedure 5. Flash chromatography (SiO₂, hexanes/ethyl acetate, 4/1 to 0/1) afforded the title compound as a colorless oil (24.0 mg, 75%).

¹H NMR (400 MHz, CDCl₃): δ = 3.69 (s, 6H), 3.18 (s, 6H), 2.59 – 2.66 (m, 4H), 2.41 ppm (t, *J* = 8.4 Hz, 4H); ¹³C NMR (100 MHz, CDCl₃): δ = 173.0, 79.6, 61.4, 32.3, 31.7, 14.4 ppm; IR (film): $\tilde{\nu}$ = 2937, 2247, 1736, 1656, 1420, 1386, 1336, 1242, 1177, 1107, 1044, 988, 917, 776, 728, 646, 606, 565, 509, 487, 437 cm⁻¹; MS (EI): m/z (%) = 256 (1), 225 (60), 196 (100), 168 (10),

124 (9), 107 (17), 94 (8), 79 (23), 60 (15), 39 (10); HRMS (ESI(pos)): m/z : calcd. for $[C_{12}H_{20}N_2O_4+Na]^+$: 279.1310, found: 279.1315.

7.4.2 RCAM Reactions

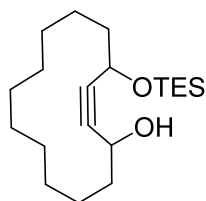
General procedure 6: Ring closing alkyne metathesis using *in situ* generated systems containing the multidentate ligand **97c** and precatalyst **73**^[42]

The diyne was stirred with MS 5 Å in toluene for 60 min at room temperature. The mixture was heated to 110 °C before a freshly prepared solution of trisilanol **97c** and complex **73** in toluene, which had been stirred for 5 min, was added. The reaction mixture was stirred for the indicated time at 110 °C before it was filtered through a pad of Celite®, which was carefully rinsed with ethyl acetate. The solvent was evaporated and the residue was purified by flash chromatography.

General procedure 7: Ring closing alkyne metathesis with catalyst **28**

The diyne was stirred with MS 5 Å in toluene for 60 min at room temperature. The mixture was heated to 110 °C before a freshly prepared solution of metathesis catalyst **28** in toluene was added in one portion. The reaction mixture was stirred for the indicated time at 110 °C before it was filtered through a pad of Celite®, which was carefully rinsed with ethyl acetate. The solvent was evaporated and the residue was purified by flash chromatography.

4-((Triethylsilyl)oxy)cyclotetradec-2-yn-1-ol (**112a**)



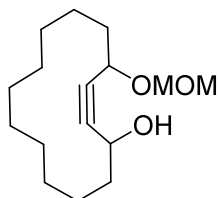
Diyne **111a** (39.3 mg, 100 μmol) was stirred with MS 5 Å (200 mg), trisilanol **97c** (19.4 mg, 22.0 μmol, 22 mol%), and complex **73** (13.3 mg, 21.2 μmol, 20 mol%) in toluene (50 mL) for 1 h according to general procedure 6. Flash chromatography (SiO₂, hexanes/ethyl acetate, 20/1 to

4/1) afforded the title compound as a colorless oil (21.8 mg, 64%, mixture of diastereomers).

¹H NMR (400 MHz, CDCl₃) δ = 4.53 – 4.41 (m, 2H), 1.74 – 1.60 (m, 5H), 1.49 – 1.25 (m, 16H), 0.98 (t, J = 7.9 Hz, 9H), 0.70 – 0.59 ppm (m, 6H); ¹³C NMR (100 MHz, CDCl₃): δ = 87.1, 86.9, 85.4, 85.1, 63.3, 63.2, 63.1, 63.0, 38.4, 38.3, 37.2, 26.60, 26.56, 26.53, 26.47, 25.84, 25.82, 25.78, 25.7, 23.89, 23.85, 23.8, 22.4, 22.3, 7.0, 4.92, 4.90 ppm; IR (fim): $\tilde{\nu}$ = 3359, 2931, 2874, 2859, 1458, 1413, 1378, 1334, 1259, 1239, 1151, 1072, 1006, 802, 726, 549, 427 cm⁻¹; MS (EI): m/z (%) = 309 (5), 121 (11), 107 (16), 105 (12), 104 (10), 103 (100), 95 (16), 93 (18), 91

(16), 87 (14), 81 (18), 79 (20), 75 (89), 67 (20), 55 (12), 47 (13); HRMS (ESI(pos)): m/z : calcd. for $[C_{20}H_{38}O_2Si+Na]^+$: 361.2521, found: 361.2533.

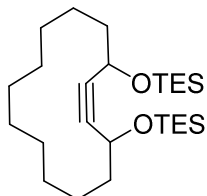
4-(Methoxymethoxy)cyclotetradec-2-yn-1-ol (**112b**)



Diyne **111b** (32.2 mg, 100 μ mol) was stirred with MS 5 Å (200 mg), trisilanol **97c** (19.4 mg, 22.0 μ mol, 22 mol%), and complex **73** (13.3 mg, 21.2 μ mol, 20 mol%) in toluene (50 mL) for 1 h according to general procedure 6. Flash chromatography (SiO₂, hexanes/ethyl acetate, 10/1 to 4/1) afforded the title compound as a colorless oil (18 mg, 67%, mixture of diastereomers).

¹H NMR (400 MHz, CDCl₃) δ = 4.92 (dd, J = 6.8, 5.5 Hz, 1H), 4.60 (dd, J = 6.8, 1.8 Hz, 1H), 4.56 – 4.40 (m, 2H), 3.38 (s, 3H), 1.89 – 1.82 (m, 1H), 1.78 – 1.63 (m, 4H), 1.56 – 1.22 ppm (m, 16H); ¹³C NMR (100 MHz, CDCl₃): δ = 94.3, 87.11, 87.06, 84.1, 83.9, 66.3, 66.1, 63.0, 55.8, 37.2, 37.1, 35.0, 34.9, 26.6, 26.50, 25.9, 25.81, 25.77, 25.7, 23.9, 23.8, 22.5, 22.4, 22.32, 22.30 ppm; IR (film): $\tilde{\nu}$ = 3400, 2928, 2859, 1459, 1429, 1338, 1260, 1213, 1150, 1097, 1026, 918, 865, 801, 731, 700, 509 cm⁻¹; MS (GC-MS): m/z (%) = 206 (5), 163 (6), 149 (11), 147 (12), 135 (19), 133 (18), 131 (13), 123 (13), 122 (11), 121 (30), 119 (21), 117 (14), 111 (17), 110 (16), 109 (33), 108 (23), 107 (42), 106 (12), 105 (28), 98 (20), 97 (29), 96 (32), 95 (66), 94 (43), 93 (56), 91 (68), 84 (17), 83 (32), 82 (37), 81 (88), 80 (61), 79 (100), 78 (19), 77 (35), 71 (13), 70 (14), 69 (35), 68 (37), 67 (93), 66 (17), 65 (19), 57 (14), 56 (11), 55 (74), 54 (25), 53 (21), 45 (79), 43 (21), 41 (59), 39 (23), 31 (26), 30 (18); HRMS (ESI(pos)): m/z : calcd. for $[C_{16}H_{28}O_2+Na]^+$: 291.1928, found: 291.1931.

3,14-bis((Triethylsilyl)oxy)cyclotetradec-1-yne (**112e**)

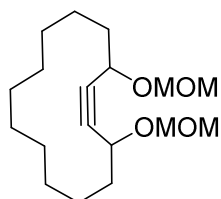


Diyne **113a** (50.7 mg, 100 μ mol) was stirred with MS 5 Å (200 mg), trisilanol **97c** (19.4 mg, 22.0 μ mol, 22 mol%), and complex **73** (13.3 mg, 21.2 μ mol, 20 mol%) in toluene (50 mL) for 3 h according to general procedure 6. Flash chromatography (SiO₂, hexanes/ethyl acetate, 1/0 to 100/1) afforded the title compound as a colorless oil (32 mg, 71%, mixture of diastereomers).

¹H NMR (400 MHz, CDCl₃) δ = 4.51 – 4.39 (m, 2H), 1.73 – 1.21 (m, 20H), 0.97 (t, J = 7.9 Hz, 18H), 0.71 – 0.56 ppm (m, 12H); ¹³C NMR (100 MHz, CDCl₃): δ = 85.9, 85.6, 63.4, 63.2, 38.7, 38.4, 26.7, 26.4, 26.1, 25.8, 24.0, 23.8, 22.4, 22.3, 7.0, 4.94, 4.88 ppm; IR (film): $\tilde{\nu}$ = 2949,

2935, 2875, 1732, 1459, 1414, 1378, 1348, 1334, 1260, 1239, 1074, 1006, 975, 843, 803, 726, 675, 533, 458 cm^{-1} ; MS (EI): m/z (%) = 425 (11), 424 (29), 423 (81), 291 (28), 217 (45), 205 (10), 190 (18), 189 (100), 161 (17), 133 (11), 121 (14), 115 (23), 107 (17), 103 (31), 95 (12), 93 (13), 87 (41), 81 (10), 75 (18), 59 (11); HRMS (ESI(pos)): m/z : calcd. for $[\text{C}_{26}\text{H}_{52}\text{O}_2\text{Si}_2+\text{Na}]^+$: 475.3404, found: 475.3398.

3,14-Bis(methoxymethoxy)cyclotetradec-1-yne (112f)

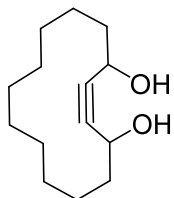


Diyne **113b** (36.7 mg, 100 μmol) was stirred with MS 5 Å (200 mg), trisilanol **97c** (19.4 mg, 22.0 μmol , 22 mol%), and complex **73** (13.3 mg, 21.2 μmol , 20 mol%) in toluene (50 mL) for 0.5 h according to general procedure 6. Flash chromatography (SiO_2 , hexanes/ethyl acetate, 20/1 to

4/1) afforded the title compound as a colorless oil (22 mg, 70%, mixture of diastereomers).

^1H NMR (400 MHz, CDCl_3): δ = 4.91 (dd, J = 6.8, 3.4 Hz, 2H), 4.59 (dd, J = 6.8, 3.0 Hz, 2H), 4.49 – 4.39 (m, 2H), 3.37 (s, 6H), 1.81 – 1.62 (m, 4H), 1.55 – 1.21 ppm (m, 16H); ^{13}C NMR (100 MHz, CDCl_3): δ = 94.3, 84.8, 84.6, 66.3, 66.2, 55.7, 35.1, 34.9, 26.6, 26.5, 25.9, 25.8, 23.82, 23.79, 22.44, 22.38 ppm; IR (film): $\tilde{\nu}$ = 2929, 2860, 2822, 2776, 1459, 1400, 1338, 1213, 1148, 1097, 1026, 919, 848, 792, 724, 704, 554, 441, 415 cm^{-1} ; MS (EI): m/z (%) = 161 (4), 147 (8), 133 (11), 121 (18), 119 (11), 109 (17), 108 (12), 107 (20), 105 (13), 97 (15), 96 (10), 95 (830), 94 (17), 93 (25), 92 (11), 91 (28), 82 (12), 81 (34), 80 (25), 79 (38), 77 (13), 69 (11), 87 (32), 55 (20), 45 (100), 41 (16); HRMS (ESI(pos)): m/z : calcd. for $[\text{C}_{18}\text{H}_{32}\text{O}_4+\text{Na}]^+$: 355.2189, found: 355.2193.

Cyclotetradec-2-yne-1,4-diol (112i)



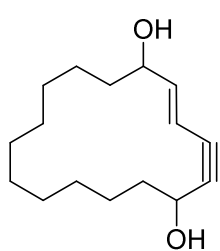
Diyne **113e** (27.8 mg, 100 μmol) was stirred with MS 5 Å (200 mg), trisilanol **97c** (19.4 mg, 22.0 μmol , 22 mol%), and complex **73** (13.3 mg, 21.2 μmol , 20 mol%) in toluene (50 mL) for 3 h according to general procedure 6. Flash chromatography (SiO_2 , hexanes/ethyl acetate, 4/1 to 1/1) afforded the title

compound as a colorless solid (11.8 mg, 53%, mixture of diastereomers).

M.p.: 110 – 111 $^\circ\text{C}$; ^1H NMR (400 MHz, CDCl_3): δ = 4.58 – 4.44 (m, 2H), 1.98 – 1.89 (m, 2H), 1.79 – 1.62 (m, 4H), 1.52 – 1.26 ppm (m, 16H); ^{13}C NMR (100 MHz, CDCl_3): δ = 86.5, 86.2, 63.04, 62.96, 37.2, 37.1, 26.53, 26.50, 25.74, 25.71, 23.8, 22.4, 22.3 ppm; IR (film): $\tilde{\nu}$ = 3273, 2923, 2856, 1729, 1457, 1443, 1341, 1297, 1146, 1107, 1020, 945, 723, 702, 590, 533, 512,

440 cm^{-1} ; MS (EI): m/z (%) = 208 (4), 206 (7), 165 (4), 163 (7), 149 (12), 135 (19), 133 (14), 131 (13), 123 (10), 122 (10), 121 (29), 119 (18), 117 (14), 111 (19), 110 (15), 109 (28), 108 (24), 107 (48), 106 (12), 105 (24), 98 (21), 97 (30), 96 (35), 95 (67), 94 (49), 93 (57), 92 (25), 91 (62), 84 (26), 83 (44), 82 (39), 81 (91), 80 (60), 79 (100), 78 (18), 77 (34), 71 (21), 70 (30), 69 (40), 68 (37), 67 (93), 66 (17), 65 (19), 57 (26), 56 (14), 55 (92), 54 (25), 53 (23), 43 (33), 42 (12), 41 (68), 39 (27); HRMS (ESI(pos)): m/z : calcd. for $[\text{C}_{14}\text{H}_{24}\text{O}_2+\text{Na}]^+$: 247.1667, found: 247.1668.

(E)-Cyclohexadec-2-en-4-yne-1,6-diol (**120b**)



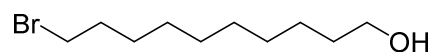
Diyne **119b** (10.0 mg, 33 μmol) was stirred with MS 5 Å (200 mg), trisilanol **97c** (6.4 mg, 7.2 μmol , 22 mol%), and complex **73** (4.4 mg, 6.6 μmol , 20 mol%) in toluene (50 mL) for 3 h according to general procedure 6. Flash chromatography (SiO_2 , hexanes/ethyl acetate, 4/1 to 0/1) afforded the title compound as a colorless solid (3.3 mg, 40%, mixture of diastereomers).

M.p. 92 – 93 $^{\circ}\text{C}$; ^1H NMR (300 MHz, CDCl_3): δ = 6.16 (ddd, J = 15.9, 6.5, 3.4 Hz, 1H), 5.71 (dt, J = 15.9, 1.6 Hz, 1H), 4.59 – 4.46 (m, 1H), 4.30 – 4.18 (m, 1H), 1.85 – 1.65 (m, 4H), 1.61 – 1.19 ppm (m, 18H); ^{13}C NMR (100 MHz, CDCl_3): δ = 146.9, 146.8, 109.70, 109.68, 91.3, 91.2, 83.99, 83.96, 72.63, 72.58, 63.37, 63.36, 37.14, 37.12, 35.54, 35.51, 28.4, 28.3, 27.9, 27.8, 27.74, 27.72, 27.69, 27.64, 27.62, 27.61, 23.57, 23.5, 22.5 ppm; IR (film): $\tilde{\nu}$ = 3670, 3309, 2923, 2852, 2219, 1633, 1459, 1407, 1342, 1292, 1168, 1115, 1015, 955, 871, 798, 710, 553, 507, 469 cm^{-1} ; MS (ESI(pos)) m/z (%) = 273.2 (100 $[\text{M}+\text{Na}]^+$); HRMS (ESI(pos)): m/z : calcd. for $[\text{C}_{16}\text{H}_{26}\text{O}_2+\text{Na}]^+$: 273.1824, found: 273.1825.

7.5 Formal Synthesis of Aspicilin

7.5.1 Synthesis of Alcohol Fragment 151

10-Bromodecane-1-ol (EP10)

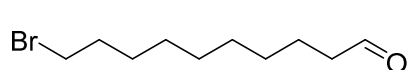


According to literature procedure^[133], HBr (48% in water, 16.3 mL, 138 mmol) was added to a suspension of 1,10-decanediol (20.0 g, 115 mmol) in toluene (250 mL). The resulting mixture was stirred at reflux temperature for 16 h. Aq. sat. Na₂S₂O₃ (50 mL) was added and the aqueous layer was extracted with ethyl acetate (3 × 200 mL). The combined extracts were dried over MgSO₄, the solvent was evaporated, and the crude product was purified by flash chromatography (silica, hexanes/ethyl acetate, 4/1 to 2/1) to give the title compound as a colorless oil (19.8 g, 73%).

¹H NMR (400 MHz, CDCl₃): δ = 3.63 (t, *J* = 6.6 Hz, 2H), 3.40 (t, *J* = 6.9 Hz, 2H), 1.88 – 1.80 (m, 2H), 1.60 – 1.51 (m, 2H), 1.46 – 1.24 (m, 13H) ppm. ¹³C NMR (100 MHz, CDCl₃): δ = 63.2, 34.2, 32.92, 32.89, 29.6, 29.49, 29.48, 28.9, 28.3, 25.8 ppm. IR (film): $\tilde{\nu}$ = 3328, 2924, 2853, 1463, 1437, 1371, 1352, 1256, 1242, 1129, 1055, 899, 756, 722, 644, 562, 505, 465, 445, 428, 417 cm⁻¹. MS (EI): *m/z* (%) = 164 (2), 162 (2), 150 (10), 148 (10), 137 (4), 135 (4), 111 (4), 110 (6), 109 (10), 97 (16), 96 (16), 95 (21), 84 (7), 83 (30), 82 (40), 81 (46), 80 (5), 79 (8), 71 (7), 70 (17), 69 (63), 68 (57), 67 (68), 66 (6), 57 (18), 56 (24), 55 (100), 54 (33), 53 (8), 44 (4), 43 (23), 42 (14), 41 (58), 39 (14), 26 (3), 31 (11), 29 (11), 27 (10); HRMS (ESI(pos)): *m/z* calcd. for [C₁₀H₂₁BrO+Na]⁺: 259.0669, found 259.0668.

The analytical and spectroscopic data are in agreement with those reported in the literature.^[134]

10-Bromodecanal (158)



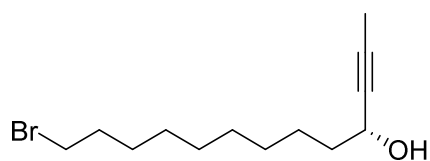
[Cu(MeCN)₄]PF₆ (744 mg, 2.00 mmol, 5 mol%), 2,2'-bipyridine (312 mg, 2.00 mmol), TEMPO (312 mg, 2.00 mmol) and *N*-methyl-imidazole (328 mg, 4.00 mmol) were added sequentially to a solution of 10-bromo-1-decanol **EP10** (10.0 g, 42.0 mmol) in acetonitrile (200 mL) in an open flask. The dark red mixture was vigorously stirred open to air for 14 h at room temperature, after which time the solution had turned blue. The reaction mixture was filtered through a plug of silica, the solvent was evaporated, and the residue was purified by flash

chromatography (silica, hexanes/ethyl acetate, 20/1 to 10/1) to give the title compound as a slightly red oil (9.00 g, 91%).

^1H NMR (400 MHz, CDCl_3): δ = 9.77 (t, J = 1.8 Hz, 1H), 3.42 (t, J = 6.8 Hz, 2H), 2.44 (td, J = 7.4, 1.8 Hz, 2H), 1.90 – 1.81 (m, 2H), 1.68 – 1.59 (m, 2H), 1.47 – 1.37 (m, 2H), 1.36 – 1.27 (m, 8H) ppm. ^{13}C NMR (100 MHz, CDCl_3): δ = 202.7, 43.9, 33.9, 32.8, 29.21, 29.18, 29.1, 28.7, 28.1, 22.1 ppm. IR (film): $\tilde{\nu}$ = 2926, 2854, 2716, 1723, 1463, 1409, 1390, 1245, 1111, 846, 723, 643, 560 cm^{-1} . MS (EI): m/z (%) = 192 (15), 190 (25), 150 (23), 148 (24), 137 (19), 135 (12), 111 (32), 109 (36), 95 (52), 83 (18), 82 (37), 81 (69), 71 (14), 70 (10), 69 (100), 68 (35), 67 (48), 57 (57), 56 (15), 55 (89), 54 (18), 53 (11), 45 (11), 44 (51), 43 (31), 42 (15), 41 (78), 39 (22), 29 (21), 27 (16); HRMS (ESI(pos)): m/z calcd. for $[\text{C}_{10}\text{H}_{19}\text{BrO}+\text{Na}]^+$: 257.0510, found 257.0512.

The analytical and spectroscopic data are in agreement with those reported in the literature.^[135]

(*R*)-13-Bromotridec-2-yn-4-ol (**159**)

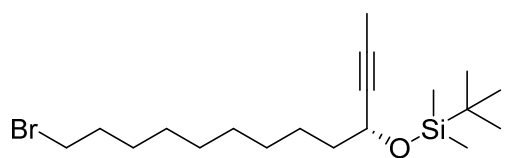


NEt_3 (3.90 mL, 27.9 mmol) was added dropwise to a suspension of $\text{Zn}(\text{OTf})_2$ (10.1 g, 27.9 mmol) and (+)-*N*-methylephedrine (5.00 g, 27.9 mmol) in toluene (120 mL) at ambient temperature. After stirring for 2 h, the reaction mixture was cooled to -78°C and liquid propyne (ca. 4 mL) was added via cannula at -78°C . The resulting mixture was allowed to warm to ambient temperature. After 1 h, a solution of aldehyde **158** (5.48 g, 23.3 mmol) in toluene (10 mL) was added dropwise over 4 h. The mixture was stirred for 14 h at room temperature before the reaction was quenched with aq. sat. NH_4Cl (20 mL). The aqueous layer was extracted with ethyl acetate (3 \times 150 mL). The water layer was acidified to pH 2 by addition of 2 M HCl and was extracted with ethyl acetate (150 mL). The combined extracts were dried over MgSO_4 , the solvent was evaporated, and the residue was purified by flash chromatography (silica, hexanes/ethyl acetate, 10/1) to give the title compound as a colorless oil (4.15 g, 65%, 94% *ee*, determined by chiral HPLC: 150 mm Chiralcell OD-3 (\varnothing 4.6 mm), *n*-heptane/2-propanol 99:1, 1.0 ml/min, 6.5 MPa, 298 K: R_t (minor enantiomer) = 11.84 min, R_t (major enantiomer) = 12.92 min)).

$[\alpha]_D^{20}$: -0.8 (c = 1, CHCl_3). ^1H NMR (400 MHz, CDCl_3): δ = 4.35 – 4.29 (m, 1H), 3.42 (t, J = 6.9 Hz, 2H), 1.85 (d, J = 2.1 Hz, 3H), 1.89 – 1.80 (m, 2H), 1.72 – 1.60 (m, 3H), 1.47 – 1.36 (m,

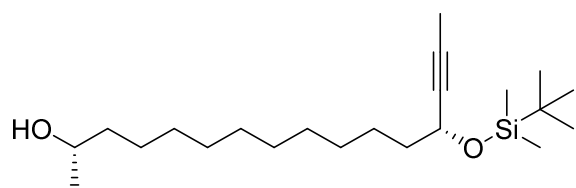
4H), 1.35 – 1.25 (m, 8H) ppm. ^{13}C NMR (100 MHz, CDCl_3): δ = 81.1, 80.6, 62.9, 38.3, 34.2, 33.0, 29.6, 29.5, 29.4, 28.9, 28.3, 25.3, 3.7 ppm. IR (film): $\tilde{\nu}$ = 3434, 2924, 2854, 2219, 1734, 1674, 1454, 1441, 1352, 1323, 1260, 1200, 1135, 1119, 1076, 1022, 988, 904, 868, 811, 723, 543, 428 cm^{-1} . MS (GC-MS): m/z (%) = 192 (1), 190 (1), 150 (1), 148 (1), 137 (1), 135 (2), 133 (1), 125 (1), 123 (1), 121 (2), 119 (1), 112 (1), 111 (3), 110 (2), 109 (4), 107 (4), 97 (9), 93 (6), 84 (23), 83 (6), 82 (9), 81 (14), 79 (10), 71 (6), 70 (8), 69 (100), 68 (15), 67 (16), 66 (5), 57 (8), 55 (19), 43 (7), 41 (16), 40 (5), 39 (8); HRMS (ESI(pos)): m/z calcd. for $[\text{C}_{13}\text{H}_{23}\text{BrO}+\text{Na}]^+$: 297.0825, found 297.0826.

(R)-((13-Bromotridec-2-yn-4-yl)oxy)(tert-butyl)dimethylsilane (160)



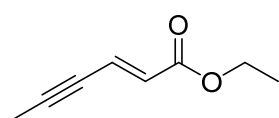
TBSCl (2.86 g, 19.0 mmol) was added to a solution of alcohol **159** (3.60 g, 13.1 mmol) and imidazole (2.66 g, 39.0 mmol) in CH_2Cl_2 (100 mL) at 0 °C. The resulting mixture was stirred at ambient temperature for 2 h. The reaction was quenched with aq. sat. NH_4Cl (30 mL) and the aqueous layer was extracted with CH_2Cl_2 (3 × 50 mL). The combined extracts were dried over MgSO_4 , the solvent was evaporated, and the residue was purified by flash chromatography (silica, hexanes/ethyl acetate, 50/1) to give the title compound as a colorless oil (4.57 g, 90%).

$[\alpha]_D^{20}$: +24.5 (c = 1, CHCl_3). ^1H NMR (400 MHz, CDCl_3): δ = 4.36 – 4.28 (m, 1H), 3.40 (t, J = 6.9 Hz, 2H), 1.82 (d, J = 2.1 Hz, 3H), 1.88 – 1.81 (m, 2H), 1.65 – 1.55 (m, 2H), 1.46 – 1.34 (m, 4H), 1.33 – 1.24 (m, 8H), 0.90 (s, 9H), 0.11 (s, 3H), 0.09 (s, 3H) ppm. ^{13}C NMR (100 MHz, CDCl_3): δ = 81.3, 79.9, 63.3, 39.1, 34.2, 33.0, 29.6, 29.5, 29.4, 28.9, 28.3, 26.0, 25.4, 18.4, 3.7, -4.3, -4.9 ppm. IR (film): $\tilde{\nu}$ = 2927, 2855, 2238, 1716, 1586, 1463, 1389, 1360, 1341, 1250, 1154, 1075, 1005, 939, 834, 775, 723, 666, 647, 563 cm^{-1} . MS (EI): m/z (%) = 389 (2), 387 (1), 375 (4), 373 (4), 334 (11), 333 (53), 332 (11), 331 (50), 207 (11), 205 (10), 184 (10), 183 (58), 177 (28), 137 (15), 135 (36), 127 (32), 123 (10), 121 (44), 109 (23), 107 (53), 98 (11), 97 (100), 95 (68), 93 (55), 83 (15), 81 (54), 79 (23), 75 (65), 67 (23), 55 (20); HRMS (ESI(pos)): m/z calcd. for $[\text{C}_{19}\text{H}_{37}\text{BrOSi}+\text{Na}]^+$: 411.1691, found 411.1689.

(2S,13R)-13-(tert-Butyldimethylsilyloxy)hexadec-14-yn-2-ol (151)

A mixture of magnesium turnings (250 mg, 10.3 mmol) and I_2 (20 mg) was vigorously stirred for 14 h at 90 °C. THF (5 mL) was added and the mixture was stirred at reflux temperature for 1 h before a solution of bromide **160** (2.00 g, 5.14 mmol) in THF (2 mL) was added over 2 min. The mixture was stirred at reflux temperature for 1 h before it was cooled to -40 °C and Li_2CuCl_4 (0.1 M in THF, 2 mL, 0.2 mmol, 4 mol%) was added. (*S*)-Propylene oxide (407 mg, 7.00 mmol, 490 μ L) was added over 5 min and the reaction mixture was allowed to reach room temperature over 14 h. The reaction was quenched by adding aq. sat. NH_4Cl (5 mL). The aqueous layer was extracted with ethyl acetate (3 \times 50 mL). The combined extracts were dried over $MgSO_4$, the solvent was evaporated and the residue was purified by flash chromatography (silica, hexanes/ethyl acetate, 50/1 to 20/1) to give the title compound as a colorless oil (1.35 g, 71%).

$[\alpha]_D^{20}$: +32.6 ($c = 1$, $CHCl_3$). 1H NMR (400 MHz, $CDCl_3$): $\delta = 4.32 - 4.25$ (m, 1H), 3.84 - 3.74 (m, 1H), 1.82 (d, $J = 2.1$ Hz, 3H), 1.65 - 1.55 (m, 2H), 1.49 - 1.33 (m, 5H), 1.32 - 1.23 (m, 14H), 1.18 (d, $J = 6.2$ Hz, 3H), 0.90 (s, 9H), 0.11 (s, 3H), 0.09 (s, 3H) ppm. ^{13}C NMR (100 MHz, $CDCl_3$): $\delta = 81.3, 79.9, 68.4, 63.4, 39.5, 39.1, 29.8, 29.7, 29.4, 26.0, 26.0, 25.9, 25.4, 23.6, 18.5, 3.7, -4.3, -4.9$ ppm. IR (film): $\tilde{\nu} = 3355, 2925, 2854, 1744, 1463, 1407, 1389, 1361, 1341, 1250, 1083, 1005, 939, 834, 775, 721, 666, 559$ cm^{-1} . MS (EI): m/z (%) = 312 (11), 311 (43), 272 (19), 271 (88), 219 (22), 184 (12), 183 (75), 163 (10), 159 (10), 153 (21), 149 (19), 145 (15), 143 (26), 137 (14), 135 (83), 127 (16), 123 (35), 121 (25), 115 (17), 109 (68), 107 (29), 105 (12), 97 (76), 95 (93), 93 (36), 83 (33), 81 (68), 79 (17), 75 (100), 73 (46), 67 (32), 57 (11), 55 (25), 45 (12); HRMS (ESI(pos)): m/z calcd. for $[C_{22}H_{44}O_2Si+Na]^+$: 391.3000, found 391.3003.

7.5.2 Synthesis of Acid Fragment 152**Ethyl-(*E*)-hex-2-en-4-ynoate (156)**

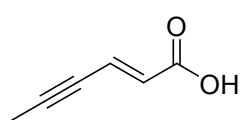
$[Pd(MeCN)_2]Cl_2$ (60.8 mg, 210 μ mol, 4 mol%) was added to a solution of ethyl-(*E*)-3-iodoacrylate^[136] (1.20 g, 5.00 mmol) and tributyl(prop-1-yn-1-yl)stannane (1.71 g, 5.20 mmol) in DMF (10 mL). The mixture was stirred at room temperature for 14 h. Aq. KF (20 mL, 0.5 M) and ethyl acetate (20 mL) were added to the mixture and stirring was continued for 2 h. The mixture was filtrated and

the aqueous layer was extracted with ethyl acetate (3 × 30 mL). The combined extracts were dried over MgSO₄, the solvent was evaporated, and the residue was purified by flash chromatography (silica, hexanes/ethyl acetate, 50/1 to 20/1) to give the title compound as a colorless oil (630 mg, 91%).

¹H NMR (400 MHz, CDCl₃): δ = 6.72 (dq, *J* = 15.8, 2.5 Hz, 1H), 6.13 (dd, *J* = 15.8, 0.6 Hz, 1H), 4.20 (q, *J* = 7.1 Hz, 2H), 2.02 (dd, *J* = 2.5, 0.6 Hz, 3H), 1.29 (t, *J* = 7.1 Hz, 3H) ppm. ¹³C NMR (100 MHz, CDCl₃): δ = 166.3, 129.4, 126.2, 96.3, 77.2, 60.8, 14.3, 4.9 ppm; MS (EI): *m/z* (%) = 138 (19), 110 (27), 95 (12), 93 (100), 82 (14), 66 (10), 65 (41), 63 (14), 39 (24); HRMS (ESI(pos)): *m/z* calcd. for [C₈H₁₀O₂+Na]⁺: 161.0575, found 161.0573.

The spectroscopic data (¹H NMR) is in agreement with the literature.^[137]

(E)-Hex-2-en-4-ynoic acid (**152**)



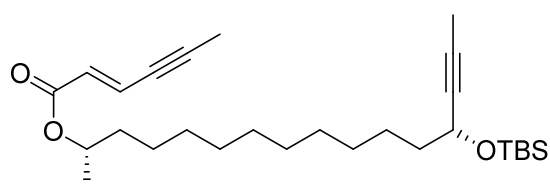
Ester **156** (950 mg, 6.88 mmol) was added to a suspension of LiOH (479 mg, 20.0 mmol) in a mixture of THF (10 mL), water (10 mL), and ethanol (2 mL). The resulting mixture was stirred for 1 h at room

temperature. The reaction was quenched with aq. sat. NH₄Cl (10 mL). The pH of the aqueous layer was adjusted to 2 by addition of 2 M HCl. The aqueous layer was extracted with ethyl acetate (3 × 50 mL). The combined extracts were dried over MgSO₄ and the solvent was evaporated to give the title compound as a colorless solid (690 mg, 91%).

M.p. = 175 – 177 °C. ¹H NMR (400 MHz, CDCl₃): δ = 11.92 (bs, 1H), 6.82 (dq, *J* = 15.8, 2.5 Hz, 1H), 6.14 (d, *J* = 15.8 Hz, 1H), 2.05 (d, *J* = 2.5 Hz, 3H) ppm. ¹³C NMR (100 MHz, CDCl₃): δ = 171.7, 129.0, 128.6, 98.6, 77.1, 5.1 ppm. IR (film): $\tilde{\nu}$ = 2925, 2582, 2216, 1674, 1614, 1452, 1421, 1310, 1279, 1210, 1172, 1033, 962, 921, 865, 677, 539, 422 cm⁻¹; MS (EI): *m/z* (%) = 110 (100), 93 (12), 82 (40), 81 (13), 65 (26), 63 (16), 39 (36); HRMS (ESI(neg)): *m/z* calcd. for [C₆H₅O₂]⁻: 109.0295, found 109.0295.

7.5.3 Completion of the Formal Total Synthesis

(2*S*,13*R*)-13-((*tert*-Butyldimethylsilyl)oxy)hexadec-14-yn-2-yl-(*E*)-hex-2-en-4-ynoate (**150**)

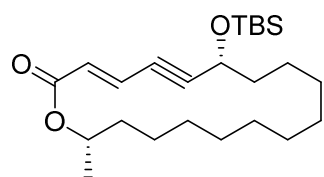


Alcohol **151** (1.50 g, 4.07 mmol) and DCC (887 mg, 4.30 mmol) were successively added to a solution of acid **152** (473 mg, 4.07 mmol) in CH₂Cl₂ (10 mL) at 0 °C. DMAP (10 mg,

0.82 mmol) was added and the resulting mixture was stirred for 2 h at this temperature. The mixture was filtered through a plug of silica, which was carefully rinsed with CH₂Cl₂. Aq. sat. NH₄Cl (5 mL) was added to the filtrate and the aqueous layer was extracted with CH₂Cl₂ (2 × 20 mL). The combined extracts were dried over MgSO₄, the solvent was evaporated, and the residue was purified by flash chromatography (silica, hexanes/ethyl acetate, 100/1 to 50/1) to give the title compound as a colorless oil (1.75 g, 93%).

$[\alpha]_D^{20}$: +35.9 (*c* = 1, CHCl₃). ¹H NMR (400 MHz, CDCl₃): δ = 6.71 (dq, *J* = 15.8, 2.4 Hz, 1H), 6.12 (d, *J* = 15.8 Hz, 1H), 5.00 – 4.90 (m, 1H), 4.32 – 4.25 (m, 1H), 2.02 (d, *J* = 2.4 Hz, 3H), 1.81 (d, *J* = 2.1 Hz, 3H), 1.66 – 1.54 (m, 3H), 1.54 – 1.24 (m, 17H), 1.23 (d, *J* = 6.3 Hz, 3H), 0.90 (s, 9H), 0.11 (s, 3H), 0.09 (s, 3H) ppm. ¹³C NMR (100 MHz, CDCl₃): δ = 166.0, 130.1, 125.9, 96.1, 81.3, 79.9, 77.3, 71.6, 63.4, 39.1, 36.1, 29.70, 29.66, 29.59, 29.4, 26.0, 25.5, 25.4, 20.1, 18.4, 4.9, 3.7, -4.4, -4.9 ppm. IR (film): $\tilde{\nu}$ = 2926, 2854, 2222, 2120, 1712, 1463, 1359, 1300, 1256, 1180, 1164, 1078, 1005, 961, 835, 776, 720, 667, 516 cm⁻¹. MS (EI): *m/z* (%) = 404 (2), 403 (7), 209 (3), 187 (3), 186 (7), 185 (53), 183 (10), 169 (6), 168 (14), 167 (100), 153 (3), 135 (2), 127 (3), 125 (2), 123 (3), 121 (2), 111 (3), 109 (5), 107 (2), 99 (2), 97 (12), 95 (8), 93 (16), 83 (2), 81 (5), 79 (2), 75 (8), 73 (7), 69 (3), 67 (3), 55 (4); HRMS (ESI(pos)): *m/z* calcd. for [C₂₈H₄₈O₃Si+Na]⁺: 483.3266, found 483.3265.

(7*R*,18*S*,*E*)-7-((*tert*-Butyldimethylsilyl)oxy)-18-methyloxacyclooctadec-3-en-5-yn-2-one (149a).

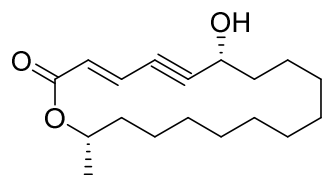


Diyne **150** (500 mg, 1.09 mmol) was added to a suspension of MS 5 Å (8 g) in toluene (800 mL) and the mixture was stirred for 1 h at room temperature. The mixture was heated to 110 °C and a solution of complex **28** (110 mg, 106 μmol, 10 mol%) in toluene (2 mL) was added over 2 min. The mixture was stirred for 10 min at 110 °C before it was filtered through a plug of Celite®, which was carefully rinsed with ethyl acetate (50 mL). The solvent was evaporated and the residue was purified by flash chromatography (silica, hexanes/ethyl acetate, 100/1 to 50/1) to give the title compound as a colorless oil (400 mg, 91%). The product contained ca. 8% of the dimeric macrocycle **149b** and was used without further purification for the next step.

¹H NMR (400 MHz, CDCl₃): δ = 6.75 (dd, *J* = 15.8, 2.1 Hz, 1H), 6.21 (d, *J* = 15.8 Hz, 1H), 5.06 – 4.93 (m, 1H), 4.54 (ddd, *J* = 7.5, 4.8, 2.1 Hz, 1H), 1.77 – 1.62 (m, 3H), 1.61 – 1.17 (m, 17H),

1.23 (d, $J = 6.3$ Hz, 3H), 0.92 (s, 9H), 0.12 (s, 3H), 0.10 (s, 3H) ppm. ^{13}C NMR (100 MHz, CDCl_3): $\delta = 165.5, 131.8, 124.9, 101.2, 82.1, 72.8, 63.6, 37.6, 34.2, 29.9, 29.8, 29.5, 29.2, 28.6, 25.9, 25.8, 25.5, 23.8, 20.3, -4.5, -4.8$ ppm. IR (film): $\tilde{\nu} = 2927, 2855, 1715, 1619, 1462, 1360, 1299, 1254, 1178, 1153, 1125, 1083, 1006, 982, 960, 940, 835, 777, 717, 669$ cm^{-1} . MS (ESI(pos)) m/z (%) = 429.3 (100 $[\text{M}+\text{Na}]^+$); HRMS (ESI(pos)): m/z calcd. for $[\text{C}_{24}\text{H}_{42}\text{O}_3\text{Si}+\text{Na}]^+$: 429.2799, found 429.2795.

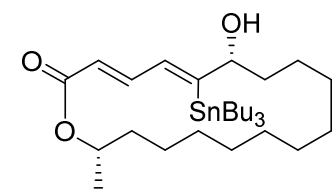
(7R,18S,E)-7-Hydroxy-18-methyloxacyclooctadec-3-en-5-yn-2-one (162a)



TBAF (1.0 M in THF, 2.00 mL, 2.00 mmol) was added to a solution of macrocycle **149a** (400 mg, 980 μmol) in THF (5 mL) at 0 °C. The mixture was warmed to room temperature and stirred for 2 h before the reaction was quenched with aq. sat. NH_4Cl (1 mL) and water (1 mL). The aqueous layer was extracted with ethyl acetate (3 \times 30 mL). The combined extracts were dried over MgSO_4 , the solvent was evaporated, and the residue was purified by flash chromatography (silica, hexanes/ethyl acetate, 20/1 to 4/1) to give the title compound as a colorless solid (243 mg, 85%).

M.p. = 62 – 63 °C. $[\alpha]_D^{20}$: +61.1 ($c = 1, \text{CHCl}_3$). ^1H NMR (400 MHz, CDCl_3): $\delta = 6.75$ (dd, $J = 15.9, 2.1$ Hz, 1H), 6.24 (d, $J = 15.9$ Hz, 1H), 5.04 – 4.94 (m, 1H), 4.61 – 4.54 (m, 1H), 2.05 – 1.16 (m, 24 H) ppm. ^{13}C NMR (100 MHz, CDCl_3): $\delta = 165.3, 132.3, 124.4, 99.9, 82.8, 72.9, 63.1, 36.6, 34.2, 29.8, 29.7, 29.5, 29.2, 29.1, 28.5, 25.4, 23.9, 20.2$ ppm. IR (film): $\tilde{\nu} = 3266, 2922, 2850, 2215, 1702, 1622, 1611, 1460, 1378, 1351, 1302, 1271, 1188, 1155, 1128, 1107, 1077, 1021, 979, 871, 755, 719, 585, 499, 410$ cm^{-1} . MS (ESI(pos)): m/z (%) = 291.2 (100 $[\text{M}+\text{Na}]^+$); HRMS (ESI(pos)): m/z calcd. for $[\text{C}_{18}\text{H}_{28}\text{O}_3]^-$: 291.1668, found 291.1966.

(3E,5E,7R,18S)-7-Hydroxy-18-methyl-6-(tributylstannyl)oxacyclooctadeca-3,5-dien-2-one (163a)

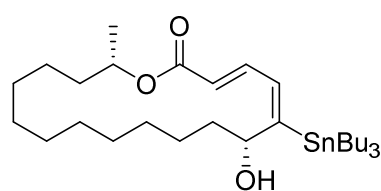


A solution of tributyltin hydride (163 mg, 0.56 mmol) in CH_2Cl_2 (1 mL) was added over 5 min to a stirred solution of enyne **162a** (150 mg, 0.51 mmol) and $[\text{Cp}^*\text{RuCl}_4]$ (10 mg, 9.0 μmol , 2 mol%) in CH_2Cl_2 (2.5 mL) at room temperature. The resulting mixture was stirred for 2 h at room temperature before all volatile materials were evaporated. Purification of the residue by flash chromatography (silica, hexanes/ethyl acetate, 20/1 to

10/1) afforded the title compound as a pale yellow oil (196 mg, 66%). A second isomer **163b** was isolated (8 mg, 3%).

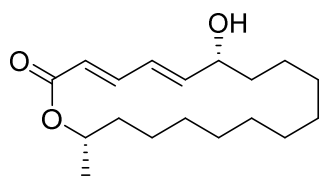
$[\alpha]_D^{20}$: -31.7 ($c = 1$, CHCl_3). ^1H NMR (400 MHz, CDCl_3) $\delta = 7.25$ (dd, $J = 15.1, 11.5$ Hz, 1H), 6.81 (d, $J = 11.6$ Hz, $J_{\text{Sn-H}} = 54.8$ Hz, 1H), 5.78 (d, $J = 15.0$ Hz, 1H), 5.05 (dq, $J = 9.3, 6.3, 2.9$ Hz, 1H), 4.31 (dt, $J = 9.3, 3.4$ Hz, $J_{\text{Sn-H}} = 26.1$ Hz, 1H), 1.71 – 1.58 (m, 2H), 1.54 – 1.38 (m, 9H), 1.35 – 1.06 (m, 22H), 1.05 – 0.91 (m, 9H), 0.84 (t, $J = 7.3$ Hz, 9H) ppm. ^{13}C NMR (100 MHz, CDCl_3): $\delta = 167.7, 166.8, 144.5, 137.0, 123.2, 80.3, 71.3, 36.1, 35.2, 29.9, 29.8, 29.5, 29.28, 29.25, 29.01, 28.96, 27.6, 25.2, 23.9, 20.6, 13.8, 11.8$ ppm. ^{119}Sn NMR (186 MHz, CDCl_3) $\delta = -56.0$ ppm. IR (film): $\tilde{\nu} = 3464, 2953, 2922, 2852, 1707, 1688, 1619, 1565, 1460, 1376, 1354, 1258, 1186, 1125, 1072, 1019, 976, 903, 863, 757, 716, 666, 595, 536, 504$ cm^{-1} ; MS (EI): m/z (%) = 531 (15), 529 (16), 528 (25), 527 (89), 526 (40), 525 (68), 524 (30), 523 (37), 513 (17), 511 (18), 510 (28), 509 (100), 508 (44), 507 (75), 506 (33), 505 (40), 251 (11), 179 (12), 177 (19), 175 (15); HRMS (ESI(pos)): m/z calcd. for $[\text{C}_{30}\text{H}_{56}\text{O}_3\text{Sn}+\text{H}]^+$: 585.3329, found 585.3324.

Stereoisomer **163b**:



^1H NMR (400 MHz, CDCl_3) $\delta = 7.51$ (ddt, $J = 15.2, 11.0, 3.3$ Hz, 1H), 6.33 (dd, $J = 11.2, 1.6$ Hz, $J_{\text{Sn-H}} = 30.8$ Hz, 1H), 5.81 (d, $J = 15.0$ Hz, 1H), 5.18 (ddp, $J = 9.5, 6.3, 3.1$ Hz, 1H), 5.03 (t, $J = 7.3$ Hz, $J_{\text{Sn-H}} = 32.0$ Hz, 1H), 1.65 – 1.11 (m, 37H), 0.99 – 0.92 (m, 5H), 0.89 (t, $J = 7.3$ Hz, 9H) ppm. ^{13}C NMR (100 MHz, CDCl_3) $\delta = 167.5, 166.5, 138.7, 134.6, 121.2, 72.2, 69.6, 37.8, 36.0, 29.8, 29.2, 28.7, 28.4, 27.7, 27.6, 26.6, 25.3, 24.2, 21.0, 13.9, 10.9$ ppm. ^{119}Sn NMR (186 MHz, CDCl_3) $\delta = -40.2$ ppm. IR (film): $\tilde{\nu} = 3500, 2953, 2923, 2854, 1710, 1691, 1569, 1460, 1419, 1376, 1357, 1337, 1268, 1186, 1125, 1072, 1021, 979, 893, 876, 845, 804, 769, 722, 665, 596, 548, 505, 435, 408$ cm^{-1} . HRMS (ESI(pos)): m/z calcd. for $[\text{C}_{30}\text{H}_{56}\text{O}_3\text{Sn}+\text{Na}]^+$: 607.3148, found 607.3143.

(3E,5E,7R,18S)-7-Hydroxy-18-methyloxacyclooctadeca-3,5-dien-2-one (**132**)



CuTC (65 mg, 340 μmol) was added to a solution of stannane **163a** (100 mg, 171 μmol) in DMF (2 mL). The mixture was stirred for 1 h at room temperature before H_2O (5 mL) was added. The aqueous layer was extracted with ethyl acetate (3×10 mL). The combined extracts were dried over MgSO_4 , the solvent was evaporated, and the residue was

purified by flash chromatography (silica, hexanes/ethyl acetate, 10/1 to 4/1) to give the title compound as a colorless oil (42 mg, 83%).

$[\alpha]_D^{20}$: +14.2 ($c = 1$, CHCl_3). ^1H NMR (400 MHz, CDCl_3): $\delta = 7.24$ (dd, $J = 15.4, 10.9$ Hz, 1H), 6.32 (dd, $J = 15.2, 10.9$ Hz, 1H), 6.07 (dd, $J = 15.2, 7.9$ Hz, 1H), 5.85 (d, $J = 15.4$ Hz, 1H), 5.02 (dq, $J = 9.4, 6.3, 3.2$ Hz, 1H), 4.27 (td, $J = 8.3, 3.7$ Hz, 1H), 1.82 – 1.73 (m, 1H), 1.69 – 1.54 (m, 4H), 1.50 – 1.37 (m, 2H), 1.28 (d, $J = 6.3$ Hz, 3H), 1.33 – 1.12 (m, 14H) ppm. ^{13}C NMR (100 MHz, CDCl_3): $\delta = 166.6, 145.1, 143.6, 128.4, 122.6, 73.3, 71.5, 35.5, 35.4, 29.7, 29.14, 29.10, 29.05, 28.8, 24.8, 23.4, 20.6$ ppm. IR (film): $\tilde{\nu} = 3412, 2925, 2854, 1701, 1644, 1618, 1460, 1355, 1296, 1260, 1178, 1124, 999, 910, 883, 730, 647, 411$ cm^{-1} . MS (EI): m/z (%) = 294 (40), 276 (10), 221 (17), 195 (32), 191 (11), 177 (27), 163 (13), 150 (14), 149 (17), 142 (17), 137 (14), 135 (22), 128 (11), 127 (10), 125 (12), 124 (23), 123 (14), 121 (28), 111 (21), 110 (31), 109 (30), 108 (14), 107 (20), 99 (100), 98 (12), 97 (40), 96 (26), 95 (51), 94 (15), 93 (16), 91 (11), 84 (11), 83 (37), 82 (54), 81 (64), 80 (13), 79 (21), 71 (14), 69 (45), 68 (12), 67 (32), 57 (20), 55 (71), 54 (12), 53 (18), 43 (27), 41 (40), 29 (10); HRMS (ESI(pos)): m/z calcd. for $[\text{C}_{18}\text{H}_{30}\text{O}_3+\text{Na}]^+$: 317.2087, found 317.2087.

7.6 Peptide Reactions

General

The peptides utilized in this work were synthesized by P. Cromm according to standard Fmoc-chemistry for SPPS using HCTU (*O*-(6-Chlorobenzotriazol-1-yl)-*N,N,N',N'*-tetramethyluronium hexafluorophosphate) and COMU (1-[(1-(Cyano-2-ethoxy-2-oxoethylideneaminoxy)-dimethylaminomorpholino)]-uroniumhexafluorophosphate) as coupling reagents. The resin bound peptides were dried prior to use in toluene over MS 5 Å for four days while exchanging the solvent daily. The resin was stored in a Schlenk tube under argon. The reactions were generally done with 5 mg of the resin bound peptides. The products were cleaved from the solid support and analyzed by analytical LC-MS.

Ring Closing Alkyne Metathesis

The resin was suspended in toluene (0.15 mL) together with MS (5 Å, sticks). A stock solution of the catalyst **28** (2 mg/mL, 1.5 equiv) in toluene was added and the reaction mixture was stirred at 40 °C for 3 h. The resin was filtered off, washed with toluene (3×), CH₂Cl₂ (3×), and dried to constant weight.

Gold Catalyzed Hydratisation

The resin (5 mg, 15.9 μmol/g, 0.08 μmmol of peptide **182b**) was suspended in MeOH (0.1 mL). A solution of 1,3-bis-(2,6-di-isopropylphenyl)-imidazol-2-ylidene-gold(I) (**186**) (15 equiv) in toluene (0.2 mL) was added and the reaction mixture was stirred at 60 °C for 2 h. Complex **186** (7 equiv) was added and stirring was continued for 14 h at 60 °C. Complex **186** (7 equiv) was added and stirring was continued for 2 h at 60 °C. The resin was filtered off, washed with toluene (3×), CH₂Cl₂ (3×), and dried to constant weight.

Click Chemistry

The resin was suspended in toluene (0.3 mL) before chloro-(1,5-cyclooctadiene)-(pentamethylcyclopentadienyl)-ruthenium(II) (**190**) (1 mg/mL in toluene, 3 equiv) was added. The azide was introduced (4-20 equiv) and the reaction mixture was stirred for 14 h at room temperature. The residue was filtered off, washed with CH₂Cl₂ (2×), MeCN/H₂O (1×), MeCN (1×), CH₂Cl₂ (3×), and dried to constant weight.

Cleavage off the Resin

The dry resin was treated with a mixture of TFA/TIPSH/H₂O (95/2.5/2.5, v/v/v, 100 μ L) for 1 h at room temperature. The solvent was evaporated and the crude material was suspended in Et₂O. The mixture was cooled with liquid N₂ until it froze before it was centrifuged (2 min, 10.000 rpm). The supernatant was removed and the crude product was dissolved in H₂O/MeCN (1/1, v/v, 0.5 mL).

Table 8.1: Overview over peptides synthesized in this work.

Entry	Sequence	Modification	HPLC (t _R , [min])	HRMS Calc.	MS (found)
1	L Y2 I F L Y1 V	Ketone 182c	2.88 ^[a]	1106.6542	1106.85 [m+H] ⁺
2	L Y2 I F L Y1 V	Benzyl 182d	2.63 ^[a]	1221.7076	1221.60 [m+H] ⁺
3	L Y2 I F L Y1 V	Sugar 182e	5.86 ^[a]	1433.7608	1433.65 [m+H] ⁺
4	L Y2 I F L Y1 V	PEG 182f	3.70 ^[a]	1343.7631	1343.75 [m+Na] ⁺
5	L Y2 I F L Y1 V	Biotin 182g	4.84 ^[a]	1532.8591	1532.60 [m+H] ⁺
6	C M W H Y2 A D Q Y1 F R S H L K	RCAM 176b	11.15 ^[b]	1071.5137	1071.52 [m+2H] ²⁺
7	C M W H Y2 A D Q Y1 F R S H L K	Ketone 176c	10.09 ^[b]	1080.5076	1080.40 [m+2H] ²⁺

[a] 50 mm Zorbax Eclipse Plus C18, 1.8 μ m, MeCN/H₂O, 0.1% TFA = 75/25, 0.5 ml/min, 308 K, 109 bar

[b] 50 mm Eclipse Plus C18, 1.8 μ m, A: Wasser + 0.1% TFA, B: MeCN + 0.1% TFA, 10% B in 20 min to 80% B, 0.5 ml/min, 308 K, 221 bar

8 Appendix

8.1 List of Abbreviations

Å	Ångström, $1 \text{ Å} = 10^{-10} \text{ m}$
AAC	Azide-alkyne cycloaddition
Ac	Acetyl
ACN	Acetonitrile
ACM	Alkyne cross metathesis
Ar	Aromatic group
aq.	Aqueous
Bn	Benzyl
bp	Boiling point
br	Broad
Bu	Butyl
Bz	Benzoyl
calc.	Calculated
cat.	Catalytic
Cl	Chemical ionization
COD	1,5-Cyclooctadiene
conc.	Concentrated
conv.	Conversion
COSY	Correlation spectroscopy
δ	Chemical shift
Δ	Reflux temperature
d	Day
d	Doublet
Da	Dalton $1 \text{ Da} = 1.660539040(20) \times 10^{-27} \text{ kg}$
DAIB	(2S)-(-)-exo-(Dimethylamino)isoborneol
DBU	1,8-Diazabicycloundec-7-ene
DCC	<i>N,N'</i> -Dicyclohexylcarbodiimide
DDQ	2,3-Dichloro-5,6-dicyano-1,4-benzoquinone

DMAP	4-(Dimethylamino)-pyridine
DME	Dimethoxyethane
DMF	<i>N,N</i> -Dimethylformamide
DMSO	Dimethyl sulfoxide
<i>dr</i>	Diastereomeric ratio
<i>ee</i>	Enantiomeric excess
EI	Electron ionization
ent	Enantiomer
ESI	Electrospray ionization
Et	Ethyl
equiv	Equivalents
eV	Electronvolt
GC	Gas chromatography
h	hour
hex	Hexyl
HMPA	Hexamethylphosphoramide
HPLC	High pressure liquid chromatography
HRMS	High resolution mass spectroscopy
Hz	Hertz, 1 Hz = 1 s ⁻¹
<i>i</i>	iso
IPr	1,3-bis(2,6-diisopropylphenyl)-imidazolium
IR	Infrared spectroscopy
J	Coupling constant
LICA	Lithium <i>N</i> -isopropylcyclohexylamide
Lit.	Literature
<i>m</i>	Meta
m	Multiplet
M	Molar: mol·l ⁻¹
m/z	Mass per charge
Me	Methyl
MOM	Methoxymethyl
Mp.	Melting point

MS	Mass spectrometry
MS	Molecular sieves
MTBE	Methyl <i>t</i> -butyl ether
<i>n</i>	Normal
NBS	<i>N</i> -Bromosuccinimide
<i>n</i> -BuLi	<i>n</i> -Butyllithium
NMI	1-Methylimidazole
NMO	<i>N</i> -Methylmorpholine- <i>N</i> -oxide
NMR	Nuclear magnetic resonance
NOE	Nuclear Overhauser effect
n.r.	No reaction
<i>p</i>	Para
<i>p</i> -TsOH	<i>p</i> -Toluenesulfonic acid
Pg	Protecting group
Ph	Phenyl
phen	1,10-Phenanthroline
ppm	Parts per million
PPTS	Pyridinium <i>p</i> -toluenesulfonate
py	Pyridine
q	Quartet
quant.	Quantitative
R	Organic substituent
rac	Racemic
RCAM	Ring closing alkyne metathesis
RCM	Ring closing olefin metathesis
rt	Ambient temperature
s	Singlet
sat.	Saturated
sm	Starting material
SPPS	Solid phase peptide synthesis
t	Tert
<i>t</i>	Triplet

T	Temperature
Tab.	Table
TBAF	Tetra- <i>n</i> -butylammoniumfluoride
TBS	<i>tert</i> -Butyldimethylsilyl
<i>t</i> -BuLi	<i>tert</i> -Butyllithium
TC	Thiophene-2-carboxylate
TEMPO	(2,2,6,6-Tetramethylpiperidin-1-yl)oxyl
<i>tert</i>	Tertiary
TES	Triethylsilyl
TFA	Trifluoroacetic acid
THF	Tetrahydrofuran
THP	Tetrahydropyran
TLC	Thin layer chromatography
TMEDA	Tetramethylethylenediamine
TMS	Trimethylsilyl
Ts	Tosyl

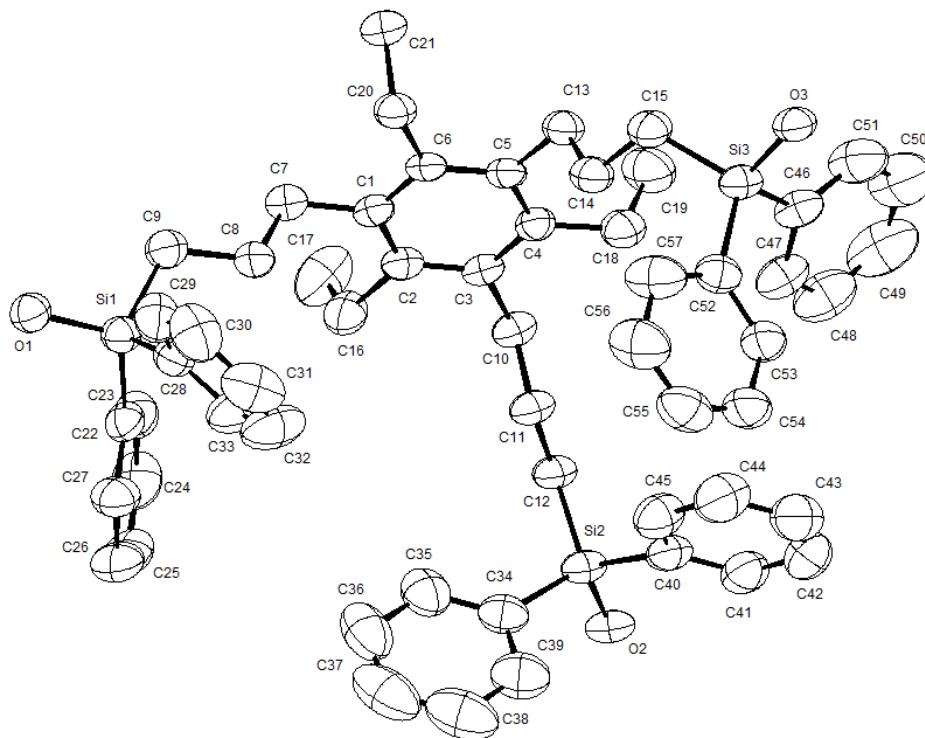
Amino acid single-letter codes

A	Alanine
R	Arginine
N	Asparagine
D	Aspartic acid
C	Cysteine
Q	Glutamine
E	Glutamic acid
G	Glycine
H	Histidine
I	Isoleucine
L	Leucine
K	Lysine
M	Methionine
F	Phenylalanine

P	Proline
S	Serine
T	Threonine
W	Tryptophan
Y	Tyrosine
V	Valine

8.2 Crystallographic Data

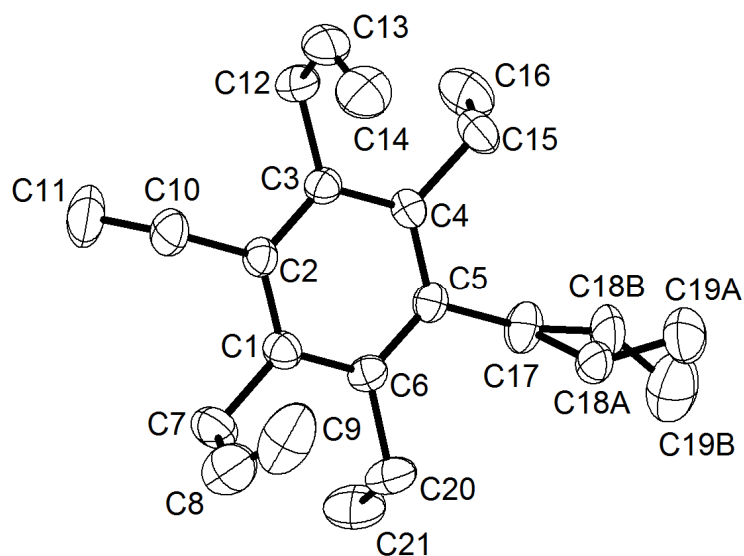
8.2.1 Crystallographic Data of 97c



Identification code	9856	
Empirical formula	$C_{57}H_{66}O_3Si_3$	
Color	colorless	
Formula weight	$883.36 \text{ g} \cdot \text{mol}^{-1}$	
Temperature	180 K	
Wavelength	0.71073 Å	
Crystal system	MONOCLINIC	
Space group	$P2_1/n$, (no. 14)	
Unit cell dimensions	$a = 15.175(4) \text{ Å}$	$\alpha = 90^\circ$.
	$b = 19.071(5) \text{ Å}$	$\beta = 95.910(5)^\circ$.
	$c = 22.799(6) \text{ Å}$	$\gamma = 90^\circ$.
Volume	$6563(3) \text{ Å}^3$	
Z	4	
Density (calculated)	$0.894 \text{ mg} \cdot \text{m}^{-3}$	
Absorption coefficient	0.105 mm^{-1}	

F(000)	1896 e	
Crystal size	0.187 x 0.110 x 0.067 mm ³	
θ range for data collection	2.728 to 26.372°.	
Index ranges	$-18 \leq h \leq 18, -23 \leq k \leq 23, -28 \leq l \leq 28$	
Reflections collected	133780	
Independent reflections	13393 [$R_{\text{int}} = 0.1537$]	
Reflections with $I > 2\sigma(I)$	6269	
Completeness to $\theta = 25.242^\circ$	99.9%	
Absorption correction	Gaussian	
Max. and min. transmission	0.99 and 0.97	
Refinement method	Full-matrix least-squares on F^2	
Data / restraints / parameters	13393 / 0 / 574	
Goodness-of-fit on F^2	0.999	
Final R indices [$I > 2\sigma(I)$]	$R_1 = 0.0599$	$wR^2 = 0.1462$
R indices (all data)	$R_1 = 0.1475$	$wR^2 = 0.1947$
Largest diff. peak and hole	0.3 and $-0.3 \text{ e} \cdot \text{\AA}^{-3}$	

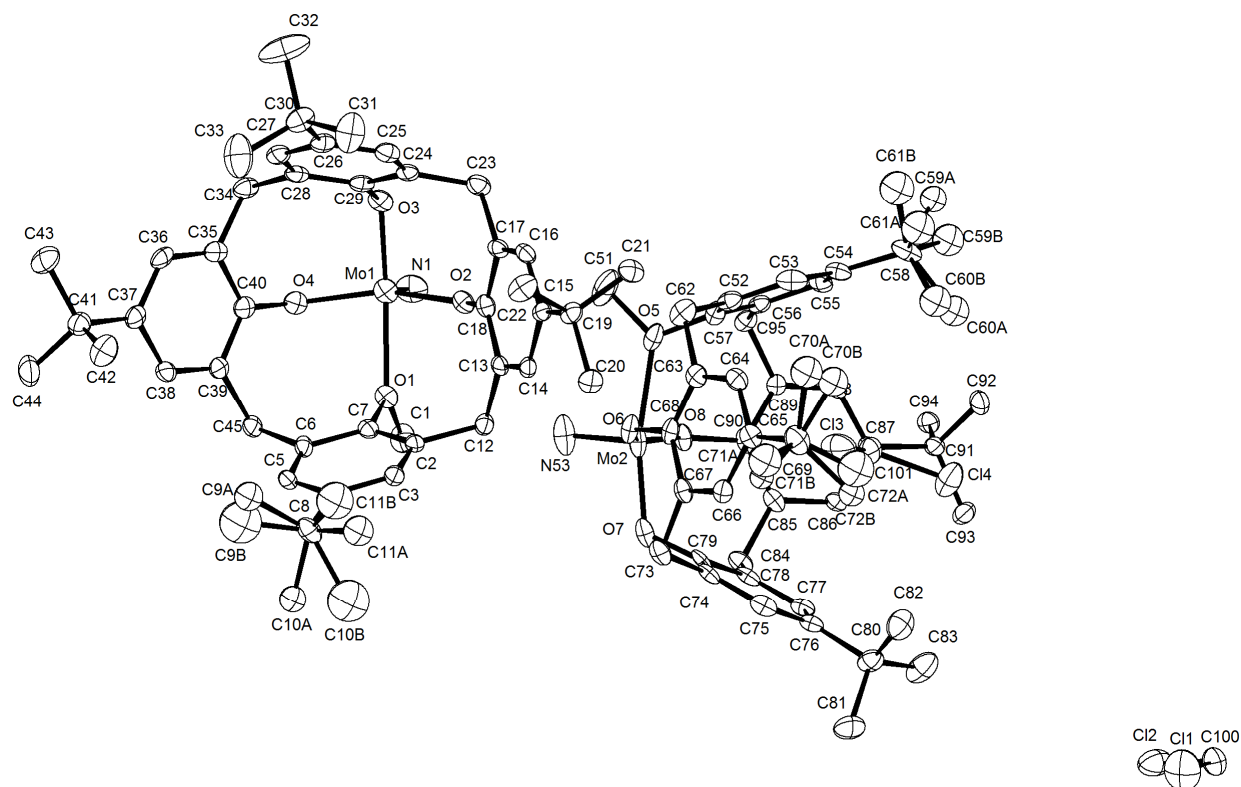
8.2.2 Crystallographic Data of 100c



Identification code	9064_SCS-SB-263_200_K	
Empirical formula	C ₂₁ H ₃₀	
Color	colorless	
Formula weight	282.45 g · mol ⁻¹	
Temperature	200 K	
Wavelength	0.71073 Å	
Crystal system	monoclinic	
Space group	P 2 ₁ /n, (no. 14)	
Unit cell dimensions	a = 8.9265(16) Å	α = 90°.
	b = 16.393(3) Å	β = 106.763(3)°.
	c = 13.113(2) Å	γ = 90°.
Volume	1837.3(6) Å ³	
Z	4	
Density (calculated)	1.021 mg · m ⁻³	
Absorption coefficient	0.057 mm ⁻¹	
F(000)	624 e	
Crystal size	0.443 x 0.240 x 0.040 mm ³	
θ range for data collection	2.043 to 30.697°.	
Index ranges	-12 h ≤ 12, -23 ≤ k ≤ 23, -18 ≤ l ≤ 18	
Reflections collected	52468	

Independent reflections	5643 [$R_{\text{int}} = 0.0449$]	
Reflections with $I > 2\sigma(I)$	3824	
Completeness to $\theta = 25.242^\circ$	99.9%	
Absorption correction	Gaussian	
Max. and min. transmission	0.99757 and 0.97850	
Refinement method	Full-matrix least-squares on F^2	
Data / restraints / parameters	5643 / 0 / 217	
Goodness-of-fit on F^2	1.030	
Final R indices [$I > 2\sigma(I)$]	$R_1 = 0.0554$	$wR^2 = 0.1502$
R indices (all data)	$R_1 = 0.0859$	$wR^2 = 0.1716$
Extinction coefficient	0	
Largest diff. peak and hole	0.341 and $-0.222 \text{ e} \cdot \text{\AA}^{-3}$	

8.2.3 Crystallographic Data of 105b



Identification code	8687	
Empirical formula	$C_{46} H_{57} Cl_2 Mo N O_4$	
Color	orange	
Formula weight	$854.76 \text{ g} \cdot \text{mol}^{-1}$	
Temperature	100 K	
Wavelength	0.71073 Å	
Crystal system	TRICLINIC	
Space group	P1, (no. 2)	
Unit cell dimensions	$a = 12.1447(11) \text{ Å}$	$\alpha = 60.091(6)^\circ$.
	$b = 21.1635(14) \text{ Å}$	$\beta = 88.852(8)^\circ$.
	$c = 21.1721(18) \text{ Å}$	$\gamma = 86.334(7)^\circ$.
Volume	$4706.9(7) \text{ Å}^3$	
Z	4	
Density (calculated)	$1.206 \text{ mg} \cdot \text{m}^{-3}$	
Absorption coefficient	0.431 mm^{-1}	
F(000)	1792 e	

Crystal size	0.18 x 0.10 x 0.02 mm ³	
θ range for data collection	2.609 to 30.036°.	
Index ranges	$-16 \leq h \leq 17$, $-29 \leq k \leq 29$, $-27 \leq l \leq 29$	
Reflections collected	69629	
Independent reflections	27332 [$R_{\text{int}} = 0.0700$]	
Reflections with $I > 2\sigma(I)$	16106	
Completeness to $\theta = 25.242^\circ$	99.7%	
Absorption correction	Gaussian	
Max. and min. transmission	0.99 and 0.95	
Refinement method	Full-matrix least-squares on F^2	
Data / restraints / parameters	27332 / 0 / 1000	
Goodness-of-fit on F^2	1.045	
Final R indices [$I > 2\sigma(I)$]	$R_1 = 0.0779$	$wR^2 = 0.1882$
R indices (all data)	$R_1 = 0.1347$	$wR^2 = 0.2121$
Largest diff. peak and hole	1.2 and $-1.1 \text{ e} \cdot \text{\AA}^{-3}$	

8.3 Bibliography

- [1] A. Fürstner, *Angew. Chem. Int. Ed.* **2013**, *52*, 2794-2819.
- [2] W. Zhang, S. Kraft, J. S. Moore, *J. Am. Chem. Soc.* **2003**, *126*, 329-335.
- [3] P. M. Cromm, J. Spiegel, T. N. Grossmann, *ACS Chem. Biol.* **2015**, *10*, 1362-1375.
- [4] J. Spiegel, P. M. Cromm, A. Itzen, R. S. Goody, T. N. Grossmann, H. Waldmann, *Angew. Chem. Int. Ed.* **2014**, *53*, 2498-2503.
- [5] S. M. Rummelt, A. Fürstner, *Angew. Chem. Int. Ed.* **2014**, *53*, 3626-3630.
- [6] P. Persich, J. Llaveria, R. Lhermet, T. de Haro, R. Stade, A. Kondoh, A. Fürstner, *Chem. Eur. J.* **2013**, *19*, 13047-13058.
- [7] a) R. R. Schrock, A. H. Hoveyda, *Angew. Chem. Int. Ed.* **2003**, *42*, 4592-4633; b) A. Deiters, S. F. Martin, *Chem. Rev.* **2004**, *104*, 2199-2238; c) S. J. Connon, S. Blechert, *Angew. Chem. Int. Ed.* **2003**, *42*, 1900-1923; d) A. Fürstner, *Angew. Chem. Int. Ed.* **2000**, *39*, 3012-3043; e) T. M. Trnka, R. H. Grubbs, *Acc. Chem. Res.* **2001**, *34*, 18-29.
- [8] a) Y. Chauvin, *Angew. Chem. Int. Ed.* **2006**, *45*, 3740-3747; b) R. H. Grubbs, *Angew. Chem. Int. Ed.* **2006**, *45*, 3760-3765; c) R. R. Schrock, *Angew. Chem. Int. Ed.* **2006**, *45*, 3748-3759.
- [9] a) A. Fürstner, P. W. Davies, *Chem. Commun.* **2005**, 2307-2320; b) R. R. Schrock, C. Czekelius, *Adv. Synth. Catal.* **2007**, *349*, 55-77; c) W. Zhang, J. S. Moore, *Adv. Synth. Catal.* **2007**, *349*, 93-120; d) X. Wu, M. Tamm, *Beilstein J. Org. Chem.* **2011**, *7*, 82-93.
- [10] F. Pennella, R. L. Banks, G. C. Bailey, *Chem. Commun.* **1968**, 1548-1549.
- [11] a) A. Mortreux, M. Blanchard, *J. Chem. Soc., Chem. Commun.* **1974**, 786-787; b) T. J. Katz, J. McGinnis, *J. Am. Chem. Soc.* **1975**, *97*, 1592-1594; c) J. H. Wengrovius, J. Sancho, R. R. Schrock, *J. Am. Chem. Soc.* **1981**, *103*, 3932-3934; d) S. F. Pedersen, R. R. Schrock, M. R. Churchill, H. J. Wasserman, *J. Am. Chem. Soc.* **1982**, *104*, 6808-6809; e) A. Fürstner, G. Seidel, *Angew. Chem. Int. Ed.* **1998**, *37*, 1734-1736; f) A. Fürstner, C. Mathes, C. W. Lehmann, *J. Am. Chem. Soc.* **1999**, *121*, 9453-9454; g) J. Heppekausen, R. Stade, R. Goddard, A. Fürstner, *J. Am. Chem. Soc.* **2010**, *132*, 11045-11057; h) K. Jyothish, W. Zhang, *Angew. Chem. Int. Ed.* **2011**, *50*, 3435-3438; i) B. Haberlag, M. Freytag, C. G. Daniliuc, P. G. Jones, M. Tamm, *Angew. Chem. Int. Ed.* **2012**, *51*, 13019-13022.

- [12] a) M. R. Churchill, J. W. Ziller, J. H. Freudenberger, R. R. Schrock, *Organometallics* **1984**, *3*, 1554-1562; b) J. H. Freudenberger, R. R. Schrock, M. R. Churchill, A. L. Rheingold, J. W. Ziller, *Organometallics* **1984**, *3*, 1563-1573.
- [13] R. Stade, PhD thesis, Technische Universität Dortmund **2012**.
- [14] a) W. Zhang, J. S. Moore, *J. Am. Chem. Soc.* **2004**, *126*, 12796-12796; b) K. Balakrishnan, A. Datar, W. Zhang, X. Yang, T. Naddo, J. Huang, J. Zuo, M. Yen, J. S. Moore, L. Zang, *J. Am. Chem. Soc.* **2006**, *128*, 6576-6577.
- [15] a) A. Fürstner, K. Grela, C. Mathes, C. W. Lehmann, *J. Am. Chem. Soc.* **2000**, *122*, 11799-11805; b) A. Fürstner, C. Mathes, *Org. Lett.* **2001**, *3*, 221-223.
- [16] R. Lhermet, A. Fürstner, *Chem. Eur. J.* **2014**, *20*, 13188-13193.
- [17] a) J. M. Tour, *Chem. Rev.* **1996**, *96*, 537-554; b) U. H. F. Bunz, *Chem. Rev.* **2000**, *100*, 1605-1644; c) D. T. McQuade, A. E. Pullen, T. M. Swager, *Chem. Rev.* **2000**, *100*, 2537-2574; d) U. H. F. Bunz, *Acc. Chem. Res.* **2001**, *34*, 998-1010; e) K. Weiss, A. Michel, E.-M. Auth, U. H. F. Bunz, T. Mangel, K. Müllen, *Angew. Chem. Int. Ed.* **1997**, *36*, 506-509.
- [18] A. Ahlers, T. de Haro, B. Gabor, A. Fürstner, *Angew. Chem. Int. Ed.* **2016**, *55*, 1406-1411.
- [19] X.-P. Zhang, G. C. Bazan, *Macromolecules* **1994**, *27*, 4627-4628.
- [20] a) S. A. Krouse, R. R. Schrock, R. E. Cohen, *Macromolecules* **1987**, *20*, 903-904; b) S. A. Krouse, R. R. Schrock, *Macromolecules* **1989**, *22*, 2569-2576; c) M. Carnes, D. Buccella, T. Siegrist, M. L. Steigerwald, C. Nuckolls, *J. Am. Chem. Soc.* **2008**, *130*, 14078-14079; d) F. R. Fischer, C. Nuckolls, *Angew. Chem. Int. Ed.* **2010**, *49*, 7257-7260; e) S. Lysenko, B. Haberlag, X. Wu, M. Tamm, *Macromol. Symp.* **2010**, *293*, 20-23; f) D. E. Bellone, J. Bours, E. H. Menke, F. R. Fischer, *J. Am. Chem. Soc.* **2014**, *137*, 850-856.
- [21] M. Bindl, R. Stade, E. K. Heilmann, A. Picot, R. Goddard, A. Fürstner, *J. Am. Chem. Soc.* **2009**, *131*, 9468-9470.
- [22] M. G. Nilson, R. L. Funk, *Org. Lett.* **2010**, *12*, 4912-4915.
- [23] M. Fouché, L. Rooney, A. G. M. Barrett, *J. Org. Chem.* **2012**, *77*, 3060-3070.
- [24] M. Bindl, L. Jean, J. Herrmann, R. Müller, A. Fürstner, *Chem. Eur. J.* **2009**, *15*, 12310-12319.
- [25] B. J. Smith, G. A. Sulikowski, *Angew. Chem.* **2010**, *122*, 1643-1646.

- [26] a) J. Heppekausen, R. Stade, A. Kondoh, G. Seidel, R. Goddard, A. Fürstner, *Chem. Eur. J.* **2012**, *18*, 10281-10299; b) A. Mayr, G. A. McDermott, *J. Am. Chem. Soc.* **1986**, *108*, 548-549; c) G. A. McDermott, A. M. Dorries, A. Mayr, *Organometallics* **1987**, *6*, 925-931; d) E. O. Fischer, A. Maasböl, *Chem. Ber.* **1967**, *100*, 2445-2456.
- [27] K. Lehr, R. Mariz, L. Leseurre, B. Gabor, A. Fürstner, *Angew. Chem. Int. Ed.* **2011**, *50*, 11373-11377.
- [28] K. Lehr, A. Fürstner, *Tetrahedron* **2012**, *68*, 7695-7700.
- [29] S. M. Rummelt, J. Preindl, H. Sommer, A. Fürstner, *Angew. Chem. Int. Ed.* **2015**, *54*, 6241-6245.
- [30] V. Hickmann, A. Kondoh, B. Gabor, M. Alcarazo, A. Fürstner, *J. Am. Chem. Soc.* **2011**, *133*, 13471-13480.
- [31] M. Fuchs, A. Fürstner, *Angew. Chem.* **2015**, *127*, 4050-4054.
- [32] a) J. Willwacher, B. Heggen, C. Wirtz, W. Thiel, A. Fürstner, *Chem. Eur. J.* **2015**, *21*, 10416-10430; b) J. Willwacher, A. Fürstner, *Angew. Chem. Int. Ed.* **2014**, *53*, 4217-4221.
- [33] L. Hoffmeister, P. Persich, A. Fürstner, *Chem. Eur. J.* **2014**, *20*, 4396-4402.
- [34] a) C. E. Laplaza, C. C. Cummins, *Science* **1995**, *268*, 861-863; b) C. E. Laplaza, M. J. A. Johnson, J. C. Peters, A. L. Odom, E. Kim, C. C. Cummins, G. N. George, I. J. Pickering, *J. Am. Chem. Soc.* **1996**, *118*, 8623-8638; c) C. C. Cummins, *Chem. Commun.* **1998**, 1777-1786.
- [35] A. Fürstner, C. Mathes, C. W. Lehmann, *Chem. Eur. J.* **2001**, *7*, 5299-5317.
- [36] A. Fürstner, D. De Souza, L. Turet, M. D. B. Fenster, L. Parra-Rapado, C. Wirtz, R. Mynott, C. W. Lehmann, *Chem. Eur. J.* **2007**, *13*, 115-134.
- [37] A. Fürstner, M. Bonnekessel, J. T. Blank, K. Radkowski, G. Seidel, F. Lacombe, B. Gabor, R. Mynott, *Chem. Eur. J.* **2007**, *13*, 8762-8783.
- [38] A. Fürstner, M. Bindl, L. Jean, *Angew. Chem. Int. Ed.* **2007**, *46*, 9275-9278.
- [39] A. Fürstner, S. Flügge, O. Larionov, Y. Takahashi, T. Kubota, J. i. Kobayashi, *Chem. Eur. J.* **2009**, *15*, 4011-4029.
- [40] J. Willwacher, N. Kausch-Busies, A. Fürstner, *Angew. Chem. Int. Ed.* **2012**, *51*, 12041-12046.
- [41] W. Zhang, S. Kraft, J. S. Moore, *J. Am. Chem. Soc.* **2004**, *126*, 329-335.
- [42] W. Zhang, Y. Lu, J. S. Moore, in *Organic Syntheses*, John Wiley & Sons, Inc., **2007**.

- [43] a) W. Zhang, S. Kraft, J. S. Moore, *Chem. Commun.* **2003**, 832-833; b) W. Zhang, J. S. Moore, *Macromolecules* **2004**, *37*, 3973-3975; c) W. Zhang, S. M. Brombosz, J. L. Mendoza, J. S. Moore, *J. Org. Chem.* **2005**, *70*, 10198-10201; d) W. Zhang, J. S. Moore, *J. Am. Chem. Soc.* **2005**, *127*, 11863-11870.
- [44] a) H. Weissman, K. N. Plunkett, J. S. Moore, *Angew. Chem. Int. Ed.* **2006**, *45*, 585-588; b) H. M. Cho, H. Weissman, J. S. Moore, *J. Org. Chem.* **2008**, *73*, 4256-4258.
- [45] K. Jyothish, Q. Wang, W. Zhang, *Adv. Synth. Catal.* **2012**, *354*, 2073-2078.
- [46] H. Yang, Z. Liu, W. Zhang, *Adv. Synth. Catal.* **2013**, *355*, 885-890.
- [47] a) R. R. Schrock, *Acc. Chem. Res.* **1986**, *19*, 342-348; b) R. R. Schrock, *Chem. Rev.* **2002**, *102*, 145-180.
- [48] C. Zhang, Q. Wang, H. Long, W. Zhang, *J. Am. Chem. Soc.* **2011**, *133*, 20995-21001.
- [49] Q. Wang, C. Yu, H. Long, Y. Du, Y. Jin, W. Zhang, *Angew. Chem. Int. Ed.* **2015**, *54*, 7550-7554.
- [50] Y. Du, H. Yang, J. M. Whiteley, S. Wan, Y. Jin, S.-H. Lee, W. Zhang, *Angew. Chem. Int. Ed.* **2016**, *55*, 1737-1741.
- [51] Y. Zhu, H. Yang, Y. Jin, W. Zhang, *Chem. Mater.* **2013**, *25*, 3718-3723.
- [52] C. M. Downing, M. N. Missaghi, M. C. Kung, H. H. Kung, *Tetrahedron* **2011**, *67*, 7502-7509.
- [53] M. Fukawa, T. Sato, Y. Kabe, *Chem. Commun.* **2015**, *51*, 14746-14749.
- [54] S. Dürr, B. Bechlars, U. Radius, *Inorg. Chim. Acta.* **2006**, *359*, 4215-4226.
- [55] J. Zeller, S. Büschel, B. K. H. Reiser, F. Begum, U. Radius, *Eur. J. Inorg. Chem.* **2005**, *2005*, 2037-2043.
- [56] Literature 26a shows that a weak donor such as Ph₃SiOH binds to [(Ph₃SiO)₃Mo≡Ph] with a Mo-O distance of 2.68(1) Å. This interaction is considered weak and the coordination site is not blocked permanently as evident from this adducts ability to catalyze alkyne metathesis reactions. In our case, the shorter Mo-O bond length of 2.228(3) Å indicates a much stronger interaction which leads to a permanent blocking of the coordination site.
- [57] J. Espinas, J. Pelletier, E. Jeanneau, U. Darbost, K. C. Szeto, C. Lucas, J. Thivolle-Cazat, C. Duchamp, N. Henriques, D. Bouchu, J.-M. Basset, H. Chermette, I. Bonnamour, M. Taoufik, *Organometallics* **2011**, *30*, 3512-3521.

- [58] H. M. Cho, H. Weissman, S. R. Wilson, J. S. Moore, *J. Am. Chem. Soc.* **2006**, *128*, 14742-14743.
- [59] S. Schaubach, K. Gebauer, F. Ungeheuer, L. Hoffmeister, M. K. Ilg, C. Wirtz, A. Fürstner, *Chem. Eur. J.* **2016**, *Accepted Article*, doi.org/10.1002/chem.201601163.
- [60] K. Gebauer, PhD thesis, Technische Universität Dortmund **2016**.
- [61] O. Hesse, *J. prakt. Chem.* **1900**, *62*, 430-480.
- [62] S. Huneck, K. Schreiber, W. Steglich, *Tetrahedron* **1973**, *29*, 3687-3693.
- [63] G. Quinkert, N. Heim, J. W. Bats, H. Oschkinat, H. Kessler, *Angew. Chem. Int. Ed.* **1985**, *24*, 987-988.
- [64] C. Raji Reddy, N. N. Rao, P. Sujitha, C. G. Kumar, *Eur. J. Org. Chem.* **2012**, *2012*, 1819-1824.
- [65] a) G. Quinkert, N. Heim, J. Glenneberg, U.-M. Billhardt, V. Autze, J. W. Bats, G. Dürner, *Angew. Chem. Int. Ed.* **1987**, *26*, 362-364; b) G. Quinkert, N. Heim, J. Glenneberg, U. Döllner, M. Eichhorn, U.-M. Billhardt, C. Schwarz, G. Zimmermann, J. W. Bats, G. Dürner, *Helv. Chim. Acta* **1988**, *71*, 1719-1794.
- [66] a) S. C. Sinha, E. Keinan, *J. Org. Chem.* **1994**, *59*, 949-951; b) S. C. Sinha, E. Keinan, *J. Org. Chem.* **1997**, *62*, 377-386.
- [67] W. Oppolzer, R. N. Radinov, J. D. Brabander, *Tetrahedron Lett.* **1995**, *36*, 2607-2610.
- [68] D. Enders, O. F. Prokopenko, *Liebigs Ann.* **1995**, *1995*, 1185-1191.
- [69] Y. Kobayashi, M. Nakano, H. Okui, *Tetrahedron Lett.* **1997**, *38*, 8883-8886.
- [70] T. Nishioka, Y. Iwabuchi, H. Irie, S. Hatakeyama, *Tetrahedron Lett.* **1998**, *39*, 5597-5600.
- [71] N. Maezaki, Y.-X. Li, K. Ohkubo, S. Goda, C. Iwata, T. Tanaka, *Tetrahedron* **2000**, *56*, 4405-4413.
- [72] D. J. Dixon, A. C. Foster, S. V. Ley, *Org. Lett.* **2000**, *2*, 123-125.
- [73] M. G. Banwell, K. J. McRae, *Org. Lett.* **2000**, *2*, 3583-3586.
- [74] S. Raghavan, T. Sreekanth, *Tetrahedron Lett.* **2006**, *47*, 5595-5597.
- [75] C. Dubost, I. E. Markó, T. Ryckmans, *Org. Lett.* **2006**, *8*, 5137-5140.
- [76] J. S. Yadav, T. S. Rao, K. Ravindar, B. V. S. Reddy, *Synlett* **2009**, *2009*, 2828-2830.
- [77] C.-Y. Wang, D.-R. Hou, *J. Chinese Chem. Soc.* **2012**, *59*, 389-393.
- [78] V. R. Gandhi, *Tetrahedron* **2013**, *69*, 6507-6511.
- [79] P. Saidhareddy, S. Ajay, A. K. Shaw, *RCS Adv.* **2014**, *4*, 4253-4259.

- [80] H. Zhang, E. C. Yu, S. Torker, R. R. Schrock, A. H. Hoveyda, *J. Am. Chem. Soc.* **2014**, *136*, 16493-16496.
- [81] P. P. Waanders, L. Thijs, B. Zwanenburg, *Tetrahedron Lett.* **1987**, *28*, 2409-2412.
- [82] G. Solladie, I. Fernandez, C. Maestro, *Tetrahedron: Asymmetry* **1991**, *2*, 801-819.
- [83] W. Oppolzer, R. N. Radinov, *J. Am. Chem. Soc.* **1993**, *115*, 1593-1594.
- [84] The entropy term is crucial for the thermodynamic equation of this reaction, which can tentatively be rationalized as follows: Two molecules of diyne **146** form one molecule of dimer **148** and two molecules of butyne (3 molecules in total). Two molecules of diyne **146** form two molecules of monomer **147** and two molecules of butyne (4 molecules in total). Therefore from an entropy point of view the formation of monomer **147** is favored as compared to the formation of dimer **148**.
- [85] *See Postdoc Report: Dr. Josep Llaveria Cros, Research Advisor: Prof. Alois Fürstner, MPI für Kohlenforschung, Mülheim a. d. Ruhr 2014.*
- [86] D. Alvarez-Dorta, E. I. León, A. R. Kennedy, A. Martín, I. Pérez-Martín, C. Riesco-Fagundo, E. Suárez, *Chem. Eur. J.* **2013**, *19*, 10312-10333.
- [87] J. M. Hoover, S. S. Stahl, *J. Am. Chem. Soc.* **2011**, *133*, 16901-16910.
- [88] G. Gao, D. Moore, R.-G. Xie, L. Pu, *Org. Lett.* **2002**, *4*, 4143-4146.
- [89] B. M. Trost, M. J. Bartlett, A. H. Weiss, A. J. von Wangelin, V. S. Chan, *Chem. Eur. J.* **2012**, *18*, 16498-16509.
- [90] D. E. Frantz, R. Fässler, E. M. Carreira, *J. Am. Chem. Soc.* **2000**, *122*, 1806-1807.
- [91] S. M. Rummelt, K. Radkowski, D.-A. Roşca, A. Fürstner, *J. Am. Chem. Soc.* **2015**, *137*, 5506-5519.
- [92] D. J. Craik, D. P. Fairlie, S. Liras, D. Price, *Chem. Biol. Drug Des.* **2013**, *81*, 136-147.
- [93] R. Dharanipragada, *Future Med. Chem.* **2013**, *5*, 831-849.
- [94] K. Fosgerau, T. Hoffmann, *Drug Discov. Today* **2015**, *20*, 122-128.
- [95] a) J. O. Agola, L. Hong, Z. Surviladze, O. Ursu, A. Waller, J. J. Strouse, D. S. Simpson, C. E. Schroeder, T. I. Oprea, J. E. Golden, J. Aubé, T. Buranda, L. A. Sklar, A. Wandinger-Ness, *ACS Chem. Biol.* **2012**, *7*, 1095-1108; b) J. M. Ostrem, U. Peters, M. L. Sos, J. A. Wells, K. M. Shokat, *Nature* **2013**, *503*, 548-551; c) K. Wennerberg, K. L. Rossman, C. J. Der, *J. Cell Sci.* **2005**, *118*, 843-846; d) F. McCormick, *Clin. Cancer Res.* **2015**, *21*, 1797-1801; e) Andrew G. Stephen, D. Esposito, Rachel K. Bagni, F. McCormick, *Cancer Cell* **2014**, *25*, 272-281; f) P. M. Cromm, J. Spiegel, T. N. Grossmann, H. Waldmann,

- Angew. Chem. Int. Ed.* **2015**, *54*, 13516-13537; g) J. Spiegel, P. M. Cromm, G. Zimmermann, T. N. Grossmann, H. Waldmann, *Nat. Chem. Biol.* **2014**, *10*, 613-622.
- [96] a) J. O. Agola, P. A. Jim, H. H. Ward, S. BasuRay, A. Wandinger-Ness, *Clin. Genet.* **2011**, *80*, 305-318; b) S. Mitra, K. W. Cheng, G. B. Mills, *Sem. Cell Dev. Biol.* **2011**, *22*, 57-68.
- [97] M. A. Klein, *ACS Med. Chem. Lett.* **2014**, *5*, 838-839.
- [98] C. Bracken, J. Gulyas, J. W. Taylor, J. Baum, *J. Am. Chem. Soc.* **1994**, *116*, 6431-6432.
- [99] D. Y. Jackson, D. S. King, J. Chmielewski, S. Singh, P. G. Schultz, *J. Am. Chem. Soc.* **1991**, *113*, 9391-9392.
- [100] A. Muppidi, Z. Wang, X. Li, J. Chen, Q. Lin, *Chem. Commun.* **2011**, *47*, 9396-9398.
- [101] K. Fujimoto, N. Oimoto, K. Katsuno, M. Inouye, *Chem. Commun.* **2004**, 1280-1281.
- [102] S. Cantel, A. Le Chevalier Isaad, M. Scrima, J. J. Levy, R. D. DiMarchi, P. Rovero, J. A. Halperin, A. M. D'Ursi, A. M. Papini, M. Chorev, *J. Org. Chem.* **2008**, *73*, 5663-5674.
- [103] L. Mendive-Tapia, S. Preciado, J. Garcia, R. Ramon, N. Kielland, F. Albericio, R. Lavilla, *Nat. Commun.* **2015**, *6*.
- [104] H. E. Blackwell, R. H. Grubbs, *Angew. Chem. Int. Ed.* **1998**, *37*, 3281-3284.
- [105] a) G. L. Verdine, G. J. Hilinski, *Drug Discov. Today Technol.* **2012**, *9*, e41-e47; b) Y.-W. Kim, T. N. Grossmann, G. L. Verdine, *Nat. Protocols* **2011**, *6*, 761-771.
- [106] F. Guillier, D. Orain, M. Bradley, *Chem. Rev.* **2000**, *100*, 2091-2158.
- [107] P. M. Cromm, S. Schaubach, J. Spiegel, A. Fürstner, T. N. Grossmann, H. Waldmann, *Nat. Commun.* **2016**, *Accepted Article*, doi.org/10.1038/ncomms11300.
- [108] N. Marion, R. S. Ramón, S. P. Nolan, *J. Am. Chem. Soc.* **2008**, *131*, 448-449.
- [109] L. Biasiolo, M. Trinchillo, P. Belanzoni, L. Belpassi, V. Busico, G. Ciancaleoni, A. D'Amora, A. Macchioni, F. Tarantelli, D. Zuccaccia, *Chem. Eur. J.* **2014**, *20*, 14594-14598.
- [110] a) L. Zhang, X. Chen, P. Xue, H. H. Y. Sun, I. D. Williams, K. B. Sharpless, V. V. Fokin, G. Jia, *J. Am. Chem. Soc.* **2005**, *127*, 15998-15999; b) B. C. Boren, S. Narayan, L. K. Rasmussen, L. Zhang, H. Zhao, Z. Lin, G. Jia, V. V. Fokin, *J. Am. Chem. Soc.* **2008**, *130*, 8923-8930; c) M. Meldal, C. W. Tornøe, *Chem. Rev.* **2008**, *108*, 2952-3015; d) G. C. Tron, T. Pirali, R. A. Billington, P. L. Canonico, G. Sorba, A. A. Genazzani, *Med. Res. Rev.* **2008**, *28*, 278-308; e) J. E. Hein, V. V. Fokin, *Chem. Soc. Rev.* **2010**, *39*, 1302-1315.
- [111] S. Díez-González, A. Correa, L. Cavallo, S. P. Nolan, *Chem. Eur. J.* **2006**, *12*, 7558-7564.

- [112] J. Xiang, R. Yuan, R. Wang, N. Yi, L. Lu, H. Zou, W. He, *J. Org. Chem.* **2014**, *79*, 11378-11382.
- [113] a) L. Pérez-Serrano, L. Casarrubios, G. Domínguez, J. Pérez-Castells, *Org. Lett.* **1999**, *1*, 1187-1188; b) J. Blanco-Urgoiti, L. Anorbe, L. Perez-Serrano, G. Dominguez, J. Perez-Castells, *Chem. Soc. Rev.* **2004**, *33*, 32-42.
- [114] B. Figadere, A. W. Norman, H. L. Henry, H. P. Koeffler, J. Y. Zhou, W. H. Okamura, *J. Med. Chem.* **1991**, *34*, 2452-2463.
- [115] S. Protti, M. Fagnoni, A. Albin, *Angew. Chem. Int. Ed.* **2005**, *44*, 5675-5678.
- [116] N. G. Pschirer, U. H. F. Bunz, *Tetrahedron Lett.* **1999**, *40*, 2481-2484.
- [117] L. Fogel, R. P. Hsung, W. D. Wulff, R. D. Sommer, A. L. Rheingold, *J. Am. Chem. Soc.* **2001**, *123*, 5580-5581.
- [118] N. Kaneta, T. Hirai, M. Mori, *Chem. Lett.* **1995**, *24*, 627-628.
- [119] M. W. Carson, M. W. Giese, M. J. Coghlan, *Org. Lett.* **2008**, *10*, 2701-2704.
- [120] R. Andrea, G. Simon, in *PCT Int. Appl., Vol. WO 2011/146974 A1*, **2011**.
- [121] Q. Huang, M. A. Campo, T. Yao, Q. Tian, R. C. Larock, *J. Org. Chem.* **2004**, *69*, 8251-8257.
- [122] M. Nouzarian, R. Hosseinzadeh, H. Golchoubian, *Synth. Commun.* **2013**, *43*, 2913-2925.
- [123] C. P. Burke, Y. Shi, *Org. Lett.* **2009**, *11*, 5150-5153.
- [124] M. Hanack, J. R. Haßdenteufel, *Chem. Ber.* **1982**, *115*, 764-771.
- [125] a) R. Chandra, S. Oya, M.-P. Kung, C. Hou, L.-W. Jin, H. F. Kung, *J. Med. Chem.* **2007**, *50*, 2415-2423; b) D. Nishimura, Y. Takashima, H. Aoki, T. Takahashi, H. Yamaguchi, S. Ito, A. Harada, *Angew. Chem. Int. Ed.* **2008**, *47*, 6077-6079; c) A. Hofmann, P. Schmiel, B. Stein, C. Graf, *Langmuir* **2011**, *27*, 15165-15175.
- [126] Y. Nishihara, Y. Okada, J. Jiao, M. Suetsugu, M.-T. Lan, M. Kinoshita, M. Iwasaki, K. Takagi, *Angew. Chem. Int. Ed.* **2011**, *50*, 8660-8664.
- [127] A. Ochida, G. Hamasaka, Y. Yamauchi, S. Kawamorita, N. Oshima, K. Hara, H. Ohmiya, M. Sawamura, *Organometallics* **2008**, *27*, 5494-5503.
- [128] R. Gauler, N. Risch, *Eur. J. Org. Chem.* **1998**, *1998*, 1193-1200.
- [129] J.-d. A. K. Twibanire, H. Al-Mughaid, T. B. Grindley, *Tetrahedron* **2010**, *66*, 9602-9609.
- [130] S. V. Kolotuchin, P. A. Thiessen, E. E. Fenlon, S. R. Wilson, C. J. Loweth, S. C. Zimmerman, *Chem. Eur. J.* **1999**, *5*, 2537-2547.

- [131] T. Höpfner, Peter G. Jones, B. Ahrens, I. Dix, L. Ernst, H. Hopf, *Eur. J. Org. Chem.* **2003**, 2003, 2596-2611.
- [132] E. K. Yum, J. W. Son, S. K. Kim, S. N. Kim, K. M. Kim, C. W. Lee, *Bull. Korean Chem. Soc.* **2010**, 31, 2097-2099.
- [133] E. Gogritchiani, S. Niebler, N. Egner, M. Wörner, A. M. Braun, T. Young, P. Gupta, A. Shi, S. H. Bossmann, *Synthesis* **2005**, 2005, 3051-3058.
- [134] S.-K. Kang, W.-S. Kim, B.-H. Moon, *Synthesis* **1985**, 1985, 1161-1162.
- [135] C. Zhou, A. V. Walker, *Langmuir* **2010**, 26, 8441-8449.
- [136] F. Muth, M. Günther, S. M. Bauer, E. Döring, S. Fischer, J. Maier, P. Drückes, J. Köppler, J. Trappe, U. Rothbauer, P. Koch, S. A. Laufer, *J. Med. Chem.* **2015**, 58, 443-456.
- [137] T. Miura, M. Shimada, P. de Mendoza, C. Deutsch, N. Krause, M. Murakami, *J. Org. Chem.* **2009**, 74, 6050-6054.